

Transcending Conventional Approaches: The AHRt of Experimental Autoimmune Prostatitis (EAP) Treatment with 2-(1' H-indole-3'-carbonyl)-thiazole-4-carboxylic acid methyl ester (ITE)

By

Robbie SJ Manuel

A dissertation submitted in partial fulfillment  
of the requirement for the degree of

Doctor of Philosophy  
(Molecular & Environmental Toxicology)

at the UNIVERSITY OF WISCONSIN-MADISON  
2024

Date of Final Oral Examination: April 16, 2024

The dissertation is approved by the following members of the Final Oral Committee:

Chad Vezina, PhD, Professor, Comparative Biosciences  
Laura Hernandez, PhD, Professor, Animal & Dairy Sciences, Obstetrics & Gynecology  
Jyoti Watters, PhD, Professor, Comparative Biosciences  
Kim Keil-Stietz, PhD, Assistant Professor, Comparative Biosciences  
LaTasha Crawford, VMD PhD, Assistant Professor, Pathobiological Sciences  
Matthew Grimes, MD, Assistant Professor, Urology

## Dedication

This thesis is dedicated to my family whose love and encouragement sustained me throughout the years. There wasn't a parenting book in the world that could have prepared you for my eccentricity, yet you endured.

Familiar generations before me have showed that education is the key to unlocking the world, and a passport to *freedom*. Here in this *freedom*, we create the highest, grandest vision possible for my life, for me to become every bit of what I believe.

---

“Who said that all of who you are has to be good? All of who you are *is who you are*. It hurts, you rage, battle it out, ask, “Why?” Then you forgive, reconcile, and use your heart, your courage and vision to fix, to heal and then, ultimately, to connect, to empathize. And that empathy creates a passion for people, and it *all* is the fuel of the warrior—a brave, experienced soldier, or fighter.”  
– Viola Davis

Robbie SJ Manuel

## Acknowledgements

The University of Wisconsin-Madison, an institution perched gracefully on the shoreline of an isthmus within a city I never envisioned as my academic haven, has proven to be the fertile soil in which my intellectual journey took root. In this city, I stumbled upon a thriving community of burgeoning academics, seasoned mentors, and benevolent locals who have collectively shaped the academic voyager I stand as today.

My heartfelt gratitude extends to Laura Hernandez, PhD the trailblazer who took a leap of faith and welcomed me into her lab as a research acolyte while I navigated the labyrinthine path to graduate programs. Little did she know, her acceptance into the fold led me to the luminous presence of Celeste Sheftel, PhD ('22), who adopted me as her protege and introduced me to esoteric theories, unconventional thoughts, and mysterious protocols. Celeste not only taught me the art of kindness but also the importance of unwavering commitment during tumultuous times. Her unyielding dedication throughout her academic journey has left me awestruck. As a scientist, parent, and partner, she stands as a paragon of inspiration and admiration that will endure eternally.

To my PhD advisor and program director, Chad Vezina, PhD, I offer my profound thanks for your unwavering support over the years and for never permitting me to throw in the academic towel. Your guidance has been the steadfast beacon from my orientation to the bittersweet final days in the laboratory. Mark Marhol, our erstwhile program coordinator and chief cheerleader, your wisdom, humor, and understanding of the human condition, the program, the campus, and

its resources remain unparalleled. I shall forever regard you as a confidant I can turn to for any discourse.

To the following members of the entering class of 2019 - Brandon Scharpf, Tyler Beams, Brenna Walton, and Thomas Peterson - my deepest thanks. We, an eclectic bunch of individuals with diverse backgrounds, expertise, and personalities, found common purpose in supporting one another. Brandon, my stalwart lab companion, your presence was a reassuring constant in the ever-changing laboratory landscape.

To my elder sibling, Andre Manuel, you have been the cornerstone of my existence, guiding me through life's battles and ensuring my dreams found their wings. Your indomitable spirit taught me that the middle stages of any journey are unique to each traveler, and complacency is a realm I must never dwell in. You instilled in me the value of self-prioritization and the relentless pursuit of personal growth.

In the annals of my academic odyssey, there exists a singular character who emerged from the desert sands of Arizona State University back in 2012 and transformed into the steadfast anchor of my journey - my confidant, partner in academic misadventures, and all-around life enthusiast. Alexander R. Tom, my best friend, and the perpetual source of laughter in even the bleakest of times, I offer my sincerest appreciation. You've been my sanity checkpoint for over a decade now. Your unwavering support and infectious humor have been the secret sauce that spiced up my life, making the journey not only bearable but genuinely enjoyable. I look forward to our continued life together, as I start anew in New York City.

Jane Austen's words in 'Northanger Abbey' resonate with me deeply: "There is nothing I would not do for those who are really my friends. I have no notion of loving people by halves; it is not my nature." Indeed, the bonds forged here transcend my tenure as a graduate student. I count myself fortunate to have crossed paths with these extraordinary individuals. Some enter our lives at precisely the right juncture for profound reasons, while others exit just when we need them most. Time plays the role of matchmaker, and we determine who remains in our narrative. My narrative would be nothing less if it weren't for these people:

Aimee Walters	Kim Castillo	Steve Schmidt
Alan Zhou	Conner Ball	Tad Simpson
Andy Sylvia	Hunter Hazel	Ryan Grosvold, PhD ('08 '11 '21)
Brandon Pivotto	Matthew Hazel	Taylor Johnson
Lt. Col Clint Carr, RET	Pinkesh Shah	*Trenell Darby, DNP ('16)
Demetrius Shaw	Rian Rainey	Zach Vruwink
James Sinigan	Ryan Hubanks	Victor Baxerres
*Jason DePhillips, MS ('23)	Ryan Spensley	*Zach Eastburn, JD ('15)
Katie Altman	Shamrock Bar & Grille	

\*University of Wisconsin-Madison Graduate

Lastly, but certainly not least, a heartfelt nod goes to Joshua L. Bernardini. Your unwavering support over the past decade has been nothing short of extraordinary. You've been there in every conceivable way, providing a steady hand on this tumultuous journey. And let's not forget your exceptional role as a co-parent to our beloved Toaster, who's been a source of boundless joy in our lives. To paraphrase JFK, "We choose to take on challenges not because they're easy, but because they're hard." Our journey has been no cakewalk, but together, we've tackled it with determination and triumphed. I'd boldly go to the moon and back with you, because the path we choose is always worth the adventure.

## Table of Contents

<i>Dedication</i> .....	<i>i</i>
<i>Acknowledgements</i> .....	<i>ii</i>
<i>List of Abbreviations</i> .....	<i>vi</i>
<b>ABSTRACT</b> .....	<b>1</b>
<i>Preface</i> .....	<b>4</b>
The Wisconsin Idea and Significance of Science Communication in Biomedical Sciences.....	<b>4</b>
<b>Chapter 1</b> .....	<b>8</b>
Pee-rless Prostates: Tiny Glands, Big Urological Discoveries! Communicating Research to Non- Scientist for the Wisconsin Initiative for Science Literacy .....	<b>8</b>
<b>Chapter 2</b> .....	<b>28</b>
Trends In Experimental Autoimmune Prostatitis: Insights into Pathogenesis, Therapeutic Strategies, And Redefinition.....	<b>28</b>
<b>Chapter 3</b> .....	<b>59</b>
The aryl hydrocarbon receptor agonist ITE reduces inflammation and urinary dysfunction in a mouse model of autoimmune prostatitis.....	<b>59</b>
<b>Chapter 4</b> .....	<b>118</b>
The Last Drop: Conclusion & Future Directions.....	<b>118</b>
<b>APPENDIX</b> .....	<b>130</b>
<b>Appendix A</b> .....	<b>131</b>
Harmony and Dissonance: Unraveling Sex-Biased Dynamics in Immunometabolism, Autoimmunity, and Chronic Unpredictable Stress for Personalized Health.....	<b>131</b>
Sex-biased Autoimmunity .....	<b>161</b>
Adopted From: Sexual Dimorphism in Immunometabolism and Autoimmunity: Impact on Personalized Medicine. ....	<b>165</b>

## List of Abbreviations

<b>5-Ari</b>	<b>5-Alpha-Reductase Inhibitor</b>
<b>5-Ht</b>	<b>5-Hydroxytryptamine (Serotonin)</b>
<b>A/J</b>	<b>Inbred Albino Mouse Strain</b>
<b>AAM</b>	<b>Alternatively Activated Macrophage</b>
<b>AARDA</b>	<b>American Autoimmune Related Diseases Association, Inc</b>
<b>ADME</b>	<b>Absorption, Distribution, Metabolism, &amp; Excretion</b>
<b>AHR</b>	<b>Aryl Hydrocarbon Receptor</b>
<b>AHRE</b>	<b>Aryl Hydrocarbon Response Element</b>
<b>Aire</b>	<b>Autoimmune Regulator (Gene)</b>
<b>AKG</b>	<b>-Ketoglutarate</b>
<b>AMPK</b>	<b>Amp-Activated Protein Kinase</b>
<b>APC</b>	<b>Antigen-Presenting Cell</b>
<b>ARNT</b>	<b>Ahr Nuclear Translocator</b>
<b>AS</b>	<b>Ankylosing Spondylitis</b>
<b>ATP</b>	<b>Adenosine Triphosphate</b>
<b>BC</b>	<b>Bladder Capacity</b>
<b>BCR</b>	<b>B Cell Receptor</b>
<b>BHLH</b>	<b>Basic Helix–Loop–Helix</b>
<b>BP</b>	<b>Baseline Pressure</b>
<b>BPH</b>	<b>Benign Prostatic Hyperplasia</b>
<b>BR</b>	<b>Broad Range</b>
<b>BRMS</b>	<b>Biomedical Research Modeling Services</b>
<b>C</b>	<b>Compliance</b>
<b>CAM</b>	<b>Classically Activated Macrophage</b>
<b>CCA</b>	<b>Citric Acid Cycle / Krebs Cycle</b>
<b>CD</b>	<b>Cluster Of Differentiation</b>
<b>CLPL</b>	<b>Colon Lamina Propria Lymphocytes</b>
<b>CMB</b>	<b>Cystometry</b>
<b>CNS</b>	<b>Central Nervous System</b>
<b>COX-</b>	<b>Cyclooxygenase</b>
<b>COX5B</b>	<b>Cytochrome C Oxidase Subunit 5b</b>
<b>CP/CPPS</b>	<b>Chronic Prostatitis/Chronic Pelvic Pain Syndrome</b>
<b>CTFH</b>	<b>Circulating-Tfh</b>
<b>CTL</b>	<b>Cytotoxic T Lymphocyte</b>
<b>DC</b>	<b>Dendritic Cell</b>
<b>DIM</b>	<b>3, 3'-Diindolylmethane</b>
<b>DMSO</b>	<b>Dimethyl Sulfoxide</b>
<b>DNA</b>	<b>Deoxyribonucleic Acid</b>
<b>dsDNA</b>	<b>Anti-Double-Stranded DNA</b>
<b>DSS</b>	<b>Dextran Sulphate Sodium</b>
<b>E</b>	<b>Efficiency</b>

<b>E2</b>	Estradiol
<b>EAe</b>	Experimental Autoimmune Encephalomyelitis
<b>EAP</b>	Experimental Autoimmune Prostatitis
<b>EAU</b>	Experimental Autoimmune Uveitis
<b>EC</b>	Endothelial Cell
<b>ERK</b>	Extracellular Signal-Regulated Kinase
<b>Fadh<sub>2</sub></b>	Fuel Oxidative Phosphorylation
<b>FAO</b>	Fatty-Acid Oxidation
<b>FFA</b>	Free Fatty Acid
<b>FICZ</b>	6-Formylindolo-(3,2-B)Carbazole
<b>Flt3</b>	Fms-Related Tyrosine Kinase 3 Ligand
<b>FOXO</b>	Forkhead Box Transcription Factors-O
<b>FOXP</b>	Forkhead Box Protein-P
<b>GH</b>	Growth Hormone
<b>GM-CSF</b>	Granulocyte-Macrophage Colony Stimulating Factor
<b>HAH</b>	Halogenated Aromatic Hydrocarbon
<b>HIF-1<math>\alpha</math></b>	Hypoxia-Inducible Factor 1-Alpha
<b>HIV</b>	Human Immunodeficiency Virus
<b>Hla</b>	Human Leukocyte Antigen
<b>HSP--</b>	Heat Shock Protein
<b>I3C</b>	Indole-3-Carbinol
<b>IAA</b>	Indole Acetic Acid
<b>IBD</b>	Irritable Bowel Disease
<b>IBS</b>	Irritable Bowel Syndrome
<b>ID</b>	Infusion Duration
<b>IDO</b>	2,3-Dioxygenase
<b>Ig-</b>	Immunoglobulin
<b>Il-</b>	Interleukin
<b>ILC</b>	Innate Lymphoid Cells
<b>iNOS</b>	Inducible Nitric Oxide Synthase
<b>IR</b>	Infusion Rate
<b>Irak-1</b>	Interleukin-1 Receptor Associated Kinase
<b>Irf-1</b>	Interferon Regulatory Factor 1
<b>IRS</b>	Insulin Receptor Substrate
<b>ITE</b>	2-(1' H-Indole-3'-Carbonyl)-Thiazole-4-Carboxylic Acid Methyl Ester
<b>IV</b>	Infused Volume
<b>IVI</b>	Intervoid Interval
<b>KYN</b>	Kynurenine
<b>Lfa-1</b>	Lymphocyte Function-Associated Antigen 1
<b>List</b>	Low-Intensity Shockwave Therapy
<b>LUT -(D)</b>	Lower Urinary Tract -Disease
<b>MAG</b>	Male Accessory Gland
<b>MAPK</b>	Mitogen-Activated Protein Kinase
<b>MBFR</b>	Mass-Based Flow Rate



<b>Mcl-2</b>	Macrophage C-Type Lectin 2
<b>Mcp-1</b>	Monocyte Chemoattractant Protein
<b>MCT</b>	Monocarboxylate Transporters
<b>MHC</b>	Major Histocompatibility Complex (1/2)
<b>MLN</b>	Mesenteric Lymph Nodes
<b>MOA</b>	Mechanism Of Action
<b>MS</b>	Multiple Sclerosis
<b>MTORr -C</b>	Mechanistic Target Of Rapamycin -Complex
<b>NADH</b>	Nicotinamide Adenine Dinucleotide
<b>NK</b>	Natural Killer
<b>NO</b>	Nitric Oxide
<b>NOD</b>	Nucleotide Oligomerization Domain
<b>NOD</b>	Non-Obese Diabetic (Mouse Strain)
<b>NPVP</b>	Normalized Peak Void Pressure
<b>NSAID</b>	Non-Steroidal Anti-Inflammatory Drugs
<b>NTP</b>	Normalized Threshold Pressure
<b>NVC</b>	Nonvoiding Contraction
<b>OXPHOS</b>	Oxidative Phosphorylation
<b>P25</b>	Prostatic Spermine-Binding Protein
<b>P4</b>	Progesterone
<b>PAg</b>	Prostate Antigen
<b>PAH</b>	Polycyclic Aromatic Hydrocarbon
<b>PAMP(S)</b>	Pathogen-Associated Molecular Pattern
<b>PAP</b>	Prostatic Acid Phosphate
<b>PBL</b>	Peripheral Blood Lymphocytes
<b>PBS</b>	Phosphate-Buffered Saline
<b>PCA</b>	Prostate Cancer
<b>PDK-1</b>	Phosphoinositide-Dependent Kinase 1
<b>PE</b>	Prostate Extract
<b>PEC</b>	Predicted Environmental Concentration
<b>PG-</b>	Prostaglandin
<b>PGC1</b>	Peroxisome Proliferator-Activated Receptor Beta
<b>pl3k</b>	Phosphoinositide 3-Kinase
<b>PIP2</b>	Phosphatidylinositol (3,4)-Bisphosphate
<b>PIP3</b>	Phosphatidylinositol (3,4,5)-Trisphosphate
<b>PKB</b>	Protein Kinase B
<b>PPP</b>	Pentose Phosphate Pathway
<b>PRR(S)</b>	Pattern Recognition Receptors
<b>PSA</b>	Prostate-Specific Antigen
<b>PSPB</b>	Prostatein Or Steroid Binding Protein
<b>PSS</b>	Prostate Symptom Score
<b>PVM</b>	Perivascular Macrophage
<b>PVP</b>	Peak Void Pressure
<b>QQK</b>	Quality Of Life

<b>RA</b>	Rheumatoid Arthritis
<b>RARC</b>	Research Animal Resources And Compliance
<b>ROS</b>	Reactive Oxygen Species
<b>RPS6</b>	Ribosomal Protein-S6
<b>RV</b>	Residual Volume
<b>SD</b>	Sprague Dawley (Rat Strain)
<b>SGEC</b>	Salivary Gland Epithelial Cell
<b>SHBG</b>	Sex Hormone-Binding Globulin
<b>SJL</b>	Swiss Jim Lambert (Mouse Strain)
<b>SLE</b>	Systemic Lupus Erythematosus
<b>SRBP-1</b>	Sterol Regulatory Element Binding Protein 1
<b>S2</b>	Sjögren's Syndrome
<b>STAT1</b>	Signal Transducer And Activation Of Transcription Factor 1
<b>SVS2</b>	Seminal Vesicle Secretory Protein 2
<b>T</b>	Testosterone
<b>T2</b>	Peptide
<b>TB</b>	Tuberculosis
<b>TCA</b>	Tricarboxylic Acid
<b>TCDD</b>	2,3,7,8-Tetrachlorodibenzodioxin
<b>TCR</b>	T Cell Receptor
<b>TFH</b>	T-Follicular Helper Cells
<b>Th-</b>	T-Helper Cell
<b>TLR</b>	Toll-Like Receptors
<b>Tp</b>	Threshold Pressure
<b>Tr1</b>	Type-1 Regulatory T Cells
<b>T<sub>reg</sub></b>	T-Regulatory Cell
<b>Tsc2</b>	Tuberous Sclerosis 2
<b>TTP</b>	Tristetraprolin
<b>UPD</b>	Up-Down
<b>VD</b>	Void Duration
<b>VFR</b>	Volume Flow Rate
<b>VFT</b>	Von Frey Filament Test
<b>Vgll3</b>	Vestigial Family Member 3
<b>VLA-4</b>	Very Late Antigen 4
<b>VSA</b>	Void Spot Assay
<b>VV</b>	Void Volume
<b>WT</b>	Wildtype

**Transcending Conventional Approaches: The AHRt of Experimental Autoimmune Prostatitis (EAP) Treatment with 2-(1' H-indole-3'-carbonyl)-thiazole-4-carboxylic acid methyl ester) (ITE)**

**Robbie SJ Manuel**

Under the supervision of Professor Chad M. Vezina at the University of Wisconsin-Madison

**ABSTRACT**

My laboratory is focused on understanding mechanisms and potential therapies for benign urological diseases. Autoimmune mediated inflammation has been identified as a mechanism of several benign prostatic diseases, but no existing therapy is approved to treat autoimmune-mediated benign urological conditions. In Chapter 2, I review the utilization of experimental autoimmune prostatitis (EAP) in rodents as a method to simulate key aspects of autoimmune-mediated Chronic Prostatitis/Chronic Pelvic Pain Syndrome (CP/CPSS). Through the examination of causative factors, immune responses, and new treatment approaches, our goal is to deepen understanding of CP/CPSS and advance the use of the EAP model for testing novel treatments. In Chapter 3, I introduced a new research model to the laboratory, the mouse EAP model. I collected and purified homogenate from rat prostate and introduced it subcutaneously in mice to initiate an immune response against rat prostate antigens. Given the close species relationship between rats and mice, the rat prostate antigen also drives an autoimmune response

to mouse prostate, leading to histological inflammation, allodynia, and changes in urinary function.

The aryl hydrocarbon receptor signaling pathway, initially identified as the pathway that mediates toxic responses to a variety of environmental contaminants, has recently been identified as a potential drug target for treating a variety of autoimmune diseases, including multiple sclerosis, inflammatory bowel disease, and other inflammatory diseases. Whether the AHR signaling pathway can also block inflammation and other adverse responses to prostate autoimmunity had not been previously addressed.

I tested whether 2-(1'H-indole-3'carbonyl)-thiazole-4-carboxylic acid methyl ester (ITE), an agonist of the AHR, protects against histological and functional disorders in EAP mice.

I found that EAP increased histological inflammation of the dorsal prostate, caused tactile allodynia, and increased non-voiding bladder contractions; ITE significantly reduced these EAP-mediated endpoints. I also identified a candidate gene for mediating inflammatory responses of EAP and the protective actions of ITE. EAP increased the abundance of three RNAs (H2-AB1, S100a8, and S100a9) and ITE protected against the EAP-mediated increase in abundance. I highlight the potential of ITE as a new treatment path for prostate diseases, revealing its ability to modulate the immune system and reprogram metabolism amid urological inflammation.

In the first two years of my PhD work, I investigated the influence of environmental chronic stress on sex-biased autoimmunity to understanding the molecular stress influence on systemic lupus erythematosus patients by utilizing a novel pTre-*Vgll3*/K14rtTA mouse model. I describe

the impact of chronic environmental stress on disease progression with the *Vgll3*-driven, lupus-prone mouse model, and identify the molecular mechanism targets underlying stress-influenced autoimmune disease progression. These results are significant because it is unknown how environmental exposures alter the risk and progression of autoimmune diseases driven by *VGLL3*. These results are shown in Appendix 1.

## **Preface**

### **The Wisconsin Idea and Significance of Science Communication in Biomedical Sciences**

---

The Wisconsin Idea is a concept in American political thought that emerged in the late 19th and early 20th centuries. It refers to the progressive reforms and policies implemented in the state of Wisconsin that aimed to improve the lives of its citizens and promote the greater good of society. The idea is often credited to Charles Van Hise, the president of the University of Wisconsin-Madison from 1903 to 1918.

At its core, the Wisconsin Idea emphasizes the notion that the boundaries of the university should not end at the campus edge. Instead, knowledge and expertise generated by the university should be used to solve problems and improve society as a whole. This concept led to closer ties between the state government, the university system, and the people of Wisconsin. Progressive reforms such as workers' compensation, labor regulations, and environmental conservation were developed and implemented based on academic research and expertise.

1. **Public Engagement:** The idea underscores the importance of universities being actively engaged with their communities. In today's interconnected world, universities have a responsibility to address local, national, and global challenges. This engagement fosters a sense of community and ensures that research and knowledge have a meaningful impact on society.
2. **Interdisciplinary Collaboration:** Many of the issues faced by society today are complex and multifaceted. The Wisconsin Idea promotes collaboration across disciplines, encouraging researchers and scholars to work together to find innovative solutions. This interdisciplinary approach is crucial in addressing contemporary challenges such as climate change, public health crises, and social inequality.
3. **Applied Research:** The Wisconsin Idea emphasizes the application of research to real-world problems. Terminal degree programs, such as PhDs and professional doctorates, are often research-intensive. Encouraging students to apply their research in practical settings helps bridge the gap between academia and the real world, ensuring that knowledge is used to solve practical problems.
4. **Social Responsibility:** Universities play a significant role in shaping the values and ethics of future leaders. The Wisconsin Idea emphasizes the social responsibility of universities to contribute positively to society. This ethos is essential in educating individuals who not only excel in their fields but also understand the ethical implications of their work and contribute positively to society.
5. **Lifelong Learning:** Education doesn't stop at graduation. The Wisconsin Idea promotes the concept of lifelong learning, encouraging individuals to continue their education and stay updated with the latest developments in their fields. This is particularly important in

today's rapidly changing world where continuous learning is essential for personal and professional growth.

6. **Global Perspective:** While the Wisconsin Idea originated at a state level, its principles can be applied globally. In an interconnected world, universities and scholars often collaborate internationally to address global challenges. The idea of universities being socially responsible and engaged with communities extends beyond national borders.

The enduring influence of the Wisconsin Idea on American public policy and education is manifest in its role as a paradigmatic model, profoundly shaping the trajectory of the nation's public university system. Rooted in the fundamental principles of public engagement, interdisciplinary collaboration, applied research, social responsibility, lifelong learning, and a global perspective, this ideological framework has endowed universities with the mandate to function as dynamic and socially conscientious institutions. Serving as a lodestar, it guides the evolution of contemporary higher education and terminal degree programs, imbuing them with a sense of purpose and a commitment to meaningful societal contributions. In this context, the Wisconsin Idea stands as an exemplar of educational philosophy, resonating far beyond its origins, and continuing to illuminate the path toward a socially impactful and globally aware academia.

In my nascent academic journey, I am profoundly grateful for the scholarly mentorship provided by my principal investigator, Dr. Chad M. Vezina, PhD, whose embodiment of the Wisconsin Idea has profoundly influenced my academic ethos. Departing from this venerable institution, I carry with me an unwavering commitment to the principles encapsulated by the Wisconsin Idea,



virtues that have been instilled in me during my tenure within the nurturing confines of our isthmus-ensconced campus. In this expansive moment of transition, I am compelled to express my profound gratitude to Laura Knoll, PhD, Associate Dean for Basic Research, whose unwavering support has served as a steadfast beacon throughout my graduate studies. I also extend my heartfelt appreciation to the entirety of my program administration and thesis committee, whose collective guidance has been indispensable in shaping my scholarly trajectory.

Chapter 1

**Pee-rless Prostates: Tiny Glands, Big Urological Discoveries! Communicating Research to Non-Scientist for the Wisconsin Initiative for Science Literacy**

Manuel, Robbie SJ

## **Why the Prostate?**

The pivotal factor driving my research focus lies in the guidance of my advisor, Dr. Chad Vezina, PhD. In the academic realm, an advisor holds a significant sway; their research direction becomes ours. In my case, Dr. Vezina's expertise leads our laboratory's research to the realm of diseases impacting the lower urinary tract in human males and dogs.

Within the Vezina Group, our concentration gravitates towards ailments afflicting the lower urinary tract in both humans and aging male dogs. These disorders, marked by symptoms such as increased urge to urinate, painful urination, excessive urination during the day or at night, and incontinence, collectively cost American seniors over \$4 billion annually[4]. Prostate-related issues, notably prostate cancer, stand out as prominent culprits behind these problems and, alarmingly, are a leading cause of mortality among American men[4].

Our mission is twofold. Firstly, we are dedicated to advancing male health by pioneering novel treatments for prostate-related urinary dysfunction and cancer in both human males and male dogs. Secondly, our commitment extends to nurturing Wisconsin's future scientific luminaries. By cultivating a new generation of exceptional scientists, we ensure a sustained effort in combating prostate-related diseases, shaping a healthier tomorrow. This commitment to transformative research and education stands as the hallmark of the Vezina Group, reinforcing our dedication to male health and scientific progress.

The study of male urological diseases, particularly those concerning the prostate, is of paramount importance due to several compelling reasons:

1. **Prevalence and Impact:** Prostate-related issues, including benign prostatic hyperplasia (BPH) and prostate cancer, are incredibly common among aging men[5]. Prostate cancer, in particular, is the second most common cancer in men worldwide. Understanding these conditions is essential due to their widespread prevalence and their significant impact on the quality of life and mortality rates of affected individuals.
2. **Health and Well-being:** Urological diseases, such as prostate cancer, profoundly affect the health and well-being of men[4]. Studying these diseases facilitates the development of early detection methods, innovative treatments, and preventive strategies, leading to improved patient outcomes and enhanced quality of life for affected individuals.
3. **Aging Population:** As the global population ages, the incidence of prostate-related diseases is expected to rise. Research in this field is crucial to address the unique challenges posed by an aging demographic, ensuring that appropriate healthcare measures are in place to cater to the needs of an increasing number of affected individuals[5-7].
4. **Economic Burden:** Prostate-related diseases pose a substantial economic burden on healthcare systems globally. By studying these diseases, researchers can identify cost-effective diagnostic methods, treatments, and management strategies. This research-

driven approach can alleviate the economic strain on healthcare infrastructures and improve resource allocation[4].

5. **Advancing Medical Science:** Research on male urological diseases, including the prostate, contributes significantly to the advancement of medical science. Discoveries in this field often have broader implications, leading to innovations in cancer research, genetics, immunology, and pharmacology. Studying these diseases provides valuable insights into the complex interplay of genetic, environmental, and lifestyle factors in disease development, fostering a deeper understanding of human biology[1, 8-11].
6. **Personalized Medicine:** In recent years, there has been a shift towards personalized medicine, tailoring treatments to an individual's genetic makeup and specific disease characteristics. Studying male urological diseases, including prostate cancer, is instrumental in advancing personalized medicine approaches. This tailored approach to treatment can lead to more effective interventions with fewer side effects, significantly improving patient outcomes[12, 13].

Therefore, studying male urological diseases and the prostate is essential for the well-being of individuals, the sustainability of healthcare systems, and the continuous progress of medical science. By delving into the intricacies of these diseases, researchers pave the way for better diagnostics, treatments, and prevention strategies, ultimately enhancing the lives of millions of men worldwide.

Ah, the prostate (**Figure 1**), that small but mighty gland in the male body, diligently producing fluids like a little factory worker. It's nestled right below the bladder, doing its part in the reproductive orchestra by mixing special juices with sperm, creating a protective environment for those little swimmers. Picture it as a bustling workshop, where workers mix ingredients to make a crucial potion for the magical journey of reproduction.

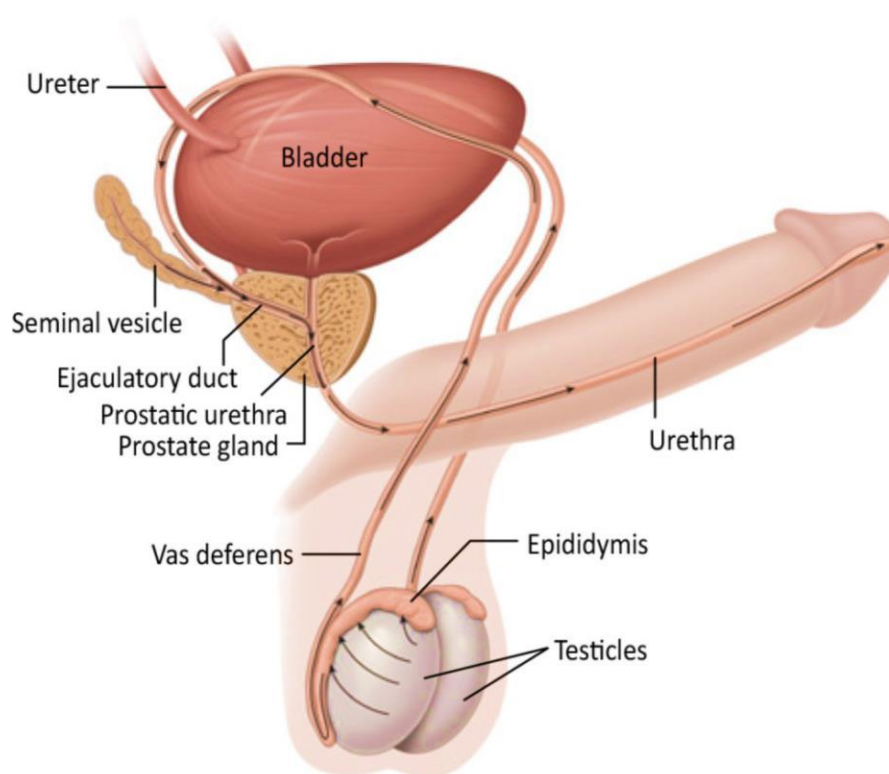


**Figure 1:** Simple anatomical diagram of the human reproductive tract

Now, as men age, this prostate can sometimes act like a grumpy old neighbor causing trouble. One issue it might stir up is an enlargement, squeezing the urethra like a kink in a garden hose, making bathroom trips a bit challenging. Or there's the worry of prostate cancer, where cells in the prostate grow unruly, creating a real medical mystery that needs solving. Just like regular

check-ups for your car, these prostate check-ups are crucial to keep your body engine running smoothly.

### **What is Prostatitis?**

Prostatitis is a condition characterized by inflammation or swelling of the prostate gland, which is a small organ located just below the bladder in men. Prostatitis can cause a variety of symptoms, which can vary in intensity and duration. Here are the common symptoms associated with prostatitis (**Figure 2**):

1. **Pain or Discomfort:** Individuals with prostatitis often experience pain or discomfort in the pelvic area, lower abdomen, lower back, or perineum (the area between the scrotum and anus). This pain can be mild to severe and may come and go[12].
2. **Painful or Difficult Urination:** Prostatitis can cause a burning or stinging sensation during urination. Some individuals may also experience pain or discomfort in the urethra (the tube that carries urine out of the body)[12].
3. **Frequent Urination:** People with prostatitis may feel the need to urinate more frequently than usual, often with only small amounts of urine being passed each time[14].  
Additionally, prostatitis can cause a sudden and urgent need to urinate, which may be difficult to control. Some individuals with prostatitis may feel like their bladder hasn't completely emptied after urination[2, 15].

4. Painful Ejaculation: Prostatitis can cause pain or discomfort during or after ejaculation. This symptom is especially common in cases of chronic prostatitis[16, 17]. Ultimately leading to sexual difficulties, including erectile dysfunction or decreased libido[18].

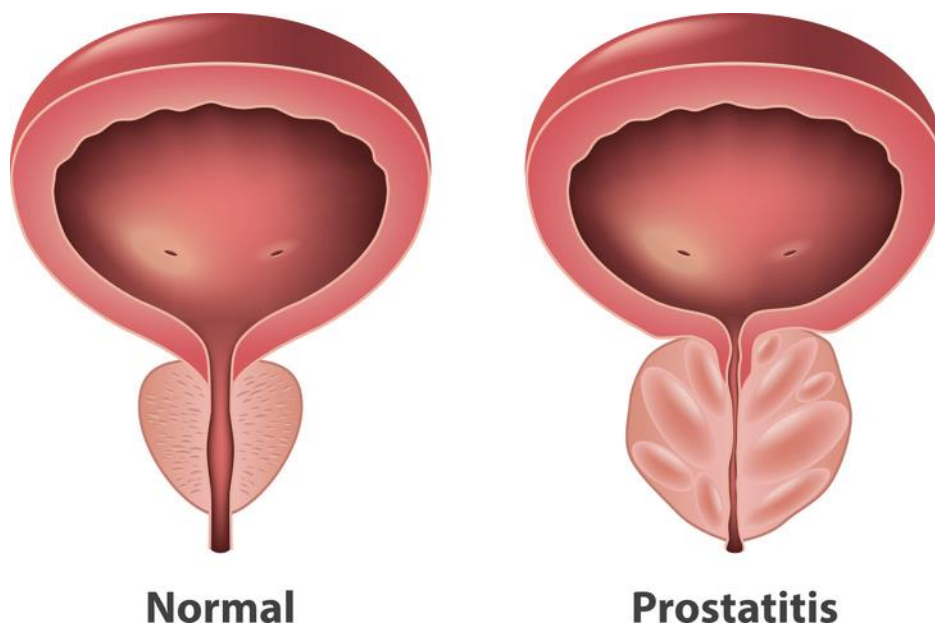


**Figure 2:** Simple diagram of a normal prostate (left) and inflamed prostate (right).

Additionally, prostatitis can be acute (sudden onset and severe) or chronic (long-lasting, with symptoms that come and go over an extended period). But wait, there's more! Along the aging journey, there's the possibility of encountering prostatitis, a condition where this little gland gets all riled up and inflamed. It's like having a grumbling stomach that just won't settle down. This inflammation can lead to discomfort and a constant urge to pee, making even the simplest activities a bit like sitting on a bed of prickly cacti.



Now, when it comes to prostatitis, there are different types, each with its own quirky personality.

1. Acute Bacterial Prostatitis: This type is caused by a bacterial infection in the prostate gland. It usually comes on suddenly and can cause symptoms like fever, chills, severe pain in the lower abdomen or back, and difficulty urinating. It's like a sudden storm hitting, causing immediate and intense discomfort[17-19].

2. Chronic Bacterial Prostatitis: Unlike the acute type, chronic bacterial prostatitis is a long-term condition where the prostate gland remains infected for a prolonged period. Symptoms might be less severe than acute bacterial prostatitis but can be persistent. It's like a lingering rain that doesn't go away completely[17-19].

3. Chronic Prostatitis/Chronic Pelvic Pain Syndrome (CP/CPSP): This is the most common type of prostatitis. It's characterized by long-term pelvic pain and discomfort without clear evidence of infection. The symptoms, which can include pain during urination, frequent urination, or pain in the genital area, can be challenging to manage. Think of it as a constant, low-level hum of discomfort in the background[17-19].

4. Asymptomatic Inflammatory Prostatitis: This type is called "asymptomatic" because it doesn't cause noticeable symptoms. Doctors might diagnose it when they find inflammation in the prostate through tests done for other reasons, even though the person doesn't feel any pain or discomfort. It's like having a quiet garden with hidden, unnoticed flowers[17-19].

## **Combining Benign Urological Research & Immunology**

In the realm of medical wonders, there's even a notion that the immune system, our body's defense army, might get a bit mixed up, attacking the prostate like an overenthusiastic guard dog barking at harmless visitors. This confusion can lead to inflammation, adding another layer to the prostatitis puzzle.

While prostatitis is not primarily classified as an autoimmune disease, some researchers have explored the possibility of autoimmune factors contributing to certain cases. Let's discuss this in a simplified manner.

Think of our immune system as a loyal guard dog, always on the lookout for intruders in our body. Normally, this guard dog does a fantastic job protecting us from harmful bacteria and viruses. However, in autoimmune diseases, this vigilant guard dog can get a bit confused. Instead of sniffing out real threats, it starts barking at innocent passersby, our healthy tissues and organs.

When it comes to prostatitis, it's like this guard dog in our immune system occasionally mistakes the prostate gland for a trespasser. It's as if the guard dog, despite no real danger, starts barking furiously at the castle walls (prostate gland), causing unnecessary chaos. This confusion triggers inflammation and discomfort, creating symptoms similar to other forms of prostatitis.

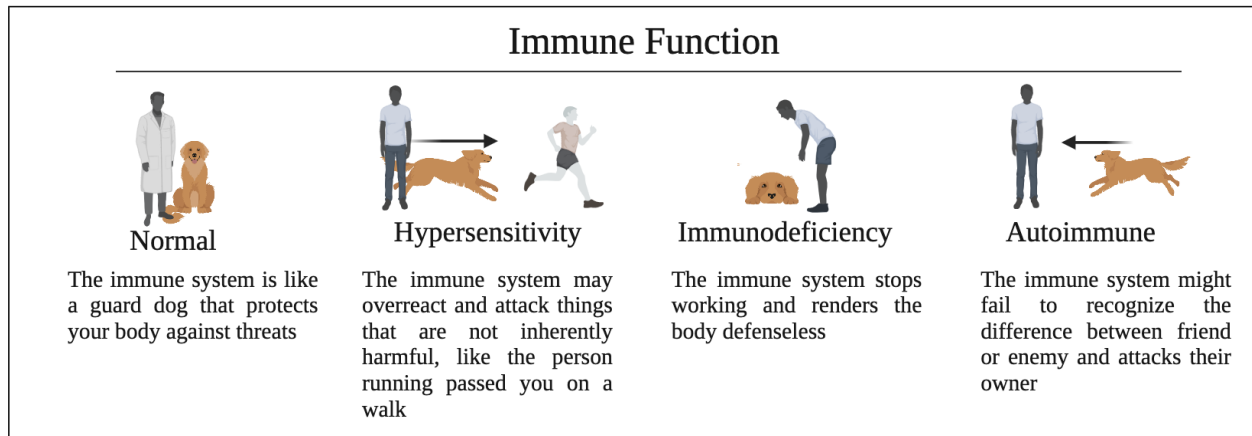


**Figure 3:** The immune system is vital for maintaining health, but abnormal responses can lead to diseases. These responses include hypersensitivity, where the immune system overreacts to harmless substances upon re-exposure, causing allergic reactions or even severe systemic conditions like anaphylaxis. Autoimmune disorders occur when the immune system mistakenly targets the body's own cells, often triggered by pathogens mimicking host markers. Diseases such as type I diabetes, rheumatoid arthritis, and multiple sclerosis result from this process. Additionally, immunodeficiency disorders compromise the immune system's ability to fight infections, whether due to inherited conditions like SCIDs, pathogenic origins like AIDS, or drug-induced suppression during transplant procedures. Immunosuppressive drugs are commonly utilized in transplants to prevent graft rejection.

In this autoimmune scenario, our loyal guard dog becomes a bit overzealous, mistakenly attacking the castle it's supposed to protect (**Figure 3**). While prostatitis isn't commonly linked to this guard dog's confusion, researchers suspect that in some cases, this mix-up might contribute to the inflammation and discomfort experienced by individuals. Understanding this canine mix-up helps us comprehend the complexities of autoimmune factors in prostatitis.

Translational models for experimental autoimmune prostatitis (EAP) provide researchers with invaluable tools to better understand the complexities of autoimmune diseases affecting the prostate gland. These models serve as bridges between basic laboratory research and potential clinical applications in humans. Here's a simplified explanation:

Imagine scientists as detectives trying to solve a mystery. In this case, the mystery is autoimmune prostatitis. To crack the case, they create translational models. Think of these models as laboratory simulations, similar to recreating a crime scene for analysis.

One common translational model involves using mice or rats. These animals are like stand-ins for humans in the lab. Researchers can manipulate their immune systems to mimic autoimmune responses seen in human prostatitis patients. It's akin to teaching these animals to display specific behaviors, helping scientists observe the disease's progression and understand its underlying mechanisms.

These translational models act as magnifying glasses for scientists, allowing them to zoom in on specific details of the disease. By studying these models, researchers can identify potential targets for treatments, test new therapies, and ultimately work toward solving the mystery of autoimmune prostatitis. While this work is complex and takes time, these models are essential tools, bringing us one step closer to effective treatments for this condition.

In the world of EAP modeling, specific prostate antigens play a crucial role in triggering the disease. Antigens are like unique nametags that the immune system recognizes. In EAP, these antigens come from the prostate gland, and the immune system, for some reason, starts attacking these "nametags" as if they were invaders.

Imagine the prostate antigens as puzzle pieces. Normally, these pieces fit perfectly into the immune system's puzzle, ensuring harmony in the body. However, in EAP, some of these pieces become misshapen or altered. It's like having a puzzle piece that doesn't quite fit anymore. The immune system, designed to protect the body, mistakenly identifies these altered pieces as foreign and dangerous.

When the immune system detects these "misfit" prostate antigens, it goes into attack mode, releasing an army of immune cells to neutralize the perceived threat. Unfortunately, instead of protecting the body, these immune cells start damaging the prostate tissue. This ongoing attack causes inflammation, pain, and discomfort, leading to the disease state characteristic of EAP.

To further simplify, it's like having a security system in a high-tech vault. Normally, the system recognizes authorized personnel (properly shaped antigens) and allows them access. But in EAP, the security system malfunctions. It starts flagging even the authorized personnel as intruders (misshapen antigens), leading to chaos and damage within the vault (prostate gland).

In the realm of experimental autoimmune prostatitis, scientists use these insights into specific prostate antigens and the immune response to create models. These models help researchers

study the disease's progression, test potential treatments, and ultimately find ways to correct the immune system's confusion. By understanding the role of these antigens, scientists can develop targeted therapies aimed at restoring the balance and stopping the immune system from attacking the prostate, offering hope for effective treatments in the future.

### **Animal Models Used to Study EAP:**

Let's delve deeper into how the immune response and specific prostate antigens are studied in translational models of EAP.

1. **Model Development:** Researchers typically start by inducing EAP in animal models, often mice or rats. They accomplish this by exposing the animals to prostate-specific antigens, such as prostate proteins or peptides, in a way that mimics the body's immune response[20]. These antigens can be modified to resemble the altered or misshapen antigens found in human prostatitis. By injecting these antigens, scientists essentially provide the immune system of these animals with a "target" to react against[3].
2. **Immune Response Observation:** Once the animals are exposed to these prostate antigens, scientists closely monitor their immune responses. They study how immune cells, especially T cells, respond to these antigens. T cells are like soldiers in the immune system, and in EAP, they play a central role in attacking the prostate tissue[11, 21-23]. By examining the behavior and interactions of these cells,

- researchers gain valuable insights into how the immune system reacts to specific prostate antigens, leading to inflammation and disease.
3. **Inflammatory Processes:** Translational models allow scientists to observe the inflammatory processes triggered by the immune response. Inflammation, characterized by the influx of immune cells and various signaling molecules, damages the prostate tissue and contributes to the disease state. Researchers can study these processes in detail, pinpointing the pathways and molecules involved. This knowledge is essential for developing targeted therapies that can interrupt these processes and reduce inflammation[2, 20, 24, 25].
  4. **Testing Therapies:** Using these models, scientists can test potential therapies. For example, they might introduce medications or immunotherapies to see if they can modulate the immune response. By observing how these treatments affect the disease progression, researchers can identify promising approaches to managing EAP. These therapies could include immunomodulatory drugs, antibodies, or even gene therapies designed to regulate the immune response[10, 26-28].
  5. **Genetic and Molecular Studies:** Translational models also facilitate genetic and molecular studies. Researchers can manipulate specific genes related to the immune system or antigens to understand their impact on EAP development. Molecular studies allow scientists to analyze the intricate biochemical reactions occurring within

immune cells when exposed to prostate antigens[2, 3, 10, 11, 20, 22, 24, 27, 29-31].

This detailed understanding informs the development of highly targeted treatments.

Translational models in EAP research provide a controlled environment to explore the immune response to specific prostate antigens. By studying the immune reactions, inflammatory processes, and testing various therapies, scientists gain critical insights. These insights pave the way for the development of precise treatments, moving us closer to effectively managing autoimmune prostatitis in humans.

### **Current Trends in Treating EAP**

In the context of immunization and autoimmune conditions like EAP, immunomodulatory drugs and adjuvants play vital roles:

#### **1. Immunomodulatory Drugs**

Immunomodulatory drugs are medications designed to regulate the immune system, either by enhancing or suppressing its activity. In autoimmune conditions like EAP, where the immune system mistakenly attacks the body's own tissues, these drugs help restore balance and prevent excessive immune responses. Here are some common types:

#### **2. Anti-Inflammatory Drugs**



These drugs, like nonsteroidal anti-inflammatory drugs (NSAIDs) or corticosteroids, reduce inflammation by blocking specific molecules in the inflammatory process. By doing so, they alleviate symptoms associated with EAP, such as pain and swelling.

### 3. Immunosuppressive Agents

Medications such as corticosteroids or certain chemotherapy drugs suppress the immune system's activity. In EAP, these drugs help dampen the immune response against prostate antigens, reducing damage to the prostate tissue. However, their use requires careful monitoring due to their impact on overall immunity.

### 4. Biological Therapies

These therapies, including monoclonal antibodies, target specific immune system molecules or cells involved in the autoimmune response. By precisely blocking these targets, biological therapies modulate the immune system, preventing it from attacking the prostate tissue excessively. They are often used in severe or refractory cases of autoimmune diseases.

## References

1. Welliver, C., et al., *Evolution of healthcare costs for lower urinary tract symptoms associated with benign prostatic hyperplasia*. *Int Urol Nephrol*, 2022. **54**(11): p. 2797-2803.
2. Mehta, V. and C.M. Vezina, *Potential protective mechanisms of aryl hydrocarbon receptor (AHR) signaling in benign prostatic hyperplasia*. *Differentiation*, 2011. **82**(4-5): p. 211-9.
3. Vezina, C.M., T.M. Lin, and R.E. Peterson, *AHR signaling in prostate growth, morphogenesis, and disease*. *Biochem Pharmacol*, 2009. **77**(4): p. 566-76.
4. Wegner, K.A., et al., *Void spot assay procedural optimization and software for rapid and objective quantification of rodent voiding function, including overlapping urine spots*. *Am J Physiol Renal Physiol*, 2018. **315**(4): p. F1067-f1080.
5. Ittmann, M., *Anatomy and Histology of the Human and Murine Prostate*. Cold Spring Harb Perspect Med, 2018. **8**(5).
6. Liu, Y., et al., *Chronic prostatitis/chronic pelvic pain syndrome and prostate cancer: study of immune cells and cytokines*. *Fundam Clin Pharmacol*, 2020. **34**(2): p. 160-172.
7. Wang, H.H., et al., *Characterization of autoimmune inflammation induced prostate stem cell expansion*. *Prostate*, 2015. **75**(14): p. 1620-31.
8. Zhang, L., et al., *Establishment of experimental autoimmune prostatitis model by T(2) peptide in aluminium hydroxide adjuvant*. *Andrologia*, 2018. **50**(3).

9. Zhang, Y., et al., *Influence of Experimental Autoimmune Prostatitis on Sexual Function and the Anti-inflammatory Efficacy of Celecoxib in a Rat Model*. *Front Immunol*, 2020. **11**: p. 574212.
10. Magistro, G., C.G. Stief, and F.M.E. Wagenlehner, [*Chronic prostatitis/chronic pelvic pain syndrome*]. *Urologe A*, 2020. **59**(6): p. 739-748.
11. Manuel, R.S.J. and Y. Liang, *Sexual dimorphism in immunometabolism and autoimmunity: Impact on personalized medicine*. *Autoimmun Rev*, 2021. **20**(4): p. 102775.
12. Yamaguchi, H., et al., [*Experimental rodent models of chronic prostatitis: effect of phosphodiesterase 5 inhibitor on chronic pelvic-pain-related behavior*]. *Nihon Yakurigaku Zasshi*, 2019. **154**(5): p. 259-264.
13. Liu, Y., et al., *Experimental autoimmune prostatitis: different antigens induction and antigen-specific therapy*. *Int Urol Nephrol*, 2021. **53**(4): p. 607-618.
14. Matsukawa, Y., et al., *Clinical features and urodynamic findings in elderly men with chronic prostatitis*. *Int J Urol*, 2022. **29**(5): p. 441-445.
15. Chen, L., M. Zhang, and C. Liang, *Chronic Prostatitis and Pelvic Pain Syndrome: Another Autoimmune Disease?* *Arch Immunol Ther Exp (Warsz)*, 2021. **69**(1): p. 24.
16. Magistro, G., et al., *Contemporary Management of Chronic Prostatitis/Chronic Pelvic Pain Syndrome*. *Eur Urol*, 2016. **69**(2): p. 286-97.
17. Stamatiou, K., E. Samara, and G. Perletti, *Sexuality, Sexual Orientation and Chronic Prostatitis*. *J Sex Marital Ther*, 2021. **47**(3): p. 281-284.
18. Ludwig, M., et al., *Immunocytological analysis of leukocyte subpopulations in urine specimens before and after prostatic massage*. *Eur Urol*, 2001. **39**(3): p. 277-82.

19. Altuntas, C.Z., et al., *A novel murine model of chronic prostatitis/chronic pelvic pain syndrome (CP/CPPS) induced by immunization with a spermine binding protein (p25) peptide*. *Am J Physiol Regul Integr Comp Physiol*, 2013. **304**(6): p. R415-22.
20. Jackson, C.M., et al., *Strain-specific induction of experimental autoimmune prostatitis (EAP) in mice*. *Prostate*, 2013. **73**(6): p. 651-6.
21. Breser, M.L., et al., *Regulatory T cells control strain specific resistance to Experimental Autoimmune Prostatitis*. *Sci Rep*, 2016. **6**: p. 33097.
22. Schaeffer, E.M., *Re: IL17 Mediates Pelvic Pain in Experimental Autoimmune Prostatitis (EAP)*. *J Urol*, 2016. **196**(3): p. 958-9.
23. Zhou, X.H., et al., *Increased inflammatory factors activity in model rats with experimental autoimmune prostatitis*. *Arch Androl*, 2007. **53**(2): p. 49-52.
24. Diserio, G.P. and E. Nowotny, *Experimental autoimmune prostatitis: dihydrotestosterone influence over the immune response*. *J Urol*, 2003. **170**(6 Pt 1): p. 2486-9.
25. Motrich, R.D., et al., *Autoimmune prostatitis: state of the art*. *Scand J Immunol*, 2007. **66**(2-3): p. 217-27.
26. Penna, G., et al., *Treatment of experimental autoimmune prostatitis in nonobese diabetic mice by the vitamin D receptor agonist elocalcitol*. *J Immunol*, 2006. **177**(12): p. 8504-11.
27. Quick, M.L., et al., *CCL2 and CCL3 are essential mediators of pelvic pain in experimental autoimmune prostatitis*. *Am J Physiol Regul Integr Comp Physiol*, 2012. **303**(6): p. R580-9.
28. Roman, K., et al., *Tryptase-PAR2 axis in experimental autoimmune prostatitis, a model for chronic pelvic pain syndrome*. *Pain*, 2014. **155**(7): p. 1328-1338.

29. Liu, K.J., et al., *Identification of rat prostatic steroid-binding protein as a target antigen of experimental autoimmune prostatitis: implications for prostate cancer therapy*. *J Immunol*, 1997. **159**(1): p. 472-80.
30. Wong, L., et al., *Experimental autoimmune prostatitis induces microglial activation in the spinal cord*. *Prostate*, 2015. **75**(1): p. 50-9.
31. Yang, J., et al., *Prostate-derived IL-3 " w r t g i w n c v g u " g z r t g u u k q p " q h paraventricular nucleus and shortens ejaculation latency in rats with experimental autoimmune prostatitis*. *Asian J Androl*, 2022. **24**(2): p. 213-218.

## Chapter 2

### **Trends In Experimental Autoimmune Prostatitis: Insights into Pathogenesis, Therapeutic Strategies, And Redefinition.**

Am J Clin Exp Urology 2024 *In Press*  
**Manuel, Robbie SJ**, and Chad Vezina

## **Trends in Experimental Autoimmune Prostatitis: Insights into Pathogenesis, Therapeutic Strategies, and Redefinition**

Robbie SJ Manuel<sup>1,2,3</sup>, and Chad Vezina<sup>1,2,3\*</sup>

<sup>1</sup> *Department of Comparative Biosciences, University of Wisconsin-Madison, Madison, WI, USA;*

<sup>2</sup> *Molecular & Environmental Toxicology, University of Wisconsin-Madison, School of Medicine & Public Health, Madison, WI, USA;*

<sup>3</sup> *Endocrinology and Reproductive Physiology, University of Wisconsin-Madison, School of Medicine & Public Health, Madison, WI, USA*

### **Acknowledgements**

We thank Brandon Scharpf, Marcela Ambrogi, Thomas Peterson, Jaskiran Sandhu, Simran Sandhu, and Sneha Chandrashekar for technical assistance. Funded by National Institutes of Health grants R01 ES001332, T32 ES007015 and U54 DK104310. The content is solely the responsibility of the authors and does not necessarily represent the official views of the National Institutes of Health. This work does not represent the views of the Department of Veterans Affairs or the United States Government

**Abstract:** Chronic prostatitis/chronic pelvic pain syndrome (CP/CPSS) is a debilitating condition characterized by prostate inflammation, pain and urinary symptoms. The immune system's response to self-antigens is a contributing factor to CP/CPSS. In this review, we examine the use of experimental autoimmune prostatitis (EAP) in rodents to model salient features of autoimmune mediated CP/CPSS. By exploring etiological factors, immunological mechanisms, and emerging therapeutic strategies, our aim is to enhance our understanding of CP/CPSS pathogenesis and promote the development of strategies to test innovative interventions using the EAP pre-clinical model.

### **Introduction:**

Prostatitis, or inflammation of the prostate gland, is a common urological condition in men. Prostatitis is responsible for nearly 2 million physician visits per year and \$84 million in associated health care expenses [32]. Prostatitis is classified as type I (acute bacterial prostatitis); type II (chronic bacterial prostatitis), type III (chronic prostatitis / chronic pelvic pain syndrome, CP/CPSS), or type IV (asymptomatic inflammatory prostatitis) [33].

CP/CPSS, the most common prostatitis form, is characterized by persistent pelvic and perineal discomfort, and may include difficult and/or painful urination and ejaculatory pain [1, 16, 17]. The medical expenses for CP/CPSS are comparable to that of peripheral neuropathy, back pain,



fibromyalgia, and rheumatoid arthritis [17]. Medical expenses associated with CP/CPSS increases with symptom severity [32]. Many men experiencing CP/CPSS also incur additional costs through work absenteeism and reduced productivity. Although antibiotics, alpha adrenoreceptor antagonists, biofeedback and dietary modifications are sometimes prescribed for CP/CPSS, no therapies are particularly effective.

The onset, progression, severity, and duration of CP/CPSS are influenced by an array of factors [16, 17, 32-34], and new research is needed to understand disease etiology and identify effective therapies. CP/CPSS is more common in middle-aged and older men than in younger men, and men over age 50 are at the highest risk [12]. A variety of potential CP/CPSS mechanisms have been examined, including infection, autoimmunity, compromised urothelial integrity and function, as well as psychosocial factors [16].

Autoimmune diseases are characterized by immune system activation against self-antigens, resulting in tissue damage and dysfunction [13]. While CP/CPSS was previously thought to be a non-inflammatory disorder, recent studies have revealed evidence of autoimmune dysregulation in this condition [1, 2, 16]. Abundance of autoantibodies against prostatic proteins is elevated in sera from many CP/CPSS patients [35]. T cells from patients with CP/CPSS exhibited increased reactivity to prostatic antigens [1, 36]. Like most autoimmune diseases, more than one autoantigen is implicated [13].

One approach for studying mechanisms and efficacy of pre-clinical treatment strategies for autoimmune mediated CP/CPSS is the rodent model of experimental autoimmune prostatitis

(EAP). EAP has been induced in rodents to test efficacy of potential therapeutics including anti-inflammatory agents, such as non-steroidal anti-inflammatory drugs (NSAIDs), corticosteroids, immunomodulatory agents (such as cyclosporine A and mycophenolate mofetil) [11, 37], herbal remedies and natural compounds [38].

EAP is initiated by immunizing rodents with prostate antigens and adjuvants [16, 35, 39]. The EAP phenotype in rodents resembles that of human CP/CPPS, and can include pro-inflammatory cytokine production, leukocyte infiltration, T-cell activation, chronic inflammation, fibrosis, and glandular atrophy [1, 2]. Factors that contribute to inflammation in rodents with EAP are summarized in **Table 1**. EAP in rodents is a progressive and chronic condition. Histological inflammation appears 5-10 days post-immunization and the timing depends on the species/strain of the host animal and the immunization strategy [1, 2, 39, 40]. Physiological phenotypes observed in rodents subjected to EAP encompass pelvic pain, quantified through Von Frey filament testing—a widely employed measure of tactile/mechanical allodynia in pain assessment utilizing animal models. Additionally, assessments reveal the presence of voiding dysfunction and sexual dysfunction, contributing to a comprehensive understanding of the physiological ramifications associated with EAP induction [11, 16, 39]. Pelvic pain appears 5 days post immunization and persists for more than 30 days as a chronic condition [39]. Histological inflammation is correlated with pain in rodents with EAP and both intensify over time [1, 20, 25, 39].

**Table 1. Summary of immunological mechanisms in EAP**

<b>Contributing factor to EAP</b>	<b>Description</b>	<b>Reference</b>
Autoantigens and T Cell Response	Self-antigens from the prostate gland are perceived as foreign, triggering an immune response. Autoantigens, including prostate-specific antigens such as prostate-specific antigen (PSA) and prostatic acid phosphatase (PAP), are presented to T cells by antigen-presenting cells (APCs) and activate and expand CD4+ T cells, to drive an immune response.	[27, 35, 39, 41-43]
Inflammatory Mediators and Cytokines	Activation of autoantigen-specific T cells leads to production of pro-inflammatory cytokines, such as interleukin-17 (IL-17), interferon (IFN)-gamma ( $-\gamma$ ), and tumor necrosis factor (TNF)-alpha ( $-\alpha$ ). These cytokines facilitate recruitment of neutrophils, macrophages, and dendritic cells into the prostate gland. Additionally, cytokines promote tissue inflammation, amplify immune responses, and contribute to the development of chronic inflammation.	[21, 25, 35, 41, 44]
Autoantibody Production	B cell activation in response to autoantigens stimulates autoantibody production, including anti-prostate antibodies. Autoantibodies may contribute to tissue damage and inflammation by forming immune	[26, 45-49]

---

complexes, activating complement cascades, and  
engaging Fc receptors on immune cells.

---

### **Experimental Models of EAP:**

Two general approaches are used to induce chronic prostatitis in rodents:

1. Immunize rodents with extracts from all male rodent accessory sex glands, extracts specifically from rodent prostate gland, or natural or synthetic proteins selectively expressed by the rodent prostate to drive autoimmunity against the prostate gland.
2. Adoptively transfer activated immune cells such as T cells, trained against antigens in the prostate, into mice expressing those antigens in the prostate [2, 24, 45].

Immunization protocols for inducing EAP differ among research groups and these differences can influence the penetrance, onset, and severity of prostate inflammation. The most notable difference in EAP protocols is the rodent strain and species from which prostate antigens are collected and the strain and species into which antigens are introduced, and these include rats (Sprague Dawley (SD), Wistar, Copenhagen, Lewis) and mice (C57BL/6, and non-obese diabetic (NOD) (summarized in **Table 2**) [3, 9, 45].

**Table 2. Immunogens used to induce EAP in mice.**

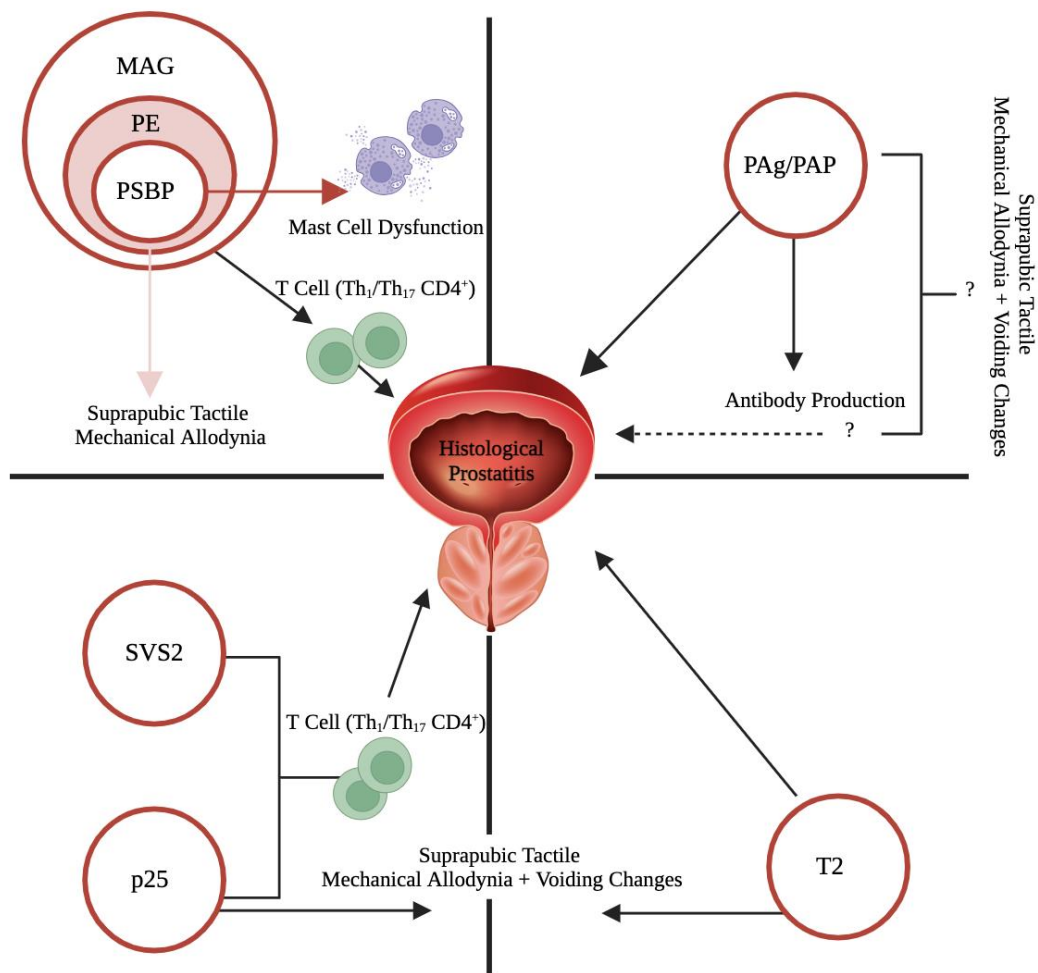
<b>Antigen</b>	<b>Mouse Strain</b>	<b>Age (wks)</b>	<b>Immunization Schedule</b>	<b>Antigen Dose per Immunization</b>	<b>Success Rate* (%)</b>	<b>Reference</b>
PE	AJ	6-8	30 days: 1 x D0	375 mg	100	[50]
PE	C57BL/6J	6-8	30 days: 1 x D0	250 mg	100	[50]
SVS2	C57BL/6J	25	42 days: 3 x D0, D14, D28	200 mg	71.4	[45]
T2	C57BL/6J	6-8	35 days: 3 x D0, D14, D28	9 mg	100	[19]
PE	NOD	6	21 days: 2 x D0, D15	1 mg	100	[47]
PSBP	NOD	6	21days: 2 x D0, D15	30 mg	80	[47]
MAG <sup>\</sup>	NOD(H2 <sup>g7</sup> )	6	10 days: 1 x D0	1 mg	100	[51]
PE	SJL/J	6-8	30 days: 1 x D0	1 mg	100	[50]
p25	SWXJ(H-2 <sup>q.s</sup> )	8	63 days: 1 x D0	200 mg	100	[20]
MAG <sup>\</sup>	NOD(H2 <sup>g7</sup> )	6	21 days: 2 x D0, D15	1 mg	37.5	[51]

<sup>\</sup>MAG antigen derived from rat

\*Percentage of animals that develop histological inflammation

Some researchers drive EAP using pooled male accessory gland extracts (MAG) that include seminal vesicles, prostate (anterior, dorsolateral, and ventral lobes), bulbourethral glands, ampullary glands, urethral glands, and preputial glands [8, 24, 46, 51].

The most widely used method to drive EAP in rodents is to immunize with prostate extracts/antigens (PAgs) pooled from the dorsolateral, anterior, and ventral prostate lobes of non-syngeneic rodents [1, 2, 40, 50]. PAg-specific lymphocytes have been identified in CP/CPPS patients [21, 25]. Intravenous PAg immunization induces a cytotoxic T-Cell (CTL) response and subsequent autoimmune prostatitis which is confined to the prostate [2]. Immunogenic peptides derived from prostatic acid phosphatase (PAP) stimulate CD4<sup>+</sup> T lymphocytes [2, 16, 20, 21]. The use of PAgs to induce EAP is specifically suited to study the adverse impact of prostatitis on fertility and mental health [11, 25] (**Figure 1**).



Other researchers drive EAP using isolated prostatic proteins from non-syngeneic hosts. Many autoantigens induce histological inflammation of the rodent prostate; however, only p25- and T2 also drive pelvic pain and urinary voiding dysfunction [2, 20, 45]. p25, a protein selectively expressed in prostate and which functions as a major mouse prostatic secretory glycoprotein, has been used to induce EAP with a phenotype that mimics the clinical presentation in humans and includes histological prostatitis, pelvic pain, and changes in voiding behavior associated with CP/CPPS [2, 20]. Rats immunized with p25 peptide exhibit urinary dysfunction, increased relative prostate weights, and heightened proinflammatory cytokines, all subsequently

ameliorated by p25-specific CD4<sup>+</sup> T cells provoking a Th1 response [20]. Remarkably, the bladder remains unaffected upon histological examination, suggesting prostate-specific pathology.

Synthetic prostatic steroid-binding proteins (PSBP) have been used to induce EAP and promote cellular- and humoral-specific autoimmune responses [29, 47, 52]. PSBP, a tetrameric protein composed of two distinct subunits, showcases a unique arrangement—the first subunit harbors C1 and C3 polypeptides, while the second subunit harbors C2 and C3 polypeptides [47]. The transcript encoding the PSBP-C1 peptide is selectively expressed in ventral prostate and not dorsal prostate, bladder or kidney[53]. Leveraging this insight, peptides corresponding to the PSBP-C1 subunit were synthesized and used to immunize mice. PSBP-C1 peptides initiate cellular and humoral autoimmune responses. PSBP-C1 peptide initiates substantial T and B cell responses in nonobese diabetic (NOD) mice, coinciding with significant lymphomononuclear cell infiltration of the prostate [2, 29, 47]. Notably, histopathological changes are observed by day 8 post-immunization, including the appearance of CD4<sup>+</sup> T cells, and ablation of CD4<sup>+</sup> T-cells confers resistance of PSBP-C1 induced prostatitis [47, 54]. The focal point of inflammation from PSBP-C1 induced prostate inflammation is in the ventral lobe, aligning with ventral prostate selective expression of PSBP. Noteworthy is the dominance of mast cells among inflammatory cells, accompanied by lymphocytes, monocytes/macrophages, histiocytes, and neutrophils contributing to epithelial atrophy [54]. Abundance of systemic inflammatory mediators IFN- $\gamma$  and IL-12 is elevated in mice with PSBP induced EAP while abundance of IL-10 is reduced. PSBP's tetrameric nature and histopathological differences from human CP/CPPS have led to the



adoption of immunogenic PSBP peptides. Limitations of PSBP as a driver of EAP include peptide cost and inconsistency of antigen presentation [1].

SVS2 and semenogelin are CP/CPPS autoantigens in mice and humans, respectively [45]. SVS2 and semenogelin derive from the seminal vesicle and not the prostate [2], and their function is to regulate seminal fluid viscosity [45]. SVS2 is implicated in spontaneous prostatitis. SVS2 expression is dependent on the autoimmune regulator (*Aire*) gene [45]. Genetic deletion of *Aire* results in multi-organ autoimmune reactivity in the eye, salivary glands, ovaries, stomach, and prostate [45, 55-58]. SVS2 reactive antibodies were detected in sera of *Aire* null mice. Wild-type mice immunized with SVS2 and *Aire*-deficient mice develop EAP [2, 45].

Despite the usefulness of the EAP model, there are some limitations that should be considered. One limitation is that the induction of EAP is highly dependent on the antigen used for immunization, and each antigen may lead to unique pathological and physiological EAP phenotypes (**Table 2**) [2, 11, 16]. Another limitation of the EAP model is that it does not fully reflect the complexity of human CP/CPPS, which involves multiple factors, such as infection, stress, and neuropathic pain [1, 2].

Haverkamp and colleagues used a unique, immunization-free approach to drive prostate inflammation in the POET-3 mouse. They collected splenocytes from Thy1.1+OT-I mice, which harbor a transgenic T cell receptor that recognizes ovalbumin. They applied ovalbumin to the splenocytes *in vitro*, and the resulting MHC class I-restricted, ovalbumin-specific, CD8<sup>+</sup> T cells were transferred into mice expressing the ovalbumin transgene in prostate luminal epithelial cells

(POET-3 and POET-3/*Luc/Pten*<sup>-/+</sup> mice) to induce prostatitis in the anterior, dorsolateral, and anterior prostate regions [59]. POET-3 mice demonstrate robust recruitment of CD4<sup>+</sup>, CD8<sup>+</sup> T-cells, and CD4<sup>+</sup>FOXP3<sup>+</sup> T-regulatory cells, elevated cytokine/chemokine expression, and sustained prostate epithelial proliferation [9, 59].

Fundamental challenges for translational urological research are the identification and appropriate use of animals to model salient features of human disease. There is significant debate over whether animal can accurately replicate human disease [60]. Some argue, and with support from the literature, that animal models are not always predictive of human outcomes and may lead to false conclusions [61]. A major problem with animal models in benign urologic research is that the models and endpoints are not standardized (for example, see the variable methods for immunization of EAP mice in **Table 1**). There is a great need for strategy homogeneity within the field to improve reproducibility and comparability between studies [2, 11, 14, 20]. Also, addressing the differences between animal and human physiology regarding disease presentation is needed to develop and achieve clinically relevant endpoints.

While whole animal models of prostatitis capture the complex interplay between prostate tissues and the immune system, alternative methods can be used to study select aspects of prostatitis:

1. *In vitro* cell culture: Primary prostate epithelial cells are stimulated with human recombinant tryptase-P/TPSB2 and co-cultured with leukocytes to examine paracrine signaling mechanisms involved in prostate inflammation. Cell based models provide a

controlled environment for studying cell-cell interactions and molecular mechanisms [28].

2. *Ex vivo* tissue explants: Human or rodent prostates are harvested and maintained in culture to study the effects of immunological stimuli or therapeutic agents [62].
3. Human tissues: Prostatic tissues from patients with CP/CPSS are analyzed to identify histological features of the disease and biomarkers of disease severity [25].
4. Computational modeling: Baker's research uses computational models to predict regulatory mechanisms of CD4<sup>+</sup> T cell functions and examine intersections between immunity and metabolism [63]. Lorenzo and colleagues modeled prostate cancer growth, an approach that could be applied to prostate hyperplastic responses to inflammation [64].

### **Current therapies for CP/CPSS**

In urological research, managing CP/CPSS presents a substantial challenge. The UPOINTS system (**Table 3**) provides a nuanced approach, considering urinary, psychosocial, organ-specific, infection, neurologic, tenderness, and sexual dysfunction factors [12, 34]. A major obstacle arises from the absence of detectable bacteria in urine, discouraging inappropriate antimicrobial therapy in favor of judicious antibiotic use [34].

**Table 3. UPOINT CP/CPPS Diagnosis and Treatment Therapies with UPOINT System****Description**

<b>UPOINT Domain</b>	<b>Clinical Presentation</b>	<b>Treatment</b>
Urinary	LUT Syndrome	Alpha Blockers
		5-Alpha-reductase inhibitors (5-ARIs)
Psychological	Depression	5-serotonin and
	Stress	norepinephrine reuptake inhibitor
Organ-Specific	Targeted palpations	Pollen Extract
	exacerbate symptoms	Eviprostat
Infection	Recurrent UTIs	Antibiotics
	Bacterial localization	Acupuncture
		Pregabalin Botulinum Toxin-A
Sexual Dysfunction	Erectile Dysfunction	Phosphodiesterase inhibitors
Tenderness	Fibromyalgia	Prostatic massage
	Tenderness	Transrectal radiofrequency
	Spasm of perineum	Hyperthermia
		Low-intensity shockwave therapy (LiST)

---

\*Adopted and revised from [12, 34]

Addressing urinary symptoms, conventional alpha-blocker treatments have shown limited improvement in prostatitis symptoms, with notable risks of adverse events like dizziness and hypotension[10]. Similarly, 5-alpha-reductase inhibitors exhibit a modest trend toward symptom relief, especially in cases concurrent with benign prostatic hyperplasia [12, 17, 34].

Psychosocial factors significantly contribute to CP/CPPS, correlating with psychiatric symptoms like depression, affecting symptom severity and quality of life [65]. Selective serotonin and norepinephrine reuptake inhibitors, such as duloxetine, effectively alleviate CP/CPPS-associated pain with favorable side effects [65-67].

Organ-specific symptom treatments like pollen extract (cernilton) and eviprostat offer relief without adverse effects [68]. In cases without bacterial prostatitis, the efficacy of antimicrobial therapy, especially combined with alpha-blockers, remains uncertain due to inconsistent outcomes [68].

Neurologic manifestations involve abdominal or pelvic pain, alleviated by treatments like acupuncture and low-intensity shockwave therapy, though long-term efficacy of low-intensity shockwave therapy remains inconclusive [38].

Painfulness in the perineum or pelvic floor requires specialized approaches such as prostatic massage (contraindicated in acute bacterial prostatitis) and transrectal radiofrequency hyperthermia showing promise in improving pain and quality of life [38].

Addressing sexual dysfunction, phosphodiesterase inhibitors like tadalafil effectively improve CP/CPPS symptoms, especially pain and polyuria [14, 69]. Traditional Chinese medicine combined with Western interventions, like alpha-blockers and phosphodiesterase inhibitors, offers a holistic approach [70, 71].

However, limitations exist in current studies due to variability in patient populations, study designs, and cultural contexts, necessitating further research to refine CP/CPPS therapeutic strategies. Recent trials challenge the efficacy of alfuzosin, an alpha-adrenergic blocker, highlighting the need for rigorous exploration of novel treatments to enhance the quality of life for CP/CPPS patients [72, 73].

Effective CP/CPPS therapies remain elusive, given the array of symptoms and multifaceted disease causes. The UPOINTS system guides treatment strategies based on symptoms and causes, employing medications like antibacterial agents, anti-inflammatory drugs, analgesics, and those for benign prostatic hyperplasia (**Table 3**). Tailored adjustments are necessary based on individual responses, often requiring a multimodal approach [1, 12, 17, 38, 67, 72]. Alpha adrenoreceptor antagonists, including tamsulosin and alfuzosin, show promise in alleviating CP/CPPS symptoms, although ongoing debate surrounds the efficacy of antibiotics and anti-inflammatory agents.

## **Emerging Therapeutic Targets for CP/CPSS**

Researchers are increasingly channeling efforts into the exploration of targeted therapies, including immunomodulatory agents and innovative drug delivery systems, to identify more efficacious remedies for CP/CPSS [33, 74]. These endeavors harbor the potential to elevate the quality of life for individuals grappling with this enigmatic condition, offering promise for future CP/CPSS therapy.

Recognizing autoimmunity as a mechanism for CP/CPSS has implications for treatment and management approaches. While conventional anti-inflammatory drugs are typically employed for inflammatory disorders, autoimmune diseases necessitate immunomodulatory therapies that specifically target the underlying autoimmune dysregulation. Adopting this new perspective could potentially pave the way for the development of more targeted and efficacious treatments for CP/CPSS. One strategy for CP/CPSS researchers is to co-opt therapeutic targets already identified in extra-prostatic autoimmune diseases [34]. One example is the aryl hydrocarbon receptor (AHR), a transcription factor activated by a variety of endogenous and exogenous chemical and which functions as a potent immunosuppressor [75-79]. AHR regulated genes vary by cell type and context, but many participate in immune function, inflammation, and xenobiotic metabolism [75, 76]. In the context of autoimmune disease, AHR activation has been shown to have anti-inflammatory effects by promoting the differentiation of regulatory T cells and inhibiting the differentiation of pro-inflammatory Th17 cells [79]. Genetic loss of AHR signaling exacerbates inflammation in a mouse model of colitis [77, 80, 81]. The AHR signaling pathway

has been experimentally manipulated with a variety of agonists, antagonists, and dietary constituents and below we focus on AHR ligands used in a preclinical setting to treat autoimmune disorders, acknowledging their broader relevance beyond the confines of prostatic pathophysiology.

The AHR agonist 2-(1'H-indole-3'-carbonyl)-thiazole-4-carboxylic acid methyl ester (ITE) reduces colitis [77]. ITE also impedes differentiation of Th17 T cells [75, 82] and suppresses production of pro-inflammatory cytokines such as IL-17 and IFN-gamma [76, 77].

The AHR agonist 6-formylindolo(3,2-b) carbazole (FICZ) has been assessed for its potential in treating irritable bowel disease [78, 79]. FICZ activates the AHR pathway and the tristetraprolin pathway to reduce cytokine abundance and inflammation in mice treated with dextran sulfate sodium to drive colitis [76, 79, 80, 82, 83].

The naturally occurring AHR agonist 3,3'-diindolylmethane (DIM) has demonstrated therapeutic promise within the experimental autoimmune encephalomyelitis (EAE) model, a relevant representation of multiple sclerosis [84, 85]. Administration of DIM post-EAE induction reduces inflammation and curtails cellular infiltration in the central nervous system [84]. DIM functions by remodeling the miRNA profile (miR-200c, miR-146a, miR-16, miR-93, and miR-22) in brain CD4<sup>+</sup> T cells, influencing cell cycle regulation and promoting apoptosis-related pathways [84].

Indole-3-carbinol (I3C), a compound derived from plants, is an AHR agonist that has been shown to curtail colonic inflammation and rectify microbial dysbiosis in intestinal inflammatory



disease [75, 79]. I3C induces proliferation of beneficial gram-positive bacteria that produce butyrate, a potent anti-inflammatory agent. I3C has been shown to increase abundance of IL-22 and modulate gut microbiota to mitigate colitis [75].

Despite promising potential for treating autoimmune disease, the use of AHR modulation as a therapeutic strategy for lower urinary tract diseases is not without challenges. One major limitation is the potential for off-target effects, as AHR is known to regulate a broad range of physiological processes beyond the immune system and tissue repair. Additionally, the lack of specific AHR agonists or antagonists with high affinity and selectivity presents a major hurdle in developing effective AHR-targeted therapies. Nonetheless, the potential benefits of AHR modulation for the effective treatment of lower urinary tract diseases warrant further investigation.

Toll-like receptor 4 (TLR4) signaling, which plays a major role in the immune response to gram-negative bacteria [86-89], is also a potential target in CP/CPSS. TLR4 signaling is activated by pathogen-associated molecular patterns (PAMPs) such as bacterial lipopolysaccharide (LPS) [87, 88] and has been linked to hyperactive immune responses, sepsis, acute lung injury, and chronic inflammation [87-90]. Genetic ablation of microRNA-155 (miR-155) was recently shown to reduce TLR4 signaling [86]. MiR-155 deficient mice are resistant to EAP-mediated pelvic tactile hypersensitivity and exhibit diminished TLR4/nuclear factor-kappa B (NF- $\kappa$ B) responses to EAP [86]. In contrast, mice that overexpress miR-155 are hypersensitive to EAP-induced prostatic inflammation and oxidative stress [86, 91].

Cyclooxygenase-(COX)-1 and -2 have been implicated in autoimmune disease and COX-2-selective inhibitors such as celecoxib are effective anti-inflammatory agents [92]. A recent study showed that celecoxib reduces depressive behaviors and increases sexual drive and improves erectile function in mice with EAP [11]. Celecoxib also reduced prostate inflammation and serum IL-1 $\beta$ /TNF- $\alpha$  concentrations and increased serum serotonin in mice with EAP [11].

Tumor necrosis factor alpha (TNF $\alpha$ ) plays a critical role in autoimmunity [10, 44, 93, 94]. Insight into the signaling cascades initiated by TNF $\alpha$  has paved the way for therapeutic breakthroughs, notably the advent of TNF $\alpha$  inhibitors such as Etanercept and Infliximab, both of which have demonstrated efficacy across various autoimmune diseases [44]. A recent study revealed an elevated prevalence of BPH in patients with autoimmune disease [44]. The use of TNF $\alpha$  antagonists for autoimmune disease appeared to reduce the risk of BPH and was associated with many outcomes that would be considered positive in CP/CPSS patients, a reduction of prostate epithelial proliferation, prostatic macrophages, and suppression of NF- $\kappa$ B activation [44].

## **Conclusion**

This review offers new insights into the mechanisms of CP/CPSS. We defined autoimmune prostatitis as a form of CP/CPSS characterized by an immune-mediated response against self-antigens within the prostate gland. This condition arises when the immune system, in a dysregulated state, recognizes proteins and antigens specific to the prostate as foreign, leading to an inflammatory response that includes T-cell activation, cytokine production, and the formation of autoantibodies. The consideration of autoimmunity as a mechanism of CP/CPSS shifts from

traditional views that bacterial infections or non-specific inflammatory processes are the sole mediators of this disease and acknowledges the complexity of CP/CPSS, integrating the role of autoimmunity as a key driver of the disease process. We have described EAP models and research involving these models which has been instrumental in redefining some forms of CP/CPSS as having an autoimmune component, raising the possibility of targeted immunomodulatory therapies for treating CP/CPSS. We also described potential new therapeutic strategies, such as the use of ITE or other short-acting AHR agonists to drive immunosuppression. This is a significant step in considering and testing new therapies that can more precisely target the underlying causes of autoimmune prostatitis, ultimately improving outcomes for patients afflicted with autoimmune mediated CP/CPSS.

## References

1. Duloy, A.M., E.A. Calhoun, and J.Q. Clemens, *Economic impact of chronic prostatitis*. *Curr Urol Rep*, 2007. **8**(4): p. 336-9.
2. DeWitt-Foy, M.E., J.C. Nickel, and D.A. Shoskes, *Management of Chronic Prostatitis/Chronic Pelvic Pain Syndrome*. *Eur Urol Focus*, 2019. **5**(1): p. 2-4.
3. Chen, L., M. Zhang, and C. Liang, *Chronic Prostatitis and Pelvic Pain Syndrome: Another Autoimmune Disease?* *Arch Immunol Ther Exp (Warsz)*, 2021. **69**(1): p. 24.
4. Liu, Y., et al., *Chronic prostatitis/chronic pelvic pain syndrome and prostate cancer: study of immune cells and cytokines*. *Fundam Clin Pharmacol*, 2020. **34**(2): p. 160-172.
5. Magistro, G., et al., *Contemporary Management of Chronic Prostatitis/Chronic Pelvic Pain Syndrome*. *Eur Urol*, 2016. **69**(2): p. 286-97.
6. Maeda, K., K. Shigemura, and M. Fujisawa, *A review of current treatments for chronic prostatitis/chronic pelvic pain syndrome under the UPOINTS system*. *Int J Urol*, 2023. **30**(5): p. 431-436.
7. Magistro, G., C.G. Stief, and F.M.E. Wagenlehner, *[Chronic prostatitis/chronic pelvic pain syndrome]*. *Urologe A*, 2020. **59**(6): p. 739-748.
8. Manuel, R.S.J. and Y. Liang, *Sexual dimorphism in immunometabolism and autoimmunity: Impact on personalized medicine*. *Autoimmun Rev*, 2021. **20**(4): p. 102775.
9. Liu, Y., et al., *Experimental autoimmune prostatitis: different antigens induction and antigen-specific therapy*. *Int Urol Nephrol*, 2021. **53**(4): p. 607-618.

10. Murphy, S.F., et al., *IL17 Mediates Pelvic Pain in Experimental Autoimmune Prostatitis (EAP)*. PLoS One, 2015. **10**(5): p. e0125623.
11. Hua, X., et al., *Pathogenic Roles of CXCL10 in Experimental Autoimmune Prostatitis by Modulating Macrophage Chemotaxis and Cytokine Secretion*. Front Immunol, 2021. **12**: p. 706027.
12. Zhang, Y., et al., *Influence of Experimental Autoimmune Prostatitis on Sexual Function and the Anti-inflammatory Efficacy of Celecoxib in a Rat Model*. Front Immunol, 2020. **11**: p. 574212.
13. Crescenze, I.M., et al., *Efficacy, Side Effects, and Monitoring of Oral Cyclosporine in Interstitial Cystitis-Bladder Pain Syndrome*. Urology, 2017. **107**: p. 49-54.
14. Capodice, J.L., et al., *Complementary and alternative medicine for chronic prostatitis/chronic pelvic pain syndrome*. Evid Based Complement Alternat Med, 2005. **2**(4): p. 495-501.
15. Rudick, C.N., A.J. Schaeffer, and P. Thumbikat, *Experimental autoimmune prostatitis induces chronic pelvic pain*. Am J Physiol Regul Integr Comp Physiol, 2008. **294**(4): p. R1268-75.
16. Liu, F., et al., *Abnormal prostate microbiota composition is associated with experimental autoimmune prostatitis complicated with depression in rats*. Front Cell Infect Microbiol, 2022. **12**: p. 966004.
17. Altuntas, C.Z., et al., *A novel murine model of chronic prostatitis/chronic pelvic pain syndrome (CP/CPPS) induced by immunization with a spermine binding protein (p25) peptide*. Am J Physiol Regul Integr Comp Physiol, 2013. **304**(6): p. R415-22.

18. Motrich, R.D., et al., *Autoimmune prostatitis: state of the art*. Scand J Immunol, 2007. **66**(2-3): p. 217-27.
19. Diserio, G.P. and E. Nowotny, *Experimental autoimmune prostatitis: dihydrotestosterone influence over the immune response*. J Urol, 2003. **170**(6 Pt 1): p. 2486-9.
20. Hou, Y., et al., *An aberrant prostate antigen-specific immune response causes prostatitis in mice and is associated with chronic prostatitis in humans*. J Clin Invest, 2009. **119**(7): p. 2031-41.
21. Jackson, C.M., et al., *Strain-specific induction of experimental autoimmune prostatitis (EAP) in mice*. Prostate, 2013. **73**(6): p. 651-6.
22. Wang, H.H., et al., *Characterization of autoimmune inflammation induced prostate stem cell expansion*. Prostate, 2015. **75**(14): p. 1620-31.
23. Orsilles, M.A., B.N. Pacheco-Rupil, and M.M. Depiante-Depaoli, *Experimental autoimmune prostatitis (EAP): enhanced release of reactive oxygen intermediates (ROI) in peritoneal macrophages*. Autoimmunity, 1993. **16**(3): p. 201-7.
24. Rivero, V.E., et al., *Non-obese diabetic (NOD) mice are genetically susceptible to experimental autoimmune prostatitis (EAP)*. J Autoimmun, 1998. **11**(6): p. 603-10.
25. Ittmann, M., *Anatomy and Histology of the Human and Murine Prostate*. Cold Spring Harb Perspect Med, 2018. **8**(5) p.1-6.
26. Keetch, D.W., P. Humphrey, and T.L. Ratliff, *Development of a mouse model for nonbacterial prostatitis*. J Urol, 1994. **152**(1): p. 247-50.
27. Breser, M.L., et al., *Regulatory T cells control strain specific resistance to Experimental Autoimmune Prostatitis*. Sci Rep, 2016. **6**: p. 33097.

28. Fu, W., et al., *The effect of chronic prostatitis/chronic pelvic pain syndrome (CP/CPPS) on semen parameters in human males: a systematic review and meta-analysis*. PLoS One, 2014. **9**(4): p. e94991.
29. Liu, K.J., et al., *Identification of rat prostatic steroid-binding protein as a target antigen of experimental autoimmune prostatitis: implications for prostate cancer therapy*. J Immunol, 1997. **159**(1): p. 472-80.
30. Rivero, V., C. Carnaud, and C.M. Riera, *Prostatein or steroid binding protein (PSBP) induces experimental autoimmune prostatitis (EAP) in NOD mice*. Clin Immunol, 2002. **105**(2): p. 176-84.
31. !!! INVALID CITATION !!! [30].
32. Penna, G., et al., *Spontaneous and prostatic steroid binding protein peptide-induced autoimmune prostatitis in the nonobese diabetic mouse*. J Immunol, 2007. **179**(3): p. 1559-67.
33. Ballotti, S., F. Chiarelli, and M. de Martino, *Autoimmunity: basic mechanisms and implications in endocrine diseases. Part I*. Horm Res, 2006. **66**(3): p. 132-41.
34. Dragin, N., et al., *Estrogen-mediated downregulation of AIRE influences sexual dimorphism in autoimmune diseases*. J Clin Invest, 2016. **126**(4): p. 1525-37.
35. Zhu, M.L., et al., *Sex bias in CNS autoimmune disease mediated by androgen control of autoimmune regulator*. Nat Commun, 2016. **7**: p. 11350.
36. Haverkamp, J.M., et al., *An inducible model of abacterial prostatitis induces antigen specific inflammatory and proliferative changes in the murine prostate*. Prostate, 2011. **71**(11): p. 1139-50.

37. Pound, P., *Scientific debate on animal model in research is needed*. *Bmj*, 2001. **323**(7323): p. 1252.
38. Akhtar, A., *The flaws and human harms of animal experimentation*. *Camb Q Healthc Ethics*, 2015. **24**(4): p. 407-19.
39. Yamaguchi, H., et al., [*Experimental rodent models of chronic prostatitis: effect of phosphodiesterase 5 inhibitor on chronic pelvic-pain-related behavior*]. *Nihon Yakurigaku Zasshi*, 2019. **154**(5): p. 259-264.
40. Roman, K., et al., *Tryptase-PAR2 axis in experimental autoimmune prostatitis, a model for chronic pelvic pain syndrome*. *Pain*, 2014. **155**(7): p. 1328-1338.
41. Centenera, M.M., et al., *A patient-derived explant (PDE) model of hormone-dependent cancer*. *Mol Oncol*, 2018. **12**(9): p. 1608-1622.
42. Baker, R., et al., *Computational modeling of complex bioenergetic mechanisms that modulate CD4+ T cell effector and regulatory functions*. *NPJ Syst Biol Appl*, 2022. **8**(1): p. 45.
43. Lorenzo, G., et al., *Tissue-scale, personalized modeling and simulation of prostate cancer growth*. *Proc Natl Acad Sci U S A*, 2016. **113**(48): p. E7663-e7671.
44. Zhang, L., et al., *Establishment of experimental autoimmune prostatitis model by T(2) peptide in aluminium hydroxide adjuvant*. *Andrologia*, 2018. **50**(3).
45. Vinnik, Y.Y., A.V. Kuzmenko, and T.A. Gyaurgiev, [*Treatment of the chronic prostatitis: current state of the problem*]. *Urologiia*, 2021(4): p. 138-144.
46. Zhang, M., et al., *Clinical study of duloxetine hydrochloride combined with doxazosin for the treatment of pain disorder in chronic prostatitis/chronic pelvic pain syndrome: An observational study*. *Medicine (Baltimore)*, 2017. **96**(10): p. e6243.



47. Iwamura, H., et al., *Eviprostat has an identical effect compared to pollen extract (Cernilton) in patients with chronic prostatitis/chronic pelvic pain syndrome: a randomized, prospective study*. BMC Urol, 2015. **15**: p. 120.
48. Tawfik, A.M., et al., *Tadalafil monotherapy in management of chronic prostatitis/chronic pelvic pain syndrome: a randomized double-blind placebo controlled clinical trial*. World J Urol, 2022. **40**(10): p. 2505-2511.
49. Pineault, K., et al., *Phosphodiesterase type 5 inhibitor therapy provides sustained relief of symptoms among patients with chronic pelvic pain syndrome*. Transl Androl Urol, 2020. **9**(2): p. 391-397.
50. Krakhotkin, D.V., et al., *Evaluation of influence of the UPOINT-guided multimodal therapy in men with chronic prostatitis/chronic pelvic pain syndrome on dynamic values NIH-CPSI: a prospective, controlled, comparative study*. Ther Adv Urol, 2019. **11**: p. 1756287219857271.
51. Mehik, A., et al., *Alfuzosin treatment for chronic prostatitis/chronic pelvic pain syndrome: a prospective, randomized, double-blind, placebo-controlled, pilot study*. Urology, 2003. **62**(3): p. 425-9.
52. Nickel, J.C., *Chronic prostatitis/chronic pelvic pain syndrome: it is time to change our management and research strategy*. BJU Int, 2020. **125**(4): p. 479-480.
53. Abron, J.D., et al., *An endogenous aryl hydrocarbon receptor ligand, ITE, induces regulatory T cells and ameliorates experimental colitis*. Am J Physiol Gastrointest Liver Physiol, 2018. **315**(2): p. G220-G230.
54. Beamer, C.A., et al., *Targeted deletion of the aryl hydrocarbon receptor in dendritic cells prevents thymic atrophy in response to dioxin*. Arch Toxicol, 2019. **93**(2): p. 355-368.

55. Boule, L.A., et al., *Aryl hydrocarbon receptor signaling modulates antiviral immune responses: ligand metabolism rather than chemical source is the stronger predictor of outcome*. *Sci Rep*, 2018. **8**(1): p. 1826.
56. Busbee, P.B., et al., *Use of natural AhR ligands as potential therapeutic modalities against inflammatory disorders*. *Nutr Rev*, 2013. **71**(6): p. 353-69.
57. Ehrlich, A.K., et al., *TCDD, FICZ, and Other High Affinity AhR Ligands Dose-Dependently Determine the Fate of CD4+ T Cell Differentiation*. *Toxicol Sci*, 2018. **161**(2): p. 310-320.
58. Mehta, V. and C.M. Vezina, *Potential protective mechanisms of aryl hydrocarbon receptor (AHR) signaling in benign prostatic hyperplasia*. *Differentiation*, 2011. **82**(4-5): p. 211-9.
59. Wang, Q., et al., *Aryl hydrocarbon receptor inhibits inflammation in DSS induced colitis via the MK2/p MK2/TTP pathway*. *Int J Mol Med*, 2018. **41**(2): p. 868-876.
60. Yue, T., et al., *The AHR Signaling Attenuates Autoimmune Responses During the Development of Type 1 Diabetes*. *Front Immunol*, 2020. **11**: p. 1510.
61. Soshilov, A.A. and M.S. Denison, *Ligand promiscuity of aryl hydrocarbon receptor agonists and antagonists revealed by site-directed mutagenesis*. *Mol Cell Biol*, 2014. **34**(9): p. 1707-19.
62. Wu, H., et al., *Synthesis and biological evaluation of FICZ analogues as agonists of aryl hydrocarbon receptor*. *Bioorg Med Chem Lett*, 2020. **30**(5): p. 126959.
63. Rouse, M., et al., *3,3'-diindolylmethane ameliorates experimental autoimmune encephalomyelitis by promoting cell cycle arrest and apoptosis in activated T cells through microRNA signaling pathways*. *J Pharmacol Exp Ther*, 2014. **350**(2): p. 341-52.

64. Kenison, J.E., et al., *Tolerogenic nanoparticles suppress central nervous system inflammation*. Proc Natl Acad Sci U S A, 2020. **117**(50): p. 32017-32028.
65. Fu, X., et al., *MicroRNA-155 deficiency attenuates inflammation and oxidative stress in experimental autoimmune prostatitis in a TLR4-dependent manner*. Kaohsiung J Med Sci, 2020. **36**(9): p. 712-720.
66. Heine, H. and A. Zamyatina, *Therapeutic Targeting of TLR4 for Inflammation, Infection, and Cancer: A Perspective for Disaccharide Lipid A Mimetics*. Pharmaceuticals (Basel), 2022. **16**(1): p. 1-26.
67. Ou, T., M. Lilly, and W. Jiang, *The Pathologic Role of Toll-Like Receptor 4 in Prostate Cancer*. Front Immunol, 2018. **9**: p. 1188.
68. Spachidou, M.P., et al., *Expression of functional Toll-like receptors by salivary gland epithelial cells: increased mRNA expression in cells derived from patients with primary Sjögren's syndrome*. Clin Exp Immunol, 2007. **147**(3): p. 497-503.
69. Vidya, M.K., et al., *Toll-like receptors: Significance, ligands, signaling pathways, and functions in mammals*. Int Rev Immunol, 2018. **37**(1): p. 20-36.
70. Haartmans, M.J.J., et al., *Evaluation of the Anti-Inflammatory and Chondroprotective Effect of Celecoxib on Cartilage Ex Vivo and in a Rat Osteoarthritis Model*. Cartilage, 2022. **13**(3): p. 19476035221115541.
71. Vickman, R.E., et al., *TNF is a potential therapeutic target to suppress prostatic inflammation and hyperplasia in autoimmune disease*. Nat Commun, 2022. **13**(1): p. 2133.

72. Tang, Y., et al., *Activated NF-kappaB in bone marrow mesenchymal stem cells from systemic lupus erythematosus patients inhibits osteogenic differentiation through downregulating Smad signaling*. *Stem Cells Dev*, 2013. **22**(4): p. 668-78.
73. Wang, Z., et al., *Muscarinic M1 and M2 receptor subtypes play opposite roles in LPS-induced septic shock*. *Pharmacol Rep*, 2019. **71**(6): p. 1108-1114.
74. Pattabiraman, G., et al., *Mast cell function in prostate inflammation, fibrosis, and smooth muscle cell dysfunction*. *Am J Physiol Renal Physiol*, 2021. **321**(4): p. F466-F479.
75. Pattabiraman, G., et al., *Tactile Allodynia in a Model of Chronic Pelvic Pain*. *Front Pain Res (Lausanne)*, 2021. **2**: p. 805136.
76. Quick, M.L., et al., *CCL2 and CCL3 are essential mediators of pelvic pain in experimental autoimmune prostatitis*. *Am J Physiol Regul Integr Comp Physiol*, 2012. **303**(6): p. R580-9.
77. Penna, G., et al., *Treatment of experimental autoimmune prostatitis in nonobese diabetic mice by the vitamin D receptor agonist elocalcitol*. *J Immunol*, 2006. **177**(12): p. 8504-11.
78. Wolf, S.J., et al., *Human and Murine Evidence for Mechanisms Driving Autoimmune Photosensitivity*. *Front Immunol*, 2018. **9**: p. 2430.
79. Thumbikat, P., et al., *Bacteria-induced uroplakin signaling mediates bladder response to infection*. *PLoS Pathog*, 2009. **5**(5): p. e1000415.
80. Ludwig, M., et al., *Immunocytological analysis of leukocyte subpopulations in urine specimens before and after prostatic massage*. *Eur Urol*, 2001. **39**(3): p. 277-82.

## Chapter 3

### **The aryl hydrocarbon receptor agonist ITE reduces inflammation and urinary dysfunction in a mouse model of autoimmune prostatitis**

**Robbie SJ Manuel**<sup>1,2,3</sup>, Allison Rundquist<sup>1,3</sup>, Marcella Ambrogi<sup>1,3</sup>, Brandon R. Scharpf<sup>1,2</sup>, Nelson T. Peterson<sup>1,2</sup>, Monica Ridlon<sup>1,2</sup>, Jaskiran K. Sandhu<sup>1</sup>, Sneha Chandrashekar<sup>1</sup>, Kimberly P. Keil-Stietz<sup>1,2,3</sup>, Richard E. Peterson<sup>4</sup> and Chad M. Vezina<sup>1,2,3</sup>

<sup>1</sup> *Department of Comparative Biosciences, University of Wisconsin-Madison;*

<sup>2</sup> *Molecular & Environmental Toxicology Graduate Program, University of Wisconsin School of Medicine & Public Health;*

<sup>3</sup> *Endocrinology and Reproductive Physiology Program, University of Wisconsin School of Medicine & Public Health, Madison, WI USA*

<sup>4</sup> *Division of Pharmaceutical Sciences, University of Wisconsin School of Pharmacy, Madison, WI USA*

## **The aryl hydrocarbon receptor agonist ITE reduces inflammation and urinary dysfunction in a mouse model of autoimmune prostatitis**

Robbie SJ Manuel<sup>1,2,3</sup>, Allison Rundquist<sup>1,3</sup>, Marcella Ambrogi<sup>1,3</sup>, Brandon R. Scharpf<sup>1,2</sup>, Nelson T. Peterson<sup>1,2</sup>, Jaskiran K. Sandhu<sup>1</sup>, Sneha Chandrashekar<sup>1</sup>, Monica Ridlon<sup>1,2</sup>, Kimberly P. Keil-Stietz<sup>1,2,3</sup>, Richard E. Peterson<sup>4</sup> and Chad M. Vezina<sup>1,2,3</sup>

<sup>1</sup> *Department of Comparative Biosciences, University of Wisconsin-Madison;*

<sup>2</sup> *Molecular & Environmental Toxicology Graduate Program, University of Wisconsin School of Medicine & Public Health;*

<sup>3</sup> *Endocrinology and Reproductive Physiology Program, University of Wisconsin School of Medicine & Public Health, Madison, WI USA*

<sup>4</sup> *Division of Pharmaceutical Sciences, University of Wisconsin School of Pharmacy, Madison, WI USA*

### **Acknowledgements**

The authors gratefully acknowledge the support and resources provided by the Research Animal Resources and Compliance (RARC) Core and Biomedical Research Modeling Services (BRMS), which greatly contributed to the successful completion of this project. We would also like to express our appreciation to the University of Wisconsin O'Brien Center Rodent Urinary Function Testing Core. This work was funded by National Institutes of Health grants R01 ES001332, T32 ES007015 and U54 DK104310. The content is solely the responsibility of the authors and does not necessarily represent the official views of the National Institutes of Health. This work does not represent the views of the Department of Veterans Affairs or the United States Government

**Address Correspondence To:** Chad M Vezina, PhD, Department of Comparative Biosciences, University of Wisconsin-Madison, 1656 Linden Drive, Hanson Biomedical Sciences Laboratory, Madison, WI 53705, USA. Phone: 608-890-3235. E-mail: cmvezina@wisc.edu

**Declaration of conflict of Interest:** None

**Abstract:**

Prostate inflammation is linked to lower urinary tract dysfunction and is a key factor in chronic prostatitis / chronic pelvic pain syndrome. Autoimmunity was recently identified as a driver of prostate inflammation. Agonists of the aryl hydrocarbon receptor (AHR), a ligand-activated transcription factor, have been used to suppress autoimmunity in mouse models of colitis, rhinitis, and dermatitis, but whether AHR agonists suppress prostate autoimmunity has not been examined. Here, we test whether ITE (2-(1H-indole-3'-carbonyl)-thiazole-4-carboxylic acid methyl ester), an AHR agonist, suppresses inflammation, allodynia, and urinary dysfunction in a mouse model of experimental autoimmune prostatitis (EAP). C57BL/6J adult male mice were immunized with rat prostate antigen to induce EAP or TiterMax Gold® adjuvant (uninflamed control). Mice were also treated with ITE (10 mg/kg/day IP for 6 d) or DMSO (5 mg/kg/day) for 6d (vehicle). EAP heightened histological inflammation in the dorsal prostate, induced tactile allodynia, and increased the frequency of non-voiding bladder contractions. ITE significantly mitigated the actions of EAP. Using the Nanostring nCounter Inflammation Panel, we evaluated the impact of EAP and ITE on prostatic RNA abundance. EAP changed abundance of 40 inflammation-related RNAs, while ITE changed abundance of 28 inflammation-related RNAs. We identified a cluster of RNAs for which ITE protected against EAP-induced changes in the abundance of *H2-Ab1*, *S100a8*, and *S100a9*. ITE also increased the abundance of the AHR-responsive *Cyp1a1* RNA. These findings support the hypothesis that ITE activates the AHR and reduces autoimmune-mediated prostatitis in mice.

**Keywords:**

CP/CPPS, Experimental Autoimmune Prostatitis, AHR, ITE, Inflammation, Inflammasome,  
Therapeutic Strategies, Autoimmunity, Urology, Translational Animal Models



**Introduction:**

Lower urinary tract dysfunction (LUTD) and chronic prostatitis/chronic pelvic pain syndrome (CP/CPSS) are urological conditions affecting men of advancing age, impose a large healthcare burden, and adversely affect quality of life for millions [1]. Male LUTD is characterized by increased urinary frequency, nocturia, urinary retention, and urinary tract infections [2]. CP/CPSS is a complex syndrome with pelvic pain as its hallmark and it manifests in urinary and sexual dysfunction [3]. LUTD and CP/CPSS pathogenesis are incompletely understood but genetic, environmental, and immunological factors are involved [3, 4]. Prostate inflammation is considered a major driver of LUTD and CP/CPSS [3, 5-7], and autoimmunity is a recognized trigger for prostate inflammation [8].

There are no currently approved therapies for prostate autoimmunity. However, agonists of the aryl hydrocarbon receptor (AHR), a ligand activated transcription factor, have been effective in reducing inflammation in preclinical models of several autoimmune diseases, including multiple sclerosis, psoriasis, atopic dermatitis and inflammatory bowel disease [9, 10]. Known or suspected exposure to AHR agonists during adulthood has been linked to a lower rate of BPH diagnoses in some human populations [11-13].

The purpose of this study was to test the hypothesis that an AHR agonist would reduce inflammation and physiological manifestations of autoimmune prostatitis in a preclinical model. Rat prostate antigen was delivered subcutaneously to C57BL/6J adult male mice to induce EAP

and control mice received adjuvant alone. Mice were also exposed to the AHR agonist 2-(1'-indole-3'-carbonyl)-thiazole-4-carboxylic acid methyl ester (ITE) [14] (10 mg/kg/day IP for 6 d) or DMSO (5 mg/kg/day IP for 6d, vehicle). EAP caused prostate histological inflammation, heightened sensitivity to dermal stimuli (allodynia), and increased non-voiding bladder contractions consistent with bladder instability. ITE significantly reduced the EAP mediated changes to prostate histology and physiology. A gene expression analysis focused on inflammation related genes found that ITE protected against the EAP mediated increase in the abundance of three RNAs (*H2-ab1*, *S100a8*, and *S100a9*).

## **Results:**

The prostate is susceptible to various inflammatory and cancerous conditions affecting men across all age groups. Interestingly, inflammation can occur without the presence of infectious agents, indicating the possibility of an autoimmune reaction [15, 16]. While AHR signaling has been shown to reduce autoimmunity in areas other than the prostate [17], the role of AHR in controlling autoimmune responses within the prostate remains unexplored. We collected and purified adult rat prostate extract (includes dorsolateral, ventral, and anterior prostate lobes, rat prostatic antigen, PAg) as described in the methods and mixed it with TiterMax Gold<sup>®</sup> adjuvant in a 1:1 ratio. EAP mice received two subcutaneous injections of PAg in equal parts (0.050 ml) into the base of tail and the posterior aspect of neck. Mice randomly selected to receive ITE were injected in the lower right ventral aspect of the abdomen with 10 mg/kg/day IP for 6 d. Age-matched control mice were immunized with DMSO and TiterMax Gold<sup>®</sup> adjuvant in a 1:1 ratio.

Prostates were collected from a subset of mice (3-5 from each experimental group) seven days after the first immunization and were fixed, embedded in paraffin, and cut to a thickness of five microns for histological analysis. EAP caused inflammation, characterized by inflammatory infiltration, and stromal thickening. Inflammatory infiltration and stromal thickening were visibly less in ITE treated mice (Fig. 2A-B).

Because prostate inflammation can be painful [18], we used the von Frey Filament Test (VFT) to determine whether EAP drives changes in tactile nociception (Fig. 3). Fibers of increasing stiffness were applied to the sural region of the hindpaw to evaluate the withdrawal reflex. VFT testing was conducted on the day of immunization and every 5 d for 4 wk. EAP significantly reduced the withdrawal threshold 5 d post-immunization ( $p = 0.0289$ ), an effect that was partially blocked by ITE ( $p = 0.0347$ ).

### **ITE Reduces Changes in Micturition Behavior Induced by EAP**

Prostate inflammation has been linked to changes in voiding behaviors like urinary retention and polyuria [19, 20]. We conducted void spot assays, 6 d after immunization, to determine whether EAP drives changes in mouse voiding behavior and whether ITE protects against these changes. Mice were placed in cages lined with filter paper for 4 h and urine was visualized with UV transillumination (Fig. 4A). We assessed urine spot number, spot size, total urine area, primary void area, corner, and center voiding (Fig. 4B). There were more void spots in EAP-immunized mice receiving ITE (+EAP/+ITE,  $p = 0.0004$ ) than in any other group. +EAP/+ITE mice voided more 0.25-0.5 cm<sup>2</sup> (larger) spots than any other group ( $p=0.0437$ ; 0.0267; 0.0037). There were no significant differences among groups in the smallest category of void spots (0-0.1 cm<sup>2</sup>), in the

spatial distribution of urine spots (spots in the center versus in the corners), or in the total voided urine area. We used anesthetized cystometry to evaluate the bladder response to filling and emptying. Cystometry was completed 6 d after immunization. Representative cystometrograms are shown in Fig. 4C. EAP increased the number of non-voiding contractions and ITE protected against this change (Fig. 4D).

### **ITE and EAP alter gene expression within dorsal prostate**

We conducted NanoString nCounter multiplex gene expression analysis using the inflammation panel to identify EAP-mediated changes in dorsal prostate RNA abundance that were mitigated by ITE. Prostates were collected 6 d after immunization for NanoString analysis. A total of 561 unique inflammation-related RNAs were quantified and EAP significantly reduced abundance of 10 RNAs and increased abundance of 30 RNAs. We performed k-means clustering on differentially expressed genes to pinpoint EAP mediated gene expression changes that were counteracted by ITE (Fig. 5A). S100 calcium-binding protein A8 and A9 (*S100a8* and *S100a9*) encode subunits of the protein calprotectin, an abundant protein in neutrophils, and were highly induced by EAP and ITE protected against the EAP-mediated increase (Fig. 5A).

Histocompatibility 2, class II antigen A (*H2-ab1*) encodes an antigen processing protein that has been linked to inflammation and autoimmunity [21]. EAP increased the abundance of *H2-ab1* RNA and ITE protected against this increase (Fig. 5A). To independently validate this observation, we used RNAScope<sup>TM</sup> to label dorsal prostate tissue sections from each of the four experimental groups with a probe against *H2-ab1* (Fig. 5B). *H2-ab1* was not detectable in dorsal prostates of mice without EAP. *H2-ab1* was abundant in dorsal prostate epithelium of EAP mice treated with DMSO but was visibly less abundant in EAP mice treated with ITE. We

also treated mice with rat prostate antigen or adjuvant alone, and then ITE or DMSO vehicle and dorsolateral prostate was collected 4 hours later, RNA was isolated, and the abundance of *Cyp11a1*, a known AHR target gene, was determined. ITE significantly increased the relative abundance of *Cyp11a1* (Fig. 6A). We also observed that EAP significantly increased the abundance of *S100a8* and *S100a9*, and EAP and ITE protected against the EAP-mediated increase (Fig. 6B-C).

### **Discussion:**

Prostate autoimmunity has been linked to several benign prostatic diseases but there are no medications currently approved to target this disease mechanism. The goal of this study was to leverage recent findings that AHR activation can reduce autoimmune-mediated inflammation in a variety of tissues and test whether the AHR agonist, ITE, reduces prostate inflammation. We collected histological, physiological, and molecular evidence that supports an ITE-mediated reduction of inflammation, pain, and voiding dysfunction in a mouse model of EAP.

In humans, the induction of inflammation within the prostate is suggested to activate efferent neural pathways, consequently precipitating a localized nociceptive response through the activation of dorsal root ganglia neurons [22]. This phenomenon is facilitated by sensory fibers in instances of prostatic inflammation, thereby contributing to the propagation of inflammatory processes [22]. We observed that induction of EAP reduces the withdrawal threshold to Von Frey filaments, a phenomenon mitigated by the treatment with ITE 5 d post immunization but not at later time points. This observation aligns with clinical manifestations in humans where the intensity of pain correlates with the frequency of symptomatic episodes, such as dysuria and

dysorgasmia (painful ejaculation), intimating that the acuteness of nociception is exacerbated during peak inflammatory states [23]. A potential limitation of this model stems from its utilization of the C57BL/6J mouse strain, noted for its comparatively subdued immune response relative to other strains [24], which might influence the generalizability of the findings.

We used the NanoString nCounter inflammation panel to identify gene expression changes driven by autoimmune prostatitis and blocked by ITE as a first step in understanding the ITE mechanism of action. We found that autoimmune prostatitis increased *H2-ab1* RNA in prostate epithelial cells and that ITE prevented the increase. Mucosal epithelial cells, such as those in the gut, use MHC II molecules, including H2-AB1, to activate CD4+ T effector cells [25] and to facilitate self-renewal of the epithelium [26]. H2-AB1 abundance in intestinal epithelial cells increases in response to inflammation and autoimmunity [27-29]. H2-AB1 is required for inflammation in a mouse model of allergic rhinitis [30] and is required in a mouse model of graft versus host disease [31]. A previous study also demonstrated the requirement for H2-AB1 in autoimmune prostatitis in non-obese diabetic mice [31]. AHR activation ligands more potent than ITE were previously shown to increase *H2-ab1* abundance in non-inflammatory research models involving jejunal epithelial cells and liver [32, 33]. Though we specifically observed an ITE mediated decrease in *H2-ab1* abundance in this study, our model involved inflammation and a different ligand. It would be worthwhile to investigate whether *H2-ab1* is required for the inhibitory actions of ITE on autoimmune prostatitis.

EAP increased the abundance of *S100a8* and *S100a9* RNAs, which encode peptides that assemble into calprotectin. ITE blocked the EAP mediated increase in *S100a8* and *S100a9*.

Calprotectin plays a crucial role in controlling inflammation, especially in autoimmune diseases [34, 35]. This protein not only regulates inflammatory responses by acting as a damage-associated molecular pattern molecule that attracts leukocytes to inflammation sites but is also pivotal in the body's defense against pathogens [35]. Elevated calprotectin abundance has been linked to the severity of rheumatoid arthritis [36], inflammatory bowel disease [37], and psoriasis [36], indicating its significant impact on the pathology of these disorders [38]. The repression of calprotectin may be a mechanism by which ITE reduces prostate inflammation in mice with EAP.

**Conclusion:**

The investigation into the etiopathogenetic mechanisms of EAP and its modulation by ITE in mouse models has yielded significant insights into potential therapeutic strategies for CP/CPPS and BPH pathologies. Our results highlight ITE's efficacy in mitigating EAP-induced histological and molecular changes, underscoring the therapeutic potential of AHR modulation in prostatitis. This study not only advances our understanding of CP/CPPS and BPH pathogenesis but also positions ITE as a promising candidate for further investigation in the context of human urological disorders. The observed modulation of gene expression profiles and reduction in inflammation and fibrosis within the prostate by ITE treatment points to the intricate role of the AHR pathway in the immune response and suggests a novel approach to managing prostatic diseases. Further research is warranted to explore the long-term effects of ITE treatment and its applicability in clinical settings, aiming to provide relief for patients suffering from these and related conditions.

**Methods:****Animals**

All experiments were conducted under an approved protocol from the University of Wisconsin Animal Care and Use Committee and in accordance with the National Institutes of Health Guide for the Care and Use of Laboratory Animals. Mice were housed in Udel® Polysulfone microisolator cages on racks or in Innocage® disposable mouse cages (Innovive, San Diego, CA) on an Innorack®; room lighting was maintained on 12-hour light and dark cycles; room temperature was typically  $20.5 \pm 5^\circ\text{C}$ ; humidity was 30–70%. Mice were fed 8604 Teklad Rodent Diet (Harlan Laboratories, Madison WI) and feed and water were available ad libitum. Cages contained corn cob bedding. C57BL/6J mice were purchased from Jackson Laboratories (stock no. 000664, Bar Harbor, ME). All end point measurements were collected in male mice ranging from 7-10 wk old with 3-6 mice used per treatment group. The treatment scheme is illustrated in Fig. 1.

**Drugs**

2-(1*H*-Indol-3-ylcarbonyl)-4-thiazolecarboxylic acid methyl ester (ITE) (Tocris Bioscience, USA. Cat. No. 1803). ITE is an endogenous aryl hydrocarbon receptor (AHR) agonist. ITE was reconstituted in DMSO and prepared in a stock solution for usage and stored at standard ambient temperature, 25 °C

**Prostate Antigen (PAG) Homogenate**



Entire Prostate glands from Wistar Rats (12-55wks) were used to prepare antigen extract. Pooled glands were homogenized in phosphate-buffered saline (PBS) at a pH of 7.2 with protease inhibitors[39]. Pooled glands were homogenized with a 40mL Bellco Glass Dounce homogenizer and pushed through a Cole-Parmer PES Sterile Chromatography Syringe Filter (cat. no. EW-15945-52). Homogenate was subsequently centrifuged at 10,000g for 30 min, and the supernatant was used as the PAg.

### **Protein Quantification**

The Qubit Protein Assay from Qubit™ Protein and Protein Broad Range (BR) Assay Kits (cat. no. Q33211). Protein concentration was analyzed for pooled PAg samples and adjusted with sterile water to a standard concentration of 10 mg/ml and stored in -80°C freezer until used.

### **Induction of EAP**

Mice were injected with 1 mg of PAg blended in an equal volume of TiterMax® Gold adjuvant (Norcross, GA) with a 26G BD General Use and Precision Glide Hypodermic Needles (0.018in) (Fisher cat. no. 305115), while animals were maintained under isoflurane anesthesia. EAP mice received two subcutaneous injections of equal parts (0.050 ml) into the base of tail and the posterior aspect of neck, following a predefined established protocol. Uninflamed control mice received a subcutaneous injection of TiterMax® Gold Adjuvant only.

### **Tissue Preparation**

Seven days after immunization, the lower urinary tracts of a subset of mice (5 mice per experimental group) were collected for histological examination. The preparation, fixation, and

sectioning of the tissues followed the methods previously outlined [40]. The procedure for removing the lower urinary tract involved severing the ureters where they enter the bladder wall, cutting the vas deferens at its entry point to the bladder neck, and slicing the urethra just above the pubic symphysis. The hemi-dorsal lobes of the prostate were then excised, fixed in a 4% solution of paraformaldehyde, and rinsed with PBS. Prostates were then dehydrated into ethanol, cleared in xylene, and infiltrated with Periplast (Leica Biosystems, Deer Park, IL). Five-micron sagittal tissue sections were mounted on Superfrost Plus Gold Slides (manufactured by ThermoFisher Scientific Waltham, MA).

### **Real-Time Quantitative-PCR (RT-qPCR)**

qPCR was conducted as described previously [41] on dorsal lateral prostate tissue sections with 3 animals per experimental treatment group using the following gene specific primers: *Cyp11a1*, 5'- TTGTGCCTGCCTCCTACTTTG -3' and 5'- CTCTGAGGCCAGGTATCTCC -3', *S100a8* 5'- TGCCGTCTGAACTGGAGAAG -3' and 5'- TGTAGAGGGCATGGTGATTTC -3', *S100a9* 5'- TGAGAAGCTGCATGAGAACA -3' and 5'- AAGGCCATTGAGTAAGCCCA -3', and peptidyl prolyl isomerase a (*Ppia*), 5'-TCTCTCCGTAGATGGACCTG-3' and 5'- ATCACGGCCGATGACGAGCC-3'. Relative mRNA abundance was determined by the  $\Delta\Delta C_t$  method as described previously [41] and normalized to *Ppia* abundance.

### **Immunofluorescent staining**

Tissues were fixed in 4% paraformaldehyde, dehydrated in alcohol, cleared in xylene, and infiltrated with paraffin. 5  $\mu$ m sections were generated, mounted on Superfrost™ Plus Gold Slides (Thermo Fisher Scientific; Waltham, MA) and immunolabeled using antibodies against

CD45 Monoclonal Antibody (30-F11), eBioscience (Catalog #14-0451-82; 1:100). Non-specific binding sites were blocked for 1 hr in TBSTw containing 1% Blocking Reagent (11096176001, Roche Diagnostics, Indianapolis, IN), 5% normal goat sera, and 1% bovine serum albumin fraction 5 (RGBTw). Tissues were incubated overnight at 4°C with primary antibodies. After several washes with TBSTw, tissues were incubated for 1 hr at room temperature with RGBTw containing 1:250 diluted fluorescent secondary antibodies Anti-Goat 488 (Jackson ImmunoResearch; 711-545-152; 1:500) 2-(4-amidinophenyl)-1H-indole-6-carboxamide (DAPI) (1:1000) was used to visualize nuclei and slides were mounted in anti-fade media (phosphate-buffered saline containing 80% glycerol and 0.2% n-propyl gallate). Staining was imaged at 40X brightfield using a Leica DM LB Microscope (Leica, Wetzlar, Germany) and QImaging Micropublisher 5.0 RTV camera and software (01-MP5.0-RTV-R-CLR-10; QImaging, Surrey, BC, Canada) or at 20x (PlanFluor, NA 0.45) using a BZ-X710 digital microscope (Keyence, Itasca, IL).

### ***In situ* detection of RNAs using RNAscope™ Multiplex Fluorescent Reagent**

#### **Kit v2**

An RNAscope<sup>1</sup> probe against human *H2-ab1* (Catalog #414739; Ventana Systems, Harvard, MA) acquired from Advanced Cell Diagnostics, Inc., [(ACD), Hayward, CA]. Sections were deparaffinized in xylene, rehydrated, air dried, treated with endogenous hydrogen peroxidase block solution at room temperature for 10 min, immersed in pretreatment 2 solution at 100–104°C for 15 min, and digested with protease solution for 30 min at 40°C. Slides were rinsed with distilled water twice after each step. Probes were then hybridized at 40°C for 2 h in a humidified chamber. After washing, signal amplification from the hybridized probes was

performed by the serial application of amplification solutions per the RNAScope<sup>®</sup> instructions. Opal dyes (Akoya Biosciences; Opal 520, FP1487001KT) were reconstituted in Dimethylsulfoxide (DMSO) and diluted in tyramide signal amplification buffer (TSA;1:1000). Horseradish peroxidase (HRP)-C1 and HRP-C2 signals were developed per the RNAScope<sup>®</sup> instructions and the slides were counterstained with DAPI, and cover slipped using antifade mounting media. Slides were imaged as described in the histology and immunostaining section.

### **Hematoxylin and Eosin Staining**

Hematoxylin and eosin staining was performed by the Histology Service in the School of Veterinary Medicine at the University of Wisconsin-Madison. Stains were imaged using a BZ-X710 digital microscope (Keyence, Itasca, IL) fitted with a ×20 (PlanFluor, numerical aperture: 0.45) objective.

### **Mechanical Sensitivity Testing**

The von Frey filament test (VFT) was employed to gauge sensitivity to non-noxious point pressure stimuli. Mice were acclimated on the testing platform for a minimum of 45 minutes or until they were calm. Calibrated filaments (0.02, 0.04, 0.07, 0.16, 0.4, 0.6, 1, and 1.4 g) were incrementally applied to the glabrous skin of the hind paw until slight buckling occurred. This process was alternated between hind paws, with each filament presented five times per paw. The tests progressed through all three filaments, with at least a 1-minute interval between presentations. Testing was paused if mice exhibited activity, resuming once they were calm. Withdrawal of the paw in response to filament pressure was documented as a positive response. The filaments were applied until a brief bending was observed, leading to filament deformation

against the paw. The force applied during this bending was recorded as the mechanical stimulation force threshold. The collected data, inclusive of force thresholds and corresponding behavioral outcomes, constituted the basis for formulating a tactile sensitivity profile specific to each subject animal under scrutiny. The analytical process was executed through the utilization of the UP-Down (UPD)-Reader software, an open-source tool.

### **Cystometry**

Anesthetized cystometry was performed as described previously by Kennedy et. al (2022) [42]. Mice were anesthetized with a subcutaneous injection of urethane (AC32554- 0500, Fisher) at a dosage of 1.43 g urethane/ kg mouse. Mice were dosed using a fresh stock solution of urethane in saline at 86 mg/ml. Mice were placed back into cages for at least 30 min prior to beginning surgery. The abdomen was opened and a purse string suture (6- 0 Silk, 501180809, Fisher) placed in the dome of the bladder. PE-50 tubing (NC9140178, Fisher) was used as a catheter and placed into the dome of the bladder using a 25 G 1.5 in needle. The needle was removed, and the purse string suture tied around the catheter. The body wall and skin were closed with a suture and the mouse was allowed to recover on a heating pad for ~60 min. Following recovery, mice were connected to an in-line pressure transducer and infusion pump. Saline was infused at a rate of 0.8 ml/hr and pressure recorded using an MLT844 physiological pressure transducer (ADInstruments) connected to an FE221 Bridge Amp (ADInstruments) with a Power lab 2/26 (PL2602) data acquisition system.

Cystometrograms were analyzed using LabChart software (ADInstruments). Recordings were conducted for 1 hr or until a steady pattern was achieved. 3-5 consecutive voids were analyzed

and averaged per animal and were selected by an individual blinded to treatment conditions. Parameters measured are described in detail previously [42] and include void duration (time between threshold pressure and baseline pressure after a void), void interval (time between baseline pressure to baseline pressure during a void cycle), normalized threshold pressure (threshold pressure - baseline pressure), normalized peak void pressure (peak void pressure - baseline pressure), non-voiding contractions (spikes in pressure before a void not leading to release of urine) and compliance (infused volume/change in pressure (threshold-baseline)).

### **Gene Expression Analysis via NanoString Profiling**

Data was analyzed by ROSALIND® (<https://rosalind.bio/>), with a HyperScale architecture developed by ROSALIND, Inc. (San Diego, CA). Read Distribution percentages, violin plots, identity heatmaps, and sample MDS plots were generated as part of the QC step. Normalization, fold changes and p-values were calculated using criteria provided by Nanostring. ROSALIND® follows the nCounter® Advanced Analysis protocol of dividing counts within a lane by the geometric mean of the normalizer probes from the same lane. Housekeeping probes to be used for normalization are selected based on the geNorm algorithm as implemented in the NormqPCR R library [43]. Abundance of various cell populations is calculated on ROSALIND using the Nanostring Cell Type Profiling Module. ROSALIND performs a filtering of Cell Type Profiling results to include results that have scores with a p value greater than or equal to 0.05. Fold changes and p values are calculated using the fast method as described in the nCounter® Advanced Analysis 2.0 User Manual. P-value adjustment is performed using the Benjamini-Hochberg method of estimating false discovery rates (FDR). Clustering of genes for the final heatmap of differentially expressed genes was done using the PAM (Partitioning Around

Medoids) method using the fpc R. Hypergeometric distribution was used to analyze the enrichment of pathways, gene ontology, domain structure, and other ontologies [43].

### **Statistical Analysis**

Statistical analyses were conducted using GraphPad Prism version 10.0.2 (GraphPad Software, La Jolla, California). We evaluated the normality of the data through the Kolmogorov-Smirnov or D'Agostino-Pearson omnibus tests within this software. Non-normal data underwent transformation (logarithmic or square root) to achieve normality. For analyses involving multiple t-tests, FDR approach was utilized to adjust for multiple comparisons. Experiments involving multiple time points used one-way or two-way ANOVA, with Tukey's multiple comparisons test for repeated measures to identify significant differences among treatment groups. A p-value of less than 0.05 was deemed to indicate statistical significance. All data shown are the means  $\pm$  SEM. The determination of a 50% threshold was facilitated by the application of the following equation:

50% Threshold =  $X_f + \kappa \times \delta$ , where  $X_f$  denotes the value (in log units) of the final von Frey filament used,  $\kappa$  represents the tabular value corresponding to the pattern of positive/negative responses, and  $\delta$  signifies the mean difference (in log units) between stimuli.

## References

1. Duloy, A.M., E.A. Calhoun, and J.Q. Clemens, *Economic impact of chronic prostatitis*. *Curr Urol Rep*, 2007. **8**(4): p. 336-9.
2. Welliver, C., et al., *Evolution of healthcare costs for lower urinary tract symptoms associated with benign prostatic hyperplasia*. *Int Urol Nephrol*, 2022. **54**(11): p. 2797-2803.
3. Chen, L., M. Zhang, and C. Liang, *Chronic Prostatitis and Pelvic Pain Syndrome: Another Autoimmune Disease?* *Arch Immunol Ther Exp (Warsz)*, 2021. **69**(1): p. 24.
4. Zhang, Y., et al., *Influence of Experimental Autoimmune Prostatitis on Sexual Function and the Anti-inflammatory Efficacy of Celecoxib in a Rat Model*. *Front Immunol*, 2020. **11**: p. 574212.
5. Liu, Y., et al., *Experimental autoimmune prostatitis: different antigens induction and antigen-specific therapy*. *Int Urol Nephrol*, 2021. **53**(4): p. 607-618.
6. Vinnik, Y.Y., A.V. Kuzmenko, and T.A. Gyaurgiev, *[Treatment of the chronic prostatitis: current state of the problem]*. *Urologiia*, 2021(4): p. 138-144.
7. Vickman, R.E., et al., *TNF is a potential therapeutic target to suppress prostatic inflammation and hyperplasia in autoimmune disease*. *Nat Commun*, 2022. **13**(1): p. 2133.



8. Liedtke, V., et al., *Benign prostatic hyperplasia - A novel autoimmune disease with a potential therapy consequence?* *Autoimmun Rev*, 2023. **23**(3): p. 103511.
9. Rikken, G., et al., *Carboxamide Derivatives Are Potential Therapeutic AHR Ligands for Restoring IL-4 Mediated Repression of Epidermal Differentiation Proteins.* *Int J Mol Sci*, 2022. **23**(3).
10. Rothhammer, V., et al., *Type I interferons and microbial metabolites of tryptophan modulate astrocyte activity and central nervous system inflammation via the aryl hydrocarbon receptor.* *Nat Med*, 2016. **22**(6): p. 586-97.
11. Gupta, A., et al., *Anthropometric and metabolic factors and risk of benign prostatic hyperplasia: a prospective cohort study of Air Force veterans.* *Urology*, 2006. **68**(6): p. 1198-205.
12. Gupta, A., et al., *Serum dioxin, testosterone, and subsequent risk of benign prostatic hyperplasia: a prospective cohort study of Air Force veterans.* *Environ Health Perspect*, 2006. **114**(11): p. 1649-54.
13. Gupta, A., et al., *Dioxin exposure and benign prostatic hyperplasia.* *J Occup Environ Med*, 2006. **48**(7): p. 708-14.
14. Song, J., et al., *A ligand for the aryl hydrocarbon receptor isolated from lung.* *Proc Natl Acad Sci U S A*, 2002. **99**(23): p. 14694-9.
15. Rivero, V.E., et al., *Autoimmune etiology in chronic prostatitis syndrome: an advance in the understanding of this pathology.* *Crit Rev Immunol*, 2007. **27**(1): p. 33-46.
16. Hou, Y., et al., *An aberrant prostate antigen-specific immune response causes prostatitis in mice and is associated with chronic prostatitis in humans.* *J Clin Invest*, 2009. **119**(7): p. 2031-41.

17. Yue, T., et al., *The AHR Signaling Attenuates Autoimmune Responses During the Development of Type 1 Diabetes*. *Front Immunol*, 2020. **11**: p. 1510.
18. Breser, M.L., et al., *Immunological Mechanisms Underlying Chronic Pelvic Pain and Prostate Inflammation in Chronic Pelvic Pain Syndrome*. *Front Immunol*, 2017. **8**: p. 898.
19. Nickel, J.C., *Prostatitis*. *Can Urol Assoc J*, 2011. **5**(5): p. 306-15.
20. Toh, K.L. and C.K. Ng, *Urodynamic studies in the evaluation of young men presenting with lower urinary tract symptoms*. *Int J Urol*, 2006. **13**(5): p. 520-3.
21. Maglakelidze, N., et al., *CKTG " F g h k e k g p e { " N g c f u " v q " v j g " F g x g Like Lesions in Mice*. *J Invest Dermatol*, 2023. **143**(4): p. 578-587.e3.
22. He, H., et al., *Autonomic Nervous System Dysfunction Is Related to Chronic Prostatitis/Chronic Pelvic Pain Syndrome*. *World J Mens Health*, 2024. **42**(1): p. 1-28.
23. Wagenlehner, F.M., et al., *National Institutes of Health Chronic Prostatitis Symptom Index (NIH-CPSI) symptom evaluation in multinational cohorts of patients with chronic prostatitis/chronic pelvic pain syndrome*. *Eur Urol*, 2013. **63**(5): p. 953-9.
24. Zhang, Q., et al., *A Preliminary Study in Immune Response of BALB/c and C57BL/6 Mice with a Locally Allergic Rhinitis Model*. *Am J Rhinol Allergy*, 2023. **37**(4): p. 410-418.
25. Dotan, I., et al., *Intestinal epithelial cells from inflammatory bowel disease patients preferentially stimulate CD4+ T cells to proliferate and secrete interferon-gamma*. *Am J Physiol Gastrointest Liver Physiol*, 2007. **292**(6): p. G1630-40.
26. Heuberger, C., J. Pott, and K.J. Maloy, *Why do intestinal epithelial cells express MHC class II? Immunology*, 2021. **162**(4): p. 357-367.

27. Lorenzo, G., et al., *Tissue-scale, personalized modeling and simulation of prostate cancer growth*. Proc Natl Acad Sci U S A, 2016. **113**(48): p. E7663-e7671.
28. Koyama, M., et al., *MHC Class II Antigen Presentation by the Intestinal Epithelium Initiates Graft-versus-Host Disease and Is Influenced by the Microbiota*. Immunity, 2019. **51**(5): p. 885-898.e7.
29. Kelly, J., D.G. Weir, and C. Feighery, *Differential expression of HLA-D gene products in the normal and coeliac small bowel*. Tissue Antigens, 1988. **31**(3): p. 151-60.
30. Tang, Z., et al., *Mice with double knockout of H2-Eb1 and H2-Ab1 exhibit reduced susceptibility to allergic rhinitis*. PLoS One, 2018. **13**(10): p. e0206122.
31. Covassin, L., et al., *Human peripheral blood CD4 T cell-engrafted non-obese diabetic-*u e k f " K N 4 -Ab1 (tmpl Grm) Tg (hündan4* leucocyte antigen D-related 4) mice: a mouse model of human allogeneic graft-versus-host disease. Clin Exp Immunol, 2011. **166**(2): p. 269-80.*
32. Fader, K.A., et al., *2,3,7,8-Tetrachlorodibenzo-p-Dioxin Alters Lipid Metabolism and Depletes Immune Cell Populations in the Jejunum of C57BL/6 Mice*. Toxicol Sci, 2015. **148**(2): p. 567-80.
33. Boverhof, D.R., et al., *Comparative toxicogenomic analysis of the hepatotoxic effects of TCDD in Sprague Dawley rats and C57BL/6 mice*. Toxicol Sci, 2006. **94**(2): p. 398-416.
34. Xu, Y.D., et al., *S100A8 protein attenuates airway hyperresponsiveness by suppressing the contraction of airway smooth muscle*. Biochem Biophys Res Commun, 2017. **484**(1): p. 184-188.
35. Carnazzo, V., et al., *Calprotectin: two sides of the same coin*. Rheumatology (Oxford), 2024. **63**(1): p. 26-33.

36. Huang, J.X., et al., *Calprotectin in psoriatic arthritis: Inflammation and beyond*. Int J Rheum Dis, 2023. **26**(1): p. 11-12.
37. Khaki-Khatibi, F., et al., *Calprotectin in inflammatory bowel disease*. Clin Chim Acta, 2020. **510**: p. 556-565.
38. Wang, S., et al., *S100A8/A9 in Inflammation*. Front Immunol, 2018. **9**: p. 1298.
39. Rudick, C.N., A.J. Schaeffer, and P. Thumbikat, *Experimental autoimmune prostatitis induces chronic pelvic pain*. Am J Physiol Regul Integr Comp Physiol, 2008. **294**(4): p. R1268-75.
40. Wegner, K.A., et al., *Void spot assay procedural optimization and software for rapid and objective quantification of rodent voiding function, including overlapping urine spots*. Am J Physiol Renal Physiol, 2018. **315**(4): p. F1067-f1080.
41. Keil, K.P., et al., *Androgen receptor DNA methylation regulates the timing and androgen sensitivity of mouse prostate ductal development*. Dev Biol, 2014. **396**(2): p. 237-45.
42. Kennedy, C.L., et al., *Developmental polychlorinated biphenyl (PCB) exposure alters voiding physiology in young adult male and female mice*. Am J Clin Exp Urol, 2022. **10**(2): p. 82-97.
43. Perkins, J.R., et al., *ReadqPCR and NormqPCR: R packages for the reading, quality checking and normalisation of RT-qPCR quantification cycle (Cq) data*. BMC Genomics, 2012. **13**: p. 296.

## Figures & Legends

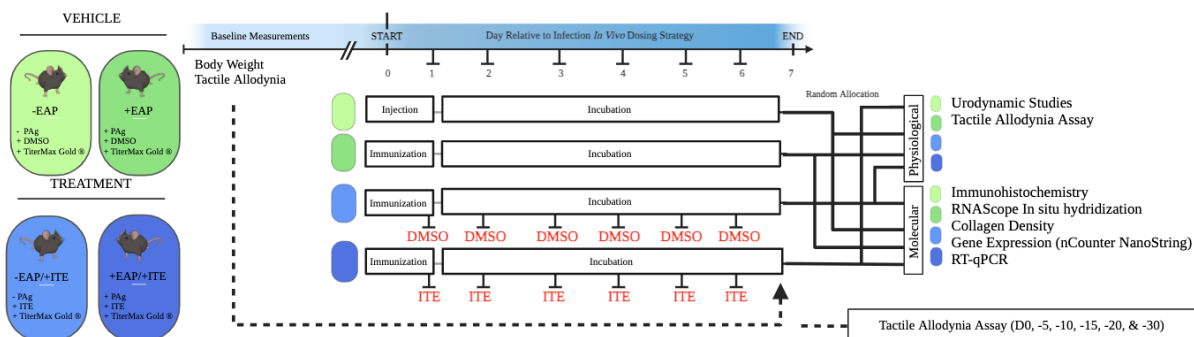


**Fig. 1: Study Design.** C57Bl/6J male mice aged 7-9wks were used, and randomly selected and placed into one of four experimental groups. A long term cohort was selected and treated in the same fashion contingent upon experimental group and received VFT testing on D0, -5, -10, -20 and -30 post immunization. All groups received TiterMax Gold<sup>®</sup> Adjuvant for immunization. Vehicle treated animals were dosed with dimethyl sulfoxide (DMSO) with or without combination injection with prostate antigen (PAg). Treatment group received 2-(1'-H-indole-3'carbonyl)-thiazole-4-carboxylic acid methyl ester (ITE) with or without combination injection with prostate antigen (PAg). Groups receiving vehicle and treatment dosing were dosed daily (qd) for 6 days. 7 days post immunization animals were evenly split randomly into physiological or molecular testing groups.

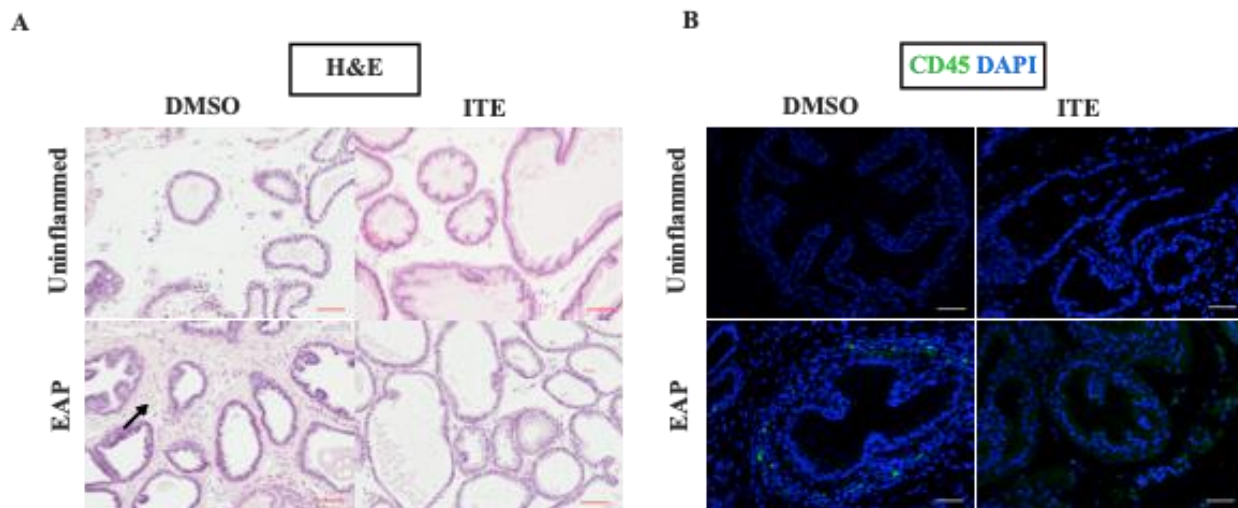


**Fig. 2. ITE protects against an EAP mediated increase in dorsal prostate inflammation.** EAP was induced and mice were treated with ITE or DMSO (vehicle) as described in Fig. 1 and dorsal prostate tissue was collected seven days after induction of EAP and 5  $\mu$ m formalin fixed, paraffin embedded tissue sections were prepared. (A) Tissue sections were stained with hematoxylin and eosin. Note the thickened periductal stroma in EAP mice (arrowhead) and that ITE protected against this histological change which is normally associated with inflammation. (B) Tissue sections were labeled with an antibody against CD45 (green, labels leukocytes) and stained with DAPI (blue) to visualize nuclei. Results are representative of three mice per group. Scale bars are 100  $\mu$ m.

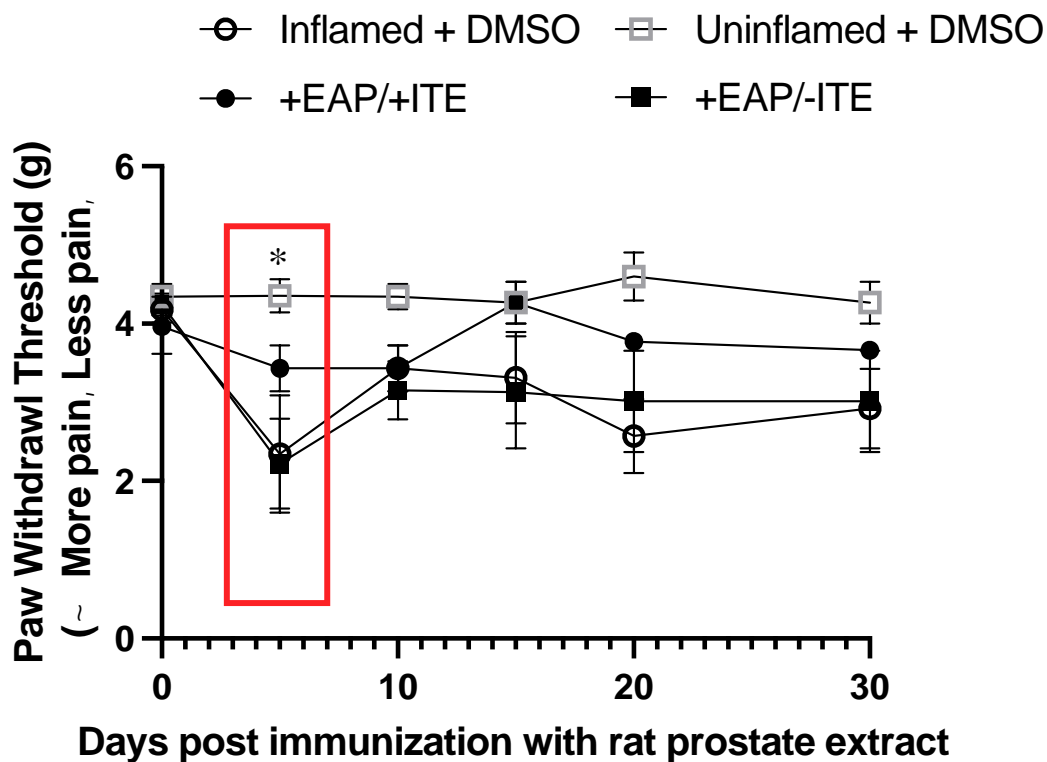


**Fig. 3. ITE protects against an EAP mediated allodynia.** EAP was induced and mice were treated with ITE or DMSO (vehicle) as described in Fig. 1. Von Frey filaments of increasing stiffness were applied to the sural region of the hind paw, every 5 days, to determine the amount of force required to induce paw withdrawal. Von Frey testing was repeated for a duration of 30 days. Results are mean  $\pm$  SEM of three mice/group. Two-way ANOVA with Tukey's multiple comparison test was used to compare means. Asterisks indicate a significant difference between groups (+EAP/+ITE v +EAP/DMSO  $p=0.0256$ ) using a paired t test.

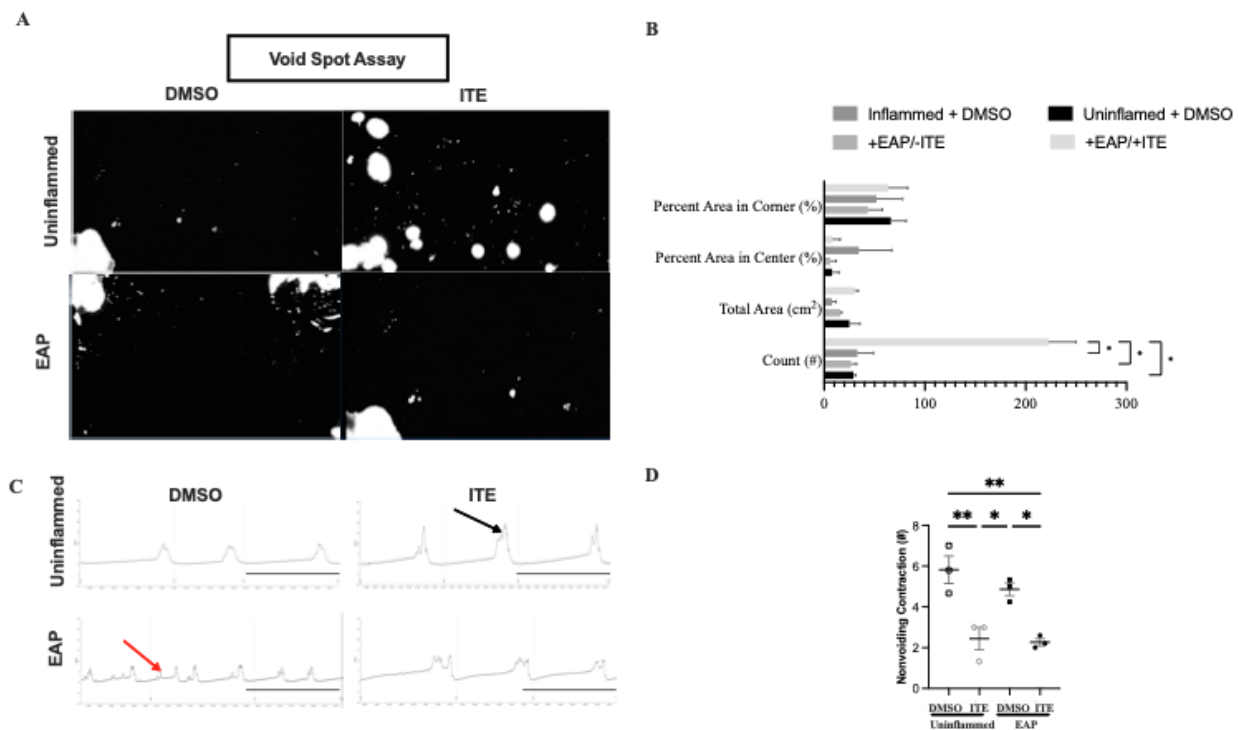


**Fig. 4. ITE protects against EAP mediated changes to voiding behavior.** EAP was induced and mice were treated with ITE or DMSO (vehicle) as described in Fig. 1 and voiding behavior was evaluated on day 7. (A). The void spot assay (VSA) was used to quantify spontaneous voiding behavior. Mice were tested in cages lined with Whatman cellulose filter paper. Representative voiding patterns are shown at the left. Total void spots were quantified in the graph at the right, results are mean  $\pm$  SEM, 3 mice per group. Differences between groups were determined using Tukey's multiple comparison test. A significant difference between groups was  $P < 0.05$ . (B) Parameters examined following the 4-hr VSA include: relative frequency (%), total area, and urine spot distribution, and total spot count. Two-way ANOVA followed by Dunnett's multiple comparison test. (C) Mice were anesthetized, a cystostomy catheter was passed through the bladder dome, and saline was infused at a rate of 1.5 ml/h while continuously measuring bladder pressure



in response to filling and emptying. Representative pressure versus time traces are shown. Intravesical pressures (mmHg) are shown on the y-axis. Scale bars: 2.5 min. Black arrows indicate bladder contractions during a voiding event, while red arrows indicate non-voiding contractions. Non-voiding contractions were quantified in the graph at the right, results are mean  $\pm$  SEM, 3 mice per group. Differences between groups were determined using two-way ANOVA. A significant difference between groups was  $P < 0.05$ .

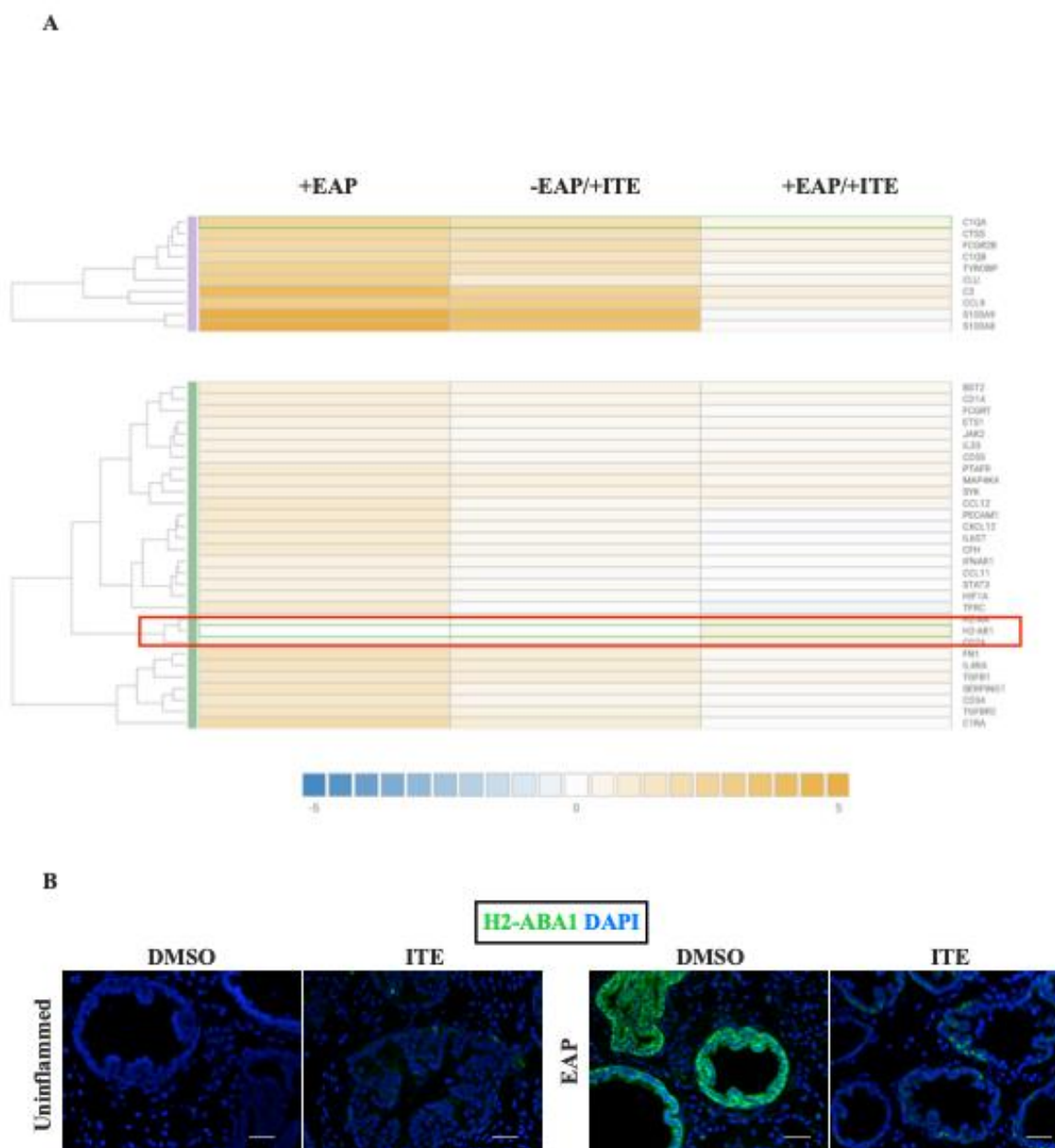


**Fig. 5. ITE protects against some EAP mediated changes in inflammatory gene expression.** EAP was induced and mice were treated with ITE or DMSO (vehicle) as described in Fig. 1 and dorsal prostate tissue was collected seven days after induction of EAP. (A) The Nanostring nCounter Inflammation panel was used to evaluate inflammatory gene expression. ITE protected

against an EAP mediated increase in a cluster of RNAs which included *H2-ab1*. (B) Tissue sections were labeled with an RNAScope™ probe against *H2-ab1* (green) and stained with DAPI (blue) to visualize nuclei. Results are representative of three mice per group. Scale bars are 100 μm.

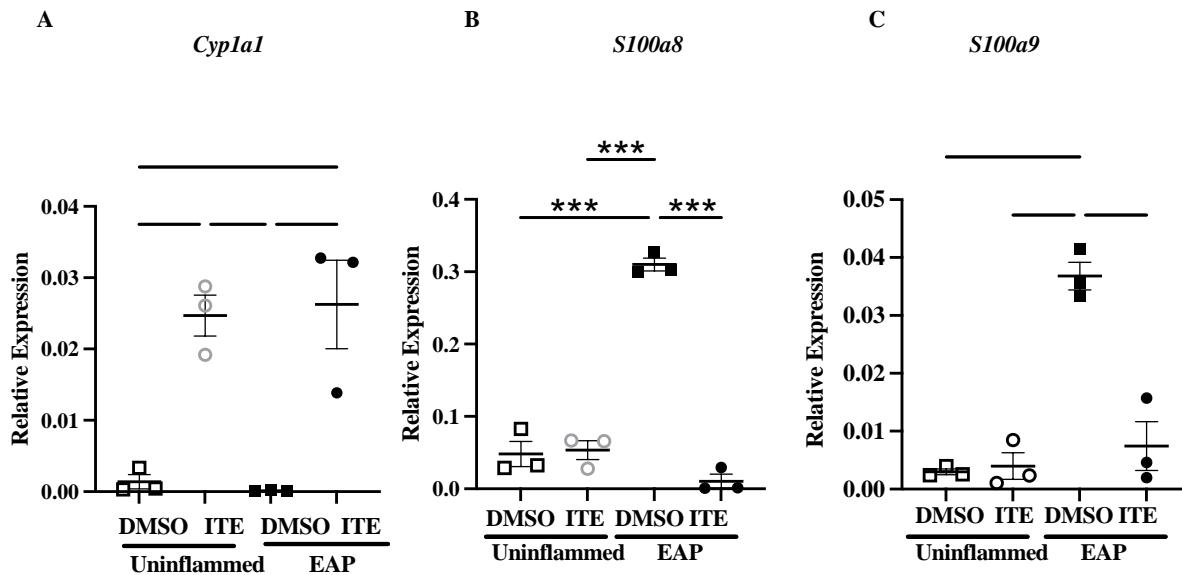


**Fig. 6. ITE increases mRNA abundance of the canonical AHR target gene, cytochrome P450 1B1 (*Cyp1a1*) and calprotectin heterodimers *S100a8* and *S100a9*.** EAP was induced and mice were treated with ITE or DMSO (vehicle) as described in Fig. 1 and prostate tissue was collected four hr later. The relative abundance of *Cyp1a1* (A), *S100a8* (B), and *S100a9* (C) were determined and normalized to the abundance of peptidyl prolyl isomerase A (*Ppia*). Results are mean  $\pm$  SEM, 3 mice per group. Differences between groups were determined using an un-paired Student's *t*-tests. A significant difference between groups was considered  $P < 0.05$ .

**Supplement Table 1: NanoString Immunology Panel**

<b>Name</b>	<b>1</b>	<b>2</b>	<b>3</b>	<b>4</b>	<b>5</b>	<b>6</b>	<b>7</b>	<b>8</b>	<b>9</b>	<b>10</b>	<b>11</b>	<b>12</b>
<b>Abl1</b>	6.60 399	6.254 89	6.44 167	6.32 458	6.62 482	6.34 035	6.78 465	6.31 407	6.50 016	6.40 732	6.93 828	7.02 502
<b>Cfd</b>	10.5 852	7.696 49	9.70 997	8.29 103	10.4 502	8.58 497	8.15 787	8.35 987	9.22 434	5.77 173	9.44 654	9.02 033
<b>Aicda</b>	2.16 105	2.852 8	0.81 7175	1.88 164	1.80 039	2.23 182	2.39 234	3.52 98	2.14 967	0.96 4375	2.25 178	1.75 824
<b>Aire</b>	2.74 601	3.045 44	2.23 221	2.20 357	2.21 543	2.23 182	3.39 234	3.16 723	2.14 967	1.96 438	3.25 178	2.92 816
<b>App</b>	10.7 913	10.90 26	10.9 665	10.9 328	10.7 292	10.7 475	10.8 211	10.8 059	10.8 776	10.8 508	10.6 333	10.9 042
<b>Arhg dib</b>	6.37 05	6.504 87	9.11 485	6.32 458	6.97 032	6.34 035	6.57 82	6.50 962	6.93 626	6.99 78	9.02 327	9.16 55
<b>Atm</b>	6.92 923	6.915 8	6.35 115	6.75 2	7.02 279	7.05 2	7.30 881	7.45 79	6.95 702	7.14 428	7.49 019	6.53 96
<b>B2m</b>	14.7 815	15.09 83	14.7 491	14.6 706	14.7 932	14.9 521	15.1 19	15.0 172	15.0 278	15.0 034	15.0 689	14.8 533
<b>Bax</b>	7.46 483	7.622 87	8.01 685	7.47 41	7.49 155	7.35 076	7.49 667	7.58 869	7.50 722	7.82 856	7.63 549	7.62 242
<b>Bcl2</b>	5.58 731	4.852 8	5.40 214	5.46 66	5.88 786	5.44 127	5.49 667	5.35 987	5.95 702	5.87 127	6.31 787	6.25 009
<b>Bcl3</b>	3.48 297	3.745 88	4.09 019	1.46 66	3.80 039	2.55 375	3.39 234	2.94 483	3.28 717	3.66 481	4.83 674	5.08 016
<b>Bcl6</b>	5.40 897	4.952 33	4.98 71	4.78 853	5.34 471	4.93 226	4.92 839	5.48 915	5.03 719	4.28 63	5.20 598	5.59 113
<b>Bid</b>	5.11 524	4.999 64	5.46 103	4.78 853	5.02 279	4.55 375	5.19 969	4.52 98	4.99 766	5.05 184	6.22 906	5.96 769
<b>Prdm 1</b>	3.48 297	3.045 44	3.62 453	3.78 853	4.21 543	4.31 928	4.39 234	4.26 676	4.14 967	4.21 23	4.25 178	4.00 616
<b>Cxcr5</b>	5.51 86	5.367 37	4.09 019	4.96 91	5.50 083	5.27 622	6.00 115	5.85 172	5.41 27	5.45 623	5.67 805	4.15 055

<b>Bst1</b>	3.33 097	3.504 87	6.84 692	2.46 66	4.02 279	3.23 182	3.77 085	4.06 031	4.22 006	5.05 184	6.60 933	5.86 676
<b>Btk</b>	3.33 097	3.745 88	5.53 599	2.88 164	3.80 039	3.93 226	3.77 085	3.68 18	4.14 967	4.71 926	5.25 178	5.80 263
<b>Serpi ng1</b>	7.91 593	8.264 61	9.38 323	8.18 085	8.25 982	8.21 481	8.14 722	8.44 733	8.58 263	8.81 612	9.57 821	10.0 144
<b>C1qa</b>	6.55 336	6.600 03	9.33 024	6.18 542	7.19 271	6.49 861	6.64 026	7.39 329	7.40 517	8.04 652	8.83 298	9.12 674
<b>C1qb</b>	7.72 329	7.752 8	10.3 596	7.34 925	8.17 543	7.83 915	7.73 574	8.53 978	8.62 54	9.16 65	9.99 325	10.1 814
<b>C1qb p</b>	8.46 025	8.367 37	8.23 221	8.52 188	8.24 885	8.48 449	8.38 782	8.42 596	8.43 876	8.13 43	8.54 64	8.46 904
<b>C2</b>	5.74 601	5.630 4	6.91 169	4.83 584	6.07 341	5.44 127	5.77 085	5.64 527	6.11 314	5.63 68	6.99 325	7.08 915
<b>Ciita</b>	4.16 105	4.132 9	4.72 407	3.58 208	3.80 039	4.13 871	4.15 787	4.81 93	5.18 529	5.21 23	4.64 41	4.00 616
<b>C3</b>	8.71 563	8.735 44	12.3 352	7.98 493	8.99 679	8.63 696	8.52 574	9.71 742	9.63 348	10.8 371	12.8 702	12.8 079
<b>C4bp</b>	4.16 105	4.504 87	4.40 214	3.34 107	3.80 039	3.81 678	3.97 73	4.75 219	4.63 509	4.54 934	5.53 718	4.71 243
<b>C6</b>	6.95 546	6.915 8	6.53 599	6.60 956	7.34 471	6.86 118	7.39 234	7.52 98	7.04 691	7.55 683	7.72 752	6.13 328
<b>C9</b>	4.33 097	4.045 44	3.23 221	3.05 156	3.91 587	4.31 928	4.24 033	4.60 78	3.73 463	4.21 23	4.49 971	2.92 816
<b>Casp 1</b>	4.40 897	4.437 76	5.62 453	3.96 91	4.38 535	4.47 975	4.15 787	4.52 98	4.78 193	5.00 877	5.77 534	6.26 603
<b>Casp 2</b>	4.86 149	4.999 64	5.11 486	4.52 55	5.16 963	5.58 937	5.31 834	5.21 785	4.63 509	5.42 381	6.05 914	5.64 088
<b>Casp 3</b>	6.99 394	7.067 81	7.44 653	6.90 401	6.98 361	7.02 624	6.90 33	6.94 483	7.00 765	7.54 18	7.38 107	7.24 205
<b>Casp 8</b>	7.19 447	7.454 83	7.65 848	7.31 627	7.36 518	7.34 035	7.33 719	7.53 978	7.36 69	7.48 794	7.75 163	7.78 614
<b>Ctnn b1</b>	10.9 457	10.97 62	11.0 738	10.9 645	10.9 695	11.0 156	11.0 633	11.1 022	11.0 869	11.0 631	11.1 884	11.2 314
<b>Runx 1</b>	6.20 544	6.022 72	6.98 04	5.73 962	6.28 152	6.38 157	6.35 581	6.50 962	6.44 245	6.44 011	7.08 467	7.34 32
<b>Runx 3</b>	4.74 601	4.689 3	3.81 717	4.27 396	4.60 775	4.31 928	4.59 397	5.16 723	5.18 529	5.09 366	5.29 618	3.34 32
<b>Ccr6</b>	3.16 105	1.045 44	2.93 265	2.46 66	3.21 543	2.23 182	2.87 776	3.94 483	1.82 774	3.87 127	3.05 914	2.08 016
<b>Cd14</b>	7.14 973	7.100 72	7.53 142	6.46 66	7.12 232	7.29 791	7.41 914	7.55 954	7.09 452	7.49 576	8.26 859	7.06 202
<b>Ctla4</b>	2.16 105	2.045 44	2.69 164	- 0.11 8361	1.21 543	1.81 678	2.87 776	3.52 98	2.41 27	2.28 63	2.83 674	2.08 016

<b>Cd19</b>	3.86 149	2.045 44	5.55 414	2.88 164	3.02 278	3.03 918	3.52 984	4.16 723	3.52 818	3.77 173	4.15 867	4.56 559
<b>Cd1d 1</b>	5.06 794	3.952 33	5.57 206	4.34 107	5.42 488	4.75 538	4.92 839	4.75 219	5.31 959	5.35 669	4.71 121	5.64 088
<b>Cd2</b>	4.96 84	3.852 8	5.38 196	4.52 55	3.38 536	4.13 871	4.87 776	4.26 676	5.11 314	4.54 934	4.64 41	5.04 364
<b>Ms4a 1</b>	4.96 84	4.437 76	7.18 641	4.92 603	4.73 899	4.55 375	4.97 73	5.16 723	4.63 509	5.48 794	5.10 976	5.68 897
<b>Cd22</b>	6.98 122	6.928 08	6.25 458	6.42 08	7.16 963	7.00 001	7.24 033	7.49 942	7.03 719	7.31 31	7.62 682	6.40 209
<b>Cd24 a</b>	12.0 175	12.45 51	12.0 542	12.4 643	12.1 927	12.2 714	12.4 606	11.9 406	12.0 646	12.4 029	12.0 046	11.6 096
<b>Cd28</b>	6.29 033	6.195 19	5.27 661	5.60 956	6.21 543	6.08 98	6.91 59	7.06 031	5.93 626	6.66 481	6.55 556	4.80 263
<b>Cd34</b>	8.65 29	8.663 83	9.78 68	8.18 998	9.05 463	8.85 021	8.60 957	8.91 446	9.10 851	9.44 416	10.1 237	10.2 187
<b>Cd36</b>	7.86 149	6.839 86	8.54 736	6.46 66	7.90 892	6.53 56	7.36 503	6.85 172	7.65 429	7.16 405	8.21 178	8.60 059
<b>Entp d1</b>	7.53 609	7.553 24	7.69 574	7.38 149	7.62 482	7.62 414	7.69 976	7.92 211	7.60 252	7.86 524	8.18 842	7.86 152
<b>Cd3d</b>	4.24 851	3.852 8	3.23 221	3.88 164	3.91 587	4.69 125	4.87 776	4.75 219	4.52 818	4.60 823	5.29 618	4.45 868
<b>Cd3e</b>	1.74 601	2.367 37	2.03 957	3.20 357	1.21 543	1.81 678	2.39 234	1.94 483	3.28 717	2.54 934	4.05 914	3.08 016
<b>Cd24 7</b>	5.94 241	5.215 37	4.69 164	4.46 66	5.07 341	5.08 98	5.42 796	6.11 476	5.63 509	5.45 623	6.03 314	5.28 18
<b>Cd4</b>	6.51 86	6.330 84	5.58 976	5.94 773	6.62 482	6.53 56	6.95 305	7.18 005	6.50 016	6.75 879	7.09 727	4.40 209
<b>Cd44</b>	8.43 717	8.195 19	8.94 989	8.45 529	8.52 377	8.51 722	8.65 161	8.64 989	8.62 864	8.53 802	9.41 417	8.92 565
<b>Cd48</b>	5.44 645	4.689 3	6.93 265	5.16 704	5.70 728	5.31 928	5.19 969	5.94 483	5.80 502	5.84 702	6.85 17	7.25 009
<b>Cd5</b>	6.44 645	6.312 23	5.42 204	6.29 103	6.65 837	6.49 861	6.85 177	6.78 614	6.20 278	6.79 727	7.08 467	5.11 579
<b>Cd53</b>	3.74 601	3.215 37	4.87 607	3.20 357	3.53 736	3.03 918	3.24 033	3.68 18	4.07 567	4.05 184	4.05 914	4.45 868
<b>Cd6</b>	2.16 105	1.630 4	1.81 717	1.88 164	3.02 278	2.23 182	3.24 033	2.35 987	1.41 27	2.28 63	2.57 371	2.08 016
<b>Cd69</b>	1.74 601	3.504 87	1.55 414	3.46 66	3.02 278	3.55 375	3.52 984	2.94 483	2.99 766	3.54 934	3.42 171	3.66 513
<b>Cd7</b>	3.16 105	3.367 37	4.03 957	1.88 164	3.53 736	4.13 871	3.39 234	4.35 987	3.82 774	4.05 184	4.49 971	3.75 824
<b>Cd79 a</b>	2.96 84	2.852 8	3.48 014	2.46 66	3.02 278	2.81 678	2.87 776	3.52 98	3.28 717	3.77 173	3.42 171	3.21 767

<b>Cd80</b>	3.16 105	3.630 4	5.20 949	3.68 899	3.80 039	3.40 175	3.87 776	5.06 031	3.73 463	4.35 669	5.05 914	5.34 32
<b>Cd81</b>	10.1 903	10.29 46	10.3 263	10.1 032	10.2 829	10.2 262	10.1 459	10.2 038	10.2 201	10.3 064	10.5 418	10.5 832
<b>Cd82</b>	8.79 04	8.776 76	8.51 761	8.97 44	8.70 327	8.83 173	8.90 33	8.89 515	8.66 694	8.84 702	8.68 641	8.70 075
<b>Cd83</b>	5.01 903	3.504 87	5.53 599	3.96 91	4.73 899	4.40 175	4.15 787	5.35 987	5.31 959	4.48 794	5.49 971	5.40 209
<b>Cd86</b>	3.33 097	4.045 44	5.31 967	3.68 899	3.91 587	3.81 678	4.39 234	4.06 031	4.47 159	4.48 794	5.33 924	5.18 45
<b>Cd8a</b>	6.20 544	6.067 81	5.31 967	5.85 892	6.16 963	6.13 871	6.67 032	6.81 93	6.09 452	6.62 259	6.71 121	4.56 559
<b>Cd8b 1</b>	2.96 84	3.504 87	2.69 164	1.46 66	3.38 536	0.23 1821	3.52 984	3.52 98	3.14 967	3.96 438	3.25 178	2.92 816
<b>Cd9</b>	10.1 398	10.02 56	9.92 831	9.87 316	9.99 679	10.0 991	10.1 958	9.92 593	10.0 348	10.0 807	10.5 267	9.96 036
<b>Cdh5</b>	5.86 149	5.402 99	6.72 407	5.52 55	5.99 679	5.55 375	5.85 177	5.91 446	5.85 011	6.09 366	6.99 325	7.61 622
<b>Cdkn 1a</b>	5.80 49	5.952 33	6.99 376	5.88 164	6.23 78	6.49 861	6.00 115	6.85 172	6.38 233	6.60 823	6.38 107	6.44 474
<b>Cebp b</b>	6.62 048	6.045 44	7.99 376	6.34 107	6.46 336	6.08 98	5.85 177	6.92 973	6.66 063	6.54 934	8.01 997	7.82 97
<b>Cfh</b>	7.74 601	7.766 54	9.23 362	7.60 956	8.41 019	8.05 837	8.07 603	8.23 024	8.28 306	8.49 576	9.22 62	9.41 466
<b>Cfi</b>	3.86 149	3.952 33	3.87 607	3.96 91	3.67 486	3.93 226	3.97 73	3.81 93	2.99 766	4.21 23	4.71 121	4.45 868
<b>Chuk</b>	8.79 767	8.881 49	8.60 29	8.94 234	8.94 675	8.93 918	9.06 193	8.92 973	8.83 617	8.85 007	8.40 153	8.75 824
<b>Cish</b>	6.57 044	6.471 7	5.60 725	6.40 52	6.94 335	6.62 414	7.07 041	7.41 515	6.75 848	6.95 306	7.14 66	5.59 113
<b>Socs3</b>	6.48 297	6.385 29	5.75 577	6.09 109	6.81 534	6.91 832	6.62 5	7.10 134	6.71 038	6.69 23	7.13 443	6.04 364
<b>Socs1</b>	4.91 593	5.254 89	5.27 661	4.96 91	5.50 083	5.13 871	5.62 5	5.40 427	5.63 509	5.45 623	6.29 618	5.98 706
<b>Clu</b>	11.4 511	11.49 1	12.4 55	10.2 556	11.5 175	10.7 327	11.5 577	11.1 013	11.1 908	12.4 894	14.3 704	13.1 939
<b>Cxcr2</b>	2.48 297	1.045 44	5.20 949	0.88 1639	2.21 543	1.81 678	2.87 776	2.35 987	1.82 774	2.77 173	5.83 674	4.66 513
<b>Cxcr3</b>	6.29 033	6.471 7	5.96 013	6.38 943	6.44 425	6.62 414	7.14 722	7.18 005	6.51 424	7.16 405	7.07 196	5.37 295
<b>Cxcr4</b>	5.11 524	4.293 37	5.25 458	4.34 107	4.53 736	4.93 226	4.87 776	5.11 476	5.28 717	4.60 823	6.03 314	5.75 824
<b>Ccr9</b>	5.48 297	4.800 33	4.44 167	4.46 66	5.07 341	5.23 182	5.07 041	5.11 476	5.14 967	5.42 381	5.53 718	5.00 616



<b>Ccr3</b>	3.86 149	2.367 37	1.55 414	2.88 164	2.53 736	2.81 678	4.07 041	3.81 93	3.73 463	3.13 43	4.05 914	3.34 32
<b>Ccr2</b>	6.29 033	5.600 03	7.54 962	5.99 016	6.85 929	6.01 318	6.52 984	6.33 715	6.67 323	6.77 173	7.30 706	7.20 945
<b>Ccr4</b>	3.16 105	2.045 44	2.40 214	2.20 357	2.53 736	2.23 182	2.39 234	2.68 18	0.82 7738	2.96 438	3.42 171	2.75 824
<b>Ccr5</b>	6.73 09	6.537 29	6.48 96	6.34 107	6.73 899	6.77 098	7.09 278	7.65 449	7.04 691	7.25 9	7.65 266	6.32 809
<b>Ccr7</b>	2.74 601	2.045 44	3.40 214	- 0.11 8361	1.80 039	3.40 175	2.87 776	3.16 723	3.14 967	2.28 63	3.57 371	3.45 868
<b>Ccr8</b>	2.74 601	2.367 37	0.76 7788	2.46 66	3.38 536	3.03 918	3.97 73	3.52 98	2.99 766	3.13 43	1.83 674	2.92 816
<b>Ccr10</b>	5.62 048	5.630 4	5.16 295	5.37 349	5.91 587	6.13 871	6.64 026	6.86 767	5.82 774	6.35 669	6.49 971	4.80 263
<b>Camp</b>	3.33 097	1.630 4	4.13 91	1.88 164	3.67 486	3.03 918	3.07 041	1.94 483	3.14 967	2.96 438	5.95 222	6.23 397
<b>Cr2</b>	2.48 297	2.367 37	2.23 221	1.46 66	3.02 278	2.23 182	1.65 537	3.52 98	2.41 27	3.87 127	2.83 674	1.75 824
<b>Crad d</b>	5.71 563	6.274 26	6.02 663	6.01 092	6.32 395	6.20 91	6.67 032	6.31 407	6.11 314	6.44 011	6.00 667	6.52 642
<b>Csf1</b>	6.44 645	6.689 3	7.73 206	6.32 458	6.75 459	6.31 928	6.52 984	6.52 98	6.66 063	6.60 823	8.08 467	8.15 912
<b>Csf1r</b>	5.88 897	5.826 8	8.12 4	5.46 66	6.28 152	6.08 98	5.68 512	6.56 932	6.28 717	7.01 966	7.83 674	8.08 467
<b>Csf2</b>	2.74 601	3.045 44	1.81 717	2.88 164	3.38 536	4.03 918	3.52 984	3.35 987	2.99 766	3.77 173	4.05 914	3.08 016
<b>Csf2r b</b>	3.16 105	2.852 8	5.75 577	3.34 107	4.21 543	3.23 182	4.15 787	4.26 676	3.52 818	4.35 669	5.83 674	5.90 798
<b>Csf3r</b>	6.40 897	6.537 29	6.65 848	6.03 139	6.62 482	6.57 167	6.97 73	7.07 412	6.64 792	6.80 987	7.55 556	6.31 283
<b>Ctsc</b>	9.15 54	9.342 36	9.89 042	9.22 371	9.29 225	9.23 182	9.27 498	9.32 277	9.29 126	9.30 2	9.58 27	9.73 695
<b>Ctsg</b>	2.96 84	2.630 4	3.23 221	2.46 66	2.53 736	3.69 125	4.31 834	4.60 78	3.63 509	4.05 184	5.05 914	6.40 209
<b>Ctss</b>	6.91 593	6.745 88	9.83 398	6.62 311	7.62 482	6.94 607	7.29 923	7.80 281	7.97 749	8.49 185	9.58 27	9.29 739
<b>Cx3cr 1</b>	4.24 851	4.630 4	5.36 15	4.68 899	4.67 486	4.03 918	4.59 397	4.68 18	4.87 213	4.91 857	5.92 421	5.08 016
<b>Cybb</b>	5.44 645	5.089 83	7.62 023	5.23 919	5.53 736	5.18 602	5.79 833	6.16 723	6.14 967	6.85 919	7.85 911	7.55 265
<b>Cd55</b>	8.38 505	8.517 12	8.78 103	8.21 703	8.38 535	8.28 167	8.70 34	8.68 18	8.62 864	8.80 673	8.81 402	8.93 316

<b>Defb1</b>	11.9 656	11.81 61	11.9 554	12.5 503	12.7 207	12.1 522	11.3 616	12.6 051	12.0 21	12.6 715	11.9 224	12.1 957
<b>Dpp4</b>	8.79 04	8.884 64	8.52 223	8.99 798	8.83 748	8.94 607	9.04 769	8.73 056	8.93 887	8.80 358	8.63 98	8.51 979
<b>Adgr el</b>	6.16 105	6.215 37	8.76 943	5.55 406	6.73 899	6.20 91	6.22 016	6.75 219	7.01 756	7.37 377	8.67 805	9.08 016
<b>Eome s</b>	6.26 957	6.045 44	5.13 91	5.60 956	5.80 039	6.23 182	6.59 397	6.80 281	6.22 006	6.65 088	6.40 153	4.66 513
<b>Fadd</b>	5.06 794	5.174 72	5.25 458	5.46 66	5.42 488	5.23 182	5.74 283	5.11 476	5.14 967	5.28 63	5.05 914	5.53 96
<b>Ptk2</b>	7.69 243	7.826 8	7.70 795	7.94 773	7.81 534	7.72 367	8.09 278	7.94 483	7.83 336	7.77 816	7.87 383	7.98 706
<b>Fas</b>	6.46 483	6.402 99	6.91 871	6.63 653	6.85 929	6.49 861	7.04 769	6.62 666	6.47 159	6.69 23	6.51 857	6.83 505
<b>Fasl</b>	4.06 794	4.569	3.81 717	4.46 66	3.53 736	4.62 414	4.65 537	4.35 987	4.28 717	4.28 63	4.77 534	4.34 32
<b>Fcer1 a</b>	4.86 149	4.999 64	5.55 414	4.92 603	4.38 535	4.62 414	4.97 73	5.06 031	4.95 702	4.71 926	5.64 41	5.64 088
<b>Fcer1 g</b>	5.16 105	5.174 72	7.95 331	4.88 164	5.16 963	4.93 226	5.27 986	5.35 987	5.97 749	6.45 623	7.68 641	7.81 893
<b>Fcgr1</b>	4.40 897	4.437 76	7.38 196	3.96 91	4.80 039	4.40 175	4.59 397	5.11 476	5.68 572	5.57 909	7.13 443	6.79 166
<b>Fcgr2 b</b>	7.67 675	7.607 68	10.4 109	6.95 846	7.90 892	7.60 686	7.72 146	8.25 469	8.21 576	8.55 683	9.87 017	9.76 105
<b>Fcgr3</b>	5.16 105	5.660 15	7.38 703	5.27 396	5.02 279	5.44 127	5.65 537	5.91 446	6.14 967	6.19 319	6.97 97	6.73 552
<b>Fcgrt</b>	7.57 044	7.667 49	8.84 508	7.38 149	7.80 789	7.79 406	7.64 026	7.81 93	7.96 729	8.21 704	8.60 051	8.60 686
<b>Fkbp 5</b>	7.09 178	7.245 11	6.92 57	7.21 256	7.55 528	7.49 861	6.57 82	7.57 904	7.13 152	7.17 383	7.22 906	7.13 328
<b>Fn1</b>	8.62 865	8.833 34	10.5 263	8.65 972	8.85 205	8.65 389	8.79 833	8.94 107	9.14 062	9.55 122	10.5 51	10.5 502
<b>Fyn</b>	5.71 563	5.537 29	6.24 344	4.92 603	5.80 039	5.58 937	5.82 53	6.14 123	6.11 314	5.82 236	6.60 933	6.71 243
<b>Gata3</b>	9.96 356	10.21 16	9.73 206	10.1 82	10.0 179	10.0 181	10.1 645	9.97 09	9.91 387	10.1 065	9.91 356	9.67 262
<b>Gfi1</b>	2.74 601	2.852 8	3.55 414	2.46 66	3.38 536	3.03 918	2.87 776	3.35 987	3.52 818	3.13 43	4.33 924	3.92 816
<b>Gp1b b</b>	3.74 601	3.504 87	3.31 967	3.05 156	3.21 543	2.55 375	4.07 041	3.52 98	3.63 509	3.77 173	3.57 371	2.56 559
<b>Lilrb 4a</b>	4.62 048	4.952 33	8.51 761	4.73 962	5.46 336	4.98 671	5.49 667	5.00 373	5.50 016	6.21 23	8.49 019	8.19 703
<b>Cmkl r1</b>	4.91 593	4.852 8	6.27 661	4.96 91	5.12 232	4.55 375	5.07 041	5.26 676	4.99 766	5.87 127	6.46 124	6.67 71

<b>Gpi1</b>	6.37 05	6.045 44	5.46 103	6.03 139	6.34 471	6.29 791	6.39 234	6.75 219	6.28 717	6.19 319	6.89 564	5.25 009
<b>Cxcl1</b>	3.96 84	2.852 8	5.70 795	3.46 66	3.02 278	4.03 918	4.31 834	4.68 18	4.07 567	4.48 794	6.08 467	6.06 202
<b>Gzma</b>	6.53 609	6.174 72	5.70 795	6.20 357	6.55 528	6.06 471	6.87 776	7.23 024	6.51 424	6.60 823	7.03 314	5.48 616
<b>Gzmb</b>	2.74 601	1.045 44	2.55 414	3.05 156	2.80 039	2.55 375	2.39 234	3.68 18	2.63 509	3.42 381	3.25 178	3.45 868
<b>H2- Aa</b>	9.39 706	9.362 85	9.28 07	9.03 392	9.60 989	9.22 617	9.73 219	9.68 405	10.4 743	9.54 558	9.48 78	9.17 186
<b>H2- Ab1</b>	8.52 299	8.584 6	8.64 372	8.61 635	8.68 304	8.30 864	8.73 574	8.83 965	9.74 958	8.75 554	8.50 445	8.51 979
<b>Cfb</b>	5.06 794	5.045 44	8.78 68	4.27 396	5.12 232	5.03 918	4.46 273	5.71 742	5.66 063	7.15 42	9.29 618	8.59 744
<b>H2- Eb1</b>	7.65 29	7.660 15	7.46 103	7.61 635	7.71 528	7.46 064	7.92 839	8.18 005	8.26 237	7.92 438	8.01 997	6.93 815
<b>H2- K1</b>	8.62 048	8.674 8	9.05 558	8.79 153	8.81 534	8.61 984	8.58 611	8.84 771	9.06 614	8.88 324	9.10 04	8.94 311
<b>H2- DMa</b>	7.31 079	6.999 64	6.62 453	6.85 892	7.41 51	7.24 305	7.63 265	7.59 828	7.67 323	7.53 423	7.69 473	6.26 603
<b>H2- DMb 2</b>	3.86 149	3.504 87	5.34 074	3.34 107	3.67 486	3.93 226	4.77 085	3.68 18	4.22 006	3.77 173	3.25 178	4.40 209
<b>H2- Ob</b>	6.65 29	6.454 83	5.46 103	6.07 146	6.53 736	6.31 928	6.85 177	7.11 476	6.23 713	6.94 166	7.24 047	5.08 016
<b>H2- Q10</b>	6.16 105	5.293 37	4.03 957	7.14 843	8.19 842	6.49 861	5.02 46	7.21 785	6.14 967	6.77 173	6.03 314	6.51 312
<b>Mr1</b>	8.55 765	8.803 66	8.48 251	8.71 769	8.62 482	8.64 545	8.84 52	8.81 52	8.66 063	8.82 236	8.37 072	8.59 744
<b>H60a</b>	3.48 297	3.215 37	2.03 957	2.20 357	2.80 039	2.81 678	2.07 041	2.68 18	2.41 27	2.96 438	2.57 371	2.56 559
<b>Hc</b>	5.83 347	5.903 42	4.09 019	4.73 962	5.16 963	5.51 722	6.22 016	6.42 596	5.50 016	6.00 877	6.00 667	4.28 18
<b>Ptpn6</b>	6.74 601	6.773 36	7.76 749	6.92 603	7.08 579	7.25 419	7.01 292	6.94 483	7.28 717	7.15 42	7.86 649	7.51 312
<b>Hfe</b>	6.99 394	6.878 33	7.51 761	6.82 415	7.14 617	6.53 56	7.07 041	6.98 923	6.92 577	7.16 405	7.48 06	7.35 069
<b>Hif1a</b>	7.20 544	7.513 05	7.99 044	7.43 623	7.50 083	7.47 975	7.31 834	7.45 79	7.62 215	7.37 377	8.39 133	8.30 898
<b>Hlx</b>	6.63 678	6.674 8	6.27 661	6.30 79	7.08 579	6.62 414	7.01 292	7.35 987	6.74 66	7.22 176	7.60 933	6.31 283
<b>Icam 1</b>	3.48 297	3.745 88	5.13 91	2.68 899	3.91 587	3.03 918	3.52 984	4.81 93	4.22 006	4.71 926	5.10 976	5.28 18
<b>Icam 2</b>	6.96 84	6.600 03	6.65 848	6.90 401	7.06 092	6.93 226	7.25 032	7.40 427	7.10 386	7.19 319	7.60 933	6.60 373

<b>Icam 5</b>	6.33 097	5.600 03	4.98 71	5.55 406	6.04 832	5.78 641	6.44 545	6.62 666	5.99 766	6.57 909	6.53 718	3.92 816
<b>Irf8</b>	5.44 645	5.174 72	5.83 213	5.16 704	5.73 899	4.98 671	5.39 234	6.03 23	5.73 463	6.09 366	5.92 421	6.18 45
<b>Irgm 1</b>	7.11 524	7.132 9	7.83 213	7.29 103	7.38 535	7.42 165	7.49 667	7.42 596	7.64 152	7.24 05	8.15 867	8.12 892
<b>Cxcl1 0</b>	5.58 731	6.111 53	5.80 207	5.63 653	5.57 298	6.11 446	6.24 033	6.44 733	6.13 152	6.59 373	6.64 41	5.31 283
<b>Ifi204</b>	5.55 336	5.089 83	7.21 521	4.40 52	5.30 289	5.62 414	5.52 984	6.11 476	5.99 766	5.94 166	7.29 618	7.41 645
<b>Ifit2</b>	5.51 86	5.132 9	6.11 486	4.96 91	5.53 736	5.47 975	5.62 5	4.88 343	5.63 509	5.21 23	5.95 222	6.37 295
<b>Ifna1</b>	3.48 297	3.367 37	3.13 91	2.46 66	3.38 536	2.23 182	2.87 776	4.06 031	2.63 509	3.28 63	4.05 914	3.45 868
<b>Ifna2</b>	3.48 297	2.852 8	2.69 164	1.46 66	3.21 543	2.81 678	3.39 234	3.52 98	3.52 818	3.13 43	3.25 178	2.56 559
<b>Ifnar 1</b>	7.78 31	7.600 03	8.43 678	7.64 319	7.72 322	7.94 607	7.51 335	8.12 806	7.95 186	7.96 438	8.43 666	8.58 478
<b>Ifnar 2</b>	7.57 89	7.529 26	7.53 599	7.12 004	7.46 336	7.47 023	7.81 188	7.76 075	7.52 818	7.66 481	8.25 178	7.64 698
<b>Ifnb1</b>	2.16 105	3.045 44	2.40 214	3.34 107	3.67 486	3.23 182	3.52 984	1.35 987	2.41 27	3.13 43	2.25 178	2.34 32
<b>Ifng</b>	2.96 84	2.367 37	2.40 214	1.46 66	2.80 039	2.55 375	3.65 537	2.94 483	2.63 509	2.77 173	4.15 867	3.08 016
<b>Ifngr 1</b>	9.52 299	9.607 68	9.62 775	9.45 718	9.54 635	9.54 243	9.65 912	9.76 075	9.67 949	9.80 358	9.66 329	9.74 123
<b>Ifngr 2</b>	7.43 717	7.358 32	7.90 464	7.64 982	7.45 384	7.71 564	7.44 545	7.41 515	7.66 694	7.70 584	7.64 41	7.79 716
<b>Cd79 b</b>	6.40 897	6.235 26	6.24 344	5.55 406	6.25 982	6.11 446	6.56 226	6.64 527	6.48 595	6.56 429	6.90 999	5.61 622
<b>Igf2r</b>	7.95 546	8.127 59	8.24 623	8.14 843	8.16 963	8.24 305	8.06 476	8.19 907	8.02 249	8.06 241	7.99 325	8.18 45
<b>Cd74</b>	9.17 507	9.269 44	9.55 639	8.98 493	9.44 184	8.92 182	9.22 776	9.47 361	10.3 785	9.53 233	9.49 496	9.10 031
<b>Ikbkb</b>	7.60 399	7.513 05	7.54 962	7.73 339	7.73 899	7.59 814	7.72 862	7.87 557	7.88 302	7.77 816	7.76 748	7.76 946
<b>Ikbkg</b>	7.00 654	6.645 35	6.37 176	6.80 05	6.46 336	6.75 538	6.62 5	6.81 93	6.35 13	6.67 862	6.31 787	6.85 627
<b>Il10</b>	3.16 105	3.504 87	2.03 957	1.46 66	2.80 039	2.81 678	3.65 537	3.68 18	2.41 27	3.28 63	3.25 178	3.21 767
<b>Il10ra</b>	4.48 297	4.293 37	5.48 014	4.46 66	4.91 587	4.98 671	4.52 984	4.81 93	4.41 27	4.91 857	5.29 618	5.31 283
<b>Il10rb</b>	6.22 713	6.111 53	7.45 138	5.78 853	6.36 518	6.11 446	6.19 969	6.31 407	6.59 592	6.74 574	7.64 41	7.56 559

<b>II1ra 1</b>	4.48 297	4.045 44	4.58 976	4.40 52	4.85 929	5.18 602	4.46 273	4.68 18	4.68 572	4.91 857	5.38 107	5.40 209
<b>II12a</b>	6.16 105	5.903 42	5.01 357	5.60 956	5.83 014	6.40 175	6.69 976	6.60 78	5.97 749	6.48 794	6.89 564	4.61 622
<b>II12b</b>	6.53 609	6.674 8	5.20 949	5.99 016	6.44 425	6.55 375	6.86 482	7.16 723	6.50 016	7.13 43	7.24 047	4.45 868
<b>II12r b1</b>	3.74 601	4.132 9	3.13 91	3.34 107	3.67 486	4.03 918	3.39 234	4.52 98	4.35 13	4.77 173	4.42 171	3.92 816
<b>II12r b2</b>	2.96 84	2.367 37	2.23 221	2.20 357	3.02 278	2.23 182	3.52 984	3.16 723	3.41 27	3.96 438	1.83 674	3.21 767
<b>II13</b>	7.10 356	6.674 8	5.84 692	6.68 899	7.14 617	6.86 118	7.52 984	7.66 365	6.95 702	7.41 559	7.60 051	6.15 055
<b>II13ra 1</b>	8.15 54	8.056 67	8.50 368	8.31 627	8.35 498	8.12 056	8.44 11	8.55 954	8.33 553	8.42 381	8.91 356	8.36 926
<b>II15</b>	7.50 977	7.385 29	7.03 957	7.33 285	7.44 425	7.15 068	7.60 179	7.35 987	7.23 713	7.28 63	6.55 556	7.09 809
<b>II15ra</b>	4.96 84	5.215 37	4.98 71	5.09 109	5.42 488	5.31 928	5.42 796	5.40 427	5.11 314	4.96 438	5.29 618	5.82 433
<b>II16</b>	3.33 097	3.630 4	4.58 976	3.20 357	4.30 289	4.47 975	4.07 041	3.68 18	4.41 27	4.28 63	4.95 222	5.11 579
<b>II17a</b>	6.04 369	5.826 8	4.62 453	5.58 208	6.12 232	5.75 538	6.49 667	6.62 666	6.22 006	6.51 896	6.71 121	4.66 513
<b>II17ra</b>	5.55 336	5.367 37	6.41 212	5.46 66	5.88 786	5.93 226	5.62 5	6.16 723	6.03 719	5.89 511	6.55 556	6.13 328
<b>II18</b>	4.68 461	5.437 76	5.55 414	5.49 635	5.25 982	5.40 175	4.87 776	4.68 18	5.50 016	5.71 926	5.25 178	5.78 06
<b>II18ra p</b>	2.16 105	3.045 44	4.36 15	2.20 357	3.80 039	3.81 678	4.07 041	3.81 93	3.73 463	2.77 173	4.15 867	4.45 868
<b>II1a</b>	5.99 394	6.045 44	5.36 15	5.81 238	5.88 786	5.62 414	6.33 719	6.71 742	6.01 756	6.42 381	6.38 107	4.28 18
<b>II1b</b>	1.74 601	2.367 37	5.74 001	0.11 8361	3.53 736	3.03 918	2.87 776	3.16 723	3.14 967	3.66 481	5.86 649	5.18 45
<b>II1r1</b>	7.56 192	7.717 87	8.68 548	7.91 506	7.85 205	7.95 974	7.67 774	7.70 86	7.80 502	7.88 324	8.69 057	9.17 82
<b>II1r2</b>	5.20 544	4.852 8	6.19 8	5.68 899	5.21 543	5.13 871	5.46 273	5.26 676	4.82 774	5.54 934	6.67 805	6.04 364
<b>Irak1</b>	8.51 86	8.389 74	7.97 705	8.46 66	8.54 635	8.55 375	8.59 789	8.45 79	8.44 979	8.44 819	8.18 842	8.40 929
<b>II1ra p</b>	6.96 84	6.731 94	6.65 006	6.78 853	6.99 679	7.13 871	7.30 881	7.48 915	6.89 383	7.39 9	7.61 81	6.41 645
<b>II1rn</b>	2.48 297	3.745 88	6.86 157	2.68 899	3.02 278	3.23 182	3.24 033	4.35 987	3.14 967	3.87 127	6.72 752	6.02 502
<b>II18r1</b>	5.06 794	5.600 03	6.55 414	5.05 156	5.80 039	5.27 622	5.31 834	5.97 458	5.31 959	6.80 987	7.54 64	6.98 706

<b>II2</b>	1.74 601	2.045 44	1.81 717	1.88 164	1.80 039	2.23 182	2.39 234	2.68 18	2.82 774	1.96 438	2.57 371	2.08 016
<b>II2ra</b>	3.86 149	4.132 9	4.09 019	3.58 208	3.91 587	4.13 871	3.87 776	4.35 987	3.91 52	4.05 184	4.25 178	3.92 816
<b>II2rb</b>	4.96 84	5.367 37	5.31 967	5.12 957	5.53 736	4.98 671	5.39 234	5.56 932	5.18 529	5.21 23	5.92 421	5.80 263
<b>II2rg</b>	6.57 044	6.689 3	6.48 96	6.46 66	6.53 736	6.64 121	7.15 787	7.29 061	6.63 509	7.06 241	7.41 165	5.92 816
<b>II3</b>	4.16 105	3.504 87	2.03 957	3.34 107	3.67 486	3.81 678	3.87 776	4.94 483	4.14 967	3.42 381	4.05 914	3.66 513
<b>II4</b>	3.33 097	1.630 4	3.55 414	0.88 1639	3.21 543	2.81 678	2.65 537	3.52 98	1.41 27	2.28 63	3.71 121	2.75 824
<b>II4ra</b>	7.12 683	6.940 26	8.41 461	6.53 985	7.08 579	7.13 871	7.12 569	7.45 79	7.08 513	7.34 808	8.56 919	8.42 712
<b>II5</b>	2.48 297	2.367 37	2.69 164	- 0.11 8361	3.53 736	1.23 182	2.39 234	3.52 98	2.63 509	0.96 4375	3.57 371	2.08 016
<b>II6</b>	6.95 546	6.852 8	5.72 407	6.48 155	6.87 364	6.95 974	7.02 46	7.24 251	6.74 66	7.28 63	7.42 171	5.84 57
<b>II6ra</b>	6.91 593	6.689 3	6.84 692	6.70 182	6.92 968	6.94 607	7.18 935	7.27 873	7.00 765	7.14 428	7.29 618	6.95 791
<b>II6st</b>	7.91 593	7.752 8	8.84 324	7.68 254	8.07 341	8.09 601	7.83 859	8.01 808	8.09 92	8.09 88	9.09 413	9.28 18
<b>II7</b>	6.33 097	6.569 607	5.87 843	6.14 843	6.59 047	6.58 937	7.02 46	7.18 005	6.39 759	6.96 438	6.72 752	5.04 364
<b>II7r</b>	7.10 356	6.645 35	6.19 8	6.40 52	6.62 482	7.01 318	7.30 881	7.29 061	6.75 848	7.24 05	7.21 757	5.64 088
<b>II9</b>	6.92 923	7.045 44	5.83 213	6.71 453	7.09 807	7.06 471	7.47 98	7.43 669	7.00 765	7.23 116	7.55 556	5.80 263
<b>IIf3</b>	6.01 903	5.928 08	6.09 019	5.90 401	6.07 341	5.81 678	6.35 581	5.88 343	6.13 152	6.21 23	6.44 161	6.02 502
<b>Irf1</b>	7.59 567	7.488 38	8.08 396	7.51 1	7.97 032	7.47 975	7.68 512	7.64 527	7.78 774	7.99 228	8.21 757	8.27 787
<b>Irf4</b>	6.91 593	6.254 89	5.83 213	6.27 396	6.60 775	6.13 871	7.18 935	7.03 23	6.52 818	6.98 674	7.13 443	5.21 767
<b>Itga2 b</b>	3.33 097	3.852 8	4.27 661	3.46 66	4.12 232	3.23 182	4.31 834	4.68 18	3.52 818	4.48 794	4.42 171	4.34 32
<b>Itga4</b>	5.88 897	5.800 33	6.23 221	5.05 156	5.94 335	6.11 446	6.57 82	6.52 98	6.20 278	6.39 064	6.97 97	6.18 45
<b>Itga5</b>	5.83 347	5.903 42	7.17 473	7.09 109	6.21 543	5.81 678	6.26 023	6.06 031	6.54 198	6.50 353	7.30 706	7.24 205
<b>Itga6</b>	8.23 251	8.122 26	8.15 405	8.42 08	8.42 8.42	8.34 035	8.36 962	8.34 856	8.24 98	8.16 895	8.24 614	8.50 978
<b>Itgal</b>	4.40 897	4.745 88	4.90 464	3.78 853	3.80 039	3.69 125	4.59 397	4.26 676	4.68 572	3.87 127	5.80 637	5.34 32

<b>Itgam</b>	4.62 048	4.630 4	7.61 592	3.68 899	4.46 336	4.81 678	5.11 48	5.16 723	5.25 4	5.98 674	7.37 072	6.92 816
<b>Itgax</b>	6.51 86	6.454 83	5.64 16	5.20 357	6.40 525	6.51 722	6.68 512	6.64 527	6.22 006	6.71 926	6.59 163	5.04 364
<b>Itgb1</b>	10.7 794	10.92 73	11.0 44	10.8 739	10.8 629	10.8 865	10.9 667	10.9 486	11.0 493	11.0 217	11.1 95	11.2 882
<b>Itgb2</b>	5.99 394	5.826 8	7.00 04	5.23 919	6.19 271	5.62 414	6.52 984	6.54 97	6.22 006	6.48 794	7.33 924	6.37 295
<b>Itln1</b>	3.48 297	3.045 44	3.13 91	3.34 107	3.38 536	3.69 125	4.39 234	3.68 18	3.41 27	3.87 127	3.83 674	3.45 868
<b>Jak1</b>	8.65 29	8.437 76	9.17 473	8.47 035	8.81 534	8.78 257	8.78 808	8.81 93	8.76 143	8.88 324	9.23 478	9.37 846
<b>Jak2</b>	8.07 991	8.116 9	8.16 59	7.68 254	7.98 361	8.15 068	8.15 256	8.37 668	8.07 567	8.30 422	8.72 346	8.45 52
<b>Jak3</b>	5.40 897	4.800 33	5.06 51	4.73 962	5.07 341	4.93 226	5.49 667	5.52 98	5.66 063	5.60 823	5.95 222	5.80 263
<b>Kit</b>	3.74 601	3.952 33	3.55 414	3.20 357	3.80 039	3.81 678	3.65 537	4.06 031	3.91 52	3.87 127	4.33 924	3.84 57
<b>Klra1</b>	3.16 105	2.045 44	2.23 221	2.68 899	2.21 543	2.55 375	2.87 776	2.94 483	1.82 774	3.66 481	4.25 178	2.56 559
<b>Klra4</b>	1.74 601	1.630 4	1.55 414	2.20 357	2.21 543	2.55 375	1.65 537	1.94 483	1.82 774	1.96 438	2.25 178	2.34 32
<b>Klra5</b>	3.16 105	1.630 4	0.81 7175	2.68 899	2.21 543	3.03 918	2.87 776	3.35 987	2.82 774	3.87 127	3.71 121	2.75 824
<b>Klra6</b>	3.48 297	4.504 87	3.55 414	3.20 357	3.02 278	4.03 918	3.07 041	4.26 676	3.73 463	3.54 934	3.95 222	3.08 016
<b>Klra7</b>	1.74 601	3.745 88	3.48 014	3.05 156	3.02 278	2.81 678	3.77 085	2.68 18	3.52 818	3.54 934	3.83 674	3.21 767
<b>Klra8</b>	1.74 601	3.504 87	3.40 214	3.20 357	3.67 486	3.23 182	4.15 787	3.94 483	3.73 463	3.13 43	3.42 171	3.66 513
<b>Klrc1</b>	3.62 048	2.045 44	2.55 414	2.46 66	3.67 486	3.69 125	3.77 085	4.06 031	3.99 766	3.96 438	3.83 674	3.21 767
<b>Klrc2</b>	4.68 461	4.367 37	2.81 717	3.68 899	4.21 543	3.81 678	4.82 53	4.16 723	3.82 774	4.82 236	4.95 222	4.28 18
<b>Klrd1</b>	3.16 105	3.630 4	4.23 221	3.58 208	3.91 587	3.93 226	3.77 085	3.81 93	4.41 27	4.21 23	4.71 121	4.88 752
<b>Lck</b>	3.96 84	4.952 33	4.23 221	4.27 396	4.60 775	4.55 375	4.59 397	4.60 78	4.58 263	4.71 926	4.05 914	4.88 752
<b>Lcp2</b>	2.96 84	4.215 37	3.81 717	3.68 899	3.91 587	3.69 125	3.07 041	3.52 98	4.28 717	4.35 669	4.49 971	3.92 816
<b>Lef1</b>	4.40 897	4.215 37	3.75 577	4.46 66	4.12 232	3.69 125	4.39 234	4.52 98	4.14 967	4.66 481	4.77 534	4.40 209
<b>Lif</b>	3.62 048	2.852 8	4.03 957	3.34 107	4.30 289	3.55 375	3.87 776	4.16 723	3.28 717	4.13 43	3.42 171	4.21 767

<b>Psemb9</b>	5.51 86	5.254 89	5.72 407	4.58 208	5.34 471	5.44 127	5.31 834	5.40 427	5.58 263	5.77 173	6.08 467	5.61 622
<b>Xcl1</b>	6.38 986	6.293 37	5.44 167	6.22 149	6.48 222	6.70 755	7.12 569	6.76 926	6.36 69	6.82 236	7.31 787	4.75 824
<b>Lta</b>	6.76 096	6.022 72	5.31 967	6.11 046	6.53 736	6.47 975	6.64 026	6.85 172	6.47 159	6.74 574	6.59 163	4.56 559
<b>Ltb</b>	3.86 149	3.630 4	5.06 51	3.96 91	4.21 543	4.40 175	4.39 234	3.81 93	4.35 13	3.77 173	4.77 534	4.96 769
<b>Ltb4r1</b>	6.16 105	5.254 89	5.06 51	5.43 623	5.46 336	5.58 937	6.31 834	6.64 527	6.03 719	6.59 373	6.33 924	5.59 113
<b>Ltbr</b>	8.13 259	8.138 2	8.42 204	8.26 966	8.29 758	8.33 511	8.15 787	8.17 365	8.36 69	8.20 278	8.66 541	8.64 088
<b>Ltf</b>	6.77 576	6.488 38	5.62 453	6.30 79	6.48 222	6.80 168	7.04 769	7.14 123	6.66 063	7.06 241	7.12 215	5.28 18
<b>Blnk</b>	9.54 691	9.615 3	9.22 939	9.45 339	9.40 525	9.50 795	9.67 959	9.50 198	9.59 095	9.62 971	9.03 642	9.19 911
<b>Il1rl1</b>	6.83 347	6.717 87	6.31 967	6.35 737	6.92 968	6.77 098	7.36 503	7.39 329	6.85 011	7.21 23	8.22 333	6.96 769
<b>Ly86</b>	5.33 097	5.689 3	7.70 795	5.20 357	5.73 899	5.18 602	4.82 53	5.71 742	6.09 452	6.37 377	7.05 914	7.19 286
<b>Ly96</b>	6.96 84	7.056 67	7.13 91	6.87 032	7.00 985	7.23 182	6.81 188	7.03 23	7.04 691	6.99 78	7.24 047	7.10 696
<b>Smad3</b>	6.74 601	6.235 26	7.15 702	6.99 016	7.19 271	7.07 731	6.85 177	6.97 458	7.05 656	7.34 808	7.49 971	7.79 716
<b>Smad5</b>	8.77 943	8.685 69	8.62 023	8.57 861	8.66 251	8.77 098	8.80 512	8.78 194	8.86 666	8.61 901	8.71 121	9.05 056
<b>Maf</b>	4.91 593	5.537 29	6.45 138	5.73 962	5.94 335	5.90 425	5.35 581	5.52 98	5.82 774	5.98 674	6.27 415	6.93 815
<b>Mapk apk2</b>	7.27 999	7.132 9	7.81 341	7.25 668	7.25 982	7.18 602	7.25 032	6.89 903	7.30 347	7.58 643	7.55 556	7.56 559
<b>Marc o</b>	2.16 105	2.630 4	3.69 164	1.46 66	2.21 543	3.23 182	2.39 234	3.16 723	3.28 717	2.96 438	5.64 41	6.83 505
<b>Masp 1</b>	5.77 576	6.274 26	6.27 661	5.81 238	5.91 587	6.13 871	6.31 834	5.52 98	5.85 011	6.32 193	6.27 415	6.21 767
<b>Masp 2</b>	1.16 105	2.852 8	1.55 414	1.46 66	3.67 486	2.23 182	1.07 041	3.16 723	3.28 717	2.96 438	3.95 222	3.21 767
<b>Mbl2</b>	1.16 105	1.630 4	1.81 717	2.20 357	1.80 039	1.23 182	2.65 537	2.68 18	2.41 27	1.54 934	1.25 178	1.34 32
<b>Mbp</b>	5.01 903	5.089 83	5.20 949	4.88 164	4.97 032	4.62 414	4.71 426	4.52 98	5.41 27	4.91 857	5.15 867	5.45 868
<b>Cd46</b>	5.91 593	5.903 42	5.13 91	5.73 962	5.80 039	5.98 671	6.71 426	6.62 666	5.97 749	6.30 423	6.44 161	4.56 559
<b>Mif</b>	8.59 984	8.692 9	8.84 324	8.67 28	8.71 129	8.62 843	8.44 11	8.76 075	8.68 882	8.61 901	9.15 265	9.09 363



<b>Cxcl9</b>	3.96 84	3.215 37	3.98 71	3.20 357	3.91 587	4.47 975	3.97 73	4.60 78	4.99 766	4.28 63	4.89 564	4.61 622
<b>Mme</b>	11.8 179	12.06 61	11.5 34	11.9 585	12.1 125	11.6 784	11.9 485	12.1 06	11.8 755	12.0 05	10.7 919	11.6 546
<b>Psmid 7</b>	10.1 297	10.15	9.91 959	10.0 947	10.0 179	10.0 804	10.2 265	10.2 022	10.1 886	10.1 192	9.75 958	10.0 574
<b>Muc1</b>	2.96 84	3.367 37	4.03 957	3.34 107	3.21 543	3.93 226	3.65 537	3.94 483	4.07 567	4.13 43	4.71 121	4.45 868
<b>Mx1</b>	6.31 079	6.839 86	6.60 725	6.63 653	6.75 459	6.67 476	6.90 33	6.75 219	6.78 193	6.78 455	6.38 107	6.92 816
<b>Myd8 8</b>	7.13 833	7.302 83	7.28 206	7.05 156	7.37 53	7.35 076	7.58 611	7.62 666	7.26 237	7.47 217	7.60 933	6.86 676
<b>Ncam 1</b>	7.39 945	7.463 29	7.36 15	7.29 949	7.45 384	7.42 165	7.74 283	7.84 369	7.53 51	7.39 9	7.88 841	7.59 113
<b>Ncf4</b>	3.16 105	4.045 44	6.44 167	3.20 357	3.80 039	3.03 918	3.97 73	4.44 733	4.35 13	4.66 481	6.60 933	6.44 474
<b>Nfatc 1</b>	4.74 601	4.569	4.98 71	4.52 55	3.67 486	4.47 975	4.77 085	5.11 476	4.68 572	4.35 669	4.71 121	5.37 295
<b>Nfatc 2</b>	4.33 097	3.504 87	4.90 464	4.20 357	4.38 535	3.81 678	4.39 234	3.52 98	4.07 567	4.21 23	5.10 976	5.34 32
<b>Nfatc 3</b>	6.73 09	6.759 69	6.74 791	6.53 985	6.62 482	6.73 962	6.92 839	6.69 972	6.87 213	7.05 184	6.69 473	6.67 71
<b>Nfil3</b>	7.13 833	6.964 3	6.67 516	6.82 415	6.77 002	7.19 761	6.47 98	7.32 566	7.15 865	6.73 256	6.67 805	7.31 283
<b>Nfkb 1</b>	7.83 347	7.999 64	8.08 396	7.88 726	8.22 106	8.24 305	8.13 11	8.38 224	8.20 278	8.17 869	8.41 165	8.04 825
<b>Nfkb 2</b>	7.03 141	6.630 4	7.60 29	6.83 584	7.03 561	6.73 962	6.78 465	6.71 742	7.21 144	7.06 241	7.72 752	7.79 716
<b>Nfkbi a</b>	6.68 461	6.759 69	6.74 001	6.27 396	6.30 289	6.44 127	6.79 833	6.75 219	6.86 116	6.70 584	7.26 301	6.83 505
<b>Cd24 4</b>	4.74 601	4.852 8	4.98 71	3.88 164	4.53 736	4.03 918	5.15 787	5.68 18	5.03 719	5.24 978	6.05 914	5.40 209
<b>Nos2</b>	5.33 097	4.569	4.40 214	4.63 653	4.53 736	4.98 671	5.59 397	5.00 373	5.31 959	5.28 63	5.53 718	5.31 283
<b>Notch 1</b>	7.19 447	7.034 12	7.36 15	7.04 151	7.27 071	7.15 068	7.01 292	7.41 515	7.19 406	7.38 223	7.25 178	7.49 295
<b>Notch 2</b>	7.42 783	7.553 24	7.34 595	7.43 623	7.73 899	7.45 099	7.79 151	7.82 748	7.52 122	7.69 908	8.09 099	7.47 934
<b>Npc1</b>	6.80 49	7.011 22	7.46 103	6.71 453	6.94 335	6.73 962	6.64 026	6.62 666	6.92 577	7.06 241	7.50 917	7.92 314
<b>Pax5</b>	6.11 524	6.174 72	5.67 516	5.34 107	5.88 786	6.18 602	6.71 426	7.03 23	6.22 006	6.48 794	6.53 718	4.88 752
<b>Pdcd 1</b>	3.33 097	3.045 44	3.03 957	3.20 357	3.38 536	3.93 226	3.77 085	3.35 987	3.73 463	3.87 127	4.05 914	3.08 016

<b>Pdcd 2</b>	7.22 713	7.011 22	6.53 599	7.07 146	7.02 279	7.11 446	7.55 422	7.70 86	7.25 4	7.57 909	7.43 169	6.08 016
<b>Pdgfb</b>	4.91 593	4.745 88	5.51 761	4.96 91	5.30 289	5.23 182	4.77 085	5.26 676	4.73 463	5.32 193	5.95 222	6.57 842
<b>Pdgfr b</b>	5.06 794	4.689 3	4.81 717	3.20 357	4.38 535	4.13 871	3.87 776	4.52 98	4.22 006	4.96 438	4.83 674	5.59 113
<b>Pecam1</b>	7.44 645	7.056 67	8.47 777	7.19 452	7.67 486	7.44 127	7.37 419	7.42 596	7.67 323	7.71 257	8.29 618	9.03 436
<b>Cfp</b>	6.22 713	6.235 26	8.66 684	5.71 453	6.60 775	6.51 722	6.68 512	7.04 637	6.88 302	7.10 393	8.17 065	8.06 202
<b>Prf1</b>	3.16 105	1.045 44	2.93 265	2.88 164	2.21 543	2.81 678	2.39 234	2.94 483	2.41 27	3.28 63	3.05 914	2.92 816
<b>Abcb 1a</b>	6.94 241	6.504 87	6.55 414	6.32 458	7.23 78	6.91 832	7.09 278	7.15 429	6.89 383	7.01 966	7.28 521	6.93 815
<b>Pigr</b>	7.56 192	7.982 08	7.75 185	7.78 853	8.28 689	7.75 538	8.03 619	7.76 075	7.96 216	8.03 046	8.88 114	7.62 86
<b>Lilra 6</b>	4.33 097	3.852 8	3.69 164	3.96 91	4.02 279	4.31 928	4.31 834	3.52 98	3.73 463	3.96 438	4.95 222	3.92 816
<b>Pirb</b>	4.48 297	4.569	6.67 516	4.12 957	4.46 336	4.31 928	4.46 273	4.88 343	4.35 13	5.45 623	6.46 124	6.51 312
<b>Prkcd</b>	9.19 447	9.215 37	9.14 211	9.30 16	9.22 386	9.19 761	9.36 503	9.53 729	9.42 579	9.41 97	9.12 83	9.25 009
<b>Pla2g 2a</b>	3.48 297	1.630 4	2.23 221	2.20 357	2.53 736	2.55 375	3.65 537	2.35 987	2.99 766	3.66 481	2.83 674	2.08 016
<b>Plau</b>	5.01 903	5.402 99	7.44 653	5.16 704	5.53 736	6.31 928	6.27 986	5.68 18	6.01 756	6.28 63	8.49 971	7.76 386
<b>Plaur</b>	4.86 149	3.630 4	6.16 295	4.27 396	4.38 535	4.47 975	4.59 397	4.81 93	4.47 159	5.09 366	6.53 718	6.73 552
<b>Pml</b>	6.91 593	6.928 08	7.29 83	6.60 956	6.88 786	6.91 832	6.81 188	7.00 373	6.97 749	6.98 674	7.05 914	7.25 009
<b>Pou2f 2</b>	3.86 149	3.745 88	4.78 68	3.58 208	3.80 039	3.03 918	4.31 834	3.35 987	3.91 52	4.35 669	5.38 107	5.40 209
<b>Pparg</b>	4.40 897	3.745 88	3.98 71	3.05 156	4.12 232	3.81 678	3.52 984	3.68 18	4.22 006	3.77 173	4.33 924	4.45 868
<b>Prim 1</b>	6.92 923	6.813 62	6.48 014	6.71 453	7.02 279	7.18 602	7.03 619	7.25 469	6.85 011	7.34 808	7.89 564	6.29 74
<b>Mapk 11</b>	2.16 105	1.630 4	3.23 221	1.88 164	3.38 536	3.03 918	3.77 085	3.52 98	3.41 27	3.42 381	1.83 674	3.75 824
<b>Psemb 10</b>	5.20 544	5.045 44	5.16 295	4.83 584	5.16 963	4.98 671	4.71 426	4.75 219	5.25 4	5.35 669	6.10 976	5.80 263
<b>Psemb 5</b>	9.68 461	9.574 87	9.45 259	9.63 82	9.59 047	9.66 645	9.79 492	9.69 972	9.54 541	9.55 309	9.42 171	9.41 108
<b>Psemb 7</b>	9.55 551	9.740 67	9.47 895	9.59 072	9.47 517	9.58 276	9.69 612	9.71 742	9.71 343	9.73 421	9.53 255	9.50 811

<b>Psmc 2</b>	10.2 748	10.29 57	10.1 406	10.2 686	10.2 027	10.2 857	10.3 753	10.3 514	10.3 581	10.3 142	9.99 493	10.2 69
<b>Ptafr</b>	6.90 251	6.615 3	7.60 29	6.58 208	6.87 364	6.69 125	7.14 722	7.27 873	7.02 741	7.49 576	7.97 288	7.19 286
<b>Ptger 4</b>	3.16 105	0.045 4404	3.69 164	3.78 853	3.80 039	3.03 918	3.97 73	3.16 723	3.52 818	3.13 43	4.15 867	4.66 513
<b>Ptgs2</b>	3.16 105	3.045 44	4.23 221	2.88 164	3.38 536	2.55 375	2.87 776	3.68 18	3.14 967	3.13 43	5.57 371	5.37 295
<b>Ptpn2</b>	7.27 999	7.022 72	7.22 657	7.12 957	7.06 092	7.26 524	7.27 986	7.42 596	7.47 879	6.91 857	7.49 019	7.34 32
<b>Ptpn2 2</b>	2.16 105	3.045 44	4.81 717	3.34 107	3.02 278	3.23 182	3.52 984	3.52 98	3.63 509	3.28 63	4.64 41	4.28 18
<b>Ptprc</b>	5.37 05	4.504 87	7.13 91	5.01 092	5.34 471	4.93 226	4.82 53	5.44 733	5.85 011	5.60 823	6.86 649	7.46 56
<b>Rag1</b>	2.96 84	3.215 37	2.03 957	1.46 66	2.53 736	3.03 918	2.07 041	2.94 483	3.14 967	2.28 63	2.25 178	2.08 016
<b>Rag2</b>	1.74 601	1.630 4	1.55 414	2.20 357	2.53 736	2.81 678	2.39 234	1.35 987	2.14 967	2.54 934	3.05 914	2.34 32
<b>Rela</b>	7.50 977	7.480 07	7.77 524	7.78 853	7.61 631	7.59 814	7.73 574	7.55 954	7.82 209	7.69 23	7.77 534	7.94 806
<b>Relb</b>	6.29 033	5.999 64	7.23 221	6.18 542	6.44 425	5.84 653	6.35 581	6.14 123	6.33 553	6.85 919	7.50 917	7.20 945
<b>Rorc</b>	7.01 903	6.731 94	6.58 094	6.60 956	6.67 486	6.97 329	7.00 115	6.95 978	7.31 959	6.60 823	6.44 161	7.00 616
<b>S100a 8</b>	6.68 461	7.056 67	11.8 061	6.51 1	7.71 528	7.03 918	7.34 653	7.30 239	7.44 979	7.37 377	12.1 784	12.1 13
<b>S100a 9</b>	6.68 461	6.865 62	12.0 175	6.14 843	7.71 528	7.02 624	7.23 028	7.07 412	6.93 626	7.60 1	12.3 074	11.8 503
<b>Msr1</b>	3.62 048	3.745 88	6.37 176	3.58 208	4.12 232	4.03 918	3.39 234	4.88 343	4.63 509	4.54 934	6.25 178	6.41 645
<b>Ccl11</b>	8.72 329	8.541 3	9.07 299	8.53 985	8.51 464	8.86 845	8.45 843	8.79 866	8.90 722	9.10 137	9.45 635	9.18 45
<b>Ccl12</b>	6.87 529	6.773 36	7.37 176	6.56 814	6.97 032	6.86 118	7.30 881	7.41 515	6.97 749	7.13 43	8.12 215	8.13 328
<b>Ccl2</b>	5.24 851	4.689 3	9.62 882	5.20 357	5.30 289	5.36 11	5.07 041	4.88 343	6.09 452	6.24 978	9.97 117	10.5 388
<b>Ccl20</b>	6.09 178	6.153 96	5.46 103	5.90 401	6.07 341	6.49 861	6.37 419	6.76 926	6.25 4	6.51 896	6.46 124	4.15 055
<b>Ccl22</b>	4.33 097	4.215 37	3.93 265	3.05 156	3.67 486	4.62 414	4.31 834	4.60 78	4.47 159	4.82 236	4.95 222	4.21 767
<b>Ccl25</b>	5.58 731	5.045 44	4.87 607	5.12 957	5.25 982	5.62 414	4.97 73	5.56 932	5.66 063	5.74 574	5.00 667	5.11 579
<b>Ccl3</b>	6.53 609	6.454 83	5.77 137	5.60 956	6.34 471	6.57 167	6.95 305	6.62 666	6.20 278	6.71 926	7.01 997	5.45 868

<b>Ccl4</b>	3.16 105	2.367 37	3.03 957	2.20 357	2.21 543	3.23 182	2.87 776	3.35 987	2.82 774	0.96 4375	3.83 674	3.21 767
<b>Ccl5</b>	4.16 105	3.367 37	4.48 014	4.12 957	4.67 486	4.40 175	4.15 787	4.52 98	5.14 967	4.87 127	6.00 667	5.18 45
<b>Ccl6</b>	5.44 645	5.367 37	9.05 876	4.68 899	5.88 786	4.75 538	5.24 033	5.88 343	6.11 314	6.48 794	7.99 325	7.84 039
<b>Ccl7</b>	3.48 297	3.215 37	7.95 331	3.88 164	4.30 289	2.81 678	4.07 041	4.16 723	4.47 159	4.21 23	7.89 564	9.31 474
<b>Ccl8</b>	2.96 84	3.852 8	9.27 25	3.68 899	5.07 341	3.81 678	4.15 787	4.52 98	5.73 463	6.48 794	9.22 045	9.69 045
<b>Ccl9</b>	6.99 394	6.800 33	10.4 984	6.34 107	7.02 279	6.67 476	7.05 909	7.14 123	7.44 979	7.72 593	9.58 27	9.67 561
<b>Cxcl1 5</b>	4.16 105	3.504 87	3.87 607	2.20 357	4.60 775	4.69 125	3.39 234	4.35 987	3.41 27	3.42 381	3.95 222	3.92 816
<b>Cx3cl 1</b>	5.16 105	4.689 3	4.75 577	4.83 584	5.07 341	5.08 98	4.59 397	4.88 343	5.41 27	5.28 63	5.10 976	4.28 18
<b>Cxcl1 2</b>	9.25 908	8.952 33	10.1 674	9.04 151	9.19 271	9.43 149	9.05 34	9.10 806	9.26 653	9.24 515	10.7 516	10.5 098
<b>Sele</b>	2.96 84	2.045 44	4.09 019	2.68 899	2.53 736	2.55 375	3.97 73	4.06 031	2.41 27	2.96 438	5.15 867	5.21 767
<b>Sell</b>	3.62 048	2.630 4	6.77 137	2.88 164	3.21 543	3.23 182	3.24 033	3.16 723	3.99 766	4.28 63	6.48 06	6.65 305
<b>Selplg</b>	2.96 84	2.630 4	2.40 214	3.20 357	3.67 486	4.13 871	3.24 033	3.81 93	3.91 52	3.54 934	4.15 867	1.75 824
<b>Foxp 3</b>	3.33 097	3.367 37	2.81 717	2.88 164	3.67 486	4.23 182	4.46 273	2.94 483	3.91 52	4.28 63	3.95 222	4.45 868
<b>Sh2d 1a</b>	3.86 149	3.215 37	3.40 214	3.96 91	3.80 039	4.13 871	4.07 041	4.60 78	3.91 52	4.28 63	4.05 914	4.15 055
<b>Ski</b>	7.42 783	7.011 22	7.03 311	7.01 092	7.51 921	7.19 761	7.30 881	7.78 614	7.53 51	7.40 732	7.86 649	7.39 486
<b>Spn</b>	3.62 048	3.045 44	4.36 15	3.78 853	3.80 039	4.31 928	4.31 834	2.94 483	3.14 967	3.96 438	5.29 618	5.04 364
<b>Src</b>	7.17 227	7.184 99	7.26 012	7.29 103	7.21 543	7.54 47	7.18 935	7.51 974	7.38 998	7.24 978	7.56 467	7.50 643
<b>Stat1</b>	6.35 087	6.067 81	7.15 108	6.29 103	6.62 482	6.40 175	6.52 984	6.71 742	7.03 719	6.75 879	7.26 301	7.28 962
<b>Stat2</b>	4.86 149	5.689 3	5.98 71	5.81 238	5.34 471	6.06 471	6.07 041	5.75 219	6.11 314	6.19 319	5.60 933	6.40 209
<b>Stat3</b>	8.73 469	8.731 94	9.41 212	8.70 182	8.82 646	8.78 257	8.82 53	8.81 52	8.86 116	8.94 452	9.77 534	9.53 96
<b>Stat4</b>	3.74 601	2.630 4	2.55 414	1.88 164	3.02 278	2.55 375	3.39 234	2.94 483	3.28 717	3.66 481	3.71 121	2.56 559
<b>Stat5 a</b>	9.54 691	9.567 04	9.30 903	9.71 611	9.51 005	9.68 097	9.75 165	9.83 56	9.61 564	9.50 741	9.13 748	9.58 796

<b>Stat5b</b>	8.48 297	8.302 83	8.11 18	8.27 396	8.51 005	8.60 251	8.58 611	8.71 742	8.49 307	8.57 909	8.81 402	8.25 409
<b>Stat6</b>	7.95 546	8.106 14	8.20 088	8.08 621	8.12 232	8.22 051	8.09 831	8.25 469	8.12 236	8.05 184	8.30 707	8.44 823
<b>Syk</b>	7.20 544	7.164 38	7.79 063	6.38 943	7.15 794	7.25 419	7.32 78	7.87 557	7.35 13	7.62 259	8.10 353	7.53 302
<b>Tal1</b>	4.33 097	4.437 76	4.27 661	4.20 357	4.38 535	3.69 125	4.87 776	4.44 733	4.82 774	4.21 23	4.71 121	4.61 622
<b>Tap1</b>	7.14 973	7.205 31	7.13 308	6.72 713	7.45 384	7.23 182	7.56 226	7.61 726	7.40 517	7.71 257	7.72 752	6.88 752
<b>Tapbp</b>	7.72 329	7.645 35	8.25 458	7.84 164	7.91 587	7.87 568	7.74 989	7.79 45	8.18 968	8.03 046	8.27 415	8.38 395
<b>Tcf4</b>	7.81 926	7.766 54	8.15 702	7.56 814	8.20 978	7.88 287	7.88 419	7.89 125	7.96 216	8.03 046	8.17 065	8.62 242
<b>Tcf7</b>	4.91 593	5.174 72	4.31 967	5.37 349	4.67 486	4.69 125	5.31 834	4.44 733	4.87 213	4.91 857	5.29 618	5.04 364
<b>Zeb1</b>	7.32 092	7.576 82	7.49 431	7.19 452	7.41 51	7.38 157	7.60 957	7.61 726	7.59 592	7.59 373	7.93 126	7.97 741
<b>Tgfb1</b>	7.21 633	7.245 11	8.15 999	6.81 238	7.09 807	6.84 653	7.23 028	7.59 828	7.31 155	7.48 008	8.41 669	8.09 809
<b>Tgfb2</b>	7.31 079	7.576 82	7.28 749	7.63 653	7.38 535	7.20 91	7.46 273	7.42 596	7.58 263	7.37 377	7.05 914	7.30 513
<b>Tgfb3</b>	6.46 483	7.022 72	6.87 607	7.05 156	6.70 728	6.72 367	7.11 48	6.81 93	6.86 116	6.79 727	7.19 43	7.45 172
<b>Tgfb1</b>	6.96 84	6.254 89	8.18 641	6.46 66	6.62 482	6.49 861	6.49 667	6.62 666	6.63 509	6.78 455	8.30 163	7.98 706
<b>Tgfb1</b>	8.01 279	7.710 78	7.95 673	7.82 415	7.73 899	7.98 671	7.88 419	8.01 808	7.83 896	7.79 092	8.17 065	8.06 658
<b>Tgfb2</b>	7.44 645	7.349 22	8.54 736	7.03 139	7.69 925	7.17 434	7.35 581	7.47 881	7.77 025	7.91 857	8.78 706	8.91 052
<b>Thy1</b>	7.39 945	7.056 67	7.32 497	7.08 131	7.44 425	7.49 861	7.34 653	7.35 987	7.44 245	7.35 669	7.97 97	8.05 286
<b>Tlr1</b>	2.96 84	2.852 8	5.62 453	1.88 164	4.46 336	3.69 125	3.52 984	3.94 483	3.82 774	4.28 63	5.20 598	5.11 579
<b>Tlr4</b>	7.91 593	7.600 03	8.30 635	7.68 899	8.00 333	7.89 716	8.22 523	8.20 536	7.92 05	8.16 405	8.63 549	7.85 627
<b>Tnf</b>	2.48 297	2.367 37	3.81 717	2.46 66	2.53 736	3.81 678	3.65 537	3.81 93	3.41 27	3.28 63	4.05 914	3.08 016
<b>Tnfai p3</b>	4.86 149	5.254 89	6.07 77	4.88 164	4.97 032	5.23 182	5.35 581	5.56 932	5.41 27	5.91 857	6.85 17	6.43 066
<b>Tnfai p6</b>	4.48 297	3.504 87	5.16 295	3.46 66	4.67 486	4.03 918	3.65 537	4.06 031	5.03 719	3.42 381	5.46 124	5.92 816
<b>Tnfri f11a</b>	5.83 347	5.826 8	6.20 949	6.11 046	6.07 341	5.90 425	5.90 33	5.60 78	6.03 719	6.15 42	6.20 598	6.40 209

<b>Tnfrs f17</b>	3.48 297	2.630 4	3.75 577	2.88 164	3.21 543	2.81 678	3.39 234	4.44 733	2.41 27	2.54 934	4.15 867	4.34 32
<b>Tnfrs f1b</b>	4.55 336	4.215 37	6.41 212	4.68 899	4.30 289	4.31 928	4.15 787	5.00 373	5.14 967	5.05 184	6.55 556	6.64 088
<b>Cd40</b>	6.16 105	6.254 89	6.10 258	6.07 146	6.62 482	5.98 671	6.82 53	7.19 276	6.36 69	6.82 236	7.20 598	5.11 579
<b>Cd27</b>	6.13 833	5.826 8	5.25 458	5.85 892	6.19 271	5.75 538	6.77 085	6.56 932	6.22 006	6.24 978	6.67 805	4.15 055
<b>Tnfrs f8</b>	2.74 601	3.852 8	3.40 214	3.05 156	3.53 736	3.69 125	3.87 776	3.81 93	3.52 818	3.28 63	4.25 178	3.45 868
<b>Tnfrs f9</b>	2.74 601	2.045 44	2.69 164	0.88 1639	3.80 039	2.55 375	2.39 234	3.16 723	2.99 766	3.28 63	3.71 121	2.34 32
<b>Tnfsf 11</b>	1.74 601	1.630 4	3.03 957	1.88 164	1.80 039	2.55 375	1.07 041	2.68 18	0.82 7738	2.77 173	3.42 171	3.92 816
<b>Tnfsf 12</b>	7.40 897	7.264 61	7.24 344	7.44 388	7.39 534	7.60 686	7.65 537	7.69 972	7.30 347	7.44 011	7.51 857	7.41 645
<b>Cd401 g</b>	6.88 897	6.674 8	5.81 717	6.52 55	6.55 528	6.91 832	7.10 383	7.54 97	6.68 572	7.24 05	7.28 521	5.25 009
<b>Tnfsf 8</b>	2.74 601	3.504 87	3.23 221	3.20 357	3.21 543	3.55 375	2.87 776	2.35 987	3.14 967	3.28 63	4.15 867	2.75 824
<b>Traf1</b>	7.56 192	7.833 34	7.51 298	7.24 796	7.55 528	7.38 157	7.64 784	7.59 828	7.58 263	7.55 683	6.62 682	6.97 741
<b>Traf2</b>	5.48 297	5.402 99	5.27 661	5.30 79	5.12 232	5.47 975	5.49 667	5.88 343	5.47 159	5.39 064	5.67 805	5.78 06
<b>Traf3</b>	7.38 986	7.067 81	6.80 964	6.88 164	7.25 982	7.27 622	7.48 826	7.86 767	7.44 245	7.84 089	7.84 424	7.02 502
<b>Traf4</b>	7.06 794	6.890 93	5.89 042	6.68 899	6.92 968	7.07 731	7.19 969	7.72 619	6.79 352	7.44 819	7.45 145	5.45 868
<b>Traf5</b>	5.29 033	5.471 7	5.93 265	5.68 899	6.04 832	5.44 127	5.49 667	5.60 78	5.66 063	5.79 727	6.22 906	6.35 815
<b>Traf6</b>	6.37 05	6.312 23	6.56 313	6.58 208	6.67 486	6.83 173	6.87 776	7.11 476	6.88 302	6.73 256	6.82 164	6.89 779
<b>Tnfsf 10</b>	4.96 84	4.903 42	5.18 641	4.68 899	5.38 535	4.47 975	5.39 234	5.31 407	5.66 063	5.66 481	6.31 787	5.90 798
<b>Tfrc</b>	8.39 945	8.588 47	8.46 823	8.38 546	8.45 86	8.74 752	8.26 023	8.42 596	8.27 895	8.49 185	10.1 481	9.75 4
<b>Trp5 3</b>	6.84 755	6.584 6	6.42 204	6.42 08	7.04 832	6.75 538	7.10 383	7.25 469	6.73 463	6.95 306	7.44 161	6.51 312
<b>Tnfrs f4</b>	4.06 794	3.745 88	3.62 453	3.20 357	4.38 535	3.81 678	3.52 984	3.35 987	4.14 967	3.28 63	4.57 371	4.21 767
<b>Tyro bp</b>	6.90 251	6.852 8	9.79 445	6.91 506	7.30 289	6.93 226	6.78 465	7.37 11	7.62 215	8.09 88	9.61 592	9.75 117
<b>Ube2l 3</b>	9.38 746	9.014 11	9.00 7	9.07 393	9.19 271	9.29 791	9.31 358	9.44 733	9.26 653	9.22 412	9.16 467	9.07 565

<b>Vcam1</b>	6.29033	6.52117	6.17473	5.9691	6.16963	6.29791	6.19969	6.62666	6.3513	6.66481	7.28521	6.21767
<b>Vtn</b>	3.62048	3.04544	3.31967	2.68899	4.21543	3.55375	3.77085	2.35987	3.28717	3.87127	4.05914	3.66513
<b>Xbp1</b>	10.9301	10.5817	10.8181	10.7689	10.7153	10.9867	10.8152	11.0758	11.0578	10.7709	10.9505	10.8765
<b>Zap70</b>	6.26957	6.17472	5.25458	5.73962	6.51921	6.69125	6.81188	6.97458	6.80502	6.88324	6.89564	5.00616
<b>Zbtb7b</b>	7.72329	7.60003	7.40214	7.50369	7.57298	7.86118	7.69246	7.5497	7.83896	7.50353	7.75958	7.82433
<b>Ikzf1</b>	3.86149	3.04544	4.40214	3.20357	2.80039	2.55375	3.87776	3.94483	2.99766	2.54934	5.15867	4.80263
<b>Ikzf2</b>	6.9684	6.8528	6.72407	6.38943	7.20411	7.22051	7.05909	6.73491	7.00765	7.1542	7.03314	7.16763
<b>Ikzf3</b>	2.48297	0.0454404	3.31967	2.88164	1.21543	1.81678	2.65537	1.94483	2.99766	2.96438	3.25178	3.3432
<b>Ikzf4</b>	7.34095	7.10072	6.43188	7.06155	7.27071	7.55375	7.55422	7.90677	7.58263	7.75228	7.6441	6.16763
<b>Xcr1</b>	2.9684	1.6304	2.69164	0.118361	1.21543	1.23182	2.07041	2.6818	2.4127	3.2863	3.05914	3.08016
<b>Clec5a</b>	2.9684	3.21537	5.62453	3.05156	2.80039	2.81678	2.39234	3.6818	3.82774	4.05184	5.80637	5.40209
<b>Ets1</b>	7.23786	7.03412	7.45138	6.82415	7.2378	7.25419	7.41026	7.40427	7.40517	7.52662	7.91712	7.72402
<b>Hcst</b>	3.48297	2.04544	2.40214	3.05156	2.21543	3.23182	3.77085	3.5298	2.4127	3.2863	3.71121	3.45868
<b>Nt5e</b>	7.23786	7.29337	7.05239	7.45907	7.38535	7.17434	7.4798	7.24251	7.4202	7.34808	7.47095	7.45172
<b>Ccl19</b>	3.74601	4.29337	5.69164	2.88164	3.91587	3.69125	3.9773	3.8193	4.28717	4.2863	5.15867	5.37295
<b>Sigirr</b>	6.62048	6.45483	6.38196	6.72713	6.69116	6.58937	6.95305	6.19276	6.50016	6.53423	6.51857	6.40209
<b>Tlr2</b>	3.86149	3.36737	4.93265	3.4666	4.30289	3.23182	3.87776	4.06031	3.73463	4.35669	5.46124	5.1845
<b>Tnfsf13b</b>	3.16105	3.21537	4.09019	3.34107	3.21543	3.81678	4.07041	3.5298	3.28717	3.96438	4.42171	4.61622
<b>Adgre5</b>	5.33097	4.99964	6.72407	5.5255	5.46336	5.75538	6.0246	5.85172	5.85011	5.96438	6.59163	6.6286
<b>Ceacam1</b>	11.0483	11.2755	10.8652	11.2995	11.1306	11.103	11.301	11.1322	11.0114	11.2058	10.3259	10.7625
<b>Map4k1</b>	3.62048	2.8528	3.40214	2.4666	3.80039	2.55375	3.07041	2.94483	2.14967	3.2863	3.57371	3.66513
<b>Map4k2</b>	7.16105	7.11153	6.54509	7.04151	7.31346	7.16256	7.3278	7.41515	6.90455	7.23116	7.46124	6.21767

<b>Mapk 1</b>	10.707	10.827	10.5468	10.6938	10.7133	10.8224	10.9369	10.8285	10.8473	10.643	10.3286	10.6704
<b>Mapk 14</b>	7.62865	7.6379	7.51298	7.65643	7.58175	7.73962	7.79833	7.92211	7.83896	7.58643	7.88841	7.99664
<b>Map4 k4</b>	7.00654	7.11153	7.87607	6.78853	6.78529	6.97329	7.03619	7.27873	7.31155	7.19319	7.99998	7.75824
<b>Pla2g 2e</b>	4.06794	3.95233	4.03957	3.58208	4.12232	3.03918	4.07041	4.44733	4.14967	4.1343	4.77534	4.66513
<b>Klrk1</b>	7.13833	6.70365	5.83213	6.56814	6.73899	6.98671	7.40133	7.39329	6.89383	7.34808	7.27415	5.64088
<b>Irf5</b>	5.06794	5.21537	6.50834	4.63653	5.16963	5.0898	5.68512	5.26676	5.50016	5.66481	6.80637	6.32809
<b>Bcap 31</b>	9.61432	9.72316	9.56201	9.56989	9.4962	9.70755	9.64972	9.86767	9.66379	9.60823	9.62899	9.67412
<b>Slamf 1</b>	2.48297	3.04544	3.03957	3.4666	2.53736	2.55375	3.39234	3.35987	3.28717	3.2863	3.95222	2.3432
<b>Nox4</b>	3.86149	3.74588	4.23221	3.05156	2.80039	4.13871	3.52984	3.8193	3.14967	3.54934	4.71121	5.00616
<b>Ebi3</b>	6.95546	6.6893	6.05239	6.48155	6.65837	7.18602	7.27008	7.20536	6.9152	7.30423	7.31787	5.82433
<b>Icosl</b>	5.16105	5.4717	5.9871	5.4666	5.91587	5.51722	5.68512	5.75219	5.68572	5.71926	6.49971	6.08016
<b>Il17rb</b>	5.6529	4.8528	5.34074	5.16704	5.02279	4.98671	5.35581	5.35987	4.78193	5.84702	5.33924	5.40209
<b>C1s1</b>	10.144	10.65	10.8423	10.7704	10.4479	10.2148	10.4734	10.1753	10.5776	10.5919	10.7426	11.1097
<b>C1ra</b>	7.56192	7.35832	9.10258	7.02119	7.68304	7.47023	6.9159	7.69972	7.90989	8.28179	9.52324	9.52311
<b>Il22</b>	3.16105	2.6304	0.232212	0.881639	0.21543	2.23182	3.39234	3.35987	2.4127	2.2863	2.83674	2.75824
<b>Tnfsf 14</b>	6.90251	6.8268	5.91871	6.4515	6.85929	6.89003	6.94077	7.23024	6.67323	7.12425	7.30706	5.1845
<b>Il27ra</b>	6.38986	6.19519	5.62453	6.01092	6.32395	6.3611	6.9033	6.89903	6.16759	6.96438	6.89564	4.88752
<b>Lair1</b>	3.48297	3.21537	5.34074	3.78853	3.38536	3.81678	4.39234	4.16723	3.63509	3.87127	5.60933	5.48616
<b>Batf</b>	5.33097	5.21537	5.81717	5.09109	5.88786	5.51722	5.42796	5.44733	5.58263	5.71926	6.15867	6.04364
<b>Cd16 4</b>	10.7337	10.7205	10.6855	10.7825	10.8004	10.8539	10.7179	10.7914	10.7622	10.8161	10.6203	10.7985
<b>Tslp</b>	4.68461	4.569	5.20949	4.4666	4.67486	4.13871	4.71426	4.26676	4.9152	5.2863	5.46124	5.94806
<b>Tlr5</b>	6.38986	6.38529	5.74001	6.14843	6.85929	6.60686	6.95305	6.85172	6.39759	6.95306	7.00667	5.75824



<b>Irf7</b>	5.16 105	4.293 37	6.38 196	4.63 653	5.64 17	5.08 98	4.87 776	5.26 676	5.63 509	5.66 481	5.53 718	6.61 622
<b>Irf3</b>	5.01 903	4.800 33	4.55 414	4.63 653	5.12 232	4.81 678	5.19 969	5.40 427	5.11 314	5.00 877	5.60 933	5.84 57
<b>Icos</b>	2.96 84	3.045 44	2.23 221	1.46 66	3.02 278	3.23 182	3.39 234	3.16 723	3.41 27	3.77 173	3.57 371	4.34 32
<b>Ccr12</b>	3.74 601	3.852 8	4.69 164	4.58 208	4.60 775	4.93 226	4.46 273	4.60 78	4.41 27	4.48 794	5.25 178	4.51 312
<b>Cd160</b>	2.96 84	1.630 4	2.40 214	0.88 1639	1.80 039	2.23 182	2.07 041	3.68 18	2.99 766	3.54 934	4.25 178	3.21 767
<b>Tollip</b>	8.99 394	9.005 44	8.96 183	9.06 403	9.02 6	9.04 56	9.19 453	9.01 808	9.00 516	8.91 566	8.82 164	9.05 515
<b>Tyk2</b>	5.29 033	5.800 33	5.74 001	5.40 52	5.70 728	5.98 671	5.90 33	6.16 723	5.95 702	5.82 236	5.77 534	5.96 769
<b>Cxcl13</b>	6.90 251	6.600 03	10.0 524	6.12 957	7.23 78	6.72 367	6.87 776	6.85 172	6.98 761	7.28 63	8.92 774	8.88 236
<b>Cxcl11</b>	4.91 593	4.215 37	3.87 607	4.20 357	4.12 232	4.13 871	4.92 839	5.56 932	4.58 263	4.77 173	5.29 618	4.45 868
<b>Il17b</b>	2.16 105	2.367 37	0.23 2212	2.68 899	2.80 039	2.55 375	2.65 537	3.52 98	2.41 27	3.13 43	3.05 914	2.92 816
<b>Abcb10</b>	5.94 241	5.903 42	5.44 167	5.66 3	5.60 775	5.72 367	6.31 834	5.68 18	5.50 016	6.19 319	5.95 222	5.82 433
<b>Ccl24</b>	3.74 601	4.215 37	7.48 488	3.05 156	3.53 736	4.23 182	4.15 787	3.16 723	4.87 213	4.60 823	5.67 805	5.04 364
<b>Tbk1</b>	6.98 122	6.674 8	6.83 213	6.80 05	7.04 832	7.11 446	7.20 996	6.92 973	7.17 647	6.96 438	7.10 976	7.16 763
<b>Ikbke</b>	6.83 347	6.645 35	7.47 539	6.71 453	6.65 837	7.02 624	6.90 33	7.21 785	6.78 193	7.14 428	7.41 165	7.49 295
<b>Clec4e</b>	3.74 601	3.367 37	7.04 599	0.88 1639	2.53 736	1.23 182	4.31 834	4.16 723	2.99 766	4.21 23	7.08 467	6.16 763
<b>Litaf</b>	7.62 865	7.622 87	8.18 35	7.57 513	7.80 789	7.76 32	8.02 46	7.89 903	7.83 896	8.06 766	8.58 27	7.77 504
<b>Ltb4r2</b>	6.22 713	5.952 33	4.98 71	5.49 635	6.53 736	6.36 11	6.47 98	7.01 808	6.20 278	6.78 455	6.69 473	4.56 559
<b>Ppbp</b>	3.86 149	3.852 8	4.09 019	2.88 164	4.53 736	4.40 175	4.15 787	3.52 98	4.14 967	4.21 23	3.71 121	3.56 559
<b>Tbx21</b>	2.16 105	3.367 37	2.69 164	2.46 66	3.02 278	3.23 182	3.24 033	3.35 987	2.63 509	3.66 481	1.25 178	2.34 32
<b>Il17re</b>	6.80 49	6.553 24	5.97 368	6.07 146	6.72 322	6.47 975	6.90 33	6.88 343	6.64 792	6.75 879	6.55 556	6.37 295
<b>Crlf2</b>	6.96 84	7.111 53	7.29 291	6.97 967	6.99 679	6.89 003	7.22 016	7.04 637	7.20 278	7.23 116	6.97 97	7.15 912
<b>Tnfrsf13b</b>	6.63 678	6.215 37	5.77 137	6.42 08	6.53 736	6.67 476	7.05 909	6.80 281	6.25 4	6.98 674	7.10 976	5.31 283

<b>Klrc3</b>	3.33 097	1.045 44	2.23 221	0.88 1639	0.21 543	3.03 918	2.65 537	2.35 987	2.99 766	1.96 438	3.05 914	1.34 32
<b>Il20</b>	6.88 897	6.385 29	5.53 599	6.14 843	6.75 459	6.53 56	7.00 115	7.14 123	6.83 896	7.01 966	7.07 196	4.61 622
<b>Pdcd 1lg2</b>	1.74 601	1.045 44	2.40 214	0.88 1639	3.21 543	2.23 182	2.87 776	2.94 483	2.63 509	3.28 63	0.25 1782	3.34 32
<b>Trem 1</b>	2.48 297	1.045 44	4.09 019	3.05 156	2.21 543	3.03 918	2.65 537	3.52 98	3.28 717	3.28 63	4.71 121	4.34 32
<b>Ackr 2</b>	2.74 601	3.215 37	2.93 265	2.88 164	2.80 039	2.23 182	2.87 776	3.16 723	2.63 509	3.13 43	3.71 121	3.21 767
<b>Il21r</b>	3.74 601	3.630 4	3.40 214	2.46 66	3.91 587	3.81 678	4.46 273	4.75 219	3.91 52	4.42 381	4.64 41	2.92 816
<b>Il21</b>	4.24 851	3.630 4	3.23 221	3.58 208	3.80 039	3.93 226	3.87 776	4.26 676	3.28 717	4.35 669	3.83 674	2.92 816
<b>Cd27 4</b>	4.48 297	4.215 37	4.31 967	3.46 66	4.67 486	4.13 871	4.46 273	3.81 93	4.47 159	3.66 481	5.20 598	4.88 752
<b>Fcam r</b>	7.04 369	6.312 23	5.84 692	6.37 349	6.84 479	6.67 476	7.37 419	7.45 79	6.69 81	6.94 166	7.05 914	5.15 055
<b>Izum o1r</b>	2.74 601	2.630 4	2.81 717	2.68 899	2.21 543	2.81 678	2.07 041	3.68 18	3.82 774	2.28 63	3.71 121	3.45 868
<b>Rae1</b>	8.21 633	8.089 83	8.04 92	8.17 626	8.09 807	8.47 499	8.14 187	8.34 856	8.25 4	8.16 895	8.08 467	8.36 557
<b>Ifitm 1</b>	7.10 356	7.045 44	6.91 871	6.70 182	7.19 271	7.29 791	7.63 265	7.52 98	7.16 759	7.64 386	8.14 053	6.73 552
<b>C8g</b>	3.74 601	3.215 37	3.62 453	3.78 853	4.46 336	4.31 928	3.77 085	3.52 98	3.28 717	3.28 63	4.15 867	3.45 868
<b>Bst2</b>	7.01 903	7.358 32	7.85 792	6.95 846	7.07 341	7.10 219	7.16 844	7.46 84	7.57 593	7.54 18	7.69 473	8.12 892
<b>Gm10 499</b>	4.91 593	4.689 3	5.29 83	4.78 853	4.85 929	4.31 928	4.92 839	5.00 373	4.41 27	5.00 877	5.20 598	4.88 752
<b>Ifi35</b>	7.90 251	7.826 8	7.95 331	7.66 3	7.78 529	7.77 098	8.09 278	7.85 172	8.08 983	7.84 089	7.87 383	7.86 152
<b>Cd20 9g</b>	6.62 048	6.703 65	7.03 311	6.05 156	7.04 832	6.91 832	7.14 722	7.27 873	6.94 668	7.24 978	7.31 787	6.72 402
<b>Cd3e ap</b>	6.84 755	6.215 37	5.67 516	6.46 66	6.50 083	6.70 755	6.71 426	7.14 123	6.75 848	6.91 857	6.88 114	5.71 243
<b>Ifih1</b>	7.07 991	7.174 72	7.47 539	7.45 15	7.49 155	7.38 157	7.60 179	7.56 932	7.56 92	7.44 011	7.36 031	7.70 075
<b>Tnfrs f13c</b>	2.16 105	2.367 37	2.93 265	2.46 66	2.53 736	3.03 918	2.39 234	2.68 18	2.63 509	1.96 438	2.83 674	2.08 016
<b>Tme m173</b>	7.22 713	7.402 99	7.52 223	7.03 139	7.24 885	7.60 686	7.74 989	7.77 772	7.29 534	7.82 856	8.18 252	7.11 579
<b>Taga p</b>	5.74 601	5.402 99	5.27 661	5.94 773	6.40 525	5.40 175	5.85 177	5.64 527	5.82 774	6.23 116	6.18 252	5.90 798

<b>Psemb11</b>	3.48 297	3.045 44	2.03 957	2.46 66	1.80 039	3.03 918	3.77 085	4.26 676	3.41 27	3.66 481	4.05 914	4.15 055
<b>Irak3</b>	7.44 645	7.205 31	7.17 473	6.83 584	7.34 471	7.43 149	7.68 512	7.59 828	7.26 237	7.62 259	7.98 649	6.94 806
<b>Slamf7</b>	3.48 297	2.367 37	4.03 957	3.34 107	3.53 736	4.40 175	4.31 834	4.81 93	5.14 967	4.21 23	5.00 667	4.56 559
<b>Adal</b>	6.06 794	5.826 8	5.75 577	5.73 962	5.94 335	5.75 538	6.26 023	6.31 407	6.13 152	5.63 68	6.20 598	6.09 809
<b>Atg1611</b>	8.25 908	7.793 63	7.59 416	7.60 274	7.99 679	8.17 434	8.33 25	8.53 48	7.99 766	8.26 358	8.16 467	7.92 314
<b>Il33</b>	7.76 838	7.330 84	8.40 714	7.37 349	7.82 276	7.65 809	7.68 512	8.12 142	7.77 025	8.01 966	8.55 556	8.07 112
<b>Cul9</b>	5.96 84	6.045 44	6.10 258	6.11 046	6.38 535	6.34 035	6.31 834	5.94 483	6.07 567	6.39 064	5.92 421	6.59 113
<b>Icam4</b>	6.84 755	6.504 87	5.34 074	6.29 103	6.51 921	6.64 121	7.31 834	7.39 329	6.48 595	6.97 56	7.04 62	4.80 263
<b>Nfkbi3</b>	6.26 957	6.195 19	6.95 331	5.94 773	6.67 486	6.47 975	6.33 719	6.46 84	6.50 016	6.74 574	7.03 314	7.36 557
<b>Cxcr6</b>	2.74 601	3.630 4	3.93 265	3.20 357	2.21 543	2.23 182	3.24 033	3.52 98	3.41 27	4.05 184	5.20 598	3.66 513
<b>Tlr9</b>	7.22 713	6.674 8	6.25 458	6.45 15	7.15 794	7.07 731	7.27 008	7.69 079	7.10 386	7.61 543	7.56 467	6.31 283
<b>Il23a</b>	3.62 048	3.215 37	2.81 717	3.46 66	4.12 232	3.93 226	4.31 834	3.81 93	3.82 774	3.96 438	3.71 121	4.08 016
<b>Trem2</b>	3.86 149	3.852 8	5.72 407	2.68 899	4.21 543	3.69 125	3.77 085	4.81 93	3.82 774	5.35 669	5.71 121	5.73 552
<b>Ham3</b>	3.16 105	3.045 44	2.23 221	3.34 107	3.80 039	3.23 182	3.52 984	1.94 483	2.99 766	2.96 438	3.95 222	1.75 824
<b>Cd96</b>	3.62 048	3.745 88	3.40 214	3.88 164	4.12 232	3.23 182	3.77 085	3.94 483	3.91 52	3.87 127	3.83 674	3.45 868
<b>Cd163</b>	4.06 794	4.367 37	6.69 982	3.58 208	4.67 486	4.03 918	4.39 234	5.21 785	4.73 463	5.00 877	5.80 637	6.45 868
<b>Klra21</b>	2.48 297	2.630 4	0.81 7175	2.20 357	1.80 039	2.81 678	3.07 041	3.94 483	2.41 27	2.77 173	2.83 674	1.34 32
<b>Phlpp1</b>	8.22 713	8.005 44	7.93 612	8.14 843	7.92 279	8.14 471	8.38 782	8.24 861	8.38 616	8.13 43	7.70 299	7.90 798
<b>Il1rl2</b>	6.13 833	6.067 81	6.31 967	6.11 046	6.40 525	6.13 871	6.74 283	6.50 962	6.48 595	6.78 455	6.93 828	6.95 791
<b>Irak2</b>	7.03 141	6.839 86	6.44 167	7.01 092	7.21 543	7.03 918	7.32 78	7.46 84	7.22 862	7.39 064	7.58 27	6.37 295
<b>C7</b>	9.29 033	9.661 99	10.0 242	8.93 421	9.67 691	9.35 594	9.58 018	9.48 915	9.52 47	9.76 204	9.37 072	9.85 758
<b>C8b</b>	7.10 356	6.569	5.57 206	6.52 55	6.83 014	6.47 975	6.95 305	6.89 903	6.44 245	7.11 412	7.39 133	4.92 816

<b>Tirap</b>	7.19 447	7.293 37	6.48 014	7.12 957	7.19 271	7.53 56	7.60 179	7.67 275	7.18 529	7.60 1	7.72 752	6.13 328
<b>Il25</b>	3.48 297	2.630 4	2.23 221	1.46 66	3.21 543	3.55 375	2.07 041	3.35 987	2.99 766	3.13 43	2.57 371	2.92 816
<b>Tlr3</b>	6.60 399	6.553 24	5.83 213	5.88 164	6.75 459	6.64 121	6.78 465	7.06 031	6.66 063	7.01 966	6.82 164	5.80 263
<b>Tlr8</b>	6.77 576	6.865 62	6.88 326	5.94 773	6.92 968	6.75 538	7.23 028	7.07 412	6.82 774	7.13 43	7.41 165	6.29 74
<b>Btla</b>	6.44 645	6.067 81	5.42 204	6.22 149	6.32 395	6.57 167	6.81 188	6.95 978	6.44 245	6.53 423	6.80 637	5.43 066
<b>Il23r</b>	3.62 048	3.367 37	2.93 265	1.88 164	3.91 587	3.69 125	3.77 085	3.94 483	3.28 717	3.66 481	4.15 867	3.66 513
<b>Nox3</b>	1.74 601	2.630 4	0.81 7175	0.88 1639	0.21 543	2.55 375	2.65 537	1.94 483	2.82 774	2.28 63	3.25 178	0.75 8236
<b>Abcf1</b>	7.94 241	7.846 34	7.29 291	7.55 406	7.94 335	7.98 671	8.09 831	8.35 422	7.93 103	8.11 919	8.10 353	7.66 513
<b>Cd22 6</b>	7.04 369	7.011 22	6.00 04	6.48 155	7.00 985	6.97 329	7.26 023	7.56 932	6.87 213	7.25 9	7.48 06	5.21 767
<b>Cxcr1</b>	3.86 149	3.367 37	3.62 453	3.34 107	3.02 278	3.69 125	4.24 033	3.81 93	4.07 567	4.28 63	4.33 924	3.92 816
<b>Ddx5 8</b>	6.26 957	6.584 6	7.80 586	6.60 956	7.07 341	6.69 125	7.13 65	6.92 973	7.09 452	7.18 354	7.77 534	7.96 769
<b>Ikbka p</b>	7.47 393	7.513 05	6.87 607	7.27 396	7.75 459	7.64 967	7.89 059	7.88 343	7.64 152	7.81 612	7.91 712	6.98 706
<b>C8a</b>	3.74 601	3.504 87	2.55 414	3.46 66	3.91 587	3.69 125	4.31 834	3.52 98	3.99 766	3.87 127	4.83 674	3.21 767
<b>Tnfrs f14</b>	5.44 645	5.504 87	6.15 108	5.23 919	5.30 289	5.27 622	5.74 283	5.31 407	5.93 626	5.74 574	6.38 107	6.48 616
<b>Lilra 5</b>	7.23 786	6.689 3	6.10 258	6.80 05	6.94 335	6.89 003	7.16 844	7.37 11	6.85 011	7.22 176	7.51 857	5.78 06
<b>Cd10 9</b>	7.39 945	6.890 93	6.59 853	6.70 182	7.34 471	7.10 219	7.55 422	7.75 219	7.38 998	7.57 909	7.95 914	6.76 946
<b>Nox1</b>	3.96 84	3.045 44	1.81 717	2.68 899	3.02 278	3.40 175	3.65 537	3.16 723	3.14 967	3.13 43	3.57 371	3.45 868
<b>Il22ra 2</b>	6.35 087	6.274 26	5.48 014	5.90 401	6.84 479	6.29 791	6.47 98	6.89 903	6.31 959	6.84 702	6.72 752	4.61 622
<b>Tnfsf 18</b>	3.62 048	2.630 4	2.40 214	2.68 899	3.21 543	3.69 125	3.39 234	3.68 18	3.14 967	2.28 63	4.05 914	3.21 767
<b>Defb1 4</b>	3.74 601	3.045 44	2.93 265	2.20 357	1.80 039	2.55 375	3.07 041	3.35 987	4.07 567	3.77 173	2.83 674	3.66 513
<b>Phlpp 2</b>	6.06 794	5.952 33	6.09 019	5.92 603	6.14 617	5.90 425	5.90 33	6.33 715	6.36 69	5.94 166	6.42 171	6.31 283
<b>Kir3d l2</b>	3.86 149	2.630 4	2.03 957	2.68 899	0.21 543	2.81 678	3.07 041	3.81 93	3.82 774	3.42 381	3.25 178	3.84 57

<b>Kir3d I1</b>	3.74 601	3.215 37	3.13 91	3.05 156	3.80 039	2.55 375	3.65 537	1.94 483	2.99 766	3.66 481	3.95 222	3.66 513
<b>Fcgr4</b>	3.74 601	3.504 87	6.17 473	2.46 66	4.53 736	2.81 678	4.24 033	3.81 93	4.28 717	4.66 481	6.27 415	5.71 243
<b>Il27</b>	3.96 84	3.952 33	2.69 164	3.05 156	4.02 279	4.03 918	4.46 273	5.06 031	4.35 13	4.42 381	4.33 924	3.34 32
<b>Ackr 4</b>	5.24 851	4.852 8	4.23 221	4.40 52	4.30 289	4.75 538	4.52 984	5.75 219	4.58 263	4.77 173	4.95 222	4.84 57
<b>Il17f</b>	2.96 84	3.745 88	3.75 577	3.05 156	4.02 279	3.03 918	2.87 776	3.52 98	3.63 509	4.05 184	5.42 171	4.34 32
<b>Nod2</b>	2.48 297	3.504 87	3.62 453	3.58 208	3.38 536	3.40 175	4.15 787	3.52 98	3.82 774	3.28 63	4.25 178	4.61 622
<b>Irak4</b>	6.44 645	6.293 37	7.21 521	6.72 713	6.77 002	6.69 125	6.42 796	6.89 903	6.83 896	6.88 324	7.39 133	7.25 009
<b>Gpr1 83</b>	3.33 097	3.215 37	4.55 414	2.46 66	3.02 278	2.23 182	3.52 984	2.68 18	3.14 967	3.42 381	4.77 534	3.92 816
<b>Tnfsf 15</b>	3.48 297	3.630 4	3.31 967	2.88 164	3.80 039	3.81 678	4.24 033	3.94 483	3.41 27	3.96 438	4.64 41	3.75 824
<b>Il19</b>	2.16 105	2.630 4	1.55 414	2.88 164	2.21 543	1.81 678	2.65 537	2.68 18	- 0.17 2262	2.54 934	2.57 371	2.08 016
<b>Cxcl3</b>	2.96 84	3.367 37	3.23 221	1.88 164	3.21 543	2.55 375	3.24 033	2.94 483	3.63 509	3.28 63	3.57 371	3.45 868
<b>Ifnl2</b>	4.96 84	4.132 9	2.93 265	3.88 164	4.97 032	4.03 918	4.92 839	4.81 93	4.82 774	4.71 926	5.25 178	4.34 32
<b>Card 9</b>	6.60 399	6.928 08	6.01 357	6.25 668	6.73 899	6.73 962	7.18 935	7.27 873	6.54 198	7.11 412	7.31 787	5.86 676
<b>Frmp d4</b>	2.48 297	3.045 44	2.93 265	3.05 156	2.53 736	2.55 375	2.87 776	3.35 987	3.28 717	2.54 934	1.83 674	2.92 816
<b>Cd59 b</b>	3.33 097	2.630 4	3.31 967	1.88 164	3.38 536	3.03 918	2.07 041	2.68 18	2.82 774	3.87 127	3.57 371	2.34 32
<b>Batf3</b>	4.74 601	4.800 33	4.09 019	4.52 55	4.91 587	4.81 678	4.52 984	4.94 483	4.47 159	4.71 926	4.25 178	4.71 243
<b>Clec4 a4</b>	0.16 1046	1.045 44	2.55 414	1.88 164	2.21 543	1.23 182	2.07 041	3.16 723	2.63 509	2.96 438	3.71 121	2.56 559
<b>Ccl26</b>	2.48 297	2.630 4	2.69 164	- 0.11 8361	2.80 039	1.23 182	4.15 787	4.06 031	2.82 774	2.77 173	3.71 121	2.56 559
<b>Btl2</b>	6.55 336	6.488 38	5.38 196	6.25 668	6.60 775	6.70 755	6.96 523	7.00 373	6.48 595	6.71 926	6.89 564	4.15 055
<b>C4a</b>	6.18 341	6.488 38	8.79 636	5.94 773	7.09 807	6.18 602	6.42 796	6.73 491	6.89 383	7.69 908	8.69 887	9.07 791
<b>Cd99</b>	7.45 567	7.480 07	7.76 359	7.40 52	7.29 225	7.39 169	6.87 776	7.01 808	7.42 02	7.48 794	7.59 163	8.11 138

<b>Btnl1</b>	6.65 29	6.330 84	5.42 204	6.37 349	6.16 963	6.49 861	7.02 46	7.14 123	6.44 245	6.94 166	6.89 564	5.00 616
<b>Tigit</b>	2.16 105	3.045 44	1.81 717	2.20 357	2.80 039	0.23 1821	2.87 776	3.52 98	2.63 509	2.77 173	2.83 674	2.75 824
<b>Klrb1</b>	2.74 601	1.630 4	0.81 7175	0.88 1639	2.21 543	2.23 182	1.65 537	1.94 483	0.82 7738	1.96 438	3.57 371	2.75 824
<b>H2-Ea-ps</b>	2.96 84	3.045 44	0.81 7175	2.20 357	3.67 486	2.55 375	3.07 041	2.94 483	2.99 766	1.96 438	3.05 914	2.75 824
<b>Gpr4 4</b>	2.48 297	2.852 8	0.81 7175	0.88 1639	2.53 736	3.03 918	2.07 041	3.52 98	2.41 27	3.28 63	3.25 178	2.75 824
<b>Name</b>	1	2	3	4	5	6	7	8	9	10	11	12
<b>Abl1</b>	6.60 399	6.254 89	6.44 167	6.32 458	6.62 482	6.34 035	6.78 465	6.31 407	6.50 016	6.40 732	6.93 828	7.02 502
<b>Cfd</b>	10.5 852	7.696 49	9.70 997	8.29 103	10.4 502	8.58 497	8.15 787	8.35 987	9.22 434	5.77 173	9.44 654	9.02 033
<b>Ahr</b>	6.26 957	6.235 26	6.55 414	6.34 107	6.14 617	6.25 419	6.39 234	5.75 219	6.71 038	6.33 941	6.74 364	6.72 402
<b>Aicda</b>	2.16 105	2.852 8	0.81 7175	1.88 164	1.80 039	2.23 182	2.39 234	3.52 98	2.14 967	0.96 4375	2.25 178	1.75 824
<b>Aire</b>	2.74 601	3.045 44	2.23 221	2.20 357	2.21 543	2.23 182	3.39 234	3.16 723	2.14 967	1.96 438	3.25 178	2.92 816
<b>App</b>	10.7 913	10.90 26	10.9 665	10.9 328	10.7 292	10.7 475	10.8 211	10.8 059	10.8 776	10.8 508	10.6 333	10.9 042
<b>Arhg dib</b>	6.37 05	6.504 87	9.11 485	6.32 458	6.97 032	6.34 035	6.57 82	6.50 962	6.93 626	6.99 78	9.02 327	9.16 55
<b>Atm</b>	6.92 923	6.915 8	6.35 115	6.75 2	7.02 279	7.05 2	7.30 881	7.45 79	6.95 702	7.14 428	7.49 019	6.53 96
<b>B2m</b>	14.7 815	15.09 83	14.7 491	14.6 706	14.7 932	14.9 521	15.1 19	15.0 172	15.0 278	15.0 034	15.0 689	14.8 533
<b>Bax</b>	7.46 483	7.622 87	8.01 685	7.47 41	7.49 155	7.35 076	7.49 667	7.58 869	7.50 722	7.82 856	7.63 549	7.62 242
<b>Bcl2</b>	5.58 731	4.852 8	5.40 214	5.46 66	5.88 786	5.44 127	5.49 667	5.35 987	5.95 702	5.87 127	6.31 787	6.25 009
<b>Bcl3</b>	3.48 297	3.745 88	4.09 019	1.46 66	3.80 039	2.55 375	3.39 234	2.94 483	3.28 717	3.66 481	4.83 674	5.08 016
<b>Bcl6</b>	5.40 897	4.952 33	4.98 71	4.78 853	5.34 471	4.93 226	4.92 839	5.48 915	5.03 719	4.28 63	5.20 598	5.59 113
<b>Bid</b>	5.11 524	4.999 64	5.46 103	4.78 853	5.02 279	4.55 375	5.19 969	4.52 98	4.99 766	5.05 184	6.22 906	5.96 769
<b>Prdm 1</b>	3.48 297	3.045 44	3.62 453	3.78 853	4.21 543	4.31 928	4.39 234	4.26 676	4.14 967	4.21 23	4.25 178	4.00 616
<b>Cxcr5</b>	5.51 86	5.367 37	4.09 019	4.96 91	5.50 083	5.27 622	6.00 115	5.85 172	5.41 27	5.45 623	5.67 805	4.15 055
<b>Bst1</b>	3.33 097	3.504 87	6.84 692	2.46 66	4.02 279	3.23 182	3.77 085	4.06 031	4.22 006	5.05 184	6.60 933	5.86 676

<b>Btk</b>	3.33 097	3.745 88	5.53 599	2.88 164	3.80 039	3.93 226	3.77 085	3.68 18	4.14 967	4.71 926	5.25 178	5.80 263
<b>Serpi ng1</b>	7.91 593	8.264 61	9.38 323	8.18 085	8.25 982	8.21 481	8.14 722	8.44 733	8.58 263	8.81 612	9.57 821	10.0 144
<b>C1qa</b>	6.55 336	6.600 03	9.33 024	6.18 542	7.19 271	6.49 861	6.64 026	7.39 329	7.40 517	8.04 652	8.83 298	9.12 674
<b>C1qb</b>	7.72 329	7.752 8	10.3 596	7.34 925	8.17 543	7.83 915	7.73 574	8.53 978	8.62 54	9.16 65	9.99 325	10.1 814
<b>C1qb p</b>	8.46 025	8.367 37	8.23 221	8.52 188	8.24 885	8.48 449	8.38 782	8.42 596	8.43 876	8.13 43	8.54 64	8.46 904

## **Chapter 4**

### **The Last Drop: Conclusion & Future Directions**

Manuel, Robbie SJ



Benign prostatic diseases, including BPH, acute prostatitis, and CP/CPSS, are prevalent and negatively impact quality of life. Current therapies address a variety of benign prostatic disease mechanisms, but fail to address autoimmunity, a cause of CP/CPSS and some forms of BPH. The incomplete understanding of autoimmune mechanisms of benign prostatic disease is a critical knowledge gap addressed in this thesis.

The AHR, a ligand-activated transcription factor, is implicated in several biological and toxicological processes. AHR induced immunosuppression was initially considered a toxic outcome of exposure to AHR agonists. It was later realized this AHR-mediated immunosuppression could be leveraged for therapeutic gain. AHR activation with selective ligands reduces autoimmunity in models of colitis, rhinitis, and dermatitis, but whether AHR activation would successfully treat prostate autoimmunity had not been previously examined.

We utilized ITE, a naturally occurring short-acting ligand for the AHR. The AHR is a ligand-activated transcription factor involved in a wide range of biological processes, including xenobiotic metabolism, cellular proliferation, differentiation, and the modulation of immune responses.

I introduced a new research model to my lab, a mouse model of autoimmune prostatitis (EAP). I obtained prostates from adult rats, collected, and filtered the homogenate, combined the homogenate with adjuvant, and injected the mixture subcutaneously into mice. The autoimmune response is characterized by low-grade inflammation (increased CD45+ leukocyte density),

allodynia, and increase in voiding frequency and increased NVCs. I used ITE to activate AHR in mice with EAP. I found that ITE significantly diminishes the presence of histological inflammation in the dorsal prostate. ITE significantly reduced allodynia two weeks post induction of EAP. ITE also protected against the EAP mediated changes in urinary behaviour, highlighted by reduction in non-voiding contractions via cystometry. Taken together, I concluded that ITE protects against prostate autoimmunity, including associated pain and urinary dysfunction that are translationally relevant for human CP/CPSS. The significance of this work lies in its potential to inform and guide future work aimed at treating autoimmune prostatitis.

A limitation of the work presented in this thesis is that the beneficial effects of ITE on prostate inflammation in mice might not be generalizable to humans. There are known species variations in responses to AHR agonists [1]. The functionality and efficacy of AHR agonists differ between mice and human, stemming from differences in ligand binding, receptor signaling, and metabolism. One source of species variation is the amino acid sequences within the AHR ligand-binding domain, which influence receptor conformation.

The signaling cascades initiated by the AHR in mice can differ from those initiated by the AHR in humans due to species differences in AHR co-activators and AHR co-repressors, and species differences in cellular signaling pathways [2]. Thus, AHR activation in mice does not always lead to the same biological outcomes as AHR activation in humans [1].

Mice metabolize AHR agonists differently than humans [1], which can potentially impact the duration of action. The mouse immune system also differs from that of humans [1]. Given the

critical function of AHR in modulating immune responses, the distinct immunological environments of mice and humans can lead to divergent outcomes following AHR activation.

While my work provides proof of concept that AHR agonists can reduce inflammation, pain and urinary dysfunction associated with autoimmune-mediated prostate inflammation, ITE may not be the ideal AHR agonist for treating human prostatitis. Understanding the species-specific dynamics of AHR agonists is crucial for the successful translation of the preclinical discoveries described in this thesis into effective clinical treatments in humans.

As our group moves forward, future research should focus on three areas.

1. ***Test the hypothesis that AHR signaling is required for the beneficial actions of ITE on autoimmune prostatitis.*** I found that ITE protects against autoimmune prostatitis in mice. While ITE was shown previously to be a selective AHR agonist [2], I did not test whether the protective effects of ITE on mouse EAP were AHR specific. Future studies should use AHR-knockout (AHRKO) mice to test the hypothesis that the AHR is required for the protective actions of ITE on EAP in mice. An assumption for these studies would be that baseline (in the absence of EAP) prostate histology, responses to tactile stimuli and voiding behaviors do not differ between AHRKO and age-matched control wild type mice. The seminal work by the Peterson group supports this assumption, as they showed AHRKO mouse prostate histology is comparable to that of wild type mice [3].
2. ***Test the hypothesis that prostate luminal epithelial cells shift energetics and cellular metabolism in response to autoimmune prostatitis.*** In Chapter 2, I used an inflammation

focused Nanostring panel to determine whether ITE blocked an EAP-mediated change in abundance of RNAs associated with inflammation. ITE blocked the EAP mediated induction of a cluster of genes involved in cellular metabolism/energetics, including *FNI*, *HIF1A*, *IFNAR1*, *IL4RA*, and *JAK2*. Prostate luminal epithelial cells secrete citrate as a critical component of seminal fluid. Citrate is normally used as part of the Krebs's cycle, and thus prostate luminal epithelial cells adapted a different mechanism to meet cellular energetic demands [4]. While it is known that prostate cells adapt new strategies for energy production during carcinogenesis, and efforts are underway to block the alternative energy production pathways to treat prostate cancer, energetic pathways have not been a focus of benign prostatic disease research.

Immune cell infiltration and inflammation, hallmarks of autoimmune prostatitis, have the potential to change prostate cell energetics. Fluorescent lifetime imaging (FLIM) is an imaging approach which measures the fluorescence lifetimes of intrinsic fluorophores like NADH and FAD, to detect shifts between oxidative phosphorylation and glycolysis [5]. These shifts are indicative of metabolic reprogramming, a hallmark of immune cell activation and a response to inflammation. Oxidative stress is a critical factor in the pathogenesis of autoimmune prostatitis, contributing to tissue damage and inflammation. FLIM can be used to assess the oxidative state within the prostate gland by monitoring changes in the redox ratio (FAD/NADH fluorescence lifetime ratio) [5]. This information can help in understanding how oxidative stress correlates with disease severity and progression. FLIM's high spatial resolution enables the mapping of metabolic heterogeneity within the prostate gland. The spatial resolution of FLIM is particularly

useful in autoimmune prostatitis, where inflammation may be patchy or localized to specific regions.

I conducted pilot studies to examine the NAD(P)H: FAD and redox ratios in uninflamed control and EAP prostate. (**Figure 1**).

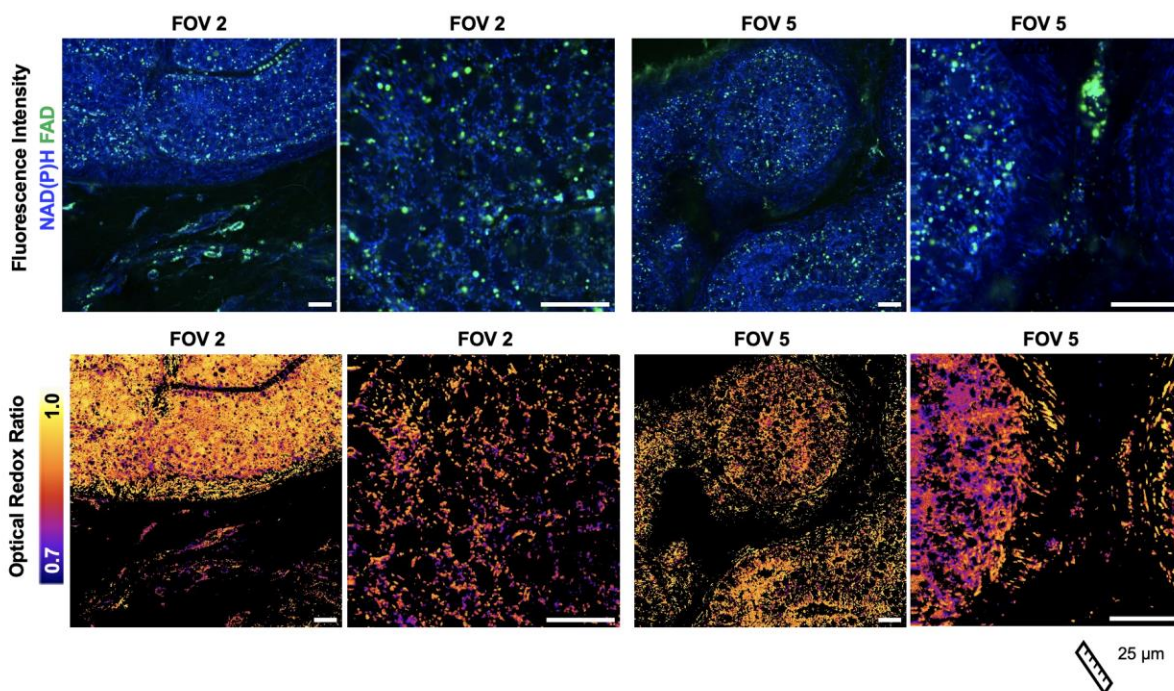


**Figure 1:** A pilot study was conducted using FLIM to image the prostate of control mice and mice with EAP. C57BL/6J adult (6-8 wk old) mice were subcutaneously injected with adjuvant or with adjuvant plus rat prostate homogenate as described in Chapter 2. Mice were euthanized by CO<sub>2</sub> asphyxiation, ventral prostates were removed and mounted immediately on glass imaging dish and imaged using a two-photon microscope. This work was performed collaboratively with Dr. Alexa Heaton, scientist in in the laboratory of Dr. Melissa Skala. The

top images reveal the fluorescence intensities of NAD(P)H (Blue) and FAD (green). The bottom images show the intensity of NADH divided by the intensity of FAD and represents cellular metabolism within the tissue. The signal to noise ratio was improved when prostate was micro-dissected and imaged separately from the rest of the urinary tract (eAp1) than when the entire mouse urinary tract was mounted on the slide and the microscope focused on the prostate (eAp2). The results are representative of two control mice and two EAP mice.

FLIM could be used alone, or in combination with other imaging techniques, to examine metabolic/energetic changes associated with autoimmune prostatitis over time, in response to treatment, and to compare metabolic/ energetic changes associated with autoimmune inflammation compared to those associated with bacterial inflammation, and cancer associated inflammation to determine whether autoimmune prostatitis drives a unique metabolic process. FLIM could also be used to compare and contrast metabolic/energetic changes associated with prostate inflammation across species, including experimental model species (mice and rats) and species in which prostate inflammation drives clinically relevant outcomes (dogs and humans). The goal would be to enhance understanding of prostate inflammation and identify energetic pathways as potential clinical targets.

The Open Field Test (OF), traditionally employed to evaluate exploratory behavior, anxiety, and locomotor activity in rodents, holds significant potential for elucidating metabolic dysfunction induced by autoimmune prostatitis. By analyzing the locomotor activity and exploratory behavior in an open arena, researchers can gain indirect insights into the energetic and metabolic

states of mice [6]. For instance, variations in locomotor activity may reflect changes in energy expenditure, indicative of underlying metabolic alterations. Similarly, a decrease in exploratory behavior might suggest impaired metabolic energy availability or modifications in neurotransmitter systems, which are known to regulate both metabolism and behavior.

Moreover, the Open Field Test can shed light on anxiety-like behaviors that are often linked to stress physiology, a critical factor in metabolic processes. The stress-related alterations observed through this behavioral assay, due to the activation of the hypothalamic-pituitary-adrenal axis, can signal changes in metabolic function, affecting glucose metabolism, fat storage, and overall energy balance. By correlating these behavioral outcomes with physiological measures of metabolism, such as blood glucose levels, insulin sensitivity, and body composition, a more comprehensive understanding of the impact of metabolic dysfunction on behavior and vice versa can be achieved.

The OFT can be particularly useful in future studies of autoimmune prostatitis. This approach will not only help in assessing the direct effects of EAP on locomotor and exploratory behaviors but also in understanding the broader implications of metabolic reprogramming associated with the disease state. Evaluating these behaviors before and after interventions aimed at correcting metabolic dysfunction or modulating the immune response in EAP (ITE treatment, for example) can provide valuable information on the efficacy of such treatments. Furthermore, the test can highlight nuanced behavior changes associated with the disease state, offering a holistic view of the organism's health that encompasses both metabolic and behavioral dimensions.

### ***3. Test the hypothesis that autoimmune prostatitis reduces male fertility.***

Chronic inflammation of the prostate gland has been shown to precipitate a range of pathophysiological alterations encompassing epithelial-mesenchymal transition, aberrant cellular proliferation, and metabolic reprogramming. Such modifications have the potential to compromise the functional integrity of the prostate, notably its seminal role in sperm transportation and seminal fluid production, both of which are pivotal for maintaining sperm viability and motility. In the realm of benign prostatic disorders, CP/CPPS emerges as a substantial contributor to male infertility, primarily attributed to the excessive generation of ROS [7]. This pathogenic process underscores the intricate link between prostatic inflammation, oxidative stress, and reproductive dysfunction, necessitating comprehensive investigations to elucidate the mechanistic pathways involved and to inform the development of targeted therapeutic interventions.

To test whether autoimmune prostatitis reduces sperm quality and whether ITE protects against this adverse outcome, I propose a series of *in vivo* experiments using the EAP mouse model. Initially, the assessment will focus on establishing baseline sperm quality parameters, including motility, concentration, and morphology, in control mice, and mice with EAP, through computer-assisted sperm analysis (CASA). This foundational data will serve as a benchmark for subsequent studies involving EAP. Following the baseline assessment, EAP mice will receive ITE at various doses and for different durations, after which sperm parameters will be reassessed and compared against untreated EAP controls and healthy counterparts.



The next step would be a longitudinal study to monitor the long-term impact of ITE on fertility and reproductive outcomes in both EAP and LUTD models. Treated mice will be mated with healthy females at selected intervals post-treatment, with a focus on evaluating mating success, litter size, and offspring health to ascertain the broader implications of ITE therapy on male reproductive success.

Moreover, to shed light on the molecular mechanisms through which ITE mediates its effects on sperm quality, transcriptomic and proteomic analyses will be conducted. These analyses aim to identify alterations in gene and protein expression related to sperm quality and inflammation in ITE-treated versus untreated mice, providing insights into the underlying biological processes influenced by ITE.

A comparative analysis involving ITE and other AHR agonists, such as I3C and its metabolite 3,3'-Diindolylmethane (DIM), will also be undertaken [8]. This comparison will help delineate the specific attributes and efficacy of ITE relative to other compounds in improving sperm quality and reproductive outcomes in the context of EAP and LUTD.

Lastly, the investigation will include a direct assessment of ITE's impact on inflammation within the prostate and lower urinary tract by employing histological and immunohistochemical techniques. This will enable a detailed evaluation of ITE's anti-inflammatory properties and its potential to mitigate tissue damage associated with EAP and LUTD, further informing the therapeutic viability of ITE in addressing male infertility related to prostatic and urinary tract

disorders. Through this comprehensive research approach, we aim to uncover novel therapeutic strategies for improving male reproductive health in the face of complex urological conditions.

## References

1. Xu, X., et al., *Species-Specific Differences in Aryl Hydrocarbon Receptor Responses: How and Why?* Int J Mol Sci, 2021. **22**(24).
2. Safe, S., et al., *Aryl Hydrocarbon Receptor (AHR) Ligands as Selective AHR Modulators (SAhRMs)*. Int J Mol Sci, 2020. **21**(18).
3. Lin, T.M., et al., *Effects of aryl hydrocarbon receptor null mutation and in utero and lactational 2,3,7,8-tetrachlorodibenzo-p-dioxin exposure on prostate and seminal vesicle development in C57BL/6 mice*. Toxicol Sci, 2002. **68**(2): p. 479-87.
4. Ahmad, F., M.K. Cherukuri, and P.L. Choyke, *Metabolic reprogramming in prostate cancer*. Br J Cancer, 2021. **125**(9): p. 1185-1196.
5. Cao, R., H. Wallrabe, and A. Periasamy, *Multiphoton FLIM imaging of NAD(P)H and FAD with one excitation wavelength*. J Biomed Opt, 2020. **25**(1): p. 1-16.
6. Bohlen, M., et al., *Experimenter effects on behavioral test scores of eight inbred mouse strains under the influence of ethanol*. Behav Brain Res, 2014. **272**: p. 46-54.
7. Ihsan, A.U., et al., *Role of oxidative stress in pathology of chronic prostatitis/chronic pelvic pain syndrome and male infertility and antioxidants function in ameliorating oxidative stress*. Biomed Pharmacother, 2018. **106**: p. 714-723.
8. Beamer, C.A., et al., *Targeted deletion of the aryl hydrocarbon receptor in dendritic cells prevents thymic atrophy in response to dioxin*. Arch Toxicol, 2019. **93**(2): p. 355-368.

**APPENDIX**

## Appendix A

### **Harmony and Dissonance: Unraveling Sex-Biased Dynamics in Immunometabolism, Autoimmunity, and Chronic Unpredictable Stress for Personalized Health**

Manuel, Robbie SJ

The work documented in this appendix was conducted under Yun Liang's supervision from December 2019 to July 2021, after which supervision was transferred to Chad Vezina in August 2021.

In the intricate landscape of autoimmune diseases, the convergence of sex, gender, biological variables, and social factors contributes to nuanced differences within and between groups. A striking observation emerges with a remarkable female predominance in autoimmune diseases, hinting at underlying fundamental distinctions in immune regulation between men and women. This phenomenon underscores the existence of molecular foundations of sexual dimorphism in immunity that, despite their indisputable presence, remain shrouded in unanswered questions.

Among the myriad of autoimmune diseases, systemic lupus erythematosus (SLE) stands as a prevalent subtype, marked by the immune system's assault on its own tissues, triggering widespread inflammation and organ damage. The burden of lupus in the United States alone surpasses 1.5 million individuals, with a staggering gender ratio of 9:1 (female to male) in the patient population, further compounded by the occurrence of multiple autoimmune diseases in half of lupus patients. The absence of a cure for lupus accentuates the emergent need to delve deeper into its molecular underpinnings.

Within the Liang Lab, our pursuit of unraveling the molecular basis of lupus is guided by a focused exploration of its female sex bias. Our analytical lens scrutinizes transcriptomic differences between female and male skin, the primary organ affected in lupus, revealing autoimmune genes characterized by female-biased expression patterns. This investigative journey led to the identification of vestigial-like family member-3 (*VGLL3*), a putative transcription factor with a female-biased disposition. *VGLL3* orchestrates a network of autoimmune genes, demonstrating a pivotal role in the regulation of immune responses.

Preliminary findings illuminate a bias in the female human skin toward heightened expression of genes associated with susceptibility to autoimmune diseases. Notably, these gene expressions operate independently of sex-hormone regulation and are under the influence of *VGLL3*, solidifying its status as a female-increased transcription factor. *VGLL3* not only facilitates the expression of immune genes, including interferon-stimulated genes (ISGs) – a hallmark of female-biased autoimmune diseases – but also correlates significantly with transcriptomic alterations observed in various female-biased autoimmune diseases, including SLE.

The translational significance of our research extends to a murine model where overexpressing *Vgll3* in the murine epidermis, driven by the keratin-5 (K5) promoter, faithfully recapitulates key features of both cutaneous and systemic lupus observed in humans. The conservation of a female sex-bias expression of *VGLL3* in the skin of wild-type (WT) mice further strengthens the premise that overexpression of a single female-biased factor, *Vgll3*, is sufficient to induce autoimmunity in mice. This discovery not only opens new avenues of opportunity for our laboratory but also marks a significant milestone in understanding the intricate molecular mechanisms underlying lupus.

While previous work from our lab identified *VGLL3* as a molecular contributor to SLE, the realm of environmental exposures and their impact on the risk and progression of autoimmune diseases driven by *VGLL3* remains uncharted. Speculations about the influence of chronic environmental stress on human health, particularly immune responses, abound; however, empirical evidence from a well-defined experimental system is conspicuously absent. In this pursuit, our mouse

model of *Vgll3* emerges as a unique lupus model, faithfully representing the effects of sex-biased, pro-autoimmune factors on autoimmune pathogenesis.

Our research trajectory involves defining the impact of environmental stress on SLE disease progression and unraveling the molecular underpinnings of stress-regulated immune responses. The overarching goal is to contribute to the development of future treatment protocols aimed at enhancing patient outcomes. A pivotal aspect of our work is testing the hypothesis that chronic stress serves as a catalyst for the progression of sex-biased lupus pathogenesis, as modeled by the *Vgll3*-overexpression mice.

The mechanistic principles governing *Vgll3*'s function in modulating stress response in vivo represent a key area of investigation. Insights gleaned from this endeavor promise to enhance our understanding of autoimmune diseases and their sex-biased characteristics. Our collaboration with rheumatologists at the University of Wisconsin School of Medicine and Public Health affords us unprecedented access to the state's only Lupus clinic, enriching our research with valuable clinical perspectives and underscoring the translational potential of our work.

Employing a multifaceted approach encompassing basic immunology, biochemistry, and animal-based modeling, our research endeavors to fill critical knowledge gaps. The diverse array of information generated holds the promise of developing an integrative strategy to aid patients grappling with SLE and a spectrum of additional autoimmune diseases characterized by similar molecular signatures.



Our exploration into the molecular intricacies of lupus, guided by a focus on its female sex bias and the role of *Vgll3*, propels us into uncharted territories of understanding. By bridging gaps in our knowledge related to gene-environment interactions, sex-specific immune regulation, and the impact of chronic stress on autoimmune disease progression, we aspire to contribute to the development of innovative therapeutic approaches. The journey outlined herein represents a concerted effort to decipher the complex tapestry of autoimmune diseases and offer potential avenues for clinical intervention and improved patient outcomes.

This study posits a hypothesis that chronic stress significantly influences the progression of sex-biased lupus pathogenesis, specifically as modeled by *Vgll3*-overexpression mice.

The importance of this research lies in its divergence from previous work, which primarily focused on successfully replicating a lupus-like phenotype within a murine model. However, the existing model lacks clarity on how genetic factors, particularly *Vgll3*, interact with environmental elements to impact disease progression, leaving a critical gap in understanding. Emerging evidence suggests that genetic factors and environmental stressors detrimentally affect the immune system's ability to discern self from non-self-antigens. Understanding these environmental influences becomes crucial, as despite indications of environmental modulation in autoimmunity pathogenesis, the precise mechanisms remain inadequately explicated. The project aims to fill this gap by identifying gene-environment interactions influencing autoimmune disease progression, elucidating fundamental disparities in immune regulation between genders under the influence of environmental stress, and providing a conceptual framework for the

development of innovative, sex-specific therapeutic approaches to enhance outcomes in autoimmune diseases.

The specific aims and experimental approach of the study involve two primary objectives:

**Aim 1:** Define the impact of chronic environmental stress and its influence on the lupus-prone, *Vgll3*-overexpressing mouse model.

**Scientific Premise:** The research employs a novel mouse model with doxycycline-inducible overexpression of murine *Vgll3* in the skin. While constitutive *Vgll3*-overexpressing mice have previously demonstrated the ability to induce lupus-like phenotypes, including cutaneous lesions (see Figure 2), the associated lethality precludes stress impact studies. To overcome this limitation, a pTre-*VGLL3*/K14rtTA model has been established, wherein *VGLL3* expression is regulated by the pTre promoter and activated by a reverse tetracycline-controlled transactivator (rtTA). Validation confirms the model's ability to recapitulate lupus-like phenotypes, including skin lesions (refer to Figure 2; data not presented).

**Experimental Approach:** Animals are subjected to a chronic unpredictable stress (CUS) paradigm, a well-established method for modeling environmental stress.

**Aim 2:** Identify the molecular mechanism(s) underlying chronic stress (CUS)-influenced

autoimmune disease progression.

**Scientific Premise:** Building on preliminary data, the hypothesis posits that the progression of lupus-like phenotypes in *Vgll3* overexpressing mice under chronic stress is mediated by the multifunctional cytokine IL-6. This cytokine is associated with responses to infections, tissue injuries, and plays a role in host defense through acute phase responses, hematopoiesis, and immune reactions. Impaired synthesis of IL-6 is linked to chronic inflammation and autoimmunity.

**Experimental Approach:** Measurement of IL-6 expression levels in serum, skin, and heart tissues, activation analysis of downstream signaling of IL-6, and evaluation of the Treg/Th17 balance by flow cytometry of PBMCs are integral components of the experimental approach. Additionally, depletion of IL-6 through administration of an anti-IL-6 monoclonal antibody is employed to establish a potential causal relationship between IL-6 and cardiac abnormalities observed in the study.

### **Establishment of a Chronic Unpredictable Stress (CUS) Paradigm:**

Representation of the schedule followed by cohorts of nulliparous male and female pTre-*Vgll3*/K14rtTA mice aged 27-32 weeks (**Table 1**):

		Monday	Tuesday	Wednesday	Thursday	Friday	Saturday	Sunday
<b>Week 1</b>	<b>AM</b>	Restraint	Multiple Cage Changes	Predator - Fox Urine	Dirty Rat Bedding	Restraint	Multiple Cage Changes	Multiple Cage Changes
	<b>PM</b>	Continuous Light (72 Hours)			Dirty Rat Bedding	Slanted Cage	No Bedding	Dirty Rat Bedding
<b>Week 2</b>	<b>AM</b>	Slanted Cage Changes	Multiple Cage Changes	Restraint	Multiple Cage Changes	Slanted Cage	Restraint	Dirty Rat Bedding
	<b>PM</b>	No Bedding	Predator - Fox Urine	Predator - Fox Urine	Dirty Rad Bedding	Continuous Light (72 Hours)		

**Table 1: Chronic Unpredictable Stress (CUS) Paradigm.** Representation of the schedule which cohorts of nulliparous male and female pTre- *Vgl3/K14rtTA* mice aged 27-32 weeks old follow. When the animal is subjected to restraints for 2 hours the animal is placed in a 50 mL conical with ample ventilating holes to allow for heat exchange. The nose/mouth of animal is then centered and stuck in the opening of the conical, where the apex of the tube has been removed. The mouse confined but in no way compressed and is able to move its body. Multiple cage changes consisted of replacing each housing cage with a new cage every 30 minutes over a period of 4 hours. Filter paper soaked in fox urine will be placed into cages for 15 minutes to simulate a predator response. Animals will have diurnal interruption with continuous light exposure for 36 hours. Soiled rat bedding will be placed into the cage of mice in order to

provoke a predator response for 12 hours. Bedding will be completely removed from cage, for 12 hours over night on a night where normal diurnal cycle is in place. Slanting the cage at 45 degrees overnight for 12 hours on a night where normal diurnal cycle is in place.

Intriguingly, the study observed a substantial burden of environmental stress on transgenic (TG) animals, with notable differences between males and females. Post-CUS treatment, male TG animals exhibited a significant 9.45% body weight loss, compared to a 2.62% loss in male wildtype (WT) animals ( $P = 0.0163$ ). Conversely, female TG animals showed a more modest 3.45% weight loss, in contrast to a 1.27% loss in female WT animals ( $n = 5$  each group). Additionally, environmental stress exacerbated skin lesions in transgenic animals of both sexes. These initial findings not only confirmed a cutaneous lupus (CL)-like phenotype with *Vgll3* overexpression but also suggested that chronic stress contributes to disease exacerbation.

It is established that CL worsens with exposures to cigarette smoke and UV light; however, associations with other environmental triggers, such as stress, remain undescribed. Furthermore, while there is an accepted association between lupus and systemic progression from skin to various organ systems, including the heart, the mechanisms and triggers behind specific organ progression are inadequately defined. To address these knowledge gaps, the study aims to:

**Aim 1.1: Determine how chronic stress impacts SLE-like skin inflammation and autoimmunity**

**Scientific Premise:** Preliminary studies successfully recapitulated CL phenotypes in the inducible *Vgll3* model, demonstrating that chronic stress exacerbates lupus-like skin lesions.

**Experimental Approach:**

- **Histological Analysis:** Employ hematoxylin and eosin (H&E) staining to assess the impact of chronic stress on histological features of cutaneous lupus.
- **Immune Cell Infiltration:** Utilize immunofluorescence staining for T cells, B cells, and dendritic cells to study immune cell populations in response to chronic stress.
- **Molecular Signatures:** Analyze the expression of interferon-stimulated genes (ISGs) and other lupus-associated markers by qPCR and western blotting.

**Assay Groups:** Utilize four experimental groups (1) TG CUS<sup>+</sup>, (2) TG CUS<sup>-</sup>, (3) WT CUS<sup>+</sup>, and (4) WT CUS<sup>-</sup>, employing litter-, sex-, and age-matched pTre-*Vgll3*/K14rtTA mice (27-32 weeks old).

**Aim 1.2: Impact of Chronic Stress on Systemic Disease Progression to the Heart**

*Vgll3* overexpression in the skin is anticipated to yield a distinct cutaneous phenotype. However, a critical aspect in lupus pathogenesis involves the progression of cutaneous manifestations to a systemic level, resulting in systemic lupus (SLE). Notably, SLE patients exhibit a threefold higher risk of fatal cardiac events compared to healthy, sex- and age-matched individuals. Premature coronary heart disease has become a significant

contributor to morbidity and mortality in SLE. Therefore, it is imperative to characterize the systemic features within this model and comprehend the role of chronic stress in influencing systemic disease progression.

In preliminary investigations, cardiac abnormalities were noted in chronically stressed (CUS+) transgenic animals, validated through 2-dimensional (2D)-echocardiogram analysis (see Figure 3). The male CUS<sup>+</sup> transgenic animal displayed a 42% increase in atrial ventricle (AV) mean velocity compared to its CUS+ wildtype (WT) counterpart, indicating stenosis. This aligns with clinical findings of progressive heart impairment, including aortic and mitral valve dysfunction, and left ventricular (LV) hypertrophy in SLE patients. Consistently, the CUS+ transgenic animal exhibited a 67% increase in LV mass difference and a 2.08-fold increase in LV/body weight ratio compared to its WT control, indicative of LV hypertrophy. The pulmonary acceleration time decreased by 16% in the TG CUS<sup>+</sup> male, raising concerns about pulmonary hypertension—an alarming complication of connective tissue diseases, notably prevalent in SLE patients. Importantly, the observed abnormalities in animals overexpressing *Vgll3* under chronic stress mirror features seen in human SLE.

To investigate whether heart inflammation underlies these abnormalities, immunofluorescence staining will be employed to analyze the infiltration of T cells, B cells, monocytes, and dendritic cells, using markers identified in sub-aim 1.1. Additionally, immunofluorescence staining will be conducted to test for the deposition of complement 3 (C3) and immunoglobulins (IgG, IgM, and IgA)—key features of SLE-

associated autoimmunity. The expression of interferon-stimulated genes, recognized hallmarks of lupus, including Mx1, IRF-7, and cGAS-MITA, will be analyzed through qPCR and western blotting. Moreover, assays will be performed to assess potential upregulation of IL-6, TNF , IL-19, and CRP, established markers of cardiac events.

**Assay Groups:** (1) TG CUS<sup>+</sup>, (2) TG CUS<sup>-</sup>, (3) WT CUS<sup>+</sup>, and (4) WT CUS<sup>-</sup>, employing litter-, sex-, and aged-matched pTre-*Vgll3*/K14rtTA mice (27-32 weeks old, corresponding to the common age of SLE onset in humans).

**Potential Caveats and Alternatives:**

Certainly, handling animals within the vivarium introduces stress. To mitigate exogenous stress beyond the CUS paradigm, handlers' gender will remain consistent, and noise and light discipline will be maintained. In the absence of changes in interferon-stimulated genes, an unbiased transcriptomic experiment will be conducted to identify stress-impacted factors associated with SLE.

**Aim 2: Unraveling the Molecular Mechanisms Underlying Chronic Stress-Influenced Autoimmune Disease Progression**

**Scientific Premise:** Building upon preliminary findings presented in Figures 2 and 3, it is evident that Chronic Unpredictable Stress (CUS) profoundly impacts facets of lupus progression, particularly the development of skin lesions. My hypothesis posits that this progression is mediated by the multifunctional cytokine Interleukin-6 (IL-6). Recognized



for its role in responding to infections and tissue injuries, IL-6 contributes to host defense by stimulating acute phase responses, hematopoiesis, and immune reactions. Impaired synthesis of IL-6 is implicated in chronic inflammation and autoimmunity. Acting as a B cell stimulatory factor, IL-6 prompts activated B cells toward antibody production. In collaboration with TGF- $\beta$ , IL-6 facilitates the differentiation of naïve CD4<sup>+</sup> T cells into Th17 while inhibiting TGF- $\beta$ -induced Treg development. This Th17/Treg imbalance may underlie the onset and progression of immune-mediated diseases. IL-6 engages two membrane receptors, IL-6R $\alpha$  receptor and glycoprotein 130 (gp130). Binding to these receptors activates the Janus Kinase/Signal Transducer and Activation of Transcription (JAK/STAT) cascade and the Mitogen-Activated Protein Kinase (MAPK) cascade. Termination of IL-6 signaling involves tyrosine phosphatases, Suppressor of Cytokine Signaling (SOCS) proteins, and Protein Inhibitor of Activated STAT (PIAS) proteins, wherein the balance between signaling pathways and suppressors modulates IL-6's ultimate cellular action.

**Experimental Approach:**

- To test the hypothesis that IL-6 mediates the chronic stress-induced progression of lupus-like phenotypes in *Vgll3*-overexpressing mice, expression levels of IL-6 will be measured in serum (ELISA) and skin/heart tissues (qPCR).
- Analysis will be sex-stratified across age-matched TG CUS<sup>+</sup>, TG CUS<sup>-</sup>, WT CUS<sup>+</sup>, and WT CUS<sup>-</sup> animals (n=12 each group).
- Downstream IL-6 signaling activation will be assessed through immunofluorescence and western blot analysis of native and phosphorylated forms of signal transducer and

- activator of transcription 3 (STAT3). Treg/Th17 balance will be examined via flow cytometry of Peripheral Blood Mononuclear Cells (PBMCs), detecting CD4/CD25/Foxp3 for Tregs and CD4/ROR $\gamma$ t/IL-17 for Th17 cells.
- To establish a potential causal link between IL-6 and cardiac abnormalities, IL-6 depletion will be conducted using anti-IL-6 monoclonal antibody (IL-6 mAb). Evaluation of IL-6 levels, skin lesions, heart function (echocardiogram), inflammatory markers, complement, and Ig deposits will be conducted, with saline-administered mice serving as controls.

**Assay Groups:** Utilize four experimental groups (1) TG CUS<sup>+</sup>, (2) TG CUS<sup>-</sup>, (3) WT CUS<sup>+</sup>, and (4) WT CUS<sup>-</sup>, employing litter-, sex-, and age-matched pTre-*Vgll3*/K14rtTA mice (27-32 weeks old).

**Potential Caveats and Alternatives:**

The primary caveat is the absence of preliminary data indicating a role for IL-6. If IL-6 is not involved, a serum cytokine array will be conducted to identify high-likelihood candidate cytokines for subsequent experiments.

**Conclusion:**

The stress response, an intricately woven biological phenomenon, extends its influence beyond the conventional understanding, revealing profound implications for the etiology of lupus—an intricate autoimmune disorder. In the realm of toxicology, stress transcends mere psychological states, transforming into a physiological condition marked by the intricate interplay of

neuroendocrine pathways. Chronic stress, characterized by persistent and prolonged activation of the stress response, introduces a multifaceted narrative into the dialogue of lupus origins and progression. Guided by McEwen's allostatic load theory, chronic stress exposes the body to prolonged periods of heightened physiological demands, resulting in wear and tear on various organ systems. This physiological strain may contribute significantly to the dysregulation of the immune system, a pivotal player in the pathogenesis of lupus.

Within the intricate web of stressors in lupus, the interplay between genetic predispositions and environmental triggers weaves a tapestry of susceptibility. The sexually dimorphic nature of stress-response pathways adds an additional layer of complexity, resembling the intricate dance of hormones and molecular signals—a Shakespearean sonnet etched into the very fabric of our genetic code. As in literature, where narratives unfold through the dynamics of male-female interactions, lupus manifests a unique stress response in males and females.

The narrative takes a bold turn as we venture into uncharted territory—a murine model, a metaphorical canvas previously untouched. The murine model, bearing unique genetic imprints, unveils molecular stresses beneath the surface of lupus progression. Analogous to Dickens unraveling societal complexities, we delve into molecular Dickensian plotlines, seeking to comprehend the stress-induced upheavals within these murine counterparts. The study, akin to a literary work, becomes an odyssey, navigating uncharted waters of stress management and unveiling a novel approach—a postmodern narrative where the essence of stress in lupus transforms into an evolving storyline.

Aligning with the ethos of modern academia, where sciences merge with humanities, this study echoes T.S. Eliot's poetic wisdom, reminding us that "humankind cannot bear very much reality." In this case, the reality of lupus, shaped by nuanced interactions of stress, genetics, and environment, becomes a tale awaiting unraveling. As this scientific narrative unfolds, akin to gripping novel chapters, it brings forth the promise of a novel clinical approach to stress management. In the grand literary tradition, this study emerges not merely as a scientific inquiry but as a compelling narrative, seeking to transform the lives of those ensnared in the intricate plotlines of lupus, offering a beacon of hope amidst the complex tapestry of stress and autoimmune disorders (**Figure 1**).

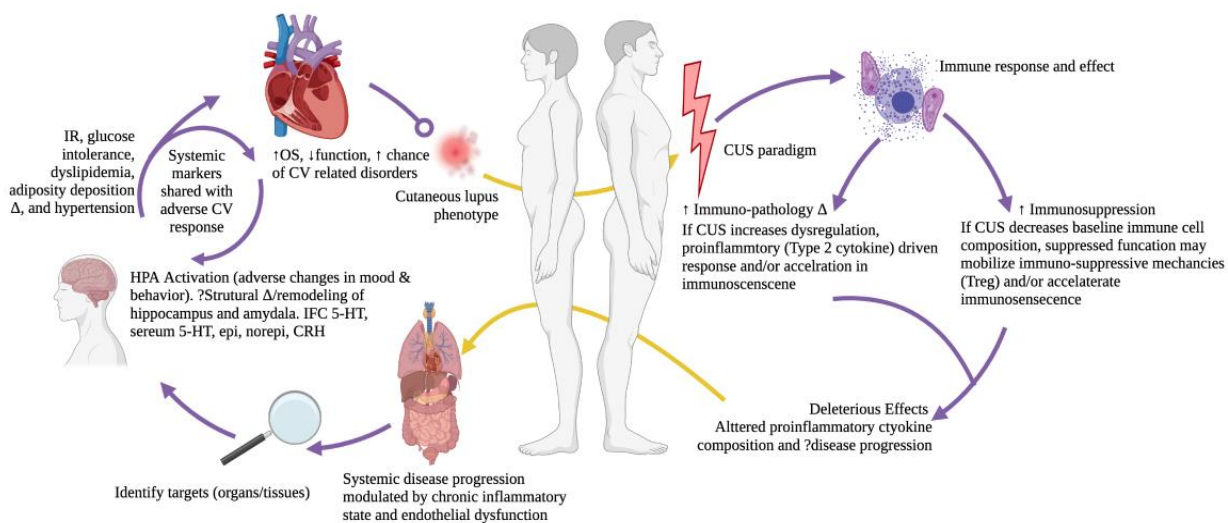


**Figure 1:** pathological sequelae of chronic stress and plausible links between systemic progression.

As we consider the broader landscape of autoimmune diseases, this study emerges as a cornerstone in translational research. Autoimmune diseases, a collective manifestation of the body's immune system turning against itself, present an intricate puzzle. Experimental autoimmune models, such as the murine model employed in this study, become invaluable tools akin to the protagonist's journey in literature—unraveling complexities, providing insights, and paving the way for translational breakthroughs. This scientific narrative, akin to a plotline in translational research, endeavors not only to uncover the mysteries of lupus but also to contribute to a broader understanding of autoimmune disorders. In this synthesis of scientific inquiry and literary metaphor, the study becomes a transformative chapter, guiding us towards innovative strategies in managing autoimmune diseases and offering a beacon of translational promise on the horizon of medical advancement.

## **Results**

Our investigation into the impact of chronic stress on body weight and metabolic parameters in a murine model has yielded compelling preliminary data. The study focused on the intricate interplay between stress, metabolic hormones, and inflammatory mediators, particularly in the context of lupus.

A noteworthy observation emerged regarding weight fluctuations in response to chronic stress. Individuals with lupus often grapple with weight changes attributed to factors such as altered appetite, dietary habits, and reduced energy and mobility. Our study sheds light on the intricate mechanisms underpinning these changes, emphasizing the role of stress-induced alterations in

metabolic pathways. The data, derived from a preliminary cohort of 60 subjects, demonstrated a statistically significant loss in body weight percentage. Specifically, the comparison between -CUS/WT Female and +CUS/TG Male revealed a significant difference ( $p=0.04$ ), as did the comparison between -CUS/WT Male and +CUS/TG Male ( $p=0.026$ ). The overall analysis employing ANOVA tests underscored a compelling significance ( $p=0.0079$ ) with an associated r-squared value of 0.2599 (**Figure 2**).

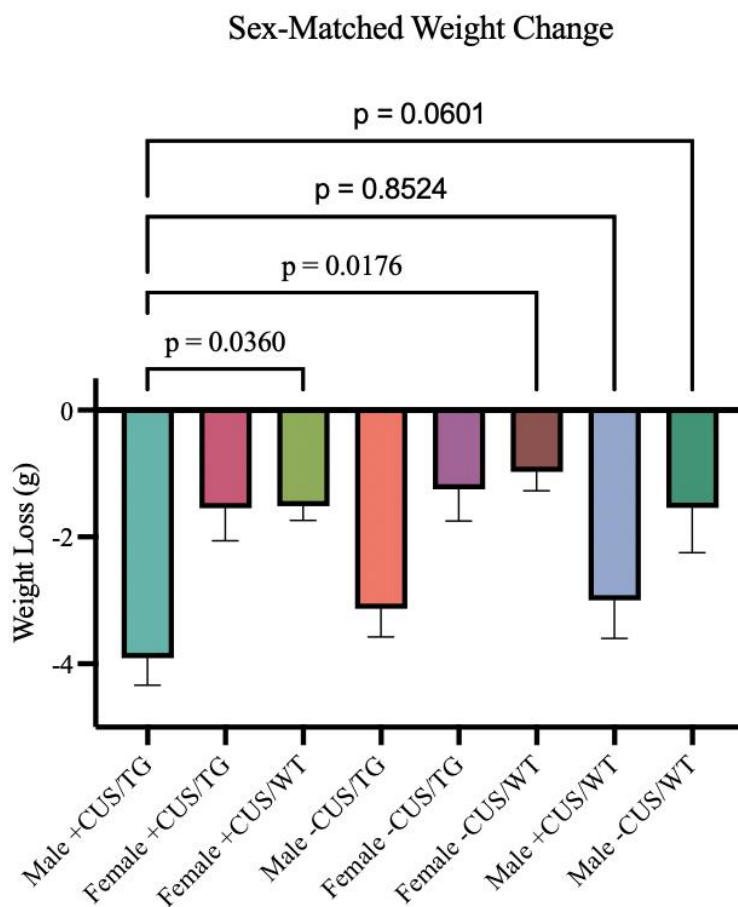


**Figure 2: Sex-Matched Weight Changes in Response to Chronic Stress and Transgenic Modification.** Sex-matched weight changes reveal significant reductions in male +CUS/TG animals compared to a majority of experimental groups across both sexes, except for Female

+CUS/TG and both -CUS/TG groups. Specifically, male +CUS/TG animals exhibit a significant weight reduction when compared to Female +CUS/WT ( $p=0.0360$ ) and Female -CUS/WT ( $p=0.0176$ ) groups. These findings highlight the nuanced impact of chronic stress and transgenic modification on sex-specific weight dynamics, with male +CUS/TG animals experiencing distinctive weight alterations in comparison to their female counterparts and other experimental groups.

The identification of significant weight loss is indicative of the intricate relationship between chronic stress and metabolic dysregulation. Importantly, our findings suggest a potential gender-specific effect, highlighting the need for further exploration in this domain. Notably, the observed r-squared value of 0.2599 prompts consideration of increasing the sample size to strengthen the effect size and enhance the robustness of our trial population.

Looking into the impact of chronic stress on stress-sensitive mice we revealed profound insights into the complex interplay between environmental factors, genotype, and behavioral responses. In response to stressful circumstances, organisms exhibit rapid adaptations in both behavior and physiological processes to maintain homeostasis. Prolonged alterations in these adaptive mechanisms are posited to contribute to an altered allostatic load, potentially leading to the development of maladaptive psychiatric states.

A key aspect of our study involved the quantification of fecal boli as a measurable parameter for early identification of behavioral and molecular markers associated with hypothalamic-pituitary-adrenal (HPA) axis alterations. Consistent with previous literature fecal boli production in mice

subjected to stress sensitivity studies, particularly in the open-field test, served as an indicator of an anxiety-like state. Notably, our findings demonstrated a significant increase in fecal boli production in TG mice compared to WT animals, with a particularly pronounced elevation in TG animals exposed to chronic unpredictable stress (+/- CUS) (**Figure 3**).

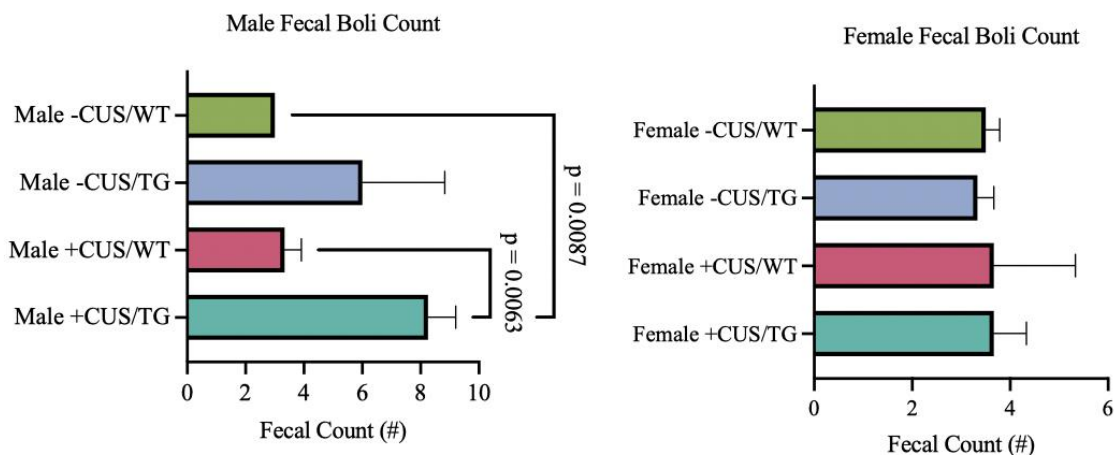


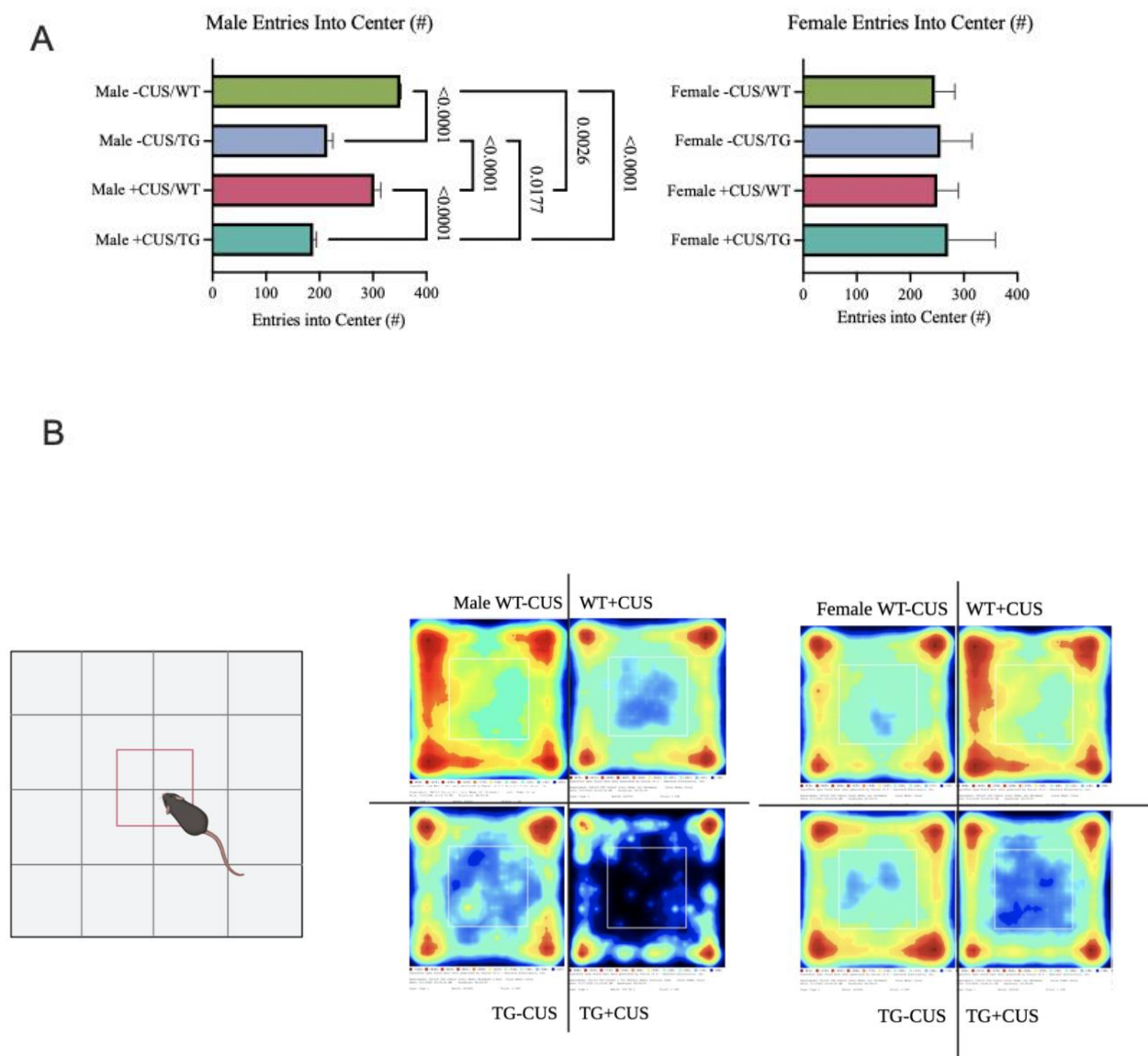
**Figure 3: Impact of Chronic Stress and Transgenic Modification on Anxiety-Related**

**Behaviors in Male and Female Mice.** Male experimental groups (left) reveal significant differences in fecal boli counts, a recognized measure of anxiety-like state in mice. Statistical analysis demonstrates notable distinctions between -CUS/WT and +CUS/TG ( $p=0.0087$ ) as well as +CUS/WT and +CUS/TG ( $p=0.0063$ ) experimental groups. Female experimental groups (right) display consistent fecal boli counts, suggesting no significant changes in anxiety-related behaviors under the experimental conditions.

Further analysis conducted in the Behavioral Testing Core is essential to comprehensively interpret the significance of these observed changes in fecal boli production. Understanding the intricate relationship between genotype, chronic stress, and behavioral responses will be crucial for elucidating the underlying mechanisms of stress-related psychiatric states.



The Open Field Test (OF), a well-established paradigm for studying spontaneous locomotion, exploration, and anxiety, provided additional insights into the behavioral outcomes of chronic stress in our experimental groups (**Figure 4**).



Specifically, comparisons between +CUS/TG and +CUS/WT revealed a highly significant difference ( $p < 0.0001$ ). Further analyses highlighted nuanced impacts of chronic stress on anxiety-related behaviors quantified by center-avoidance, with significant differences observed between +CUS/TG and -CUS/TG ( $p=0.0177$ ), +CUS/TG and -CUS/WT ( $p < 0.0001$ ), +CUS/WT and -CUS/TG ( $p < 0.0001$ ), +CUS/WT and -CUS/WT ( $p=0.0026$ ), and -CUS/TG and -CUS/WT ( $p < 0.0001$ ). (B) Schematic representation of the Open Field (OF) testing setup.

A comprehensive investigation into the cardiac implications of chronic stress, particularly in transgenic animals overexpressing *Vgll3*, has unearthed significant findings indicative of a potential link to human SLE. Utilizing 2-dimensional echocardiogram technology, we observed striking cardiac abnormalities in +CUS transgenic animals, providing valuable insights into the nuanced impact of chronic stress on cardiovascular health.

In Figure x, the representative image illustrates the disease progression in TG animals compared to their WT counterparts. Particularly noteworthy is the discernible increase in pericardial fat surrounding the cardiac organ in +CUS transgenic animals, a feature not observed in the WT group. This visual manifestation underscores the intricate relationship between chronic stress, genetic factors, and cardiac morphology.

Our observations also unveiled a sexually dimorphic aspect, with male animals exhibiting a heightened cardiac insult compared to females. This gender-specific difference was consistently observed across our study population ( $n=5$  per group), adding a layer of complexity to our understanding of the interplay between stress, genetic predisposition, and cardiac outcomes.

Further, our echocardiographic analysis demonstrated specific alterations in cardiac parameters in +CUS transgenic animals. The TG CUS+ male animal exhibited a 42% increase in atrial AV mean velocity compared to its WT CUS+ control, indicative of stenosis. This finding aligns with clinical observations in SLE patients, who often experience progressive heart impairment, including aortic and mitral valve dysfunction, and LV hypertrophy (**Figure 5**). Consistent with these clinical parallels, our study revealed LV hypertrophy in +CUS transgenic animals, characterized by a 67% increase in LV mass difference and a 2.08-fold increase in LV/body weight ratio compared to WT controls (**Figure 5**). These findings provide compelling evidence of the impact of chronic stress on cardiac structure and function, mirroring key aspects of human SLE-associated cardiac pathology.

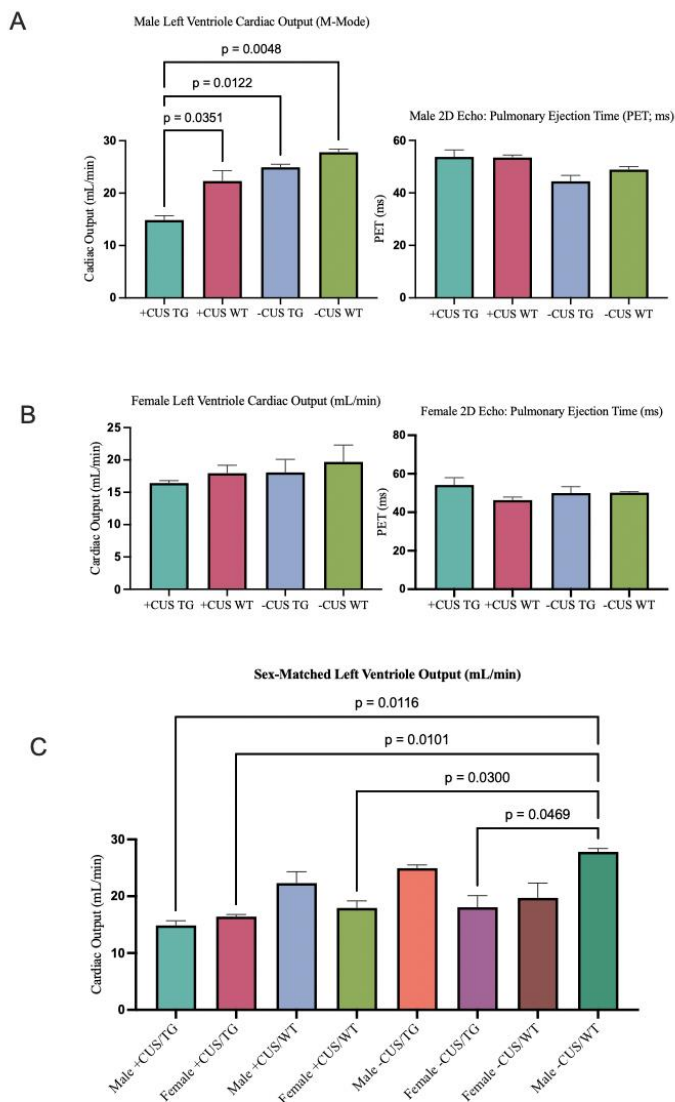


## Figure 5: Cardiac Output and Ejection Dynamics in Response to Catecholamine Unloading and Transgenic Modification.

### (A) Male left ventricular (LV) cardiac output (CO) in the +CUS/TG experimental group exhibited a significant dampening compared to both wild-type (WT) and control animals.

Statistical analysis revealed significant differences between +CUS/TG and +CUS/WT ( $p=0.0351$ ), +CUS/TG and -CUS/TG ( $p=0.0122$ ), as well as +CUS/TG and -CUS/WT ( $p=0.0048$ ) groups. No significant variance was observed among the experimental groups concerning pulmonary ejection time.

(B) Female LV CO and pulmonary ejection time demonstrated consistent values across all treatment groups, with no statistically significant differences.

(C) Sex-matched LV output analysis unveiled notable distinctions between Male and Female +CUS/TG experimental groups, displaying significant variations ( $p=0.0116$ ;  $p=0.0101$ ) compared to Male -CUS/WT experimental animals.

Furthermore, concerns about pulmonary hypertension were raised, as the TG CUS+ male exhibited a 16% decrease in pulmonary acceleration time compared to the control. This observation underscores the potential systemic consequences of chronic stress on cardiovascular health, extending beyond the primary effects on the left ventricle.

Our initial findings offer crucial insights into the interplay of chronic stress, metabolism, and weight regulation in the context of lupus. Gender-specific distinctions underscore the nuanced nature of these interactions, prompting further investigation. This study establishes a foundational understanding, providing a springboard for extensive research aimed at unraveling the underlying mechanisms and potential therapeutic interventions for weight fluctuations in lupus.

Furthermore, we emphasize the intricate interplay between chronic stress, genotype, and behavioral responses in stress-sensitive mice. Notably, observed changes in fecal boli production and anxiety-like behaviors offer valuable insights into early markers of HPA axis dysregulation. This sets the stage for in-depth investigations into the molecular and neural mechanisms associated with stress-induced psychiatric states.

In cardiology studies, we lay a robust foundation for comprehending the intricate relationship among chronic stress, genetic factors, and cardiac abnormalities, mirroring aspects of human SLE. These findings open avenues for further exploration into the molecular mechanisms governing stress-induced cardiac pathology. Moreover, they hold promise for informing future

therapeutic strategies targeting cardiovascular complications linked to chronic stress in autoimmune disorders.

## **Discussion**

The presented findings elucidate the intricate relationship between transgenic modification, chronic stress exposure, and ensuing physiological responses, with a specific emphasis on anxiety-like states and weight dynamics. Our investigative focus on TG experimental groups subjected to CUS has yielded noteworthy outcomes that enhance our understanding of the multifaceted nature of these interactions.

Male TG mice exposed to CUS exhibited a heightened incidence of anxiety-like states, as indicated by significant alterations in fecal boli counts. This behavioral manifestation aligns coherently with prior research linking transgenic modifications to augmented anxiety responses in rodent models. Notably, the observed anxiety-like states in male TG mice were concomitant with transit anorexia, evidenced by a substantial reduction in body weight compared to several experimental groups. This underscores the intricate interplay between behavioral and physiological responses, portraying a comprehensive picture of the impact of chronic stress and transgenic modification.

Further exploration into the cardiovascular consequences of these stressors uncovered left ventricular (LV) cardiac output dampening in male TG mice subjected to CUS. This physiological alteration introduces an additional layer of complexity to the observed responses, hinting at a potential linkage between the neuroendocrine effects of chronic stress, transgenic modifications, and cardiac function.

The sex-specific nature of these responses was a salient aspect, underscoring the necessity for a nuanced comprehension of the interactions between genetic factors, stress, and physiological outcomes. In contrast, female experimental groups exhibited consistent weight dynamics and anxiety-related behaviors under the experimental conditions, highlighting the divergence in responses between sexes.

The intricate relationship between chronic stress, transgenic modification, and physiological outcomes holds potential implications for susceptibility to autoimmune diseases. Existing research posits a bidirectional relationship between stress and autoimmune disorders, with stress contributing to disease onset and exacerbating existing conditions. The observed systemic effects in male TG mice, including weight reduction and cardiac output dampening, may signify a broader impact on immune function.

Understanding the role of chronic stress and transgenic modification in systemic disease progression is pivotal for elucidating potential pathways linking these factors to autoimmune diseases (**Figure 6**). The alterations in quality of life, manifested through anxiety-like states and weight dynamics, contribute to a more comprehensive understanding of the complex interplay between psychological stressors and autoimmune processes.



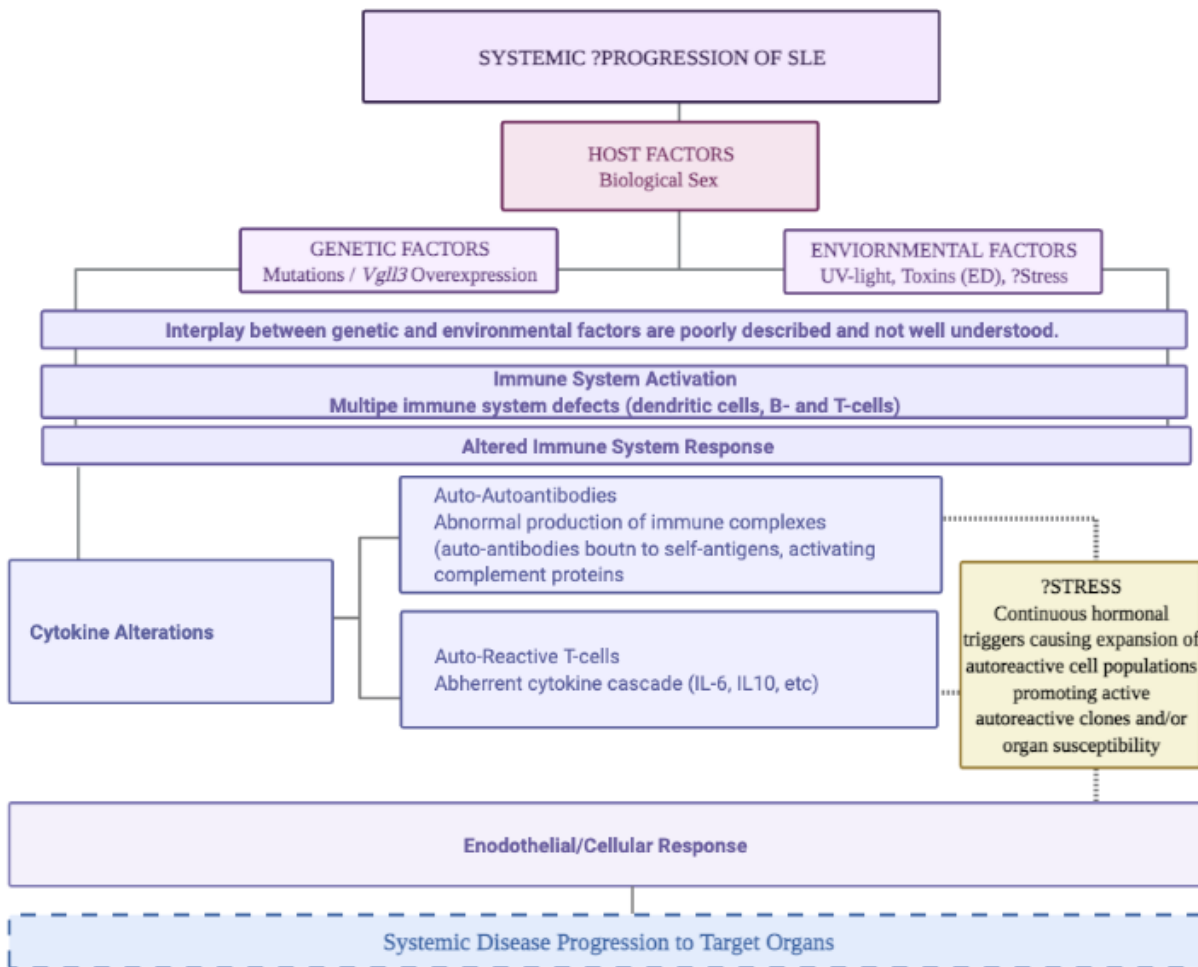


**Figure 6: Visual overview of our research project, focusing on unraveling the connections between chronic stress, transgenic modification, and systemic disease progression, particularly in the context of autoimmune diseases.** Divided into two sections, the schematic illustrates the multifaceted impact of chronic stress on physiological responses and molecular cascades, the genetic alterations resulting from TG modification, and the progression of autoimmune diseases with a spotlight on immune dysregulation and molecular signaling pathways. This schematic serves as a concise and informative guide, facilitating a visual comprehension of the project's central hypothesis and providing a valuable tool for readers to

navigate the intricate web of interactions between chronic stress, TG modification, and autoimmune disease progression.

Consideration of pathology is indispensable in assessing potential implications for autoimmune diseases. The observed physiological responses in male TG mice may signify underlying changes in immune function, creating an environment conducive to autoimmune pathology. Further investigations into immune markers and inflammatory mediators are warranted to elucidate the specific mechanisms through which chronic stress and transgenic modification may influence susceptibility to autoimmune diseases.

In conclusion, our study provides valuable insights into the intricate interplay of transgenic modification, chronic stress, and physiological responses, particularly in male mice. These findings contribute to the growing body of knowledge surrounding the complex mechanisms governing stress-related disorders and set the stage for further exploration into potential therapeutic interventions targeting these interconnected pathways.

## **Sex-biased Autoimmunity**

Sex-biased autoimmunity, a captivating facet of immune system dynamics, refers to the substantial and often perplexing differences observed in the susceptibility, prevalence, and severity of autoimmune diseases between males and females. This phenomenon underscores the intricate interplay between genetic, hormonal, and environmental factors that shape the immune landscape in a sexually dimorphic manner. The immunological journey diverges along gender lines, leading to distinctive disease patterns and responses to therapeutic interventions.

In the realm of autoimmunity, the disparities between the sexes are conspicuous, with certain autoimmune diseases exhibiting a notable predilection for one gender over the other. Systemic lupus erythematosus (SLE), multiple sclerosis, rheumatoid arthritis, and thyroid disorders are among the conditions that vividly manifest sex-biased patterns, often presenting a higher prevalence or more severe outcomes in females. These distinctions extend beyond mere numerical imbalances, as emerging evidence suggests that the underlying immunopathology may differ fundamentally between male and female individuals.

The intricate orchestration of sex hormones, particularly estrogen and testosterone, emerges as a central player in this symphony of sex-biased autoimmunity. Hormonal influences on immune function, immune cell development, and the regulation of inflammatory responses contribute to the observed disparities. Androgens, typified by testosterone, generally exhibit immunosuppressive effects, potentially offering a protective shield against certain autoimmune

conditions in males. Conversely, estrogen, with its immunoenhancing properties, may contribute to the heightened vulnerability of females to autoimmune diseases.

The multifaceted nature of sex-biased autoimmunity is further complicated by the diverse spectrum of autoimmune disorders, each governed by distinct genetic predispositions, environmental triggers, and immunological mechanisms. Exploring the intricacies of sex-biased responses in autoimmunity not only unravels the scientific nuances of disease pathogenesis but also holds profound implications for personalized medicine. Understanding how sex-specific factors shape immune responses offers a transformative lens through which we can tailor therapeutic strategies, moving beyond a one-size-fits-all approach to address the unique needs of individuals based on their gender and underlying immune dynamics.

Moreover, the intersection of sex-biased autoimmunity with toxicology and reproductive physiology introduces another layer of complexity. Reproductive physiology, intimately linked with hormonal regulation, plays a pivotal role in shaping the immune landscape, and disruptions in this delicate equilibrium can influence susceptibility to autoimmune diseases. In the realm of toxicology, where environmental exposures wield a profound impact on immune function, understanding the gender-specific responses becomes imperative. Investigating the interconnections between sex-biased autoimmunity, toxicological insults, and reproductive physiology unveils a comprehensive understanding of how external factors may trigger or exacerbate autoimmune conditions in a sex-specific manner. This intricate interplay forms the backdrop against which my exploration of stress in the context of lupus, followed by a review on

sexual dimorphism in immunometabolism, takes place, offering insights into the intricate relationship between sex, autoimmunity, and broader physiological contexts.

Having navigated the intricate landscape of autoimmune disorders, my journey converged with a comprehensive review that meticulously dissected the dimensions of sexual dimorphism in autoimmunity. The preceding exploration unfolded the saga of stress's intricate dance with lupus, a narrative wherein molecular stresses intertwined with the genetic and environmental intricacies of autoimmune diseases. Now, I embarked on a scholarly voyage that illuminated the profound impact of sexual dimorphism on immunometabolism and, consequently, on the clinical management of autoimmune diseases.

The realms of immunometabolism and sex-specific immune responses proved to be interconnected chapters in the grand narrative of human health. The immune cells, architects of metabolic homeostasis, harbored sex-specific nuances, influencing not only normal physiological transitions but also the trajectory of various immune and metabolic disorders. The shift in prevalence observed in autoimmune diseases, with females being disproportionately affected, stood in stark contrast to infectious diseases, where males often bore a greater burden. This divergence laid the foundation for my exploration of sex-specific regulatory mechanisms that governed immune functions.

The dynamic interplay between sex hormones and the immune system emerged as a pivotal plotline. Androgens, exemplified by testosterone, wielded immunosuppressive effects, while estrogen, its counterpart, orchestrated immunoenhancing mechanisms. These hormonal

orchestrations, coupled with distinct metabolic regulations across genders, contributed to the intricate tapestry of autoimmune pathogenesis. It was within this backdrop of sex-biased effector molecules, cell-type-specific functions, and the intricate interweaving of metabolic and immune functions that I unfolded in this dissertation.

In delving into this scholarly review, I was poised to unravel recent findings that dissected the critical questions surrounding sexual dimorphism in immunometabolism. I embarked on a mission to uncover the sex-biased effector molecules residing within metabolic tissues and immune cell types. My pursuit extended to identifying cell-type-specific functions of these molecules, ultimately seeking to elucidate the intricate dance between sex differences in metabolic and immune functions during autoimmune pathogenesis. The revelations encapsulated in this review transcended mere scientific inquiry; they held profound translational implications for the clinical management of autoimmune diseases.

The journey through these dual narratives—my exploration of stress in the context of lupus and the impending review on sexual dimorphism in immunometabolism—unfurled a comprehensive understanding of autoimmune disorders. Together, they constituted my scholarly odyssey where the intricate plots of stress, sex-specific immune responses, and metabolic regulation converged, opening avenues for innovative perspectives in personalized medicine.

**Adopted From: Sexual Dimorphism in Immunometabolism and Autoimmunity:  
Impact on Personalized Medicine.**

*Autoimmunity Reviews* 2022

Robbie S. J. Manuel<sup>1,2,3</sup>, Yun Liang<sup>2</sup>

<sup>1</sup>*Molecular & Environmental Toxicology Graduate Program, University of Wisconsin School of Medicine & Public Health;*

<sup>2</sup>*Endocrinology & Reproductive Physiology Graduate Program, University of Wisconsin School of Medicine & Public Health;*

<sup>3</sup>*Department of Medical Microbiology and Immunology, University of Wisconsin-Madison, Madison, WI 53706, USA*

**Acknowledgements**

R.M. is funded by the Molecular and Environmental Toxicology T32 Training Grant (T32 ES007015). Y.L. is funded by the US National Institutes of Health (K01-AR073340) and Wisconsin Partnership Program New Investigator Award.

**Abstract**

Immune cells play essential roles in metabolic homeostasis and thus, undergo analogous changes in *normal* physiology (e.g., puberty and pregnancy) and in various metabolic and immune diseases[108-110]. An essential component of this close relationship between the two is sex differences. Many autoimmune diseases, such as systemic lupus erythematosus and multiple sclerosis, feature strikingly increased prevalence in females, whereas in contrast, infectious diseases, such as Ebola and Middle East Respiratory Syndrome, affect more men than women [111-114]. Therefore, there are fundamental aspects of metabolic homeostasis and immune functions that are regulated differently in males and females. This can be observed in sex hormone-immune interaction where androgens, such as testosterone, have shown immunosuppressive effects whilst estrogen is on the opposite side of the spectrum with immunoenhancing facilitation of mechanisms[115, 116]. In addition, the two sexes exhibit significant differences in metabolic regulation, with estrous cycles in females known to induce variability in traits and more pronounced metabolic disease phenotype exhibited by males. It is likely that these differences underlie both the development of metabolic and autoimmune diseases and the response to current treatment options[108]. Sexual dimorphism in immunometabolism has emerged to become an area of intense research, aiming to uncover sex-biased effector molecules in the various metabolic tissues and immune cell types, identify sex-biased cell-type-specific functions of common effector molecules, and understand whether the sex differences in metabolic and immune functions influence each other during autoimmune pathogenesis[117-119]. In this review, we will summarize recent findings that address these



critical questions of sexual dimorphism in immunometabolism as well as their translational implications for the clinical management of autoimmune diseases.

## **Introduction**

Sexual dimorphism, or biological differences between male and female (the sexes of a species), can be noted throughout countless developmental, pathological, and physiological processes which humans go through[120-122]. Sex disparity in the manifestation of autoimmune disease represents one of the most remarkable and unexplained examples of the biological differences between men and women[112, 114, 122, 123]. According to the American Autoimmune Related Diseases Association (AARDA), there are 80-100 different autoimmune diseases ranging from the rare disorders such as Asherson's Syndrome to common disorders such as type 1 diabetes. Notably, rheumatic diseases including systemic lupus erythematosus (SLE, female: male 9:1) and Sjögren's syndrome (SS, female: male 20-9:1) are chronic systemic autoimmune disorders that predominantly affect women. Other common autoimmune diseases have moderately skewed ratios between the sexes, i.e., multiple sclerosis (MS, female: male 2-3:1). It is important to note that there are few known autoimmune diseases that are exceptions – these diseases processes are ankylosing spondylitis (AS, male: female 2-3:1), type 1 diabetes (male: female 3:2), and psoriasis (male: female 2:1)[123-125].

To better understand the sexually dimorphic basis of autoimmune etiology, sex as a biological variable has become, in the last decade, a standard of research design and analysis in vertebrate animal and human studies – backed by peer-review literature that the consideration of sex is

critical to the interpretation, validation, and generalizability of research findings[126, 127]. Though mechanisms have been put forward in order to elucidate sex bias in immune processes, its molecular underpinnings and their translation into disease phenotype have yet to fully come to fruition[108, 118, 122, 128].

One intriguing mechanism for sex-biased autoimmunity that emerged from recent study is sexual dimorphism in immunometabolism, which describes the changes in intracellular metabolic pathways in immune cells that alter their function. Fundamental metabolic pathways are essential for mammalian cells to produce energy, precursors for biosynthesis of macromolecules, and reducing power in redox regulations. There is a growing interest in the role of immunometabolism as a critical regulator of the fate and homeostatic function of immune cells. Changes in metabolic pathways within immune cells can be triggered by events of nutrient loss or anoxia, and by immune signals and regulation. Other than energy production and biosynthesis, distinct metabolic pathways can govern the phenotype and function of immune cell subtypes.

Systemic and cellular metabolism of specific immune cell populations highlight novel targets for immune-based therapies. Further understanding of sex differences in immunometabolic regulation will guide personalized medicine for immune-associated diseases. This review aims to highlight key discoveries and unanswered questions in sexual dimorphism in immunometabolism, paving the way for future studies that explore new prevention and treatment strategies for autoimmune diseases.

## **1 Sexual dimorphism in the immune system**

Sex differences in autoimmune diseases can be incompletely elucidated by known differences in the immune system<sup>3, 21, 58-60</sup>. The following sections will outline observed sexual dimorphism in the immune system and their molecular basis.

## **2.1 Sexual dimorphism in innate and adaptive immunity**

Sex differences in humans are exhibited by both the innate and adaptive immune systems.

During an innate immune response, Toll-like receptors (TLRs) are able to sense bacterial and viral components and provoke the stimulation of the cell in order to eliminate the infection[90, 91]. In addition, TLRs are found to regulate development of dendritic cells (DCs) and initiate antigen-specific adaptive immune responses as they bridge the innate and adaptive immunity[91]. In the context of autoimmunity, TLR dysregulation is central to disease pathogenesis because when inappropriately activated by self-components, a sustained or exacerbated TLR stimulation can lead to an overproduction of proinflammatory mediators, resulting in sterile inflammation and autoimmunity[91].

Importantly, TLR pathways exhibit sexual dimorphism. Souyris and colleagues have shown sex-biased expression of genes from the TLR pathway, including increased expression of TLR7 in females compared to males in B cells and myeloid cells[91, 129]. It has been shown that peripheral blood lymphocytes (PBLs) from women produce higher amounts of IFN- $\gamma$  after stimulation by TLR7 and TLR9 ligands[129, 130]. Similarly, upon TLR7 stimulation, human female plasmacytoid dendritic cells (pDCs)[131] produce higher amounts of IFN- $\gamma$  than their male counterpart, in addition to increased levels of IRF5 at basal state in females compared to males[130, 132].

While peripheral blood mononuclear cells (PBMCs) from men produce less IFN- $\gamma$  after TLR7 stimulation, upon TLR9 stimulation, they produce higher levels of the anti-inflammatory cytokine IL-10 than their female counterparts[133-135]. Additionally, male neutrophils have higher levels of TLR4 and produce more TNF than female neutrophils both at basal state and after stimulation with LPS[136], a TLR4 ligand[91, 109]. Consequently, the increased reactivity of male neutrophils to LPS and resultant increased secretion of proinflammatory cytokines justifies increased risk for septic shock in males[94].

In addition to innate immunity, the human adaptive immune system shows strong evidence of sexual dimorphism[91, 137]. Varying differences are found with immune cell counts dependent on cell type. For examples, higher counts of the cluster of differentiation-4 (CD4<sup>+</sup>) T cells and increased CD4<sup>+</sup>/CD8<sup>+</sup> ratio are found in females versus males[91, 131, 138, 139]. Differences in cell function are also observed as CD4<sup>+</sup> T cells in females produce higher levels of IFN- $\gamma$ , and proliferate quicker than CD4<sup>+</sup> T cells from men[135]. Male activated CD4<sup>+</sup> T cells have a greater tendency for IL-17 production versus females[135, 140]. Although B cell counts of the two sexes appear to be comparable, the concentration of serum immunoglobulins (Ig) differs between the sexes[129, 141].

In summary, the two sexes exhibit significant differences in both innate and adaptive immunity, which is thought to underlie the observed sex bias in autoimmune diseases (Figure 1).

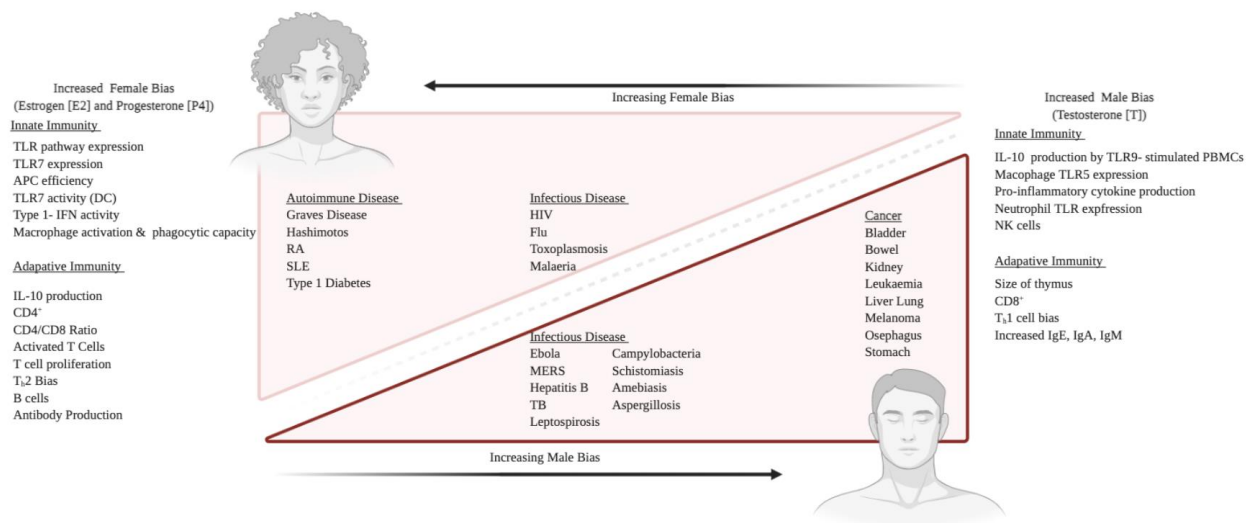


**Figure 1: Summary of sexually dimorphic factors which contribute to sex bias in immune-associated diseases.** Females and males differ in regulation of both innate and adaptive immunity, including female-biased TLR7 expression, type I – IFN activity, CD4<sup>+</sup> T cell count (left) and male-biased IL-10 production and CD8<sup>+</sup> T cell count (right). The sexual dimorphism of immunological factors is consistent with the sex bias observed in shown disease processes, where incidence rates, prevalence, susceptibility to and even prognosis of single diagnoses are different for male and females in most cases.

## 2.2 Causes of sexual dimorphism in immunity

Numerous factors could hypothetically contribute to sex differences in immune cell functions, but several have stood out in the last few years – sex hormones[108, 126, 127], sex chromosomes[108, 126, 127], epigenetics[108, 115, 142], and environmental factors[108, 115, 143]. It is highly important to note that established sex differences in immune cell function change with age and are altered during puberty and pregnancy and parturition[131, 144]. These changes are associated with lifespan milestones where hormone levels within the body are

changed significantly and confirm that sex hormones as well as their regulators play a role in immune responses[108]. Androgens, such as testosterone (T), have shown immunosuppressive effects whilst estrogen is on the opposite side of the spectrum with immunoenhancing facilitation of mechanisms (Table 1)[131, 145-147].

Testosterone influences the immune system by altering T-helper 1 (T<sub>h</sub>1) response and the action of CD8<sup>+</sup> cells whilst down-regulating natural killer (NK) cell response and production of TNF $\alpha$ [135]. Furthermore, testosterone is found to increase the production of anti-inflammatory cytokines such as IL-10[133]. Consistently, the presence of testosterone leads to higher production of T<sub>h</sub>1 by peripheral blood cells, signified by a higher T<sub>h</sub>1:T<sub>h</sub>2 ratio in men[148]. Further sexual dimorphic behavior was shown in immune cell subtypes in a humanized mouse model (DRAG mouse - HLA-DRA,HLA-DRB1\*0401[149]) of inflammation where exogenous supplementation of estradiol (E2) in castrated male mice led to an surge in autoimmunity by amplifying Major Histocompatibility Complex II (MHC2) expression and moderating B cell function (Table 1)[148]. The regulation of immune response of estrogen can be seen by the impairment of B cells and skewing of T<sub>h</sub>1 response[120, 148] and has been confirmed in rheumatoid arthritis (RA) mouse model (DRAG mouse- HLA-DR4/DQ8[150]). A summary of the effect of sex hormones on immune cells can be found in Table 1.

<b>Estrogen</b>		<b>Prolactin</b>		<b>Testosterone</b>	
Cell Type	Effect	Cell Type	Effect	Cell Type	Effect

---

B cell	Retarded B cell maturation	B cell	Increased induction of CD40	B Cell	Increased B cells and decreased IgM and lymphopoiesis
	Increased plasma cell and autoantibody producing cells		Decreased B cell receptor mediated activation threshold		
	Increased expression in CD22, SHP-1, and BCL-2		Increased IgM and IgG secretion		
			Increased JAK2 expression via B cell autoreactivity.		
			Increased STAT phosphorylation and up-regulation		
			Decreased B cell apoptosis related to increased BAFF		

---

		production and BCL-2 expression.			
DCs	Retarded DC maturation	DCs	Increased expression of CD80/86 via enhanced MHC-II	DCs	Decreased MHC-2 and CD86
	Altered regulation of cytokine and chemokine expression (IL-6, IL-10, IL-12, IL-23, CCL2, and TGF		Increased maturation of APCs		Decreased proinflammatory cytokines and TLR-mediated activation
					Increased anti-inflammatory cytokines
Macrophage	Altered chemotaxis and phagocytic activity	Macrophage	Increased in TNF , IFN , IL-1 , and IL-12	Macrophage	Decreased in TNF , TLR4, as well as eosinophil mediated chemokines
			Increased secretion of MCP		



	Increased		Controversial		Increase in M2
	induction of		increase of IL-10		and decreased
	IL-6 and		contingent upon		MCP-1
	TNF		concentration		
Neutrophils	Increased	Granulocytes	Increased	Neutrophils	Increase in
	induction of		regulation of IRF-		granulopoiesis
	TNF , IL-		1 and iNOS		and IL-10 and
	1 , and IL-6				TGF
			Increased		concentrations
			activation of		
			MAPK pathways		Decrease in
			via STAT1		ROS and
					proinflammatory
					cytokines and
					chemokines
Th1	Increased	NKCs	Increased	Th1	Decrease in Th1
	IFN		secretion of IFN		bias
	expression				
			Increased		
	Increase in		proliferation and		
	Th1 bias		cytotoxic activity		

Th2	Decrease in T <sub>h</sub> 2 bias	T cell	Increased adhesion of ECs by LFA-1 and VLA-4	Th2	Increase in T <sub>h</sub> 2 bias
Treg	Increase in regulation of FOXP3 and CTLA-4			T cell	Increased apoptosis and decreased proliferation
				Mast cell	Increased IL-6 production

**Table 1: Hormonal effects on immune processes**[58, 128, 137-139, 151-158]. The table summarizes the influence of estrogen, prolactin, and testosterone on different cell types of the immune system.

The X chromosome encodes the largest number of immune related genes[126], and a large portion of these genes escape from X chromosome inactivation leading to female-biased expression[108]. The human males produce two types of sex chromosomes, X and Y. Hence, the gametes produced by them are also of two types- one bearing X chromosome and the other bearing the Y chromosome. Thus, human males are said to be heterogametic, and deleterious recessive alleles in X-linked genes (i.e., TLR7, FOXP3, CD4<sup>+</sup>, and IRAK1) are more likely to cause immune phenotypes in males than in females[126, 127]. TLR7 and IRAK1 proteins play critical roles in pathogen recognition and induction of a proinflammatory immune response,

ensuing in type I IFN production and induction of the IFN inducible genes[91, 129]. The TLR7 gene escapes X inactivation, leading to gene dosage effects[126] that may be relevant for the recognition of both viral and self-RNA-related antigens during autoimmune pathogenesis [159-161]. Additionally, the X chromosome contains a large amount of microRNAs associated with the immune system, further contributing to sex differences in metabolic and immune function[108]. Sex differences in immune response are suggestive that sex-specific treatments would be efficacious for clinical and acute care treatment within these population groups.

### **3. Metabolic regulation of the immune system and its sexual dimorphism**

Immune and metabolic functions closely regulate each other at a systemic level, which suggests that crosstalk, as well as, cross-inhibition plays a role in the regulation of their sexually dimorphic functions[108]. Therefore, immunometabolism, the study of the multilayered interactions between immune and metabolic systems, has emerged as an exciting and important area of scientific investigation. It is expected that a better understanding of sex differences in immunometabolic regulation will help guide personalized, sex-specific treatment of autoimmune diseases.

#### **3.1. Concept of immunometabolism**

The immune system encompasses a heterogeneous populace of cells that are relatively quiescent in the steady state but share the ability to rapidly respond to infection and inflammation[125].

The ability to mount an inflammatory reaction requires considerable energy expense rapidly and effectively and is accompanied by metabolic changes. Metabolism consists of exceedingly interconnected, and complicated biochemical pathways within the human body [117, 128, 154].

The major metabolic pathways are: glycolysis, where glucose is oxidized in order to generate ATP, albeit in a relatively inefficient manner; citric acid cycle (CCA) cycle, a nexus for multiple nutrients inputs that is used for efficient ATP generation; the pentose phosphate pathway (PPP), allowing diversion of intermediates from glycolysis towards the production of nucleotide and amino acid precursors; fatty acid oxidation, allowing the conversion of fatty acids into downstream products for energy generation; fatty acid synthesis, generating lipids for cellular growth and proliferation; amino acid metabolic pathways, using amino acids for protein synthesis and signaling regulation[139].

Cells use intricate mechanisms to sense levels of metabolites produced by these metabolic pathways and activate signaling pathways accordingly to maintain metabolic homeostasis. Of these mechanisms, one central metabolic regulator of immunity is the mechanistic target of rapamycin (mTOR) – AMP kinase (AMPK) pathway[139, 159, 162, 163]. mTOR is the catalytic subunit of mTOR complex (mTORC-) 1 and 2 which sense amino acids and growth factors and promote mRNA translation[164]. Additionally, mTORC1/2 signaling contributes to lipid synthesis and cell growth[164]. Intriguingly, in the immune system, mTOR signaling facilitates events critical for T cell and monocyte differentiation, suggesting immunometabolic crosstalk. Nutrient deprivation signals to AMP kinase, which promotes catabolism of free fatty acids (FFA) and inhibits mTOR activity, thus limiting immune cell activation[164].

mTOR function is regulated by the protein kinase B (PKB/Akt), which is known to play a critical role in cell growth, metabolism, proliferation, and survival. PKB/Akt activation is controlled by a complex stepwise progression that involves phosphoinositide-3-kinase (PI3K)[165-167].

Stimulated receptors incite class 1A PI3Ks that triggers the activation of PI3K and conversion by its catalytic domain of phosphatidylinositol (3,4)-bisphosphate (PIP<sub>2</sub>) lipids to phosphatidylinositol (3,4,5)-trisphosphate (PIP<sub>3</sub>). Subsequently, PKB/Akt binds to PIP<sub>3</sub>, permitting PDK1 to access and phosphorylate T308 in the activation loop, leading to partial activation of PKB/Akt[165]. Successively this activate mTOR-complex 1 (mTORC1) by phosphorylating and inhibiting tuberous sclerosis protein 2 (TSC2)[166].

mTORC1 substrates are found to further phosphorylate ribosomal protein-S6 (RPS6), promoting protein synthesis and cellular proliferation[165]. Depletion of energy leads to inactivation of mTORC1, activation of AMPK, forkhead box transcription family-O (FOXO), and promotes constitution of mTORC2 that leads to phosphorylation of Akt[165-167]. Akt can also be activated without PI3K; which appears to be advantageous in situations like nutrition deprivation, where insulin/insulin growth factor signaling is not optimal[166]. An applied example of this can be seen when CD3/CD28 ligation activates CD4<sup>+</sup> T cells, leading to signaling through PI3K/Akt/mTOR. PI3K/Akt/mTOR signaling subsequently leads to activation of glycolysis and mitochondrial oxidative phosphorylation (OXPHOS), resulting in CD4<sup>+</sup> activation<sup>7-8, 19-23,[167]</sup> (Table 2).

In addition to CD4<sup>+</sup> T cells, PI3K/Akt/mTOR/AMPK regulates immunometabolic functions in a variety of immune cells. A summary of immunometabolic pathways regulating immune cell function can be found in Table 2.

Cell Type	Inducers	Mediators	Effectors	Outcome	Reference
Activated CD4 <sup>+</sup> T Cell	CD3/CD28	PI3K/Akt/mTOR ERK/MAPKc- MyHIF-1 $\alpha$	Glycolysis, Mitochondr ial OXPHOS	Activation, Proliferation, Cytokine production	7-8, 19-23
Activated Dendritic Cell	PAMPs	PI3K/AktHIF-1 $\alpha$	Glycolysis	Presentation, Cytokine production	7
B Cell	PAMPs	PI3K/Akt	Glycolysis	Activation, Proliferation	7, 20
Memory CD8 <sup>+</sup> T Cell	IL-15	AMPK	FAO	Survival, Quiescence	7, 24-28
Naïve CD4 <sup>+</sup> T Cell	IL-7	PI3K/Akt	Mitochondr ial OXPHOS, FAO	Survival	7-8, 22- 23, 28-30
Neutrophil	PAMPs,	HIF-1 $\alpha$	Glycolysis	ROS	7
Resting Dendritic Cell	Growth factors (GM-CSF, FLT3)	-	FAO	Growth, Survival Activation	7, 31-32

**Table 2: Immunometabolic pathways in immune cells.** Components of the inflammatory

response where ‘inducers, sensors, mediators, effectors, and outcomes’ are associated with specific metabolic processes. Herein, inducers of inflammation activate ‘mediator’ signaling, resulting in modulation of ‘effector’ metabolic pathways, and leading to cellular outcomes such as activation, proliferation, and cytokine production.

The direct regulation of immune processes by metabolism can further be observed within various immune cell types where they switch between distinctive metabolic pathways to respond to changes in a dynamic immune response[164]. For example, an inflammatory M1 macrophage uses the glycolysis pathway to support phagocytosis and inflammatory cytokine production, and utilizes the pentose phosphate pathway to support nucleotide and ROS production[164]. Another depiction of this specific pathway reliance can be observed in regulatory T cells when utilizing the CCA pathway instead of FFA oxidation because an suppressive function is needed versus the generation of T<sub>reg</sub> cells in response to tolerogenic stimuli[164].

### **3.2 Sexual dimorphism in immunometabolism**

While historically metabolism has been studied with the assumption that basic cellular machineries operate in the same way in males and females, it has been recently accepted that the two sexes exhibit significant differences in metabolic regulation. Estrous cycles in females are known to induce variability in traits, and males can exhibit more pronounced metabolic disease phenotype than females[164].

Similarly, sex-biased regulation of immunometabolism is supported by the finding that the sex steroid regulator sex hormone-binding globulin (SHBG) regulates the tissue availability of sex

steroids and influences E2 signaling in lymphocytes, which possibly underlies the female bias in multiple sclerosis[168]. At the intersection of immune and metabolic functions, SHBG also contributes to pathogenesis of metabolic diseases such as obesity and metabolic syndrome[169].

In addition, in research of the immunometabolic alterations in diabetes, it was found that sex hormones regulate visceral adipose tissue mesenchymal stromal cells and their production of IL-33, which could account for differences in regulatory T cells (Tregs) in basal or obese state between males and females[170, 171].

With the last decades seeing a growing interest in immunometabolism research, the recent recognition of sex differences being a fundamental feature of immunometabolism calls for attention from the scientific community. A better understanding of sexual dimorphism in immunometabolism will provide scientific basis to develop sex-based precision medicine for immune and metabolic diseases.

#### **4. Metabolic alterations in autoimmune disease and immunometabolism as a fundamental mechanism for sexual dimorphism in autoimmunity**

With mounting evidence supporting the metabolic regulation of immune functions, it is not surprising that metabolic alterations in autoimmune disease have been documented[48, 113, 121, 124, 172]. The findings highlighting major metabolic alterations in autoimmunity are summarized below.

##### **4.1 Systemic lupus erythematosus**



Systemic lupus erythematosus (SLE) is an autoimmune disease that is characterized by chronic inflammation[121, 125, 173]; often illustrated by the involvement of multiple organs and clinical displays of nephritis, vasculitis and pathogenic autoantibodies such as anti-double stranded DNA (dsDNA)[174, 175]. In addition to altered function of immune cells[120, 128] including CD4<sup>+</sup> T Cells[137, 176, 177], dendritic cells (DC)[178], macrophages[119, 125, 178-182], and neutrophils[119], metabolic systems play an integral role in checkpoints that control immune cell fate and function[117, 139, 183, 184]. Therefore, it is crucial to examine the relationship between mitochondrial dysfunction, oxidative stress, and abnormal metabolism that involves glucose, lipid, and amino acid metabolism of immune cells to understand the underlying pathogenic mechanisms of SLE[118, 160, 185]. Notably, metabolite intermediates that are produced within mitochondria have been found to serve as inflammatory signals (e.g., succinate in myeloid cells)[134, 160]. A seminal breakthrough by Frauwirth and colleagues[186] highlighted the activation of CD28 by glycolysis in T cells, leading to a large push in researchers looking to elucidate the regulation of T cells by metabolic substrates[117, 128, 154, 176, 187]. It is now understood that resting T cells are influenced by mitochondrial oxidative phosphorylation (OXPHOS) and that antigen-mediated stimulation and acquisition of effector functions elicit a striking metabolic reprogramming, shown an upregulation of glucose use followed by the activation of mitochondria-independent glycolysis as the major source of building blocks necessary to cope with considerable proliferation as well as production of effector molecules[118, 140, 187].

Glucose is a fundamental energy source for most cells and aids cellular proliferation, development, and survival[139, 177]. It is known that activated T cells enhance glucose

metabolism in order to meet requirements of cellular proliferation and differentiation.

Subsequently, glucose deficiency leads to decreased levels of ATP and AMP-activated protein kinase (AMPK) activation[188], which in the *normal* setting has a positive homeostatic effect on signaling pathways that compensate for cellular ATP. This can be shown in the activation of AMPK promoting GLUT4 transcription and translocation to promote glucose intake[177]. Conversely, AMPK negatively modulates key proteins in ATP-consuming reactions such as mTORC2[139, 159, 163], glycogen synthase, sterol regulatory element binding protein 1 (SREBP-1) and tuberous sclerosis 2 (TSC2), leading to inhibition of gluconeogenesis as well as glycogen, lipid, and protein synthesis[177]. It is important to note that GLUT1 overexpression in CD4<sup>+</sup> T cells has an influence on Treg cell expansion, which has led to the concept that there is a difference in glucose metabolism for regulatory and effector T cells. GLUT1 is induced by HIF1 $\alpha$ , which ultimately aids in Th17 differentiation[135, 177, 189]. Additionally, the increase in GLUT1 expression and glucose uptake occurs in a PI3K/Akt-dependent manner, allowing cells to maintain their mitochondrial potential and ATP homeostasis[177]. Correspondingly, in the absence of sufficient extrinsic signals, cell surface GLUT1 expression decreases, resulting in diminished glucose uptake, drop in mitochondrial membrane potential and ATP synthesis, and cell death[177]. Since this decline in viability occurs in the presence of appropriate glucose and oxygen, it suggests that growth factor signaling is indispensable for maintenance of metabolic homeostasis in naïve CD4<sup>+</sup> T cells[160, 177, 187].

Yet, the inhibition of AMPK and the downstream mTORC1 activation by Roquin-1 promotes a lupus-prone phenotype[176]. Roquin-1 blocks AMPK activation, allowing the function of mTORC1 and mTORC2, which are known to impact T helper follicular (Tfh) cell differentiation

[190]. In addition, recent studies have found that retention of activated mTORC1 during asymmetric cell division in CD8<sup>+</sup> T cells presents the daughter cell with effector functions, whereas the mTORC1-low daughter cell acquires memory properties. It is likely that a similar asymmetric distribution of mTORC1 exists between effector and memory CD4<sup>+</sup> T cells[162]. Dysregulation of Tfh, CD8<sup>+</sup> and CD4<sup>+</sup> T cell differentiation altogether may underlie the lupus-prone phenotype induced by Roquin-1.

Similarly, mTORC1 activation was observed in CD4<sup>+</sup> T cells from several strains of lupus-prone mice. Interestingly, treatment of these mice with 2-Deoxy-D-glucose (2-DG) and metformin normalized mTORC1 activation concomitant with disease reversal[160].

Consistent with mouse model studies, mTORC1 activation has been demonstrated in CD4<sup>+</sup> T cells of SLE patients and has been proposed to serve as a biomarker of autoimmune inflammation[163, 177]. Treatment with rapamycin, which inhibits mTOR and enhances Treg suppressive function, is effective in SLE patients and in lupus-prone New Zealand mixed (NZW/NZW F1) mice[139, 159, 163, 177, 191]. Therefore, targeting of mTORC, the critical player integrating environmental cues, nutrient levels, and immune response output, is promising in treatment of SLE (Figure 2).

Although most research has been conducted on the influence of glucose metabolism in SLE T cells[128, 139, 177, 185], glucose is also important to other immune cell types. It has been shown that B cells in the lupus-prone NZW/NZW F1 mice exhibit a highly glycolytic phenotype[160]. However, their mechanistic actions remain unsettled [177].

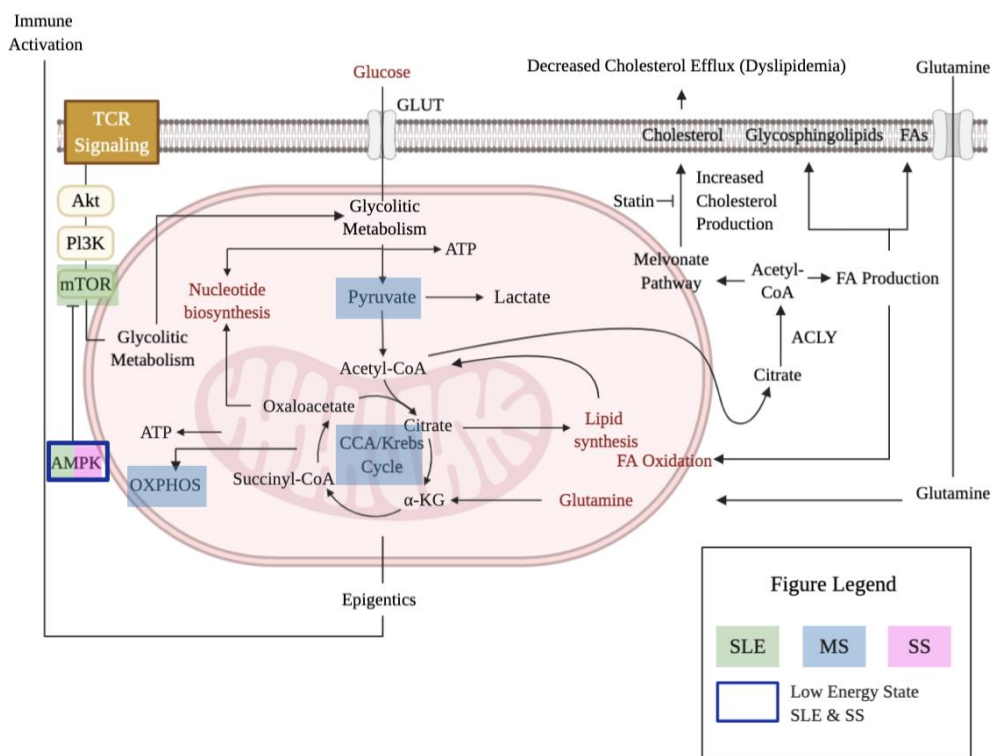


**Figure 2: Potential metabolic pathways of intervention in autoimmune diseases.** Schematic representing important metabolic targets in SLE treatment in efforts to correct the immunometabolic alterations, as AMPK and mTORC are mechanistically critical for SLE pathogenesis (green). In a similar fashion, pyruvate metabolism, OXPHOS, and CCA are highlighted as targets for MS (blue). Low energy level is associated with both SS (pink) and SLE which can be linked to the antiapoptotic effects of adiponectin mediated by phosphorylation of AMPK (blue box).

#### 4.2 Sjögren's syndrome

Sjögren's syndrome (SS) is a systemic autoimmune disease that is characterized by infiltration of lymphocytes into the exocrine glands, inflammation, tissue damage, and dysfunctional glandular secretion[188, 192, 193]. Destruction of the lacrimal and salivary glands, which typically occurs in patients with SS, results in ocular dryness (keratoconjunctivitis sicca) and oral dryness (xerostomia)[188]. Patients with SS often have extra-glandular complications such as non-erosive polyarthritis, arthralgias, vasculitis, and chronic fatigue[188]. Furthermore, patients with SS have an increased incidence of progression to various non-Hodgkin lymphomas, which may influence the rate of morbidities[188, 193]. The pathogenesis of SS is mediated by complex mechanisms involving infiltration by lymphocytes (mainly T and B cells) of target organs during a dysregulated adaptive immune response[188, 192]. In the T- and B-cell-containing ectopic lymphoid structures in the salivary and lacrimal glands, hyperactivated B cells produce autoantibodies, e.g., anti-SSA/Ro and -SSB/La, against small RNA molecules and rheumatoid factors[188, 192, 193]. Activation of B cells by follicular helper T (Tfh) cells is crucial for the clonal selection and affinity maturation[176, 190].

Since metabolic aberrations of immune cells drive immune regulation in mammals, it was postulated that the "immune" phenotype of salivary gland epithelial cell (SGEC) undergoes similar control by their metabolism and may actively shape the autoimmune response in SS[141, 188]. SGEC are secretory cells with constant high energy demands and their metabolic machinery is expected to suit their lifestyle[188]. Disturbances of this process may be enforced by insufficient energy supply, endoplasmic reticulum (ER) stress or even chronic stress, leading to metabolic reprogramming and eventually immunogenic cell death characterized by the release of cellular autoantigens[188]. Differential adiponectin production by SGEC in SS indicates a low

energy phenotype and the antiapoptotic effects of adiponectin mediated by phosphorylation of AMPK provide a robust paradigm for the interconnection between metabolism and immune functions of SGEc in the context of glandular lesion in SS[188] (Figure 2).

### **4.3 Multiple sclerosis**

Multiple sclerosis (MS) is a chronic inflammatory demyelinating disease of the central nervous system (CNS)[152]. The incursion of the brain by activated immune cells across the endothelial cells (ECs) of the blood brain barrier is due to the loss of immune self-tolerance[152]. MS is characterized by inflammation, demyelination, nonspecific reactive changes of glial cells, and neuronal loss. From a pathological perspective, the presence of perivascular lymphocytic infiltrates are indicative of the disease process, with consequent macrophage degradation of myelin sheaths that surround neurons[152]. The MS predominance ratio of female to male has increased within the last few decades from 2.3-3 – 5:1. This is suggestive that the presence of hormone receptors associated with immune cells and sex hormones (androgens, estrogens, progesterone, and prolactin) have a great influence on immune system function and disease progression[147, 152, 156, 158, 191, 194].

Biochemical studies regarding MS have established the notion of defective pyruvate metabolism, in addition to increased sera concentrations of citric acid cycle (CCA) acid such as - ketoglutarate (AKG)[195] and citrate (Figure 2). AKG is one of the most important nitrogen transporters in metabolic pathways, produced by oxidative decarboxylation via isocitrate dehydrogenase as well as oxidative deamination of glutamate via glutamate dehydrogenase[195]. MS patients are found to have elevated serum and cerebrospinal fluid pyruvate levels, as well as

antibodies that were reactive with triose phosphate isomerase and GAPDH and inhibit glycolytic activity of GAPDH[151, 156]. In regard to altered OXPHOS, there is a striking reduction of ATP synthase and increased activation of mitochondrial electron transport chain[156]. Therefore, correcting deficiencies in pyruvate metabolism is critical to managing MS clinically (Figure 2).

Reiterated from the glucose metabolism of SLE above, the metabolism of glucose in the setting of MS is the same. The foundation of glucose metabolism starts with glucose entering cells via GLUT transporters and being phosphorylated by hexokinase[158]. The product glucose 6-phosphate can be metabolized via glycolysis – producing pyruvate, ATP, and NADH, where pyruvate enters the mitochondria and is metabolized via the CCA cycle and OXPHOS[118, 140, 187, 196]. It is important to mention that pyruvate can also be reduced to lactate-by-lactate dehydrogenase and released into extracellular space via monocarboxylate transporters (MCTs). Additionally, glucose 6-phosphate can be taken through PPP or converted to glycogen via glycogenesis in astrocytes in the brain[139]. However, unlike the role of insulted glucose metabolism in SLE, the role of glucose metabolism in MS is still incompletely understood.

#### **4.4 Immunometabolism as a fundamental mechanism for sexual dimorphism in autoimmunity**

It has been discussed that maintaining metabolic homeostasis is critical in the prevention of autoimmunity. A bulk of metabolism, including energy balance – glucose and lipid metabolism, are regulated in a sexually dimorphic manner and successively influence the pathogenesis of autoimmune disease. However, the fundamental question of why sex differences in autoimmunity exist remains unanswered. To address this question, researchers such as

Pagenkopf and colleagues[114, 122] have focused on immunometabolic functions of transcriptional cofactors that provide an evolutionary validation for sexual dimorphism in autoimmunity. An example of this can be highlighted within the female-biased gene network that has been described in human skin that is associated significantly with the susceptibility to female-biased autoimmunity. An upstream regulator of this gene network, vestigial family member-3 (*VGLL3*), exhibits female-biased expression in healthy human skin and is further upregulated in autoimmune diseases including SLE, SS and systemic sclerosis[114]. In secondary studies from this group, their results demonstrated that energy deficiency is a critical trigger that upregulates *VGLL3* and that female-biased expression of *VGLL3* helps cells adapt to metabolic stress. Intriguingly, when placental mammals evolved, the need to feed a developing embryo posed significant challenge to metabolic pathways[197]. Therefore, the finding that *VGLL3* helps non-placental tissue such as the skin adapt to energy stress provides an evolutionary rationale for the selection of its increased expression in females. This study further identifies nutritional deficiency as a trigger that can turn this evolutionary strength into weakness by causing autoimmune pathogenesis, and highlights the importance of maintaining metabolic homeostasis in prevention of autoimmunity[122].

## **5. Translational Implications**

It can be inferred that immunometabolism in regard to autoimmune disease since its inception has primarily focused on glycolysis, the CCA cycle, OXPHOS, and free fatty acids (FFA) synthesis and oxidation. This is based on the findings of pathways associated with the energy needs of cell growth, membrane rigidity, cytokine production and proliferation. Seemingly



translational immunometabolism is suggestive of a repositioning of metabolic drugs that exploit new targets.

Novel drugs which modulate metabolic processes have the potential to correct the aberrant immune responses and be used to treat autoimmune disease patients (Figure 2). Looking at SLE specifically, strategies targeting mTOR activation, including use of rapamycin, could be promising ways to diminish the disease severity in SLE patient populations[139, 159, 162, 163].

Additionally, tuning of FFA pathways, including that seen in glucocorticoid (prednisone) treatment, has been directly linked to leptin reduction through inhibition of mTOR in SLE patient populations[159, 163, 173]. Also, the complex interaction among mitochondrial, and mTOR signaling pathways and their ability to control the chemotaxis of neutrophils suggest metabolic options to restore normal neutrophil functions in SLE[159]. Based on the finding that macrophage polarization follow distinct metabolic pathways, the translation of metabolic shifts to disease has gained importance, especially for diseases that clearly lean toward either phenotype (M1 vs M2)[159]. Notably, the influence of macrophage polarization has met with relative success clinically for ovarian carcinoma, showing that therapeutically targeting macrophage metabolism might be a viable option in the future for SLE and MS[159].

Symptomatically, fatigue and low energy states are commonly reported amongst patients hindering with SLE and MS. Defining fatigue can be tricky, where varying definitions can be grouped according to type (i.e., subjective, physiological, and/or performance). Herein this review, we define fatigue as insufficient cellular capacity or system-wide energy to maintain the

original level of activity and/or processing by using normal resources. Furthermore, physiological processes have been described to play a role in fatigue that include oxygen/nutrient supply and metabolism - which are exaggerated by inflammation. Effects contributing to fatigue are associated with enhanced inflammation and increased cytokine expression amongst others[198]. In addition, with nutritional deficiency as an autoimmune trigger, it is reasonable to assume that nutritional monitoring strategies can be employed to develop in order to prevent and/or treat autoimmune disorders.

This is not without considering the impact the biological sex has on personal immunity. Clear differences in male and female immunity contribute to variations in disease predisposition, severity, and drug responses (Figure 1). Additional co-factors that influence sex hormones, such as environment stress and toxin exposure, could also impact immunometabolic responses and autoimmune pathogenesis in a dynamic manner (i.e., change with age and events in life). One prominent example of sex-specific drug response is the impact of gender on immune checkpoint inhibitors-induced autoimmunity. Using the example of MS, Golden and colleagues[116] were able to elucidate the efficacious clinical benefit of discussing sex differences with treatment options of patients. Taking these observations to the laboratory bench allowed researchers to describe the mechanisms underlying sex differences, and to investigate therapeutics based on findings. Continually examining sex differences in the same “bedside to bench to bedside” fashion will bare endless novel therapeutics and treatment strategies following the identification of sex-specific disease drivers. In addition, sexual dimorphic studies will allow us to design sex-stratified treatment strategies that maximize efficiency and minimize side effects in both male and female patients.

## **6. Conclusions**

There is a growing amount of academic literature on immunometabolism that provides novel insights into autoimmune pathogenesis. When adding in additional contributory factors such as sex and its biological implications the complexity of the topic grows. Notably, the biological sex effects the production, maturation, differentiation, metabolism and ultimately the functioning of cells, in both physiology and pathology of the immune system. Taken together the topics covered can shed light on how sex-specific metabolic reprogramming therapeutic can be implored to enhance outcomes in autoimmune diseases.

## References

1. Liu, Y., et al., *Chronic prostatitis/chronic pelvic pain syndrome and prostate cancer: study of immune cells and cytokines*. *Fundam Clin Pharmacol*, 2020. **34**(2): p. 160-172.
2. Liu, Y., et al., *Experimental autoimmune prostatitis: different antigens induction and antigen-specific therapy*. *Int Urol Nephrol*, 2021. **53**(4): p. 607-618.
3. Jackson, C.M., et al., *Strain-specific induction of experimental autoimmune prostatitis (EAP) in mice*. *Prostate*, 2013. **73**(6): p. 651-6.
4. Welliver, C., et al., *Evolution of healthcare costs for lower urinary tract symptoms associated with benign prostatic hyperplasia*. *Int Urol Nephrol*, 2022. **54**(11): p. 2797-2803.
5. Mehta, V. and C.M. Vezina, *Potential protective mechanisms of aryl hydrocarbon receptor (AHR) signaling in benign prostatic hyperplasia*. *Differentiation*, 2011. **82**(4-5): p. 211-9.
6. Vezina, C.M., T.M. Lin, and R.E. Peterson, *AHR signaling in prostate growth, morphogenesis, and disease*. *Biochem Pharmacol*, 2009. **77**(4): p. 566-76.
7. Wegner, K.A., et al., *Void spot assay procedural optimization and software for rapid and objective quantification of rodent voiding function, including overlapping urine spots*. *Am J Physiol Renal Physiol*, 2018. **315**(4): p. F1067-f1080.
8. Ittmann, M., *Anatomy and Histology of the Human and Murine Prostate*. Cold Spring Harb Perspect Med, 2018. **8**(5).

9. Wang, H.H., et al., *Characterization of autoimmune inflammation induced prostate stem cell expansion*. Prostate, 2015. **75**(14): p. 1620-31.
10. Zhang, L., et al., *Establishment of experimental autoimmune prostatitis model by T(2) peptide in aluminium hydroxide adjuvant*. Andrologia, 2018. **50**(3).
11. Zhang, Y., et al., *Influence of Experimental Autoimmune Prostatitis on Sexual Function and the Anti-inflammatory Efficacy of Celecoxib in a Rat Model*. Front Immunol, 2020. **11**: p. 574212.
12. Magistro, G., C.G. Stief, and F.M.E. Wagenlehner, [*Chronic prostatitis/chronic pelvic pain syndrome*]. Urologe A, 2020. **59**(6): p. 739-748.
13. Manuel, R.S.J. and Y. Liang, *Sexual dimorphism in immunometabolism and autoimmunity: Impact on personalized medicine*. Autoimmun Rev, 2021. **20**(4): p. 102775.
14. Yamaguchi, H., et al., [*Experimental rodent models of chronic prostatitis: effect of phosphodiesterase 5 inhibitor on chronic pelvic-pain-related behavior*]. Nihon Yakurigaku Zasshi, 2019. **154**(5): p. 259-264.
15. Matsukawa, Y., et al., *Clinical features and urodynamic findings in elderly men with chronic prostatitis*. Int J Urol, 2022. **29**(5): p. 441-445.
16. Chen, L., M. Zhang, and C. Liang, *Chronic Prostatitis and Pelvic Pain Syndrome: Another Autoimmune Disease?* Arch Immunol Ther Exp (Warsz), 2021. **69**(1): p. 24.
17. Magistro, G., et al., *Contemporary Management of Chronic Prostatitis/Chronic Pelvic Pain Syndrome*. Eur Urol, 2016. **69**(2): p. 286-97.
18. Stamatiou, K., E. Samara, and G. Perletti, *Sexuality, Sexual Orientation and Chronic Prostatitis*. J Sex Marital Ther, 2021. **47**(3): p. 281-284.

19. Ludwig, M., et al., *Immunocytological analysis of leukocyte subpopulations in urine specimens before and after prostatic massage*. Eur Urol, 2001. **39**(3): p. 277-82.
20. Altuntas, C.Z., et al., *A novel murine model of chronic prostatitis/chronic pelvic pain syndrome (CP/CPPS) induced by immunization with a spermine binding protein (p25) peptide*. Am J Physiol Regul Integr Comp Physiol, 2013. **304**(6): p. R415-22.
21. Breser, M.L., et al., *Regulatory T cells control strain specific resistance to Experimental Autoimmune Prostatitis*. Sci Rep, 2016. **6**: p. 33097.
22. Schaeffer, E.M., *Re: IL17 Mediates Pelvic Pain in Experimental Autoimmune Prostatitis (EAP)*. J Urol, 2016. **196**(3): p. 958-9.
23. Zhou, X.H., et al., *Increased inflammatory factors activity in model rats with experimental autoimmune prostatitis*. Arch Androl, 2007. **53**(2): p. 49-52.
24. Diserio, G.P. and E. Nowotny, *Experimental autoimmune prostatitis: dihydrotestosterone influence over the immune response*. J Urol, 2003. **170**(6 Pt 1): p. 2486-9.
25. Motrich, R.D., et al., *Autoimmune prostatitis: state of the art*. Scand J Immunol, 2007. **66**(2-3): p. 217-27.
26. Penna, G., et al., *Treatment of experimental autoimmune prostatitis in nonobese diabetic mice by the vitamin D receptor agonist elocalcitol*. J Immunol, 2006. **177**(12): p. 8504-11.
27. Quick, M.L., et al., *CCL2 and CCL3 are essential mediators of pelvic pain in experimental autoimmune prostatitis*. Am J Physiol Regul Integr Comp Physiol, 2012. **303**(6): p. R580-9.
28. Roman, K., et al., *Tryptase-PAR2 axis in experimental autoimmune prostatitis, a model for chronic pelvic pain syndrome*. Pain, 2014. **155**(7): p. 1328-1338.

29. Liu, K.J., et al., *Identification of rat prostatic steroid-binding protein as a target antigen of experimental autoimmune prostatitis: implications for prostate cancer therapy*. *J Immunol*, 1997. **159**(1): p. 472-80.
30. Wong, L., et al., *Experimental autoimmune prostatitis induces microglial activation in the spinal cord*. *Prostate*, 2015. **75**(1): p. 50-9.
31. Yang, J., et al., *Prostate-derived IL-3 " w r t g i w n c v g u " g z r t g u u k q p " q h paraventricular nucleus and shortens ejaculation latency in rats with experimental autoimmune prostatitis*. *Asian J Androl*, 2022. **24**(2): p. 213-218.
32. Duloy, A.M., E.A. Calhoun, and J.Q. Clemens, *Economic impact of chronic prostatitis*. *Curr Urol Rep*, 2007. **8**(4): p. 336-9.
33. DeWitt-Foy, M.E., J.C. Nickel, and D.A. Shoskes, *Management of Chronic Prostatitis/Chronic Pelvic Pain Syndrome*. *Eur Urol Focus*, 2019. **5**(1): p. 2-4.
34. Maeda, K., K. Shigemura, and M. Fujisawa, *A review of current treatments for chronic prostatitis/chronic pelvic pain syndrome under the UPOINTS system*. *Int J Urol*, 2023. **30**(5): p. 431-436.
35. Murphy, S.F., et al., *IL17 Mediates Pelvic Pain in Experimental Autoimmune Prostatitis (EAP)*. *PLoS One*, 2015. **10**(5): p. e0125623.
36. Hua, X., et al., *Pathogenic Roles of CXCL10 in Experimental Autoimmune Prostatitis by Modulating Macrophage Chemotaxis and Cytokine Secretion*. *Front Immunol*, 2021. **12**: p. 706027.
37. Crescenze, I.M., et al., *Efficacy, Side Effects, and Monitoring of Oral Cyclosporine in Interstitial Cystitis-Bladder Pain Syndrome*. *Urology*, 2017. **107**: p. 49-54.

38. Capodice, J.L., et al., *Complementary and alternative medicine for chronic prostatitis/chronic pelvic pain syndrome*. *Evid Based Complement Alternat Med*, 2005. **2**(4): p. 495-501.
39. Rudick, C.N., A.J. Schaeffer, and P. Thumbikat, *Experimental autoimmune prostatitis induces chronic pelvic pain*. *Am J Physiol Regul Integr Comp Physiol*, 2008. **294**(4): p. R1268-75.
40. Liu, F., et al., *Abnormal prostate microbiota composition is associated with experimental autoimmune prostatitis complicated with depression in rats*. *Front Cell Infect Microbiol*, 2022. **12**: p. 966004.
41. Pattabiraman, G., et al., *Mast cell function in prostate inflammation, fibrosis, and smooth muscle cell dysfunction*. *Am J Physiol Renal Physiol*, 2021. **321**(4): p. F466-F479.
42. Pattabiraman, G., et al., *mMCP7, a Mouse Ortholog of delta Trypsin, Mediates Pelvic Tactile Allodynia in a Model of Chronic Pelvic Pain*. *Front Pain Res (Lausanne)*, 2021. **2**: p. 805136.
43. Pattabiraman, G., et al., *o O E R 9 . " c " O q w u g " Q t v j q n q i " q h " " V t { r* *Tactile Allodynia in a Model of Chronic Pelvic Pain*. *Front Pain Res (Lausanne)*, 2021. **2**: p. 805136.
44. Vickman, R.E., et al., *TNF is a potential therapeutic target to suppress prostatic inflammation and hyperplasia in autoimmune disease*. *Nat Commun*, 2022. **13**(1): p. 2133.
45. Hou, Y., et al., *An aberrant prostate antigen-specific immune response causes prostatitis in mice and is associated with chronic prostatitis in humans*. *J Clin Invest*, 2009. **119**(7): p. 2031-41.



46. Orsilles, M.A., B.N. Pacheco-Rupil, and M.M. Depiante-Depaoli, *Experimental autoimmune prostatitis (EAP): enhanced release of reactive oxygen intermediates (ROI) in peritoneal macrophages*. *Autoimmunity*, 1993. **16**(3): p. 201-7.
47. Rivero, V., C. Carnaud, and C.M. Riera, *Prostatein or steroid binding protein (PSBP) induces experimental autoimmune prostatitis (EAP) in NOD mice*. *Clin Immunol*, 2002. **105**(2): p. 176-84.
48. Wolf, S.J., et al., *Human and Murine Evidence for Mechanisms Driving Autoimmune Photosensitivity*. *Front Immunol*, 2018. **9**: p. 2430.
49. Thumbikat, P., et al., *Bacteria-induced uroplakin signaling mediates bladder response to infection*. *PLoS Pathog*, 2009. **5**(5): p. e1000415.
50. Keetch, D.W., P. Humphrey, and T.L. Ratliff, *Development of a mouse model for nonbacterial prostatitis*. *J Urol*, 1994. **152**(1): p. 247-50.
51. Rivero, V.E., et al., *Non-obese diabetic (NOD) mice are genetically susceptible to experimental autoimmune prostatitis (EAP)*. *J Autoimmun*, 1998. **11**(6): p. 603-10.
52. Fu, W., et al., *The effect of chronic prostatitis/chronic pelvic pain syndrome (CP/CPPS) on semen parameters in human males: a systematic review and meta-analysis*. *PLoS One*, 2014. **9**(4): p. e94991.
53. . !!! INVALID CITATION !!! [30].
54. Penna, G., et al., *Spontaneous and prostatic steroid binding protein peptide-induced autoimmune prostatitis in the nonobese diabetic mouse*. *J Immunol*, 2007. **179**(3): p. 1559-67.
55. Ballotti, S., F. Chiarelli, and M. de Martino, *Autoimmunity: basic mechanisms and implications in endocrine diseases. Part II*. *Horm Res*, 2006. **66**(3): p. 142-52.

56. Ballotti, S., F. Chiarelli, and M. de Martino, *Autoimmunity: basic mechanisms and implications in endocrine diseases. Part I*. Horm Res, 2006. **66**(3): p. 132-41.
57. Dragin, N., et al., *Estrogen-mediated downregulation of AIRE influences sexual dimorphism in autoimmune diseases*. J Clin Invest, 2016. **126**(4): p. 1525-37.
58. Zhu, M.L., et al., *Sex bias in CNS autoimmune disease mediated by androgen control of autoimmune regulator*. Nat Commun, 2016. **7**: p. 11350.
59. Haverkamp, J.M., et al., *An inducible model of abacterial prostatitis induces antigen specific inflammatory and proliferative changes in the murine prostate*. Prostate, 2011. **71**(11): p. 1139-50.
60. Pound, P., *Scientific debate on animal model in research is needed*. BMJ, 2001. **323**(7323): p. 1252.
61. Akhtar, A., *The flaws and human harms of animal experimentation*. Camb Q Healthc Ethics, 2015. **24**(4): p. 407-19.
62. Centenera, M.M., et al., *A patient-derived explant (PDE) model of hormone-dependent cancer*. Mol Oncol, 2018. **12**(9): p. 1608-1622.
63. Baker, R., et al., *Computational modeling of complex bioenergetic mechanisms that modulate CD4+ T cell effector and regulatory functions*. NPJ Syst Biol Appl, 2022. **8**(1): p. 45.
64. Lorenzo, G., et al., *Tissue-scale, personalized modeling and simulation of prostate cancer growth*. Proc Natl Acad Sci U S A, 2016. **113**(48): p. E7663-E7671.
65. Vinnik, Y.Y., A.V. Kuzmenko, and T.A. Gyaurgiev, *[Treatment of the chronic prostatitis: current state of the problem]*. Urologiia, 2021(4): p. 138-144.

66. Kuzmenko, A.V., et al., [*The use of bioregulatory peptides in the treatment of men with benign prostatic hyperplasia and chronic prostatitis*]. *Urologia*, 2021(3): p. 70-74.
67. Zhang, M., et al., *Clinical study of duloxetine hydrochloride combined with doxazosin for the treatment of pain disorder in chronic prostatitis/chronic pelvic pain syndrome: An observational study*. *Medicine (Baltimore)*, 2017. **96**(10): p. e6243.
68. Iwamura, H., et al., *Eviprostat has an identical effect compared to pollen extract (Cernilton) in patients with chronic prostatitis/chronic pelvic pain syndrome: a randomized, prospective study*. *BMC Urol*, 2015. **15**: p. 120.
69. Tawfik, A.M., et al., *Tadalafil monotherapy in management of chronic prostatitis/chronic pelvic pain syndrome: a randomized double-blind placebo controlled clinical trial*. *World J Urol*, 2022. **40**(10): p. 2505-2511.
70. Pineault, K., et al., *Phosphodiesterase type 5 inhibitor therapy provides sustained relief of symptoms among patients with chronic pelvic pain syndrome*. *Transl Androl Urol*, 2020. **9**(2): p. 391-397.
71. Yang, X., et al., *Complex regulation of human androgen receptor expression by Wnt signaling in prostate cancer cells*. *Oncogene*, 2006. **25**(24): p. 3436-44.
72. Krakhotkin, D.V., et al., *Evaluation of influence of the UPOINT-guided multimodal therapy in men with chronic prostatitis/chronic pelvic pain syndrome on dynamic values NIH-CPSI: a prospective, controlled, comparative study*. *Ther Adv Urol*, 2019. **11**: p. 1756287219857271.
73. Mehik, A., et al., *Alfuzosin treatment for chronic prostatitis/chronic pelvic pain syndrome: a prospective, randomized, double-blind, placebo-controlled, pilot study*. *Urology*, 2003. **62**(3): p. 425-9.

74. Nickel, J.C., *Chronic prostatitis/chronic pelvic pain syndrome: it is time to change our management and research strategy*. BJU Int, 2020. **125**(4): p. 479-480.
75. Beamer, C.A., et al., *Targeted deletion of the aryl hydrocarbon receptor in dendritic cells prevents thymic atrophy in response to dioxin*. Arch Toxicol, 2019. **93**(2): p. 355-368.
76. Boule, L.A., et al., *Aryl hydrocarbon receptor signaling modulates antiviral immune responses: ligand metabolism rather than chemical source is the stronger predictor of outcome*. Sci Rep, 2018. **8**(1): p. 1826.
77. Abron, J.D., et al., *An endogenous aryl hydrocarbon receptor ligand, ITE, induces regulatory T cells and ameliorates experimental colitis*. Am J Physiol Gastrointest Liver Physiol, 2018. **315**(2): p. G220-g230.
78. Busbee, P.B., et al., *Use of natural AhR ligands as potential therapeutic modalities against inflammatory disorders*. Nutr Rev, 2013. **71**(6): p. 353-69.
79. Ehrlich, A.K., et al., *TCDD, FICZ, and Other High Affinity AhR Ligands Dose-Dependently Determine the Fate of CD4+ T Cell Differentiation*. Toxicol Sci, 2018. **161**(2): p. 310-320.
80. Wang, Q., et al., *Aryl hydrocarbon receptor inhibits inflammation in DSS-induced colitis via the MK2/pMK2/TTP pathway*. Int J Mol Med, 2018. **41**(2): p. 868-876.
81. Yue, T., et al., *The AHR Signaling Attenuates Autoimmune Responses During the Development of Type 1 Diabetes*. Front Immunol, 2020. **11**: p. 1510.
82. Soshilov, A.A. and M.S. Denison, *Ligand promiscuity of aryl hydrocarbon receptor agonists and antagonists revealed by site-directed mutagenesis*. Mol Cell Biol, 2014. **34**(9): p. 1707-19.

83. Wu, H., et al., *Synthesis and biological evaluation of FICZ analogues as agonists of aryl hydrocarbon receptor*. *Bioorg Med Chem Lett*, 2020. **30**(5): p. 126959.
84. Rouse, M., et al., *3,3'-diindolylmethane ameliorates experimental autoimmune encephalomyelitis by promoting cell cycle arrest and apoptosis in activated T cells through microRNA signaling pathways*. *J Pharmacol Exp Ther*, 2014. **350**(2): p. 341-52.
85. Kenison, J.E., et al., *Tolerogenic nanoparticles suppress central nervous system inflammation*. *Proc Natl Acad Sci U S A*, 2020. **117**(50): p. 32017-32028.
86. Fu, X., et al., *MicroRNA-155 deficiency attenuates inflammation and oxidative stress in experimental autoimmune prostatitis in a TLR4-dependent manner*. *Kaohsiung J Med Sci*, 2020. **36**(9): p. 712-720.
87. Heine, H. and A. Zamyatina, *Therapeutic Targeting of TLR4 for Inflammation, Infection, and Cancer: A Perspective for Disaccharide Lipid A Mimetics*. *Pharmaceuticals (Basel)*, 2022. **16**(1).
88. Ou, T., M. Lilly, and W. Jiang, *The Pathologic Role of Toll-Like Receptor 4 in Prostate Cancer*. *Front Immunol*, 2018. **9**: p. 1188.
89. Spachidou, M.P., et al., *Expression of functional Toll-like receptors by salivary gland epithelial cells: increased mRNA expression in cells derived from patients with primary Sjogren's syndrome*. *Clin Exp Immunol*, 2007. **147**(3): p. 497-503.
90. Spachidou, M.P., et al., *Expression of functional Toll-like receptors by salivary gland epithelial cells: increased mRNA expression in cells derived from patients with primary Sjögren's syndrome*. *Clin Exp Immunol*, 2007. **147**(3): p. 497-503.
91. Vidya, M.K., et al., *Toll-like receptors: Significance, ligands, signaling pathways, and functions in mammals*. *Int Rev Immunol*, 2018. **37**(1): p. 20-36.

92. Haartmans, M.J.J., et al., *Evaluation of the Anti-Inflammatory and Chondroprotective Effect of Celecoxib on Cartilage Ex Vivo and in a Rat Osteoarthritis Model*. *Cartilage*, 2022. **13**(3): p. 19476035221115541.
93. Tang, Y., et al., *Activated NF-kappaB in bone marrow mesenchymal stem cells from systemic lupus erythematosus patients inhibits osteogenic differentiation through downregulating Smad signaling*. *Stem Cells Dev*, 2013. **22**(4): p. 668-78.
94. Wang, Z., et al., *Muscarinic M1 and M2 receptor subtypes play opposite roles in LPS-induced septic shock*. *Pharmacol Rep*, 2019. **71**(6): p. 1108-1114.
95. Shen, J.D., et al., *Review of Animal Models to Study Urinary Bladder Function*. *Biology (Basel)*, 2021. **10**(12).
96. Fraser, M.O., et al., *Best practices for cystometric evaluation of lower urinary tract function in muriform rodents*. *Neurourol Urodyn*, 2020. **39**(6): p. 1868-1884.
97. Cannon, A.S., P.S. Nagarkatti, and M. Nagarkatti, *Targeting AhR as a Novel Therapeutic Modality against Inflammatory Diseases*. *Int J Mol Sci*, 2021. **23**(1).
98. Song, J., et al., *A ligand for the aryl hydrocarbon receptor isolated from lung*. *Proc Natl Acad Sci U S A*, 2002. **99**(23): p. 14694-9.
99. Ito, T., et al., *TCDD exposure exacerbates atopic dermatitis-related inflammation in NC/Nga mice*. *Toxicol Lett*, 2008. **177**(1): p. 31-7.
100. Benson, J.M. and D.M. Shepherd, *Aryl hydrocarbon receptor activation by TCDD reduces inflammation associated with Crohn's disease*. *Toxicol Sci*, 2011. **120**(1): p. 68-78.
101. Kummari, E., et al., *TCDD attenuates EAE through induction of FasL on B cells and inhibition of IgG production*. *Toxicology*, 2021. **448**: p. 152646.

102. Huang, Y., et al., *Aryl Hydrocarbon Receptor Regulates Apoptosis and Inflammation in a Murine Model of Experimental Autoimmune Uveitis*. *Front Immunol*, 2018. **9**: p. 1713.
103. Bradley, W.E., *Electroencephalography and bladder innervation*. *J Urol*, 1977. **118**(3): p. 412-4.
104. Heppner, T.J., et al., *Transient contractions of urinary bladder smooth muscle are drivers of afferent nerve activity during filling*. *J Gen Physiol*, 2016. **147**(4): p. 323-35.
105. Bohlen, M., et al., *Experimenter effects on behavioral test scores of eight inbred mouse strains under the influence of ethanol*. *Behav Brain Res*, 2014. **272**: p. 46-54.
106. Kennedy, C.L., et al., *Developmental polychlorinated biphenyl (PCB) exposure alters voiding physiology in young adult male and female mice*. *Am J Clin Exp Urol*, 2022. **10**(2): p. 82-97.
107. Gonzalez-Cano, R., et al., *Up-Down Reader: An Open Source Program for Efficiently Processing 50% von Frey Thresholds*. *Front Pharmacol*, 2018. **9**: p. 433.
108. Mishra, S., G. Bassi, and Y.X.Z. Xu, *Sex Differences in Immunometabolism: An Unexplored Area*. *Methods Mol Biol*, 2020. **2184**: p. 265-271.
109. Nusbaum, J.S., et al., *Sex Differences in Systemic Lupus Erythematosus: Epidemiology, Clinical Considerations, and Disease Pathogenesis*. *Mayo Clin Proc*, 2020. **95**(2): p. 384-394.
110. Pacini, G., et al., *Epigenetics, pregnancy and autoimmune rheumatic diseases*. *Autoimmun Rev*, 2020. **19**(12): p. 102685.
111. Billi, A.C., et al., *The female-biased factor VGLL3 drives cutaneous and systemic autoimmunity*. *JCI Insight*, 2019. **4**(8).

112. Liang, Y., J.M. Kahlenberg, and J.E. Gudjonsson, *A vestigial pathway for sex differences in immune regulation*. Cell Mol Immunol, 2017. **14**(7): p. 578-580.
113. Liang, Y., et al., *VGLL3-regulated gene network as a promoter of sex biased autoimmune diseases*. Nat Immunol, 2017. **18**(2): p. 152-60.
114. Pagenkopf, A.C. and Y. Liang, *A New Driver for Lupus Pathogenesis is conserved in Humans and Mice*. Lupus (Los Angel), 2019. **4**(2).
115. Edwards, M., R. Dai, and S.A. Ahmed, *Our Environment Shapes Us: The Importance of Environment and Sex Differences in Regulation of Autoantibody Production*. Front Immunol, 2018. **9**: p. 478.
116. Golden, L.C. and R. Voskuhl, *The importance of studying sex differences in disease: The example of multiple sclerosis*. J Neurosci Res, 2017. **95**(1-2): p. 633-643.
117. Ganeshan, K. and A. Chawla, *Metabolic regulation of immune responses*. Annu Rev Immunol, 2014. **32**: p. 609-34.
118. Takeshima, Y., et al., *Metabolism as a key regulator in the pathogenesis of systemic lupus erythematosus*. Semin Arthritis Rheum, 2019. **48**(6): p. 1142-1145.
119. Tomczynska, M., I. Salata, and J. Saluk, *[The role of gender in the pathogenesis and development of autoimmune diseases]*. Pol Merkur Lekarski, 2016. **41**(243): p. 150-155.
120. Bhatia, A., H.K. Sekhon, and G. Kaur, *Sex hormones and immune dimorphism*. ScientificWorldJournal, 2014. **2014**: p. 159150.
121. Christou, E.A.A., et al., *Sexual dimorphism in SLE: above and beyond sex hormones*. Lupus, 2019. **28**(1): p. 3-10.



122. Pagenkopf, A. and Y. Liang, *Immunometabolic function of the transcription cofactor VGLL3 provides an evolutionary rationale for sexual dimorphism in autoimmunity*. FEBS Lett, 2020.
123. Liang, Y., et al., *SOCS signaling in autoimmune diseases: molecular mechanisms and therapeutic implications*. Eur J Immunol, 2014. **44**(5): p. 1265-75.
124. Ostensson, M., et al., *A possible mechanism behind autoimmune disorders discovered by genome-wide linkage and association analysis in celiac disease*. PLoS One, 2013. **8**(8): p. e70174.
125. Kaul, A., et al., *Systemic lupus erythematosus*. Nat Rev Dis Primers, 2016. **2**: p. 16039.
126. Markle, J.G. and E.N. Fish, *SeXX matters in immunity*. Trends Immunol, 2014. **35**(3): p. 97-104.
127. vom Steeg, L.G. and S.L. Klein, *SeXX Matters in Infectious Disease Pathogenesis*. PLoS Pathog, 2016. **12**(2): p. e1005374.
128. Freitag, J., et al., *Immunometabolism and autoimmunity*. Immunol Cell Biol, 2016. **94**(10): p. 925-934.
129. Souyris, M., et al., *TLR7 escapes X chromosome inactivation in immune cells*. Sci Immunol, 2018. **3**(19).
130. Lu, J., et al., *Changes in peripheral blood inflammatory factors (TNF- $\alpha$ , IL-1 $\beta$ , IL-6) and N intestinal flora in AIDS and HIV-positive individuals*. J Zhejiang Univ Sci B, 2019. **20**(10): p. 793-802.
131. Jaillon, S., K. Berthenet, and C. Garlanda, *Sexual Dimorphism in Innate Immunity*. Clin Rev Allergy Immunol, 2019. **56**(3): p. 308-321.

132. Shen, H., et al., *Gender-dependent expression of murine Irf5 gene: implications for sex bias in autoimmunity*. J Mol Cell Biol, 2010. **2**(5): p. 284-90.
133. Beebe, A.M., D.J. Cua, and R. de Waal Malefyt, *The role of interleukin-10 in autoimmune disease: systemic lupus erythematosus (SLE) and multiple sclerosis (MS)*. Cytokine Growth Factor Rev, 2002. **13**(4-5): p. 403-12.
134. Stojic-Vukanic, Z., et al., *Sex Bias in Pathogenesis of Autoimmune Neuroinflammation: Relevance for Dimethyl Fumarate Immunomodulatory/Anti-oxidant Action*. Mol Neurobiol, 2018. **55**(5): p. 3755-3774.
135. Talaat, R.M., et al., *Th1/Th2/Th17/Treg cytokine imbalance in systemic lupus erythematosus (SLE) patients: Correlation with disease activity*. Cytokine, 2015. **72**(2): p. 146-53.
136. Millett, C.E., B.E. Phillips, and E.F.H. Saunders, *The Sex-specific Effects of LPS on Depressive-like Behavior and Oxidative Stress in the Hippocampus of the Mouse*. Neuroscience, 2019. **399**: p. 77-88.
137. Schneider-Hohendorf, T., et al., *Sex bias in MHC I-associated shaping of the adaptive immune system*. Proc Natl Acad Sci U S A, 2018. **115**(9): p. 2168-2173.
138. Gold, S.M., et al., *Sex differences in autoimmune disorders of the central nervous system*. Semin Immunopathol, 2019. **41**(2): p. 177-188.
139. Stathopoulou, C., D. Nikoleri, and G. Bertsias, *Immunometabolism: an overview and therapeutic prospects in autoimmune diseases*. Immunotherapy, 2019. **11**(9): p. 813-829.
140. Kaufmann, U., et al., *Calcium Signaling Controls Pathogenic Th17 Cell-Mediated Inflammation by Regulating Mitochondrial Function*. Cell Metab, 2019. **29**(5): p. 1104-1118.e6.

141. Trzeciak, M., et al., *Immune Response Targeting Sjogren's Syndrome Antigen Ro52 Suppresses Tear Production in Female Mice*. *Int J Mol Sci*, 2018. **19**(10).
142. Chiaroni-Clarke, R.C., J.E. Munro, and J.A. Ellis, *Sex bias in paediatric autoimmune disease - Not just about sex hormones?* *J Autoimmun*, 2016. **69**: p. 12-23.
143. Roberts, M.H. and E. Erdei, *Comparative United States autoimmune disease rates for 2010-2016 by sex, geographic region, and race*. *Autoimmun Rev*, 2020. **19**(1): p. 102423.
144. Quintero, O.L., et al., *Autoimmune disease and gender: plausible mechanisms for the female predominance of autoimmunity*. *J Autoimmun*, 2012. **38**(2-3): p. J109-19.
145. Skakkebaek, N.E., et al., *Male Reproductive Disorders and Fertility Trends: Influences of Environment and Genetic Susceptibility*. *Physiol Rev*, 2016. **96**(1): p. 55-97.
146. Slominski, A., et al., *Steroidogenesis in the skin: implications for local immune functions*. *J Steroid Biochem Mol Biol*, 2013. **137**: p. 107-23.
147. Hughes, M., et al., *Gender-related differences in systemic sclerosis*. *Autoimmun Rev*, 2020. **19**(4): p. 102494.
148. Taneja, V., *Sex Hormones Determine Immune Response*. *Front Immunol*, 2018. **9**: p. 1931.
149. Gomez, A., et al., *Loss of sex and age driven differences in the gut microbiome characterize arthritis-susceptible 0401 mice but not arthritis-resistant 0402 mice*. *PLoS One*, 2012. **7**(4): p. e36095.
150. Behrens, M., et al., *B cells influence sex specificity of arthritis via myeloid suppressors and chemokines in humanized mice*. *Clin Immunol*, 2017. **178**: p. 10-19.

151. Adiele, R.C. and C.A. Adiele, *Metabolic defects in multiple sclerosis*. Mitochondrion, 2019. **44**: p. 7-14.
152. Bhargava, P., et al., *Metabolic alterations in multiple sclerosis and the impact of vitamin D supplementation*. JCI Insight, 2017. **2**(19).
153. Bizzarri, C., et al., *Sexual dimorphism in growth and insulin-like growth factor-I in children with type 1 diabetes mellitus*. Growth Horm IGF Res, 2014. **24**(6): p. 256-9.
154. Gaber, T., C. Strehl, and F. Buttgereit, *Metabolic regulation of inflammation*. Nat Rev Rheumatol, 2017. **13**(5): p. 267-279.
155. Li, R., et al., *Sex differences in outcomes of disease-modifying treatments for multiple sclerosis: A systematic review*. Mult Scler Relat Disord, 2017. **12**: p. 23-28.
156. Mathur, D., et al., *Perturbed glucose metabolism: insights into multiple sclerosis pathogenesis*. Front Neurol, 2014. **5**: p. 250.
157. Poddighe, S., et al., *Metabolomic analysis identifies altered metabolic pathways in Multiple Sclerosis*. Int J Biochem Cell Biol, 2017. **93**: p. 148-155.
158. Sheikh, M.H., et al., *Immuno-metabolic impact of the multiple sclerosis patients' sera on endothelial cells of the blood-brain barrier*. J Neuroinflammation, 2020. **17**(1): p. 153.
159. Huang, N. and A. Perl, *Metabolism as a Target for Modulation in Autoimmune Diseases*. Trends Immunol, 2018. **39**(7): p. 562-576.
160. Li, W., et al., *Metabolic Factors that Contribute to Lupus Pathogenesis*. Crit Rev Immunol, 2016. **36**(1): p. 75-98.
161. Syrett, C.M., et al., *Altered X-chromosome inactivation in T cells may promote sex-biased autoimmune diseases*. JCI Insight. **4**(7).

162. Pollizzi, K.N., et al., *Asymmetric inheritance of mTORC1 kinase activity during division dictates CD8(+) T cell differentiation*. Nat Immunol, 2016. **17**(6): p. 704-11.
163. Suto, T. and T. Karonitsch, *The immunobiology of mTOR in autoimmunity*. J Autoimmun, 2020. **110**: p. 102373.
164. Mauvais-Jarvis, F., A.P. Arnold, and K. Reue, *A Guide for the Design of Pre-clinical Studies on Sex Differences in Metabolism*. Cell Metab, 2017. **25**(6): p. 1216-1230.
165. Hemmings, B.A. and D.F. Restuccia, *PI3K-PKB/Akt pathway*. Cold Spring Harb Perspect Biol, 2012. **4**(9): p. a011189.
166. Vadlakonda, L., et al., *The Paradox of Akt-mTOR Interactions*. Front Oncol, 2013. **3**: p. 165.
167. Xu, F., et al., *Roles of the PI3K/AKT/mTOR signalling pathways in neurodegenerative diseases and tumours*. Cell Biosci, 2020. **10**: p. 54.
168. Balogh, A., et al., *Sex hormone-binding globulin provides a novel entry pathway for estradiol and influences subsequent signaling in lymphocytes via membrane receptor*. Sci Rep, 2019. **9**(1): p. 4.
169. Thaler, M.A., V. Seifert-Klauss, and P.B. Lippa, *The biomarker sex hormone-binding globulin - from established applications to emerging trends in clinical medicine*. Best Pract Res Clin Endocrinol Metab, 2015. **29**(5): p. 749-60.
170. Li, C., et al., *TCR Transgenic Mice Reveal Stepwise, Multi-site Acquisition of the Distinctive Fat-Treg Phenotype*. Cell, 2018. **174**(2): p. 285-299.e12.
171. Vasanthakumar, A., et al., *The transcriptional regulators IRF4, BATF and IL-33 orchestrate development and maintenance of adipose tissue-resident regulatory T cells*. Nat Immunol, 2015. **16**(3): p. 276-85.

172. Billi, A.C., J.M. Kahlenberg, and J.E. Gudjonsson, *Sex bias in autoimmunity*. *Curr Opin Rheumatol*, 2019. **31**(1): p. 53-61.
173. Wu, T., et al., *Metabolic disturbances associated with systemic lupus erythematosus*. *PLoS One*, 2012. **7**(6): p. e37210.
174. Lewis, M.J., et al., *Autoantibodies targeting TLR and SMAD pathways define new subgroups in systemic lupus erythematosus*. *J Autoimmun*, 2018. **91**: p. 1-12.
175. Liang, Y.C., et al., *[Role of circulating T follicular helper subsets and T follicular helper effector memory cells in systemic lupus erythematosus]*. *Zhonghua Yi Xue Za Zhi*, 2019. **99**(3): p. 164-168.
176. Crotty, S., *T Follicular Helper Cell Biology: A Decade of Discovery and Diseases*. *Immunity*, 2019. **50**(5): p. 1132-1148.
177. Palmer, C.S., et al., *Regulators of Glucose Metabolism in CD4(+) and CD8(+) T Cells*. *Int Rev Immunol*, 2016. **35**(6): p. 477-488.
178. Doerner, J., et al., *Fn14 deficiency protects lupus-prone mice from histological lupus erythematosus-like skin inflammation induced by ultraviolet light*. *Exp Dermatol*, 2016. **25**(12): p. 969-976.
179. Lee, T.P. and B.L. Chiang, *Sex differences in spontaneous versus induced animal models of autoimmunity*. *Autoimmun Rev*, 2012. **11**(6-7): p. A422-9.
180. Palomar, A.P.D., et al., *The Innate Immune Cell Profile of the Cornea Predicts the Onset of Ocular Surface Inflammatory Disorders*. *J Clin Med*, 2019. **8**(12).
181. Wang, K., et al., *The Properties of Cytokines in Multiple Sclerosis: Pros and Cons*. *Am J Med Sci*, 2018. **356**(6): p. 552-560.

182. Yurkovetskiy, L., et al., *Gender bias in autoimmunity is influenced by microbiota*. *Immunity*, 2013. **39**(2): p. 400-12.
183. Singh, H., A.A. Khan, and A.R. Dinner, *Gene regulatory networks in the immune system*. *Trends Immunol*, 2014. **35**(5): p. 211-8.
184. Triggianese, P., et al., *Immune checkpoint inhibitors-induced autoimmunity: The impact of gender*. *Autoimmun Rev*, 2020. **19**(8): p. 102590.
185. Yang, Z., et al., *T-cell metabolism in autoimmune disease*. *Arthritis Res Ther*, 2015. **17**(1): p. 29.
186. Frauwirth, K.A., et al., *The CD28 signaling pathway regulates glucose metabolism*. *Immunity*, 2002. **16**(6): p. 769-77.
187. He, N., et al., *Metabolic control of regulatory T cell (Treg) survival and function by Lkb1*. *Proc Natl Acad Sci U S A*, 2017. **114**(47): p. 12542-12547.
188. Katsiogiannis, S., R. Tenta, and F.N. Skopouli, *Autoimmune epithelitis (Sjögren's syndrome); the impact of metabolic status of glandular epithelial cells on auto-immunogenicity*. *J Autoimmun*, 2019. **104**: p. 102335.
189. Yasuda, K., Y. Takeuchi, and K. Hirota, *The pathogenicity of Th17 cells in autoimmune diseases*. *Semin Immunopathol*, 2019. **41**(3): p. 283-297.
190. Crotty, S., *T follicular helper cell differentiation, function, and roles in disease*. *Immunity*, 2014. **41**(4): p. 529-42.
191. Merrheim, J., et al., *Estrogen, estrogen-like molecules and autoimmune diseases*. *Autoimmun Rev*, 2020. **19**(3): p. 102468.

192. Fernández-Ochoa, Á., et al., *Discovering new metabolite alterations in primary sjögren's syndrome in urinary and plasma samples using an HPLC-ESI-QTOF-MS methodology*. J Pharm Biomed Anal, 2020. **179**: p. 112999.
193. Hwang, S.H., et al., *Metabolic abnormalities exacerbate Sjögren's syndrome by and is associated with increased the population of interleukin-17-producing cells in NOD/ShiLtJ mice*. J Transl Med, 2020. **18**(1): p. 186.
194. Recalde, G., et al., *Contribution of sex steroids and prolactin to the modulation of T and B cells during autoimmunity*. Autoimmun Rev, 2018. **17**(5): p. 504-512.
195. Wu, N., et al., *Alpha-Ketoglutarate: Physiological Functions and Applications*. Biomol Ther (Seoul), 2016. **24**(1): p. 1-8.
196. Cronin, S.J.F., et al., *The Role of Iron Regulation in Immunometabolism and Immune-Related Disease*. Front Mol Biosci, 2019. **6**: p. 116.
197. Della Torre, S., et al., *Energy metabolism and fertility: a balance preserved for female health*. Nat Rev Endocrinol, 2014. **10**(1): p. 13-23.
198. Zielinski, M.R., D.M. Szymon, and N.R. Rose, *Fatigue, Sleep, and Autoimmune and Related Disorders*. Front Immunol, 2019. **10**: p. 1827.